

RECOMMENDED PRACTICE

DNVGL-RP-C203

Edition September 2019
Amended January 2020

Fatigue design of offshore steel structures

The electronic PDF version of this document, available at the DNV GL website dnvgl.com, is the official, binding version.

FOREWORD

DNV GL recommended practices contain sound engineering practice and guidance.

© DNV GL AS September 2019

Any comments may be sent by e-mail to *rules@dnvgl.com*

This service document has been prepared based on available knowledge, technology and/or information at the time of issuance of this document. The use of this document by others than DNV GL is at the user's sole risk. DNV GL does not accept any liability or responsibility for loss or damages resulting from any use of this document.

CHANGES – CURRENT

This document supersedes the April 2016 edition of DNVGL-RP-C203.

Changes in this document are highlighted in red colour. However, if the changes involve a whole chapter, section or subsection, normally only the title will be in red colour.

Amendments January 2020

Topic	Reference	Description
Correction	Table A-5	Figure 4 and Figure 5 have been replaced.

Amendments December 2019

Topic	Reference	Description
Nominal stress and SCF in simple tubular joints	Figure F-17	An error in the figure showing the potential fatigue cracks with nominal stress and stress concentration factors has been corrected and explanatory text has been added.

Changes September 2019

Topic	Reference	Description
Application	[1.4]	The validity of the recommended practice for use in seawater with cathodic protection has been increased from 690 MP to 759 MPa.
Fatigue analysis based on S-N data	[2.3.2]	Added more information.
	[2.4.3]	Text related to the reference thickness has been corrected.
	[2.4.6]	Text has been added to explain the difference in S-N curves for the outside and the inside of tubular joints welded from the outside only.
	[2.9]	A section on friction welded bolts has been added.
Stress concentration factors	[3.1]	The recommended values of δ_0 has been changed for plated structures.
	[3.3.7.2]	Sentence with SCF = 1.0 for the inside has been removed as this is not always correct.
		The recommended values of δ_0 has been changed for tubular structures.
	[3.3.7.3]	The recommended values of δ_0 has been changed at girth welds in tubular structures with thickness transitions.
	[3.3.9]	Reference has been added to [F.17] with stress concentration factors where the thickness of the conical section is different from the tubular.

Changes - current

<i>Topic</i>	<i>Reference</i>	<i>Description</i>
Calculation of hot spot stress by finite element analysis	[4.2]	Text has been added to explain that the dynamic stresses in the chord may increase the hot spot stress at the crown position of tubular joints. Also, a section on relation between stub length and effect on stress concentration factors at tubular joints and at the girth weld to the brace has been added.
	[4.3]	Guidance on hot spot stress derivation in thick plates has been added.
	[4.3.4]	More explanation has been added on stress range calculation where the direction of the stresses can change during a load cycle.
Classification of structural details	[A.2]	Additional text with respect to fabrication tolerances for bolts has been added. The explanation of difference in classification of cut and rolled threads has been improved. The classification of cut threads has been increased from W3 to G.
		A detail with friction welded bolts to base material has been added.
	[A.5]	The text related to δ_0 has been corrected to correspond to the changes made in [3.1] and [3.3.7].
	[A.6]	A detail showing grinding of single side welded joints to achieve C-N class C1 has been added.
	[A.7]	A clarification on potential fatigue cracking has been added.
Stress concentration factors for tubular joints	[B.1]	Equation (6b) and equation (7b) have been corrected. The SCF value for the attachment has been reduced from 1.27 to 1.20.
S-N curves for base material of high strength steel	[D.2]	This section has been revised.
Application of the effective notch stress method for fatigue assessment of structural details	[E.3]	Text has been added to explain that the target value corresponds to a plate thickness equal 25 mm.
Commentary	[F.10]	This section has been revised to be more in line with experience and performed detail analyses.
	[F.12]	This is a new section that has been added for time domain analysis where the principal stress direction changes during a load cycle.
	[F.14]	The text has been revised and an equation for stress concentration factor for the inside has been added.
	[F.17]	A new section on stress concentration factors for conical transitions have been added.

Editorial corrections

In addition to the above stated changes, editorial corrections may have been made.

Contents

Changes – current.....	3
Section 1 General.....	8
1.1 Introduction.....	8
1.2 Objective.....	8
1.3 Scope.....	8
1.4 Application.....	9
1.5 Definitions.....	9
1.6 Symbols and abbreviations.....	12
Section 2 Fatigue analysis based on S-N data.....	15
2.1 Introduction.....	15
2.2 Fatigue damage accumulation.....	19
2.3 Fatigue analysis methodology and calculation of stresses.....	19
2.4 S-N curves.....	25
2.5 Mean stress influence on fatigue strength.....	36
2.6 Effect of fabrication tolerances.....	38
2.7 Requirements to non-destructive examination and acceptance criteria.....	38
2.8 Design chart for fillet and partial penetration welds.....	38
2.9 Bolts.....	39
2.10 Pipelines.....	40
2.11 Combined eccentricity for seamless riser pipes.....	43
2.12 Guidance to when a detailed fatigue analysis can be omitted.....	44
Section 3 Stress concentration factors.....	46
3.1 Stress concentration factors.....	46
3.2 Stress concentration factors for ship details.....	53
3.3 Tubular joints and members.....	53
Section 4 Calculation of hot spot stress by finite element analysis.....	74
4.1 General.....	74
4.2 Tubular joints.....	74
4.3 Welded connections in plated structures.....	77
Section 5 Simplified fatigue analysis.....	94
5.1 General.....	94
5.2 Fatigue design charts.....	95

Contents

5.3 Example of use of design charts.....	100
5.4 Fatigue capacity of connectors.....	101
Section 6 Fatigue analysis based on fracture mechanics.....	107
6.1 General on analysis methodology.....	107
Section 7 Improvement of fatigue life by fabrication.....	109
7.1 General.....	109
7.2 Weld profiling by machining and grinding.....	109
7.3 Weld toe grinding.....	110
7.4 TIG dressing.....	112
7.5 Hammer peening.....	112
Section 8 Extended fatigue life.....	114
8.1 Methodology.....	114
Section 9 Uncertainties in fatigue life prediction.....	115
9.1 Calculated probabilities of fatigue failures.....	115
9.2 Requirements to in-service inspection for fatigue cracks.....	119
Section 10 References.....	120
10.1 List of references.....	120
Appendix A Classification of structural details.....	126
A.1 Non-welded details.....	126
A.2 Bolted connections.....	128
A.3 Continuous welds essentially parallel to the direction of applied stress.....	130
A.4 Intermittent welds and welds at cope holes.....	133
A.5 Transverse butt welds, welded from both sides.....	134
A.6 Transverse butt welds, welded from one side.....	139
A.7 Welded attachments on the surface or the edge of a stressed member.....	141
A.8 Welded joints with load carrying welds.....	146
A.9 Hollow sections.....	150
A.10 Details relating to tubular members.....	153
Appendix B Stress concentration factors for tubular joints.....	156
B.1 Stress concentration factors for simple tubular joints and overlap joints.....	156
Appendix C Stress concentration factors for penetrations with reinforcements..	172

Contents

C.1 Stress concentration factors for small circular penetrations with reinforcement.....	172
C.2 Stress concentration factors at man-hole penetrations.....	200
C.3 Results.....	202
Appendix D S-N curves for base material of high strength steel.....	215
D.1 S-N curves for components of high strength steel subjected to high mean tensile stress.....	215
D.2 S-N curves for high strength steel for subsea applications.....	215
Appendix E Application of the effective notch stress method for fatigue assessment of structural details.....	222
E.1 General.....	222
E.2 Calculation of effective notch stress.....	222
E.3 Validation of analysis methodology.....	223
Appendix F Commentary.....	226
F.1 Comm. 1.2.3 low cycle and high cycle fatigue.....	227
F.2 Comm. 1.3 methods for fatigue analysis.....	228
F.3 Comm. 2.2 combination of fatigue damages from two dynamic processes.....	229
F.4 Comm. 2.3.2 plated structures using nominal stress S-N curves...	231
F.5 Comm. 2.4.3 S-N curves and joint classification.....	233
F.6 Comm. 2.4.9 S-N curves and efficiency of corrosion protection....	238
F.7 Comm. 2.4.14 qualification of new S-N curves based on fatigue test data.....	239
F.8 Comm. 2.10.3 fatigue analysis of pipes and cylindrical tanks subjected to cyclic internal pressure.....	247
F.9 Comm. 3.3 stress concentration factors.....	251
F.10 Comm. 3.3.3 tubular joints welded from one side.....	251
F.11 Comm. 4.3.7 verification of analysis methodology for finite element hot spot stress analysis.....	256
F.12 Comm. 4.3.4 Multidirectional fatigue analysis.....	265
F.13 Comm. 5 simplified fatigue analysis.....	270
F.14 Comm. 2.10.1 stresses at girth welds in pipes and S-N data.....	273
F.15 Comm. 7. improvement of fatigue life by fabrication.....	276
F.16 Comm. 3.3.12 joints with gusset plates.....	277
F.17 Comm. 3.3.9 stress concentration factors for conical transitions.....	279
Changes – historic.....	282

SECTION 1 GENERAL

1.1 Introduction

The aim of fatigue design is to ensure that the structure or the structural component has an adequate fatigue life.

The following design methods may be used when assessing fatigue life, where the choice of S-N curve depends on the selected design method:

- Nominal stress method which is typically used where the nominal stresses are well defined from structural analysis
- Hot spot stress method which is typically used in fatigue assessment of details in plated structures analysed by the finite element method
- Notch stress method which is typically used for details where it is difficult to arrive at a reliable design by using one of other methods

Selection of an S-N curve implies certain requirements to fabrication and inspection during fabrication to assure necessary quality to avoid that fatigue crack growth will occur from significant defects. This is further described in [DNVGL-OS-C401](#), NORSO M-101, ISO 5817:2014.

This recommended practice has been produced with the purpose of assessing fatigue damage in the high cycle region. For low cycle fatigue, see [DNVGL-RP-C208](#).

Calculated fatigue lives also form the basis for efficient inspection programmes during fabrication and the operational life of the structure, see [DNVGL-RP-C210](#).

1.2 Objective

The objective of this recommended practice is to provide methods for fatigue assessment of offshore steel structures and structural components with the aim to ensure safe fatigue design.

1.3 Scope

This recommended practice gives methods for fatigue analyses based on S-N data from testing for the following steel structures and components:

- Fixed and floating steel structures used for exploitation and for production of oil and gas
- Risers and pipelines
- Support structures for wind turbines
- Different types of welded connections
- Cast and forged joints
- Bolted connections
- Connectors
- Small diameter umbilicals made of super duplex steel.

The document specifies and gives guidelines for:

- S-N data in air environment, seawater with cathodic protection and seawater with free corrosion
- stress concentration factors for some details where these can be derived from analytical considerations or from detailed finite element analysis
- simplified fatigue design based on allowable stress ranges for various S-N data and Weibull long-term stress distributions
- the use of various design methods based on nominal stress, hot spot stress or notch stress
- post weld improvement such as grinding, TIG dressing and hammer peening.

1.4 Application

This recommended practice is valid for carbon manganese steel materials (C-Mn) in air with yield strength less than 960 MPa. For the carbon and low alloy machined forgings for subsea applications in [D.2] the S-N curves are valid for steels with yield strength up to 759 MPa and tensile strength up to 897 MPa in air environment.

For steel (C-Mn) materials in seawater with cathodic protection or steel with free corrosion the recommended practice is valid up to a yield strength 759 MPa and a tensile strength 897 MPa. This limit applies also to the carbon and low alloy machined forgings for subsea applications in [D.2].

This recommended practice is also valid for bolts in air environment or with protection corresponding to that condition of grades up to 10.9, ASTM A490 or equivalent.

This recommended practice is valid for material temperatures of up to 100°C for C-Mn steels in air condition.

1.5 Definitions

Table 1-1 Definition of verbal forms

Term	Description
shall	verbal form used to indicate requirements strictly to be followed in order to conform to the document
should	verbal form used to indicate that among several possibilities one is recommended as particularly suitable, without mentioning or excluding others
may	verbal form used to indicate a course of action permissible within the limits of the document

Table 1-2 Definition of terms

Term	Definition
butt weld	a butt weld is used to describe the weld between two plates or tubular sections that can be welded from both sides (double side weld) or from one side (single side weld)
classified structural detail	a structural detail containing a structural discontinuity including a weld or welds, for which the nominal stress approach is applicable, and which appear in the tables of this recommended practice Also referred to as standard structural detail.
constant amplitude loading	a type of loading causing a regular stress fluctuation with constant magnitudes of stress maxima and minima
crack propagation rate	amount of crack propagation during one stress cycle
crack propagation threshold	limiting value of stress intensity factor range below which the stress cycles are considered to be non-damaging
design fatigue factor	factor on fatigue life to be used for design
eccentricity	misalignment of plates at welded connections measured transverse to the plates
effective notch stress	notch stress calculated for a notch with a certain effective notch radius
fatigue action	load effect causing fatigue

Term	Definition
fatigue damage	ratio of number of applied load cycles and the corresponding number of cycles to failure at a constant stress range
fatigue life	number of stress cycles at a particular magnitude required to cause fatigue failure of the component
fatigue limit	fatigue strength under constant amplitude loading corresponding to a high number of cycles large enough to be considered as infinite by a design code
fatigue resistance	structural detail's resistance against fatigue actions in terms of S-N curve or crack propagation properties
fatigue strength	magnitude of stress range leading to a particular fatigue life
fracture mechanics	a branch of mechanics dealing with the behaviour and strength of components containing cracks
geometric stress	see hot spot stress
girth weld	a welded butt weld around the circumference between tubular sections having the same or a similar longitudinal axis (this is not defined as a tubular joint)
hot spot	a point in structure where a fatigue crack may initiate due to the combined effect of structural stress fluctuation and the weld geometry or a similar notch in the base material
hot spot stress	the value of structural stress on the surface at the hot spot (also known as geometric stress or structural stress)
local nominal stress	nominal stress including macro-geometric effects, concentrated load effects and misalignments, disregarding the stress raising effects of the welded joint itself
local notch	a notch such as the local geometry of the weld toe, including the toe radius and the angle between the base plate surface and weld reinforcement The local notch does not alter the structural stress but generates non-linear stress peaks.
macro-geometric discontinuity	a global discontinuity, the effect of which is usually not taken into account in the collection of standard structural details, such as large opening, a curved part in a beam, a bend in flange not supported by diaphragms or stiffeners, discontinuities in pressure containing shells, eccentricity in lap joints
macro-geometric effect	a stress raising effect due to macro-geometry in the vicinity of the welded joint, but not due to the welded joint itself
membrane stress	average normal stress across the thickness of a plate or shell
miner sum	sum of individual fatigue damage ratios caused by each stress cycle or stress range block according to Palmgren-Miner rule
misalignment	axial and angular misalignments caused either by detail design or by fabrication
M-N curve	graphical presentation of the dependence of fatigue life (N) on fatigue moment capacity (M)
nominal stress	a stress in a component, resolved, using general theories such as beam theory
nonlinear stress peak	the stress component of a notch stress which exceeds the linearly distributed structural stress at a local notch

Term	Definition
notch stress	<p>total stress at a notch taking into account the stress concentration caused by the local notch</p> <p>Thus the notch stress consists of the sum of the structural stress and the non-linear stress peak.</p>
notch stress concentration factor	the ratio of notch stress to structural stress
Paris' law	an experimentally determined relation between crack growth rate and stress intensity factor range
Palmgren-Miner rule	<p>fatigue failure is expected when the Miner sum reaches unity</p> <p>See also Sec.9 on uncertainties.</p>
rainflow counting	a standardised procedure for stress range counting
shell bending stress	bending stress in a shell or plate like part of a component, linearly distributed across the thickness as assumed in the theory of shells
S-N curve	graphical presentation of the dependence of fatigue life (N) on fatigue strength (S)
stress cycle	a part of a stress history containing a stress maximum and a stress minimum
stress intensity factor	factor used in fracture mechanics to characterise the stress at the vicinity of a crack tip
stress range	the difference between stress maximum and stress minimum in a stress cycle
stress range block	a part of a total spectrum of stress ranges which is discretized in a certain number of blocks
stress range exceedances	<p>a tabular or graphical presentation of the cumulative frequency of stress range exceedances, i.e. the number of ranges exceeding a particular magnitude of stress range in stress history</p> <p>Here frequency is the number of occurrences.</p>
stress ratio	ratio of minimum to maximum value of the stress in a cycle
structural discontinuity	<p>a geometric discontinuity due to the type of welded joint, usually found in tables of classified structural detail</p> <p>The effects of a structural discontinuity are (i) concentration of the membrane stress and (ii) formation of secondary bending stress.</p>
structural stress	<p>a stress in a component, resolved taking into account the effects of a structural discontinuity, and consisting of membrane and shell bending stress components</p> <p>Also referred to as geometric stress or hot spot stress.</p>
structural stress concentration factor	<p>the ratio of hot spot (structural) stress to local nominal stress</p> <p>In this RP the shorter notation: stress concentration factor (SCF) is used.</p>
tubular joint	welded connection between intersecting tubular members
variable amplitude loading	a type of loading causing irregular stress fluctuation with stress ranges (and amplitudes) of variable magnitude

1.6 Symbols and abbreviations

Table 1-3 Symbols and abbreviations

<i>Symbol</i>	<i>Description</i>
BOP	blowout preventer
C	material parameter
D	accumulated fatigue damage, diameter of chord
DFF	design fatigue factor
D _j	cylinder diameter at junction
E	Young's modulus
EC	eddy current
F	fatigue life
FE	finite element
I	moment of inertia of tubulars
K _{max} K _{min}	maximum and minimum stress intensity factors respectively
K _w	stress concentration factor due to weld geometry
ΔK	K _{max} - K _{min}
L	length of chord, length of thickness transition
MPI	magnetic particle inspection
N	number of cycles to failure
N _i	number of cycles to failure at constant stress range Δσ _i
N	axial force in tubular
NDT	non-destructive testing
R	outer radius of considered chord, reduction factor on fatigue life, stress ratio
SCF	stress concentration factor
SCF _{AS}	stress concentration factor at the saddle for axial load
SCF _{AC}	stress concentration factor at the crown for axial load
SCF _{MIP}	stress concentration factor for in plane moment
SCF _{MOP}	stress concentration factor for out of plane moment
SMTS	specified minimum yield strength
SMYS	specified minimum tensile strength
XT	christmas tree
R _a	surface roughness (mean)

Symbol	Description
R_T	reduction factor on fatigue resistance due to temperature
R_{y5}	surface roughness (largest amplitude measured in 5 cycles)
R_z	surface roughness (largest amplitude out of 10)
RF	fatigue life reduction factor
T	thickness of chord
T_e	equivalent thickness of chord
T_d	design life in seconds
Q	probability for exceedance of the stress range $\Delta\sigma$
a	crack depth, distance between braces in K-joints
a_i	half crack depth for internal cracks
\bar{a}	intercept of the design S-N curve with the log N axis
d	diameter of brace
e^{-a}	$\exp(-a)$
g	gap = a/D, factor depending on the geometry of the gap between the brace intersections with the chord in for example a K-joint
h	Weibull shape parameter, weld size or weld leg length
k	number of stress blocks, exponent on thickness
l	segment lengths of a tubular
m	negative inverse slope of the S-N curve, crack growth parameter
n_i	number of stress cycles in stress block i
n_o	is the number of cycles over the time period for which the stress range level $\Delta\sigma_o$ is defined
t_{ref}	reference thickness
t	plate thickness, thickness of brace member
t_c	cone thickness
t_p	plate thickness
Q	Weibull scale parameter
Γ	gamma function
η	usage factor
α	the slope angle of the cone, $\alpha = L/D$ (parameter used in equation for stress concentration factors for T- and Y-joints)
β	d/D
δ	Eccentricity

<i>Symbol</i>	<i>Description</i>
δ_0	eccentricity inherent in the S-N curve
γ	R/T
v_o	average zero-up-crossing frequency
ν	Poisson's ratio
σ_{local}	local stress
σ_{nominal}	nominal stress
$\sigma_{\text{hot spot}}$	hot spot stress or geometric stress
σ_x	maximum nominal stresses due to axial force
$\sigma_{my}\sigma_{mz}$	maximum nominal stresses due to bending about the y-axis and the z-axis
$\Delta\sigma$	stress range
$\Delta\sigma_0$	stress range exceeded once out of n_0 cycles
τ	t/T, shear stress

SECTION 2 FATIGUE ANALYSIS BASED ON S-N DATA

2.1 Introduction

2.1.1 General

The main principles for fatigue analysis based on fatigue tests are described in this section. The fatigue analysis may be based on nominal S-N curves for plated structures when appropriate. Additional stresses resulting from fabrication tolerances for butt welds and cruciform joints should be considered when the fabrication tolerances exceed that inherent the S-N data, see [3.1] and [3.3].

When performing finite element (FE) analysis for design of plated structures it is often found more convenient to extract hot spot stress from the analysis than that of a nominal stress. Guidance on finite element modelling and hot spot stress derivation is presented in [4.3]. The calculated hot spot stress is then entered a hot spot S-N curve for derivation of cycles to failure. Also here additional stresses resulting from fabrication tolerances for butt welds and cruciform joints should be considered.

For design of simple tubular joints it is standard practice to use parametric equations for derivation of stress concentration factors (SCF) to obtain hot spot stress for the actual geometry. Then this hot spot stress is entered a relevant hot spot stress S-N curve for tubular joints.

Results from performed fatigue analyses are presented in Sec.5 in terms of design charts that present allowable stresses as function of the Weibull shape parameter. The basis for the design charts is that long term stress ranges can be described by a two parameter Weibull distribution. The procedure can be used for different design lives, different design fatigue factors (DFFs) and different plate thickness.

2.1.2 Methods for fatigue analysis

To ensure that the structure will fulfil its intended function, a fatigue assessment, supported where appropriate by a detailed fatigue analysis, should be carried out for each individual member, which is subjected to fatigue loading. See also [2.12]. It should be noted that any element or member of the structure, every welded joint and attachment or other form of stress concentration, is potentially a source of fatigue cracking and should be individually considered.

The fatigue analysis should be based on S-N data, determined by fatigue testing of the considered welded detail, and the linear damage hypothesis. When appropriate, the fatigue analysis may alternatively be based on fracture mechanics. If the fatigue life estimate based on S-N data is short (shorter than 15 years) for a component where a failure may lead to severe consequences, a more accurate investigation considering a larger portion of the structure, or a fracture mechanics analysis, should be performed. For calculations based on fracture mechanics, it should be documented that there is a sufficient time interval between time of crack detection during in-service inspection and the time of unstable fracture.

All significant stress ranges, which contribute to fatigue damage, should be considered. The long term distribution of stress ranges may be found by deterministic or spectral analysis, see also /1/. Dynamic effects shall be duly accounted for when establishing the stress history. A fatigue analysis may be based on an expected stress history, which can be defined as expected number of cycles at each stress range level during the predicted life span. A practical application of this is to establish a long term stress range history that is on the safe side. The part of the stress range history contributing most significantly to the fatigue damage should be most carefully evaluated. See also [F.2] for guidance.

It should be noted that the shape parameter h in the Weibull distribution has a significant impact on calculated fatigue damage. For effect of the shape parameter on fatigue damage see also design charts in Figure 5-1 and Figure 5-2. Thus, when the fatigue damage is calculated based on closed form solutions with an assumption of a Weibull long term stress range distribution, a shape parameter to the safe side should be used.

2.1.3 Validity

This recommended practice is valid for carbon manganese steel materials (C-Mn) in air with yield strength less than 960 MPa. For the carbon and low alloy machined forgings for subsea applications in [D.2] the S-N curves are valid for steels with yield strength up to 759 MPa and tensile strength up to 897 MPa in air environment.

For steel (C-Mn) materials in seawater with cathodic protection or steel with free corrosion the recommended practice is valid up to a yield strength 759 MPa and a tensile strength 897 MPa. This limit applies also to the carbon and low alloy machined forgings for subsea applications in [D.2].

This recommended practice is also valid for bolts in air environment or with protection corresponding to that condition of grades up to 10.9, ASTM A490 or equivalent.

This recommended practice may be used for stainless steel.

2.1.4 Temperature

For higher temperatures than 100°C the fatigue resistance data for C-Mn steels in air condition may be modified with a reduction factor given as:

$$R_T = 1.0376 - 0.239 \cdot 10^{-3} T - 1.372 \cdot 10^{-6} T^2 \quad (2.2.1)$$

where T is given in °C (derived from figure in IIW document XII-1965-03/XV-1127-03). Fatigue resistance is understood to mean strength capacity. The reduced resistance in the S-N curves can be derived by a modification of the $\log \bar{\alpha}$ as:

$$\log \bar{\alpha}_{RT} = \log \bar{\alpha} + m \log R_T \quad (2.2.2)$$

2.1.5 Low cycle and high cycle fatigue

This recommended practice has been produced with the purpose of assessing fatigue damage in the high cycle region. See also [F.1]. For low cycle fatigue see DNVGL-RP-C208.

2.1.6 Requirements to fabrication

Selection of an S-N curve implies certain requirements to fabrication and inspection during fabrication to assure necessary quality that fatigue crack growth will not occur from significant defects. See DNVGL-OS-C401, NORSO M-101, ISO 5817:2014 and [F.6].

2.1.7 Fatigue failure modes

The following fatigue cracking failure modes are considered in this document, see also Figure 2-1:

- Fatigue crack growth from the weld toe into the base material.

In welded structures fatigue cracking from weld toes into the base material is a frequent failure mode. The fatigue crack is initiated at small defects or undercuts at the weld toe where the stress is highest due to the weld notch geometry. A large amount of the content in this RP is made with the purpose of achieving a reliable design with respect to this failure mode.

- Fatigue crack growth from the weld root through the fillet weld.

Fatigue cracking from root of fillet welds with a crack growth through the weld is a failure mode that can lead to significant consequences. Use of fillet welds should be avoided in connections where the failure consequences are large due to less reliable non-destructive examination (NDE) of this type of connection compared with a full penetration weld. However, in some welded connections use of fillet welds can hardly be avoided and it may also be efficient for fabrication. The specified design procedure in this document is considered to provide reliable connections also for fillet welds.

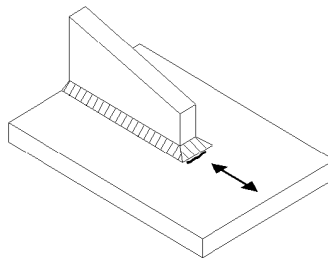
- Fatigue crack growth from the weld root into the section under the weld.

Fatigue crack growth from the weld root into the section under the weld is observed during service life of structures and in laboratory fatigue testing. The number of cycles to failure for this failure mode is of a similar magnitude as fatigue cracking from the weld toe in as-welded condition. There is no methodology that can be recommended used to avoid this failure mode except from using alternative types of welds locally. This means that if fatigue life improvement of the weld toe is required, the connection is subjected to high dynamic stress ranges. Thus, the connection becomes also highly utilised with respect to dynamic loading and it is also required to make improvement for the root. This can be performed using a full penetration weld along some distance of the stiffener nose.

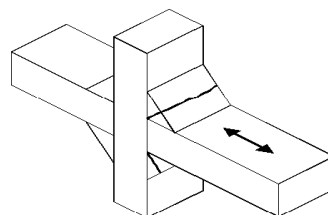
- Fatigue crack growth from a surface irregularity or notch into the base material.

Fatigue cracking in the base material is a failure mode that is of concern in components with high stress cycles. Then the fatigue cracks often initiate from notches or grooves in the components or from small surface defects/irregularities. The specified design procedure in this document is considered to provide reliable connections also with respect to this failure mode.

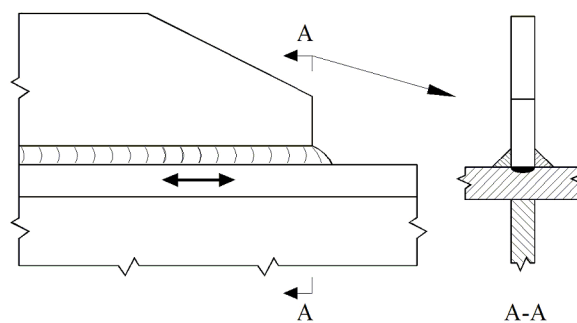
a) Fatigue crack growth from the weld toe into the base material.



b) Fatigue crack growth from the weld root through the fillet weld.



c) Fatigue crack growth from the weld root into the section under the weld.



d) Fatigue crack growth from a surface irregularity or notch into the base material.

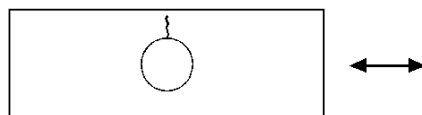


Figure 2-1 Explanation of different fatigue failure modes

2.2 Fatigue damage accumulation

The fatigue life may be calculated based on the S-N fatigue approach under the assumption of linear cumulative damage (Palmgren-Miner rule).

When the long-term stress range distribution is expressed by a stress histogram, consisting of a convenient number of constant stress range blocks $\Delta\sigma_i$ each with a number of stress repetitions n_i , the fatigue criterion reads:

$$D = \sum_{i=1}^k \frac{n_i}{N_i} = \frac{1}{\bar{a}} \sum_{i=1}^k n_i \cdot (\Delta\sigma)^m \leq \eta = \frac{1}{DFF} \quad (2.2.1)$$

where:

D = accumulated fatigue damage

\bar{a} = intercept of the design S-N curve with the log N axis

m = negative inverse slope of the S-N curve

k = number of stress blocks

n_i = number of stress cycles in stress block i

N_i = number of cycles to failure at constant stress range $\Delta\sigma_i$

usage factor

η = $1/\text{design fatigue factor from DNVGL-OS-C101 Ch.2 Sec.5 [1.2] Design fatigue factors.}$

DFF = design fatigue factor.

Applying a histogram to express the stress distribution, the number of stress blocks, k , should be large enough to ensure reasonable numerical accuracy, and should not be less than 20. Due consideration should be given to selection of integration method as the position of the integration points may have a significant influence on the calculated fatigue life dependent on integration method.

See [Sec.5](#) for calculation of fatigue damage using design charts based on a two-parameter Weibull distribution of the long term stress ranges.

See [\[F.3\]](#) for derivation of fatigue damage calculated from different processes.

2.3 Fatigue analysis methodology and calculation of stresses

2.3.1 General

Fatigue analysis may be based on different methodologies depending on what is found most efficient for the considered structural detail. Different concepts of S-N curves are developed and referred to in the literature and in this RP. It is thus important that the stresses are calculated in agreement with the definition of the stresses to be used together with a particular S-N curve. Three different concepts of S-N curves are defined:

- Nominal stress S-N curve that is described in [\[2.3.2\]](#).
- Hot spot stress S-N curve that is described in [\[2.3.3\]](#) for plated structures and in [\[2.3.4\]](#) for tubular joints.
- Notch stress S-N curve that is presented in [App.E](#). This notch stress S-N curve can be used together with finite element analysis where the local notch is modelled by an equivalent radius. This approach is

foreseen used only in special cases where it is found difficult to reliably assess the fatigue life using other methods, see [App.E](#) for more guidance.

Nominal stress is understood to be a stress in a component that can be derived by classical theory such as beam theory. In a simple plate specimen with an attachment as shown in [Figure 4-2](#) the nominal stress is simply the membrane stress that is used for plotting the S-N data from the fatigue testing. An example of fatigue design using this procedure is shown in the commentary section (example with fatigue analysis of a drum in [\[F.13\]](#)).

Hot spot stress is understood to be the geometric stress created by the considered detail. (The notch stress due to the local weld geometry is excluded from the stress calculation as it is assumed to be accounted for in the corresponding hot spot S-N curve. The notch stress is defined as the total stress resulting from the geometry of the detail and includes the non-linear stress field due to the notch at the weld toe).

Derivation of stresses to be used together with the different S-N curves are described in more detail in the following section.

The procedure for the fatigue analysis is based on the assumption that it is only necessary to consider the ranges of cyclic stresses in determining the fatigue endurance (i.e. mean stresses are neglected for fatigue assessment of welded connections due to presence of residual stresses).

The presence of residual tensile stresses at welds means also that compressive stress ranges may result in fatigue crack initiation and further fatigue crack growth until the crack has grown out of the tensile stress field. This means that also the stress range resulting from the minimum principal stress may need to be analysed in addition to the stress range from the maximum principal stress, see e.g. [\[4.3.4\]](#).

The selection of S-N curve is dependent on amount and type of inspection during fabrication, see [App.A](#). The size of defects inherent the S-N data are described in [\[F.5\]](#).

2.3.2 Plated structures using nominal stress S-N curves

The joint classification and corresponding S-N curves takes into account the local stress concentrations created by the joints themselves and by the weld profile. The design stress can therefore be regarded as the nominal stress, adjacent to the weld under consideration. However, if the joint is situated in a region of stress concentration resulting from the gross shape of the structure, this shall be taken into account. As an example, for the weld shown in [Figure 2-2 a\)](#), the relevant local stress for fatigue design would be the tensile stress, σ_{nominal} . For the weld shown in [Figure 2-2 b\)](#), the stress concentration factor for the global geometry shall in addition be accounted for, giving the relevant local stress equal to $\text{SCF} \cdot \sigma_{\text{nominal}}$, where SCF is the stress concentration factor due to the hole. Thus the local stress is derived as:

$$\sigma_{\text{local}} = \text{SCF} \sigma_{\text{nominal}} \quad (2.3.1)$$

σ_{local} shall be used together with the relevant S-N curves D through G, dependent on joint classification (as welded condition with potential fatigue crack growth from the weld toe).

The maximum principal stress is considered to be a significant parameter for analysis of fatigue crack growth. When the principal stress direction is different from that of the normal to the weld toe, it becomes conservative to use the principle stress range together with a classification of the connection for stress range normal to the weld toe as shown in [Figure 2-3](#). As the angle between the principal stress direction and the normal to the weld, φ , is increased further, fatigue cracking may no longer initiate along the weld toe, but may initiate in the weld and grow normal to the principal stress direction as shown in [Figure 2-4](#). This means that the notch at the weld toe no longer significantly influences the fatigue capacity and a higher S-N curve applies for this stress direction.

For welded details, in the as welded condition, one can calculate separate fatigue damages for fatigue cracking along the weld toe and transverse to the weld toe. An example of this is shown in [\[F.11\]](#).

More guidance on this for use of nominal S-N curves is presented in [\[F.4\]](#)

Stress ranges calculated based on von Mises form of component stress ranges can be used for fatigue analysis of notches in base material where initiation of a fatigue crack is a significant part of the fatigue life. More information on this is presented in [D.2].

2.3.3 Plated structures using hot spot stress S-N curves

For detailed finite element analysis of welded plate connections other than tubular joints it may also be convenient to use the alternative hot spot stress for fatigue life assessment, see [4.3] for further guidance. A relation between nominal stress and hot spot stress may be defined as:

$$\sigma_{\text{hot spot}} = \text{SCF} \sigma_{\text{nominal}} \quad (2.3.2)$$

where SCF is structural stress concentration factor normally denoted as stress concentration factor.

The effect of stress direction relative to the weld toe as shown in Figure 2-3 and Figure 2-4 when using finite element analysis and hot spot stress S-N curve is presented in [4.3.4].

2.3.4 Tubular joints

For a tubular joint, i.e. brace to chord connection, the stress to be used for design purpose is the range of idealised hot spot stress defined by: the greatest value of the extrapolation of the maximum principal stress distribution immediately outside the region effected by the geometry of the weld. The hot spot stress to be used in combination with the T-curve is calculated as:

$$\sigma_{\text{hot spot}} = \text{SCF} \sigma_{\text{nominal}} \quad (2.3.3)$$

where:

SCF = stress concentration factor as given in [3.3].

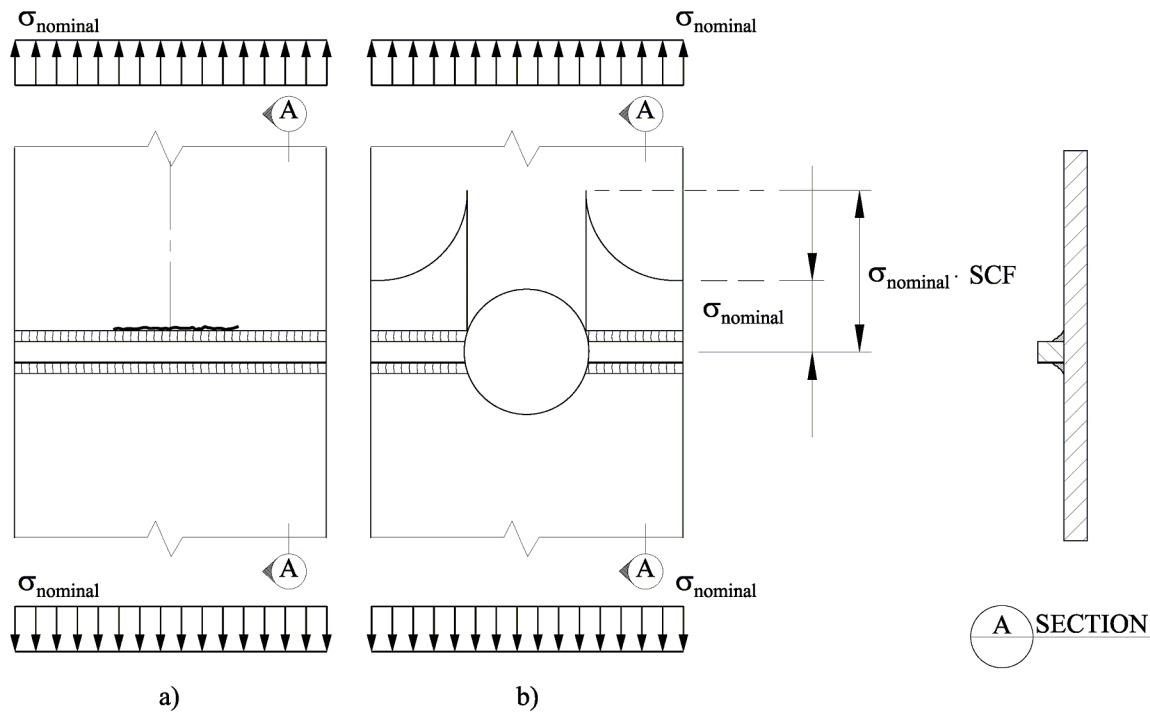


Figure 2-2 Explanation of local stresses

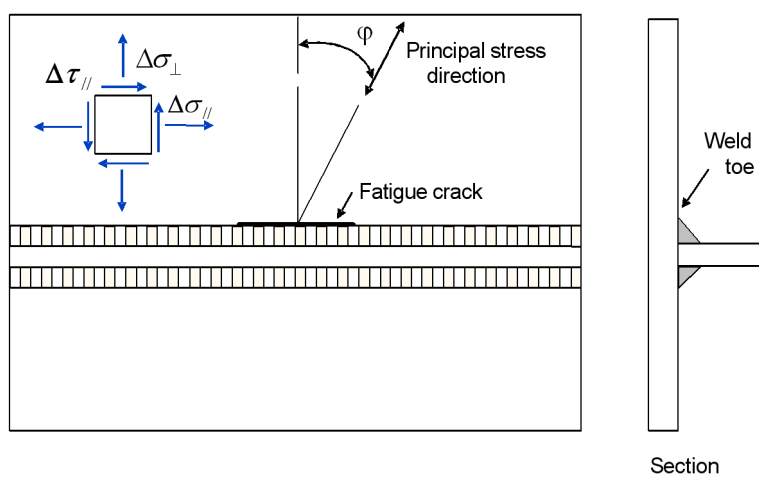


Figure 2-3 Fatigue cracking along weld toe

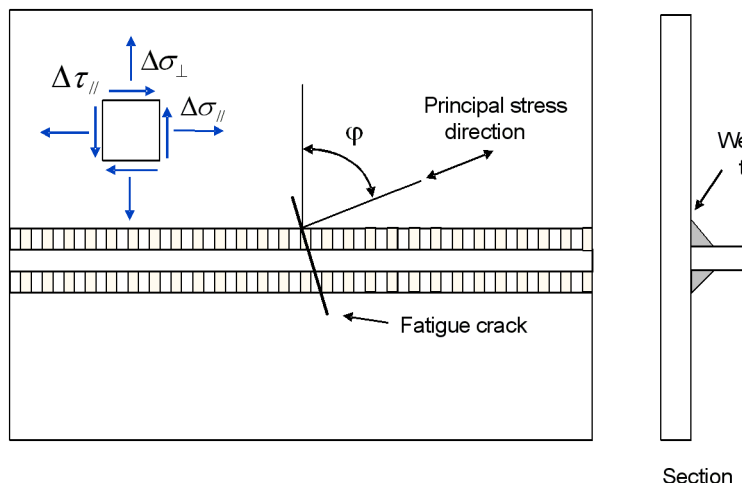


Figure 2-4 Fatigue cracking when principal stress direction is more parallel with weld toe

2.3.5 Fillet welds at load carrying joints

The relevant stress range for potential cracks in the weld throat of load-carrying fillet-welded joints and partial penetration welded joints may be calculated as:

$$\Delta\sigma_w = \sqrt{\Delta\sigma_{\perp}^2 + \Delta\tau_{\perp}^2 + 0.2\Delta\tau_{\parallel}^2} \quad (2.3.4)$$

where the stress components are explained in [Figure 2-5](#).

The total stress fluctuation (i.e. maximum compression and maximum tension) should be considered to be transmitted through the welds for fatigue assessments.

See [Table A-8](#) for selection of S-N curve.

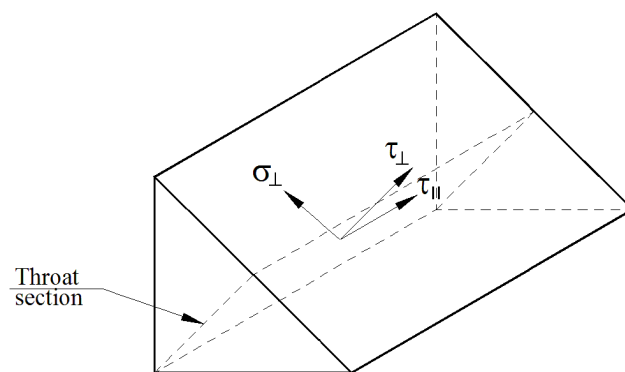


Figure 2-5 Explanation of stresses on the throat section of a fillet weld

2.3.6 Fillet welds at doubling plates

Fillet welds at doubling plates as shown in Figure 2-6 will be subjected to bending stress over the throat thickness when the doubling plate is loaded by an axial force or a bending moment. It is recommended to perform a finite element analysis for assessment of fatigue of these connections. The bending stress can be analysed using a modelling of the weld with at least 2 second order solid elements over the throat thickness where each element represents a linear stress distribution. The calculated stress components at a position 0.25 a and 0.75 a, where a is throat thickness, can be extrapolated to the weld root where these stresses are used to calculate the principal stress. The range of the maximum principal stress can then be used together with the F3 curve for calculation of fatigue damage. The S-N curve for air environment can be used for fatigue assessment if there is a closure weld all around the detail.

Alternatively the notch stress methodology described in App.E can be used for fatigue analysis of the weld root.

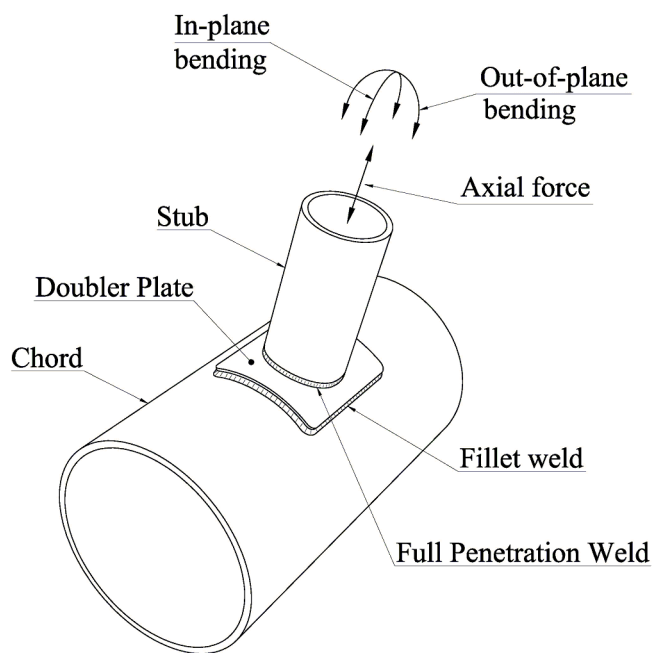


Figure 2-6 Fillet welded doubling plate

2.3.7 Fillet welded bearing supports

Where support plating below bearings are designed with fillet welded connection, it should be verified that fatigue cracking of the weld will not occur. Even though the joint may be required to carry wholly compressive stresses and the plate surfaces may be machined to fit, the total stress fluctuation should be considered to be transmitted through the welds for fatigue assessment.

If it is assumed that compressive loading is transferred through contact, it should be verified that the contact will not be lost during the welding. The actual installation condition including maximum construction tolerances should be accounted for.

2.4 S-N curves

2.4.1 General

The fatigue design is based on use of S-N curves, which are obtained from fatigue tests. The design S-N curves which follows are based on the mean-minus-two-standard-deviation curves for relevant experimental data. The S-N curves are thus associated with a 97.7% probability of survival.

2.4.2 Failure criterion inherent the S-N curves

Most of the S-N data are derived by fatigue testing of small specimens in test laboratories. For simple test specimens the testing is performed until the specimens have failed. In these specimens there is no possibility for redistribution of stresses during crack growth. This means that most of the fatigue life is associated with growth of a small crack that grows faster as the crack size increases until fracture if the connection otherwise does not show significant redistribution of stress flow during crack growth.

For details with the same calculated damage, the initiation period of a fatigue crack takes longer time for a notch in base material than at a weld toe or at a weld root. This also means that with a higher fatigue resistance of the base material as compared with welded details, the crack growth will be faster in base material when fatigue cracks are growing as the stress range in the base material may be significantly higher than at the welds if they are designed with the same fatigue utilization.

For practical purpose one defines these failures as being crack growth through the thickness.

When this failure criterion is transferred into a crack size in a real structure where some redistribution of stress is more likely, this means that this failure criterion corresponds to a crack size that is somewhat less than the plate thickness.

The test specimens with tubular joints are normally of a larger size. These joints also show larger possibility for redistribution of stresses as a crack is growing. Thus a crack can grow through the thickness and also along a part of the joint before a fracture occur during the testing. The number of cycles at a crack size through the thickness is used when the S-N curve for tubular joints is derived. As these tests are not very different from that of the actual behaviour in a structure, this failure criterion for the S-N curve for tubular joints corresponds approximately to the thickness at the hot spot (chord or brace as relevant).

2.4.3 S-N curves and joint classification for plated structures

For practical fatigue design, welded joints are divided into several classes, each with a corresponding design S-N curve. All tubular joints are assumed to be class T as specified in [Table 2-3](#). Other types of joint, including tube to plate, may fall in one of the 14 classes specified in [Table 2-1](#), [Table 2-2](#) and [Table 2-4](#), depending upon:

- the geometrical arrangement of the detail
- the direction of the fluctuating stress relative to the detail
- the method of fabrication and inspection of the detail.

Each construction detail at which fatigue cracks may potentially develop should, where possible, be placed in its relevant joint class in accordance with criteria given in [App.A](#). It should be noted that, in any welded joint, there are several locations at which fatigue cracks may develop, e. g. at the weld toe in each of the parts joined, at the weld ends, and in the weld itself. Each location should be classified separately.

The basic design S-N curve is given as:

$$\log N = \log \bar{a} - m \log \Delta\sigma \quad (2.4.1)$$

- N = predicted number of cycles to failure for stress range $\Delta\sigma$
 $\Delta\sigma$ = stress range with unit [MPa]
 m = negative inverse slope of S-N curve
 $\log \bar{a}$ = intercept of the design S-N curve with the log N-axis by S-N curve.

$$\log \bar{a} = \log a - 2 s_{\log N} \quad (2.4.2)$$

where:

- $\log a$ = intercept of mean S-N curve with the log N axis
 $s_{\log N}$ = standard deviation of $\log N$, see [F.5].

The fatigue strength of welded joints is to some extent dependent on plate thickness. This effect is due to the local geometry of the weld toe in relation to thickness of the adjoining plates. See also effect of profiling on thickness effect in [7.2]. It is also dependent on the stress gradient over the thickness, see [F.5]. The thickness effect is accounted for by a modification of the stress range such that the design S-N curve for thickness larger than the reference thickness reads:

$$\log N = \log \bar{a} - m \log \left(\Delta\sigma \left(\frac{t}{t_{ref}} \right)^k \right) \quad (2.4.3)$$

where:

- t_{ref} = reference thickness equal 25 mm for welded connections other than simple tubular joints. For simple tubular joints the reference thickness is 16 mm when using the T-curve. The reference thickness is equal 25 mm when other S-N curves are used for fatigue analysis of tubular joints. For bolts $t_{ref} = 25$ mm
 t = thickness through which a crack will most likely grow. $t = t_{ref}$ is used for thickness less than t_{ref}
 k = thickness exponent on fatigue strength as given in Table 2-1, Table 2-2, Table 2-3 and Table 2-4.
 k = 0.10 for tubular girth welds made from one side with fatigue cracking from the weld root
 k = 0.25 for threaded bolts subjected to stress variation in the axial direction.

In general the thickness exponent is included in the design equation to account for a situation that the actual size of the considered structural component is different in geometry from that the S-N data are based on. The thickness exponent is considered to account for different size of plate through which a crack will most likely grow. To some extent it also accounts for local geometry at the weld toe. However, it does not account for weld length or length of component different from that tested such as e.g. design of mooring systems with a significant larger number of chain links in the actual mooring line than what the test data are based on. Then the size effect should be carefully considered using probabilistic theory to achieve a reliable design, see [F.5].

The thickness or size effect is also dependent on width of butt welds and attachment length in cruciform connections. This parameter is denoted L_t in Figure 2-7. For butt welds where the widths L_t may be different

on the two plate sides, the width L_t for the considered hot spot side should be used. The size effect is lower than predicted from equation (2.4.3) for short lengths of L_t . Thus the thickness t in equation (2.4.3) for butt welds and cruciform joints may be replaced by an effective thickness t_{eff} which may be derived as:

$$t_{eff} = \min ((14\text{ mm} + 0.66L_t), T) \quad (2.4.4)$$

where the parameters L and T are measured in [mm] and are defined in [Figure 2-7](#). t_{eff} should not be less than t_{ref} . It should be noted that the width L_t for butt weld may be somewhat wider than that of the weld groove depending on the welding process. Also the possibility for weld repair should be considered when the width L_t to be used for fatigue analysis is decided.

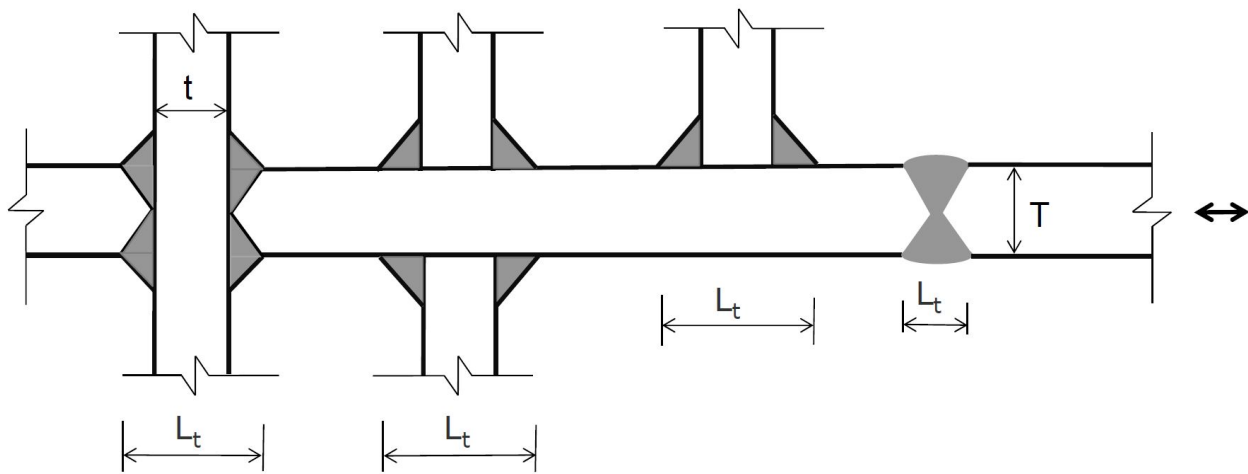


Figure 2-7 Definition of attachment length in cruciform joints and weld width in butt welds

2.4.4 S-N curves in air

S-N curves for air environment are given in [Table 2-1](#) and [Figure 2-8](#). The T curve for tubular joints is shown in [Table 2-3](#) and [Figure 2-10](#).

The maximum stress range is that of the B1 curve as shown in [Figure 2-8](#). However, for offshore structures subjected to typical wave and wind loading the main contribution to fatigue damage is in the region $N > 10^6$ cycles and the bilinear S-N curves defined in [Table 2-1](#) can be used.

Table 2-1 S-N curves in air

S-N curve	$N \leq 10^7$ cycles		$N > 10^7$ cycles $\log \bar{a}_2$ $m_2 = 5.0$	Fatigue limit at 10^7 cycles [MPa] *)	Thickness exponent k	Structural stress concentration embedded in the detail (S-N class), see also equation (2.3.2)
	m_1	$\log \bar{a}_1$				
B1	4.0	15.117	17.146	106.97	0	
B2	4.0	14.885	16.856	93.59	0	
C	3.0	12.592	16.320	73.10	0.05	
C1	3.0	12.449	16.081	65.50	0.10	
C2	3.0	12.301	15.835	58.48	0.15	
D	3.0	12.164	15.606	52.63	0.20	1.00
E	3.0	12.010	15.350	46.78	0.20	1.13
F	3.0	11.855	15.091	41.52	0.25	1.27
F1	3.0	11.699	14.832	36.84	0.25	1.43
F3	3.0	11.546	14.576	32.75	0.25	1.61
G	3.0	11.398	14.330	29.24	0.25	1.80
W1	3.0	11.261	14.101	26.32	0.25	2.00
W2	3.0	11.107	13.845	23.39	0.25	2.25
W3	3.0	10.970	13.617	21.05	0.25	2.50

*) See also [2.12].

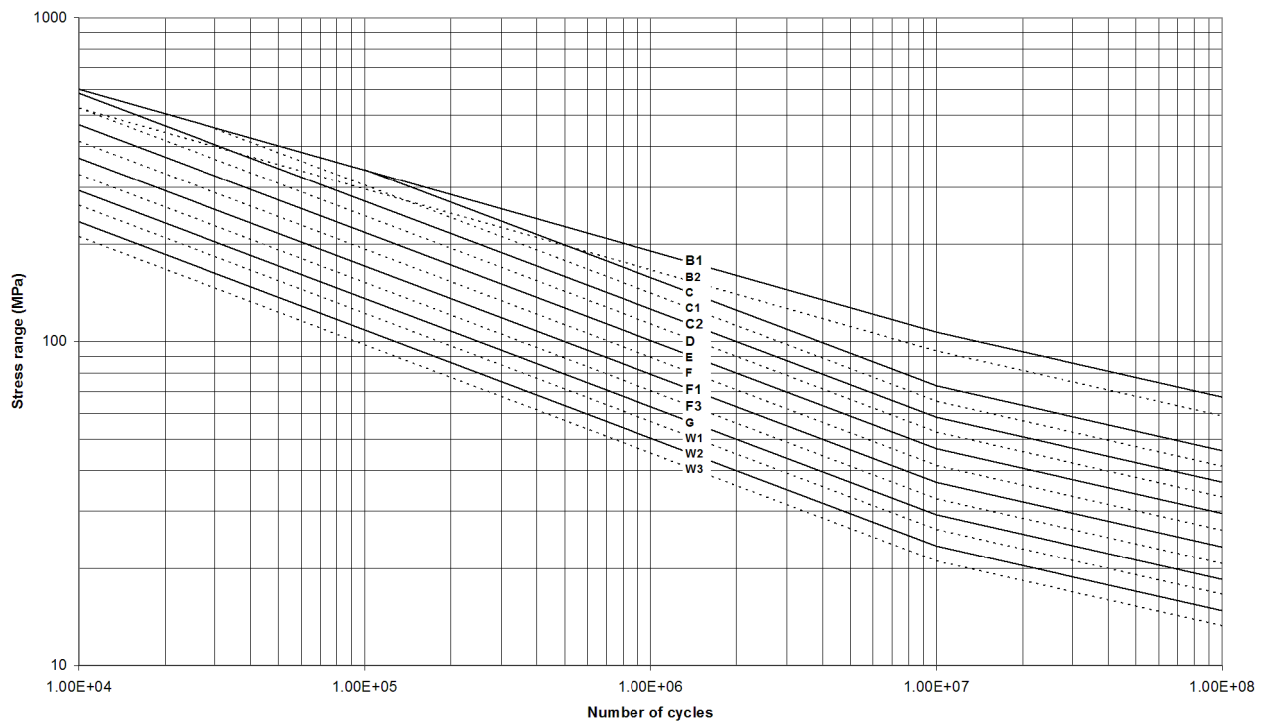


Figure 2-8 S-N curves in air

2.4.5 S-N curves in seawater with cathodic protection

S-N curves for seawater environment with cathodic protection are given in [Table 2-2](#) and [Figure 2-9](#). The T curve is shown in [Table 2-3](#) and [Figure 2-10](#). For shape of S-N curves see also comment in [\[2.4.4\]](#).

Table 2-2 S-N curves in seawater with cathodic protection

S-N curve	$N \leq 10^6$ cycles		$N > 10^6$ cycles $\log \bar{a}_2$ $m_2 = 5.0$	Fatigue limit at 10^7 cycles [MPa] *)	Thickness exponent k	Structural stress concentration embedded in the detail (S-N class), see also equation (2.3.2)
	m_1	$\log \bar{a}_1$				
B1	4.0	14.917	17.146	106.97	0	
B2	4.0	14.685	16.856	93.59	0	
C	3.0	12.192	16.320	73.10	0.05	
C1	3.0	12.049	16.081	65.50	0.10	
C2	3.0	11.901	15.835	58.48	0.15	
D	3.0	11.764	15.606	52.63	0.20	1.00
E	3.0	11.610	15.350	46.78	0.20	1.13

S-N curve	$N \leq 10^6$ cycles		$N > 10^6$ cycles $\log \bar{a}_2$ $m_2 = 5.0$	Fatigue limit at 10^7 cycles [MPa] *)	Thickness exponent k	Structural stress concentration embedded in the detail (S-N class), see also equation (2.3.2)
	m_1	$\log \bar{a}_1$				
F	3.0	11.455	15.091	41.52	0.25	1.27
F1	3.0	11.299	14.832	36.84	0.25	1.43
F3	3.0	11.146	14.576	32.75	0.25	1.61
G	3.0	10.998	14.330	29.24	0.25	1.80
W1	3.0	10.861	14.101	26.32	0.25	2.00
W2	3.0	10.707	13.845	23.39	0.25	2.25
W3	3.0	10.570	13.617	21.05	0.25	2.50

*) See also [2.12].

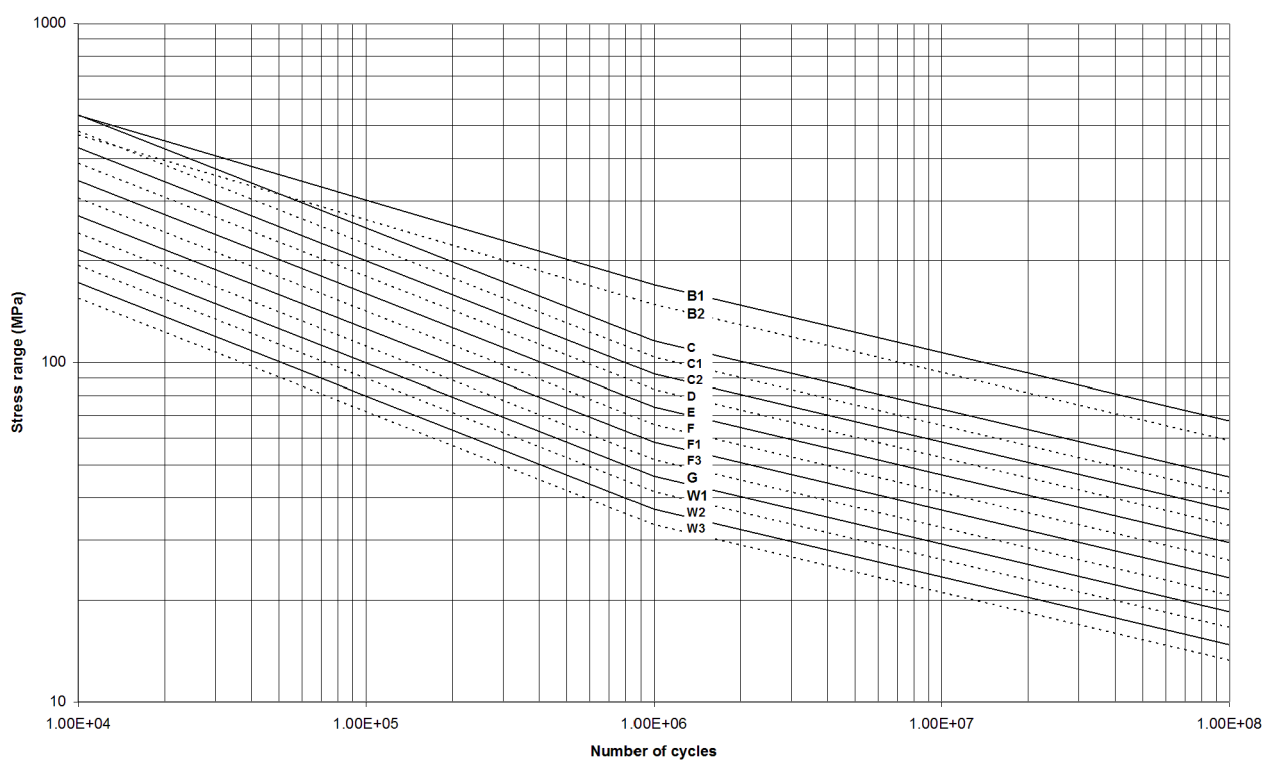


Figure 2-9 S-N curves in seawater with cathodic protection

2.4.6 S-N curves for tubular joints

S-N curves for tubular joints in air environment, seawater with cathodic protection and free corrosion are given in [Table 2-3](#) and [Figure 2-10](#). These S-N curves are denoted T-curves and apply to the outside hot spots at tubular joints. The T-curves are used for the outside hot spots for tubular joints that are welded from both outside and inside as well as for tubular joints welded from the outside only. Only the outside of a tubular joint needs to be assessed with respect to fatigue when it is welded from both outside and inside. The reference thickness is 16 mm for these S-N curves. For tubular joints welded from outside only see [\[3.3.3\]](#). The reference thickness for S-N curves used for the weld root in tubular joints welded from the outside only is listed in [\[2.4.3\]](#).

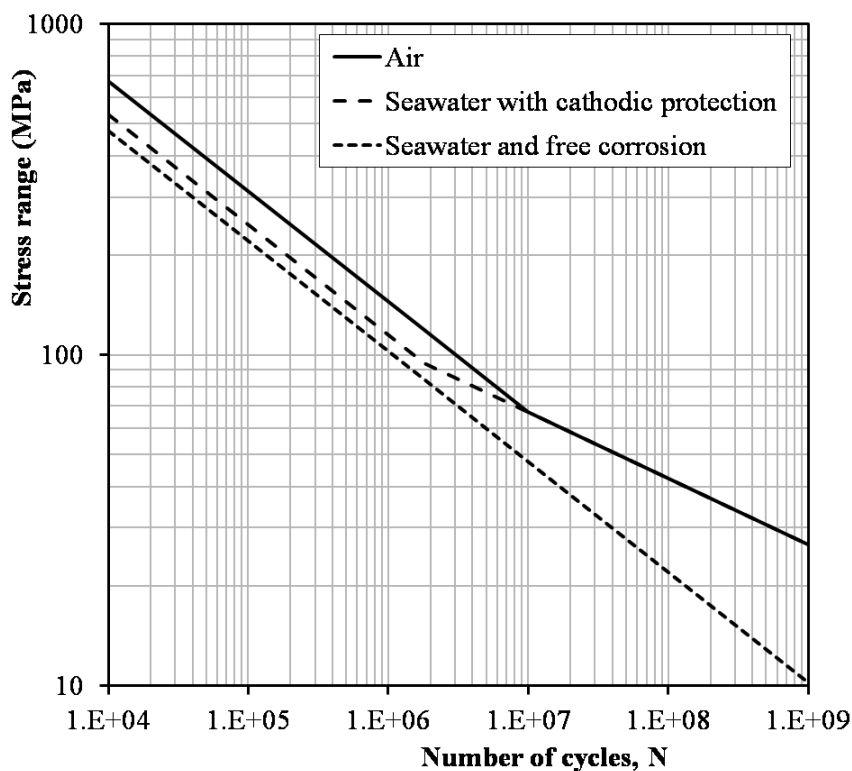


Figure 2-10 S-N curves for tubular joints in air and in seawater with cathodic protection

Table 2-3 S-N curves for tubular joints

Environment	m_1	$\log \bar{a}_1$	m_2	$\log \bar{a}_2$	Fatigue limit at 10^7 cycles [MPa]*)	Thickness exponent k
Air		$N \leq 10^7$ cycles		$N > 10^7$ cycles		
	3.0	12.48	5.0	16.13	67.09	0.25
Seawater with cathodic protection		$N \leq 1.8 \cdot 10^6$ cycles		$N > 1.8 \cdot 10^6$ cycles		
	3.0	12.18	5.0	16.13	67.09	0.25
Seawater free corrosion	3.0	12.03	3.0	12.03	0	0.25

*) See also [2.12].

2.4.7 S-N curves for cast nodes

It is recommended to use the C-curve for cast nodes. Tests may give a more optimistic curve. However, the C-curve is recommended in order to allow for weld repairs after possible casting defects and possible fatigue cracks after some service life. The probability of a repair during service life depends on accumulated fatigue damage. See [9.1] and Figure 9-3 which indicates fatigue failure probability as function of the design fatigue factor that is used.

For cast nodes a reference thickness $t_{ref} = 38$ mm may be used provided that any possible repair welds have been ground to a smooth surface.

For cast nodes with a stress gradient over the thickness a reduced effective thickness may be used for assessment of thickness effect. The effective thickness to be used in equation (2.4.3) can be calculated as:

$$t_e = t_{actual} \left(\frac{S_i}{S_0} \right)^{1/k} \quad (2.4.5)$$

where:

- S_0 = hot spot stress range on surface
- S_i = stress range 38 mm below the surface, under the hot spot
- t_{actual} = thickness of cast piece at considered hot spot measured normal to the surface
- t_e = effective thickness. t_e shall not be less than 38 mm
- k = thickness exponent = 0.15.

2.4.8 S-N curves for forged nodes

The B1 curve may be used for forged nodes designed with a design fatigue factor equal to 10. For designs with DFF less than 10 it is recommended to use the C-curve to allow for weld repair if fatigue cracks should occur during service life.

2.4.9 S-N curves for free corrosion in plated structures

S-N curves for free corrosion in plated structures, i.e. without corrosion protection, are given in Table 2-4.

See also [F.6] for consideration of corrosion protection of connections in the splash zone and inside tanks in FPSOs.

Table 2-4 S-N curves in seawater for free corrosion

<i>S-N curve</i>	$\log \bar{a}$ <i>For all cycles m = 3.0</i>	<i>Thickness exponent k</i>
B1	12.436	0
B2	12.262	0
C	12.115	0.15
C1	11.972	0.15
C2	11.824	0.15
D	11.687	0.20
E	11.533	0.20
F	11.378	0.25
F1	11.222	0.25
F3	11.068	0.25
G	10.921	0.25
W1	10.784	0.25
W2	10.630	0.25
W3	10.493	0.25

2.4.10 S-N curves for base material of high strength steel

The fatigue capacity of the base material is depending on the surface finish of the final component and its yield and tensile strength. S-N curves for components of high strength steel with yield strength above 500 MPa subjected to high mean tensile stress such as in tether connectors are presented in [D.1].

S-N curves for high strength steel for subsea applications are presented in [D.2].

2.4.11 S-N curves for stainless steel

For duplex and for super duplex steel one may use the same classification as for C-Mn steels.

Also for austenitic steel one may use the same classification as for C-Mn steels.

2.4.12 S-N curves for small diameter umbilicals

For fatigue design of small diameter pipe umbilicals (outer diameter in the range 10 -100 mm) made of super duplex steel with a yield strength larger than 500 MPa with thicknesses in the range 1.0 to 10 mm the following S-N curve can be used for fatigue assessment:

For $N \leq 10^7$:

$$\log N = 15.301 - 4.0 \log \left\{ \Delta\sigma \left(\frac{t}{t_{ref}} \right)^{0.25} \right\} \quad (2.4.6)$$

and for $N > 10^7$

$$\log N = 17.376 - 5.0 \log \left\{ \Delta\sigma \left(\frac{t}{t_{ref}} \right)^{0.25} \right\}$$

where:

t = actual thickness of the umbilical

t_{ref} = 1.0 mm.

A normal good fabrication of the umbilicals is assumed as basis for this design S-N curve. The welds on the inside and outside of the pipes should show a smooth transition from the weld to the base material without notches and/or undercuts. A detailed NDE inspection for each connection is assumed.

The NDE methods are visual inspection and X-ray. For single pass welds, no indications are acceptable. For multipass welds the acceptance criteria shall be according to ASME B31.3, chapter IX high pressure service girth groove. Dye penetrant shall be used as a surface test in addition to visual inspection when relevant indications, as defined by ASME VIII div. 1, app.4. are found by X-ray.

The S-N curve is based on fatigue testing of specimens subjected to a mean stress up to 450 MPa.

The given S-N curve is established from test specimens that are not prestrained from reeling. However, based on a few test data with prestrained specimens it is considered acceptable to use the S-N curve also for umbilicals that have been reeled. Thus this S-N curve applies also when number of cycles under reeling is less than 10 and the total strain range during reeling is less than 2%.

The following design S-N curve can be used for the base material of umbilical tubes:

For $N \leq 10^7$:

$$\log N = 15.301 - 4.0 \log \Delta\sigma \quad (2.4.7)$$

and for $N > 10^7$

$$\log N = 17.376 - 5.0 \log \Delta\sigma$$

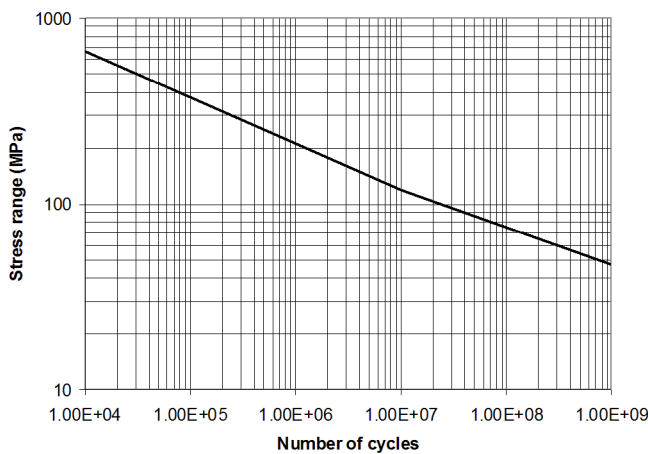


Figure 2-11 S-N curve for small diameter pipe for umbilicals

2.4.13 S-N data for piles

The transition of the weld to base material on the outside of tubular girth welds can normally be classified to S-N curve E. If welding is performed in a flat position, it can be classified as D. If welding is performed from outside only, it should be classified as F3 for the weld root.

S-N curve E applies to weld beads.

S-N data corresponding to air environment condition can be used for the pile driving phase.

S-N data corresponding to environment of seawater with cathodic protection can be used for the operational life when the structure above the mud line is cathodically protected.

The effect of toe grinding is described in [7.3] and [F.15]. When flush grinding of the weld is performed, the improvement is obtained through use of a better S-N curve as presented in Table A-5.

2.4.14 Qualification of new S-N curves based on fatigue test data

For qualification of new S-N data to be used in a project it is important that the test specimens are representative for the actual fabrication and construction. This includes possibility for relevant production defects as well as fabrication tolerances. The sensitivity to defects may also be assessed by fracture mechanics.

For new types of connections it is recommended to perform testing of at least 15 specimens in order to establish a new S-N curve. At least three different stress ranges should be selected in the relevant S-N region such that a representative slope of the S-N curve can be determined, see [F.7], for a broader assessment of how to derive S-N curves from few fatigue test data.

See also /55/, /76/, /86/, /89/ for statistical analysis of the fatigue test data. Normally fatigue test data are derived for number of cycles less than 10^7 . It should be noted that for offshore structures significant fatigue damage occurs for $N \geq 10^7$ cycles. Thus how to extrapolate the fatigue test data into this high cycle region is important in order to achieve a reliable assessment procedure. In addition to statistical analysis one should use engineering judgement based on experience for derivation of the S-N data in this region. It is well known that good details where fatigue initiation contribute significantly to the fatigue life show a more horizontal S-N curve than for less good details where the fatigue life consists mainly of crack growth. See also S-N curves with different slopes shown in this chapter.

The residual stresses at weld toes of small scale test specimens are normally small as compared with that in actual full size structures due to different restraints during fabrication. This is an item that is of importance when planning fatigue testing and for assessment of design S-N curves, see [F.7]

It should also be remembered that for $N \geq 10^7$ cycles there is additional uncertainty due to variable amplitude loading. This is an issue that should be kept in mind if less conservative S-N curves than given in this RP are aimed for by qualifying a new S-N curve.

Also the probability of detecting defects during a production should be kept in mind in this respect. The defects that normally can be detected by an acceptable probability are normally larger than that inherent in the test specimens that are produced to establish test data for a new S-N curve.

Fatigue testing may be needed when stainless steel is used in corrosive environment like scour service, see DNVGL-RP-F108 App.C.

2.5 Mean stress influence on fatigue strength

2.5.1 Base material without significant residual stresses

For fatigue analysis of regions in the base material not significantly affected by residual stresses due to welding or cold forming, the stress range may be reduced if part of the stress cycle is in compression.

This reduction may e.g. be carried out for cut-outs in the base material. The calculated stress range obtained may be multiplied by the reduction factor f_m as obtained from Figure 2-12 before entering the S-N curve.

In this figure σ_m = mean stress. If the residual stress is known, this stress can be added to the tensile part of the stress and subtracted for the compressive part before the reduction factor in equation (2.5.1) is calculated.

The reduction factor can be derived from the following equation:

$$f_m = \frac{\sigma_t + 0.6|\sigma_c|}{\sigma_t + |\sigma_c|} \quad (2.5.1)$$

where:

σ_t = maximum tension stress where tension is defined as positive

σ_c = maximum compression stress where compression is defined as negative.

This implies in particular that f_m is 1.0 when the material is in tension during the entire stress cycle, 0.8 when it is subject to zero-mean stress, and 0.0 when it is in compression during the entire stress cycle provided low residual stresses can be documented. If the stress exceeds the yield stress locally also during compressive stress cycles, residual stresses may be introduced in the base material and this reduction factor should not be used.

It should be noted that cold forming of tubular sections implies yielding in the circumferential and the longitudinal directions of the sections being formed meaning that significant residual stresses may be left in both directions in the base material. The residual stresses are compressive on the inside and tensile on the outside of the formed tubular section. Therefore stress reduction should not be accounted for in cold formed tubulars with residual tensile stresses.

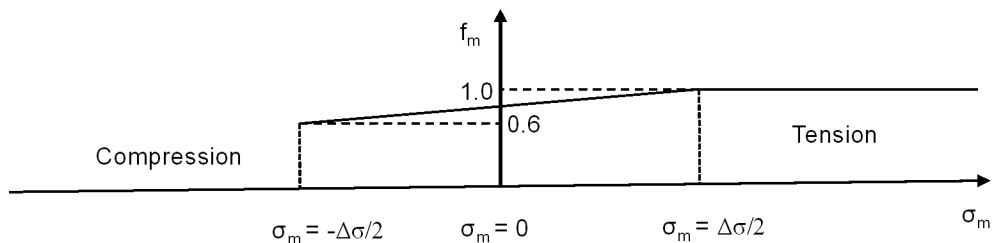


Figure 2-12 Stress range reduction factor to be used with the S-N curve for base material

2.5.2 Welded connections without significant residual stresses

For fatigue analysis of regions in welded structural details, which have been subject to post weld heat treatment or where correspondingly low residual stresses can be documented, the stress ranges may be reduced prior to the fatigue analysis depending on whether part of the stress range is tensile stress or compressive stress.

The calculated stress range at the hot spot may be multiplied by the reduction factor f_m as obtained from Figure 2-13 before entering the S-N curve. In this figure σ_m = mean stress.

The reduction factor can be derived from the following equation:

$$f_m = \frac{\sigma_t + 0.8|\sigma_c|}{\sigma_t + |\sigma_c|} \quad (2.5.2)$$

where:

σ_t = maximum tension stress where tension is defined as positive

σ_c = maximum compression stress where compression is defined as negative.

This implies in particular that f_m is 1.0 when the material is in tension during the entire stress cycle, 0.9 when it is subject to zero-mean stress, and 0.8 when it is in compression during the entire stress cycle provided low residual stresses can be documented. If the stress exceeds the yield stress locally also during compressive stress cycles, residual stresses may be introduced in the connection and this reduction factor should not be used.

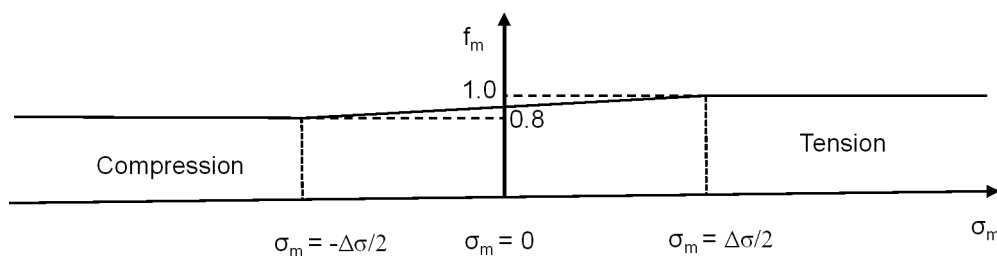


Figure 2-13 Stress range reduction factor at post weld heat treated connections or welds with corresponding low residual stresses

2.6 Effect of fabrication tolerances

Normally larger fabrication tolerances are allowed in real structures than that accounted for in the test specimens used to derive S-N data, see [DNVGL-OS-C401 Fabrication and testing of offshore structures](#). Therefore, additional stresses resulting from normal fabrication tolerances should be included in the fatigue design. Special attention should be given to the fabrication tolerances for simple butt welds in plates and tubulars as these give the most significant increase in additional stress. Stress concentration factors for butt welds in plated structures are given in [\[3.1.2\]](#) and at tubular circumferential welds in [\[3.3.7\]](#).

2.7 Requirements to non-destructive examination and acceptance criteria

See [DNVGL-OS-C401 Fabrication and testing of offshore structures](#) for requirements to non-destructive examination (NDE). See also [DNVGL-OS-C401](#) with respect to acceptance criteria. Some acceptance criteria related to the different classification of structural details are also presented in [App.A](#), see also [\[F.5\]](#).

For umbilical pipes requirements to NDE are presented in [\[2.4.12\]](#). For partial penetration welds requirements to NDE are presented in [\[2.8\]](#).

In general the requirements to NDE and acceptance criteria are being increased when going from the lower to the high level S-N curves. This should also be considered when designing connections showing a high fatigue utilisation, see also [\[F.5\]](#).

2.8 Design chart for fillet and partial penetration welds

Design should be performed such that fatigue cracking from the weld root is less likely than from the toe region. The reason for this is that a fatigue crack at the toe can be found by in-service inspection while a fatigue crack starting at the root cannot be discovered before the crack has grown through the weld. Thus the design of the weld geometry should be performed such that the fatigue life for cracks starting at the root is longer than the fatigue life of the toe. [Figure 2-15](#) can be used for evaluation of required penetration. The notation used is explained by [Figure 2-14](#).

It should be added that it is difficult to detect internal defects by NDE in fillet/partial penetration welds. Such connections should therefore not be used in structural connections of significant importance for the structural integrity.

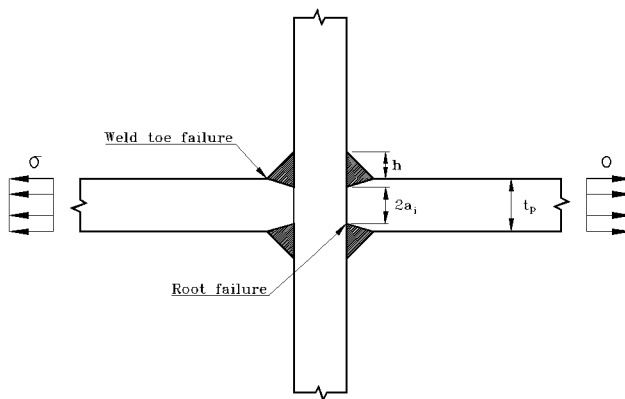


Figure 2-14 Welded connection with partial penetration weld

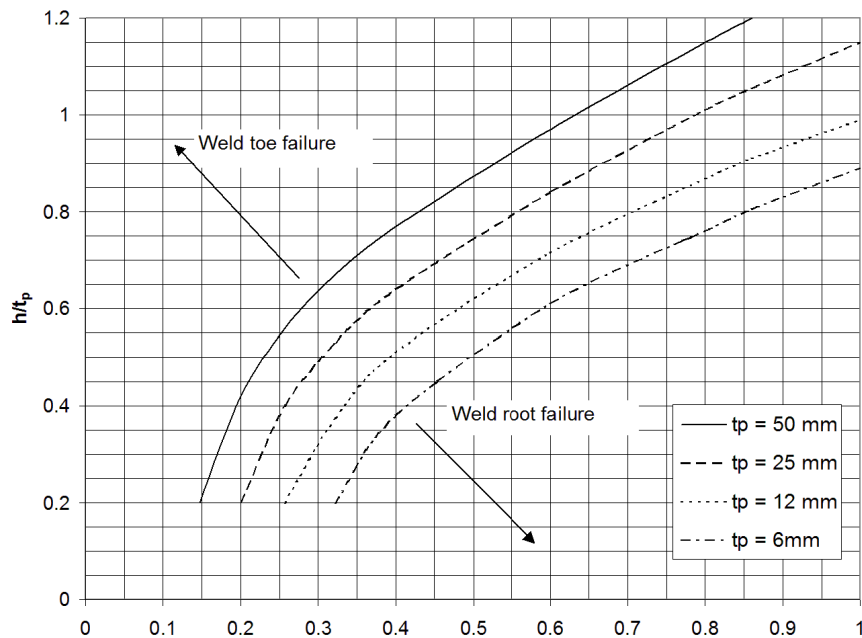


Figure 2-15 Weld geometry with probability of root failure equal to toe failure

2.9 Bolts

2.9.1 General

A bolted joint connection subjected to dynamic loading should be designed with pretensioned bolts. The pretension should be high enough to avoid slipping after relevant loss of pretension during service life.

It is recommended to develop a technical specification for procurement of heavy-duty bolts for marine structures. Some guidance can be found in /103/. General thread tolerances for bolts and nuts are defined in ISO 965-1 /117/.

2.9.2 Bolts subjected to tension loading

Connections where the pretensioned bolts are subjected to dynamic axial forces should be designed with respect to fatigue taking into account the stress range in the bolts resulting from tension and compression range. The stress range in the bolts may be assessed based on e.g. *Maskindeler 2* /23/, or *Systematic Calculation of High Duty Bolted Joints* /26/. The cyclic stress in the bolts may be a combination of membrane stress (constant over the cross-section) and bending stress (linear over the cross-section). The bolt stress should include the sum of the membrane stress and the bending stress.

For S-N classification see [Table A-2](#). The stress in the bolt should be calculated based on the bolt stress area (which is different from the root area, see equations for the bolt stress area in for example /103/).

2.9.3 Bolts subjected to shear loading

For bolts subject to shear loading the following methodology may be used for fatigue assessment. The threads of the bolts should not be in the shear plane. The methodology may be used for fitted bolts or for

normal bolts without load reversal. The shear stress to be calculated based on the shank area of the bolt. Then number of cycles to failure can be derived from:

$$\log N = 16.301 - 5.0 \log \Delta\sigma \quad (2.9.1)$$

where:

$\Delta\sigma$ = shear stress based on shaft area of bolt.

2.9.4 Friction welded bolts

Fatigue tests of friction welded bolts installed below or above water give S-N curve C1 as shown in [Table A-2](#) and [/114/](#).

2.10 Pipelines

2.10.1 Stresses at girth welds in pipes and S-N data

Welds in pipelines are normally made with a symmetric weld groove with welding from the outside only. The tolerances are rather strict compared with other structural elements with eccentricity less than 0.05 t or maximum 3 mm (t = wall thickness). The fabrication of pipelines also implies a systematic and standardised NDT of the weld root area where defects are most critical. Provided that the same acceptance criteria are used for pipelines with larger wall thickness as for that used as reference thickness (25 mm), a thickness exponent $k = 0$ may be used for the hot spot at the weld root and $k = 0.15$ for the weld toe without grinding of the weld. Provided that these requirements are fulfilled, the detail at the root side may be classified according to the S-N curves in [Table 2-5](#) with SCF from equation (2.10.8).

See [Table 2-5](#) for ground welds and welds made from both sides.

The following stress concentration for the weld toe due to maximum allowable eccentricity should be included:

$$SCF_{cap} = 1 + \frac{6\delta_m e^{-\alpha}}{t_c \left(1 + \left(\frac{T}{t_c} \right)^\beta \right)} \quad (2.10.1)$$

where:

$$\alpha = \frac{1.82 L_{cap}}{\sqrt{D t_c} \left(1 + \left(\frac{T}{t_c} \right)^\beta \right)} \quad (2.10.2)$$

$$\beta = 1.5 - \frac{1.0}{\log \left(\frac{D}{t_c} \right)} + \frac{3}{\left(\log \left(\frac{D}{t_c} \right) \right)^2} \quad (2.10.3)$$

$$T = t_c + [hi/lo_{cap} - hi/lo_{root}] \quad (2.10.4)$$

T and t_c = wall thickness of the pipes on either side of the girth weld, $T > t_c$

- δ_m = misalignment (wall thickness differences, out-of-roundness, centre eccentricities, etc.)
 D = outside diameter of pipe.

It is acceptable to calculate the SCF based on the following expression, see [Figure 2-16](#).

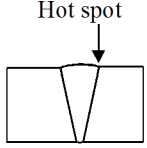
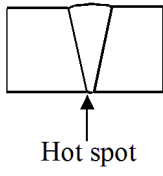
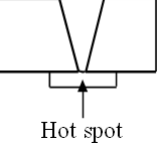
$$\delta_m = \frac{hi/lo_{cap} + hi/lo_{root}}{2} \quad (2.10.5)$$

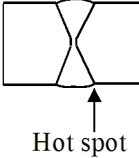
The hi/lo should be in accordance with [DNVGL-ST-F101 Table D-4](#). However, operators or weld contractors often specify minimum hi/lo values that are smaller than these hi/lo values. It is acceptable to specify smaller hi/lo values than the maximum values stated in [DNVGL-ST-F101](#) if such values are substantiated.

The nominal stress on the outside of the pipe should be used for fatigue assessment of the outside and the nominal stress on the inside of the pipe should be used for fatigue assessment of the inside. The membrane stress in the considered section should be used for calculation of local bending stress over the thickness together with stress concentration factor from equation (2.10.1).

See also [\[F.14\]](#) where a more detailed guidance on stress range calculation in pipes subjected to combined axial load and bending is included.

Table 2-5 Classification of welds in pipelines

Description		Tolerance requirement (mean hi/lo-value)	S-N curve	Thickness exponent k	Stress concentration factor
Welding	Geometry and hot spot				
Single side			D	0.15	Eq. (2.10.1)
Single side		$\delta_m \leq 1.0 \text{ mm}$	E	0.00	Eq.(2.10.8)
		$1.0 \text{ mm} < \delta_m \leq 2.0 \text{ mm}$	F	0.00	
		$2.0 \text{ mm} < \delta_m \leq 3.0 \text{ mm}$	F1	0.00	
Single side on backing		$\delta_m \leq \min(0.1t, 2 \text{ mm})$	F	0.00	Eq. (2.10.8)
		$\delta_m > \min(0.1t, 2 \text{ mm})$	F1	0.00	

Description		Tolerance requirement (mean hi/lo-value)	S-N curve	Thickness exponent k	Stress concentration factor
Welding	Geometry and hot spot				
Double side			D	0.15	Eq. (2.10.1)
Ground weld outside and inside			C	0.00	Eq. (2.10.1) for outside and Eq. (2.10.8) for inside

The width of the girth welds in the root in pipelines and risers may be larger than that shown in [Figure 3-8](#) and may also be narrower on the outside to reduce the welding volume and increase fabrication efficiency. A more typical weld section through a girth weld is shown in [Figure 2-16](#). For this geometry the stress due to local bending is less for the root than for the weld toe (weld cap). The local bending stress at the weld toe due to axial misalignment, δ_m , and membrane stress, σ_m , can be expressed as:

$$\sigma_{bt} = (SCF_{cap} - 1)\sigma_m \quad (2.10.6)$$

The width of the weld at the root in [Figure 2-16](#) is L_{Root} . Then the bending stress in the pipe wall at the transition from the weld to the base material at the root can be obtained from the linearized moment in [Figure 2-16](#) as:

$$\sigma_{br} = \sigma_{bt} \frac{L_{root}}{L_{cap}} \quad (2.10.7)$$

Thus, for the weld root the effect of axial misalignment can be included by the following SCF for the weld root:

$$SCF_{root} = 1 + (SCF_{cap} - 1) \frac{L_{root}}{L_{cap}} \quad (2.10.8)$$

where:

SCF_{cap} is defined by equation (2.10.1).

If knowledge about the weld shape is missing, one may put L_{root} equal L_{cap} in equation (2.10.8) such that it reduces to that of equation (2.10.1). The background for this equation is presented in /103/.

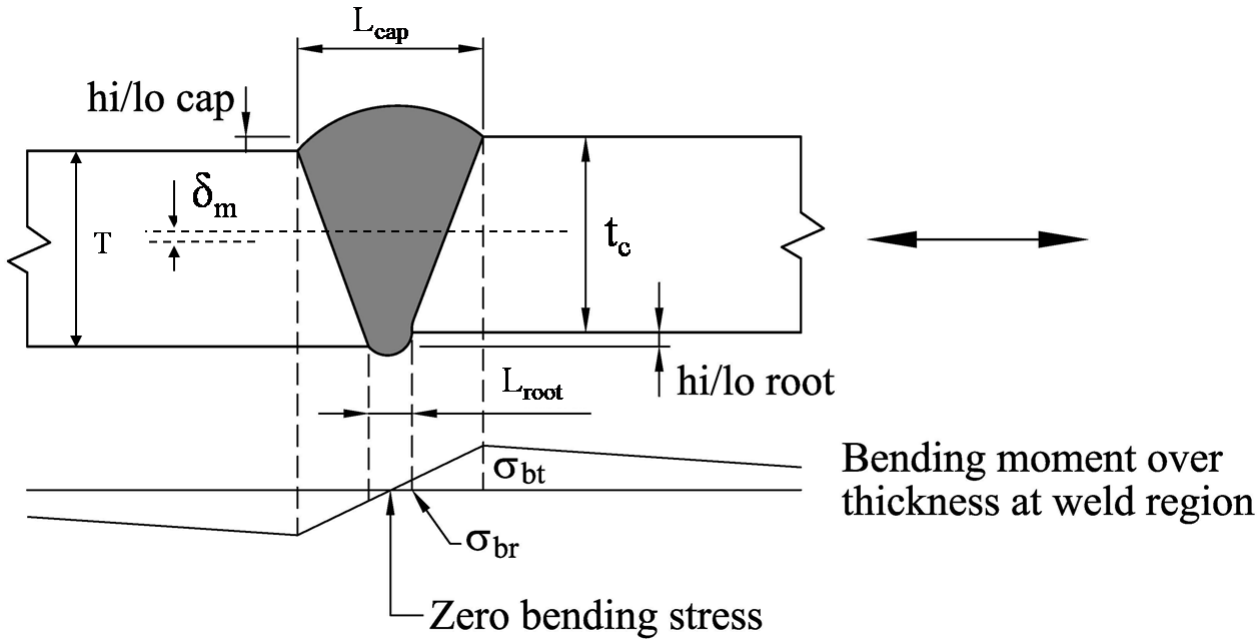


Figure 2-16 Stress distribution due to axial misalignment at single-sided welds in tubular members

2.10.2 Fatigue analysis of pipes and cylindrical tanks subjected to cyclic internal pressure

Pipes and cylindrical tanks may be subjected to fatigue from cyclic loading when subjected to significant variation in internal pressure. See [F.8] for stress concentration factors for thickness transitions at girth welds and at ring stiffeners/supports. It also gives stress concentration factors for the longitudinal welds (or seam weld) due to out-of-roundness of pipes and cylindrical tanks. For very long welds the fatigue capacity is considered to be reduced due to a system effect. The fatigue capacity for long welds can be accounted for as described under system effects in [F.5].

2.11 Combined eccentricity for seamless riser pipes

For seamless pipes the eccentricity is governed by the thickness and out of roundness tolerances. A resulting tolerance at girth welds for use in equation (2.10.1) for calculation of stress concentration factor may also be obtained as:

$$\delta_m = \sqrt{\delta_{Thickness}^2 + \delta_{Out\ of\ roundness}^2} \quad (2.11.1)$$

where:

$$\delta_{Thickness} = (t_{max} - t_{min})/2$$

$$\delta_{Out\ of\ roundness} = D_{max} - D_{min} \text{ if the pipes are supported such that flush outside at one point is achieved (no pipe centralising)}$$

- $\delta_{Out\ of\ roundness}$ = $(D_{max} - D_{min})/2$ if the pipes are centralised during construction
- $\delta_{Out\ of\ roundness}$ = $(D_{max} - D_{min})/4$ if the pipes are centralised during construction and rotated until a good fit around the circumference is achieved (if one part is made perfect circular by machining, this equation is not applicable).if one part is made perfect circular by machining, this equation is not applicable).

See [DNVGL-RP-F108](#) /109/, for measurements of tolerances..

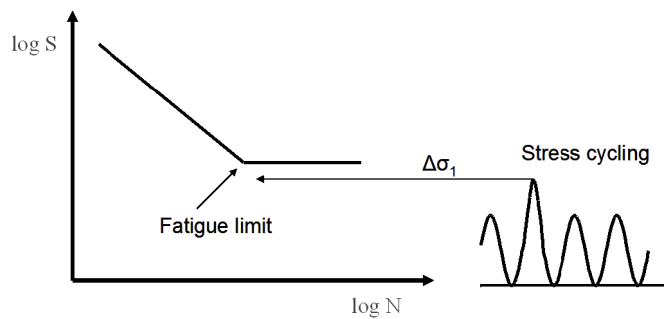
2.12 Guidance to when a detailed fatigue analysis can be omitted

A detailed fatigue analysis can be omitted if the largest local stress range for actual details defined in equation (2.3.1) is less than the fatigue limit at 10^7 cycles in [Table 2-1](#) for air and [Table 2-2](#) for seawater with cathodic protection. For design fatigue factors larger than one the allowable fatigue limit should also here be reduced by a factor $(DFF)^{0.33}$. See also /103/ for a more detailed derivation. For definition of DFF see [DNVGL-OS-C101](#) /28/.

Requirements to detailed fatigue analysis may also be assessed based on the fatigue assessment charts in [Figure 5-1](#) and [Figure 5-2](#).

The use of the fatigue limit is illustrated in [Figure 2-17](#) a) for DFF = 1.0 and in [Figure 2-17](#) b) for DFF larger than 1.0. A detailed fatigue assessment can be omitted if the largest stress cycle is below the fatigue limit. However, in the example in [Figure 2-18](#) there is one stress cycle $\Delta\sigma_1$ above the fatigue limit. This means that a further fatigue assessment is required and the fatigue damage from the stress cycles $\Delta\sigma_2$ has also to be included in the fatigue assessment.

a) DFF = 1.0



b) DFF larger than 1.0.

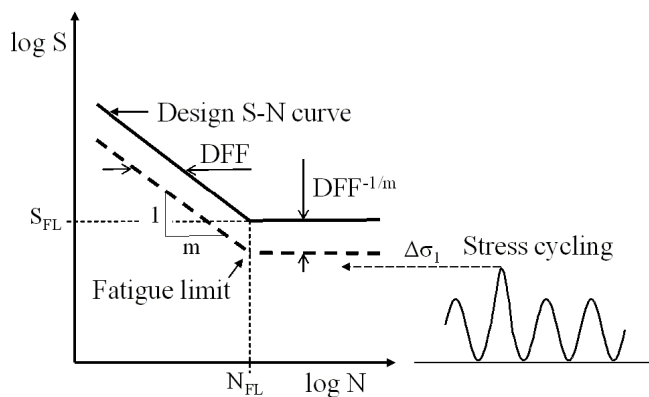


Figure 2-17 Stress cycling where further fatigue assessment can be omitted

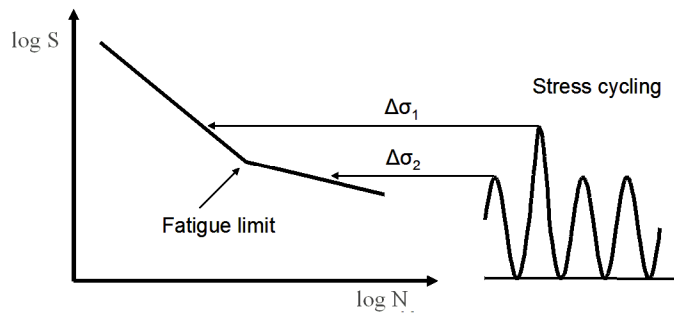


Figure 2-18 Stress cycling where a detailed fatigue assessment is required

SECTION 3 STRESS CONCENTRATION FACTORS

3.1 Stress concentration factors

3.1.1 General

A stress concentration factor is defined as the ratio of hot spot stress range over nominal stress range. Fabrication tolerances increase the stress range at butt welds and cruciform joints. For as welded butt welds and cruciform joints there are already included some tolerances in the S-N curves that are used. However, the value of fabrication tolerance to be included in design calculation depends also on what is the expected as-built tolerance as compared with that required in the fabrication standard. This means that for some details a misalignment value δ_0 may be subtracted from the fabrication tolerance when the stress concentration factor to be used in design is calculated. See [Table 3-1](#) for recommended δ_0 for butt welds in different structural details.

Table 3-1 Recommended values of δ_0 for butt welds in different types of structures

Structural detail	As welded	Ground flush
Plated structures	0.05t	0
Tubular girth welds in structures	0.05t	0
Girth welds in tethers	0	0
Girth welds in pipelines and risers	0	0

3.1.2 Stress concentration factors for butt welds in plated structures

The eccentricity between welded plates with a similar thickness may be accounted for in the calculation of stress concentration factor. The following formula applies for a butt weld in an unstiffened plate:

$$SCF = 1 + \frac{3(\delta_m - \delta_0)}{t} \quad (3.1.1)$$

where δ_m is eccentricity (misalignment) and t is plate thickness, see [Figure 3-8](#).

$\delta_0 = 0.05t$ is misalignment inherent in the S-N data for butt welds and analysis procedure for plated structures with an expected fabrication tolerance that is lower than that allowed in fabrication specification and as used in design, see also [Table 3-1](#). See [DNVGL-OS-C401](#) for fabrication tolerances.

The stress concentration for the weld between plates with different thickness in a plate field on the side of the thickness transition may be derived from the following formula:

$$SCF = 1 + \frac{6(\delta_m + \delta_t - \delta_0)}{t \left[1 + \frac{T^{1.5}}{t^{1.5}} \right]} \quad (3.1.2)$$

where:

δ_m = maximum fabrication misalignment

$\delta_t = \frac{1}{2} (T - t)$ eccentricity due to change in thickness

Note: this applies also at transitions sloped as 1:4.

$\delta_0 = 0.05t$ is misalignment inherent in the S-N data for butt welds and analysis procedure for plated structures with an expected fabrication tolerance that is lower than that allowed in fabrication specification and as used in design, see also [Table 3-1](#)

See [DNVGL-OS-C401](#) for fabrication tolerances

T = thickness of thicker plate

t = thickness of thinner plate.

See also [Figure 3-8](#).

The stresses at the weld on the opposite side of the thickness transition in the plate can be calculated using the following formula for stress concentration factor:

$$SCF = 1 - \frac{6(\delta_t + \delta_0 - \delta_m)}{t \left[1 + \frac{T^{1.5}}{t^{1.5}} \right]} \quad (3.1.3)$$

This equation applies to the weld on the opposite side of the thickness transition with $\delta_0 = 0.05t$ when the butt weld is made from both sides. For the root side of a single sided weld $\delta_0 = 0.0$ should be used together with a relevant S-N curve. The value of δ_0 is based on actual tolerances accounted for in S-N curves and experience from fabrication of different structural details. Thus, it is also based on the relation between specified tolerances in fabrication standards versus actual fabricated values.

3.1.3 Stress concentration factors for cruciform joints in plated structures

The stress concentration factor for cruciform joint at plate thickness t_i may be derived from the following formula:

$$SCF = 1 + \frac{6t_i^2(\delta - \delta_0)}{l_i \left(\frac{t_1^3}{l_1} + \frac{t_2^3}{l_2} + \frac{t_3^3}{l_3} + \frac{t_4^3}{l_4} \right)} \quad (3.1.4)$$

where:

$\delta = (\delta_m + \delta_t)$ is the total eccentricity

$\delta_0 = 0.15 t_i$ is misalignment embedded in S-N data for cruciform joints and analysis procedure when including effect of fabrication tolerances

See [DNVGL-OS-C401](#) for fabrication tolerances.

t_i = thickness of the considered plate ($i = 1, 2$)

l_i = length of considered plate ($i = 1, 2$).

The other symbols are defined in [Figure 3-1](#).

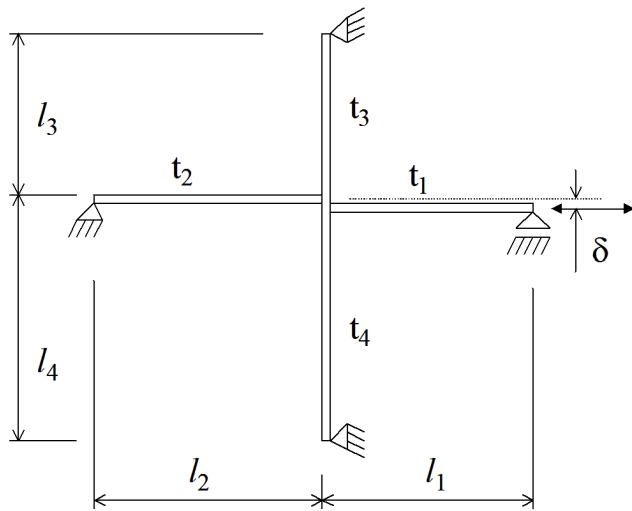


Figure 3-1 Cruciform joint

3.1.4 Stress concentration factors for rounded rectangular holes

Stress concentration factors for rounded rectangular holes are given in Figure 3-2 based on analytical expressions presented in the literature /106/.

Where there is one stress raiser close to another detail being evaluated with respect to fatigue, the interaction of stress between these should be considered. An example of this is a welded connection in a vicinity of a hole. Then the increase in stress at the considered detail due to the hole can be evaluated from Figure 3-3.

Some guidelines on effect of interaction of different holes can be found in Peterson's *Stress Concentration Factors*, /15/.

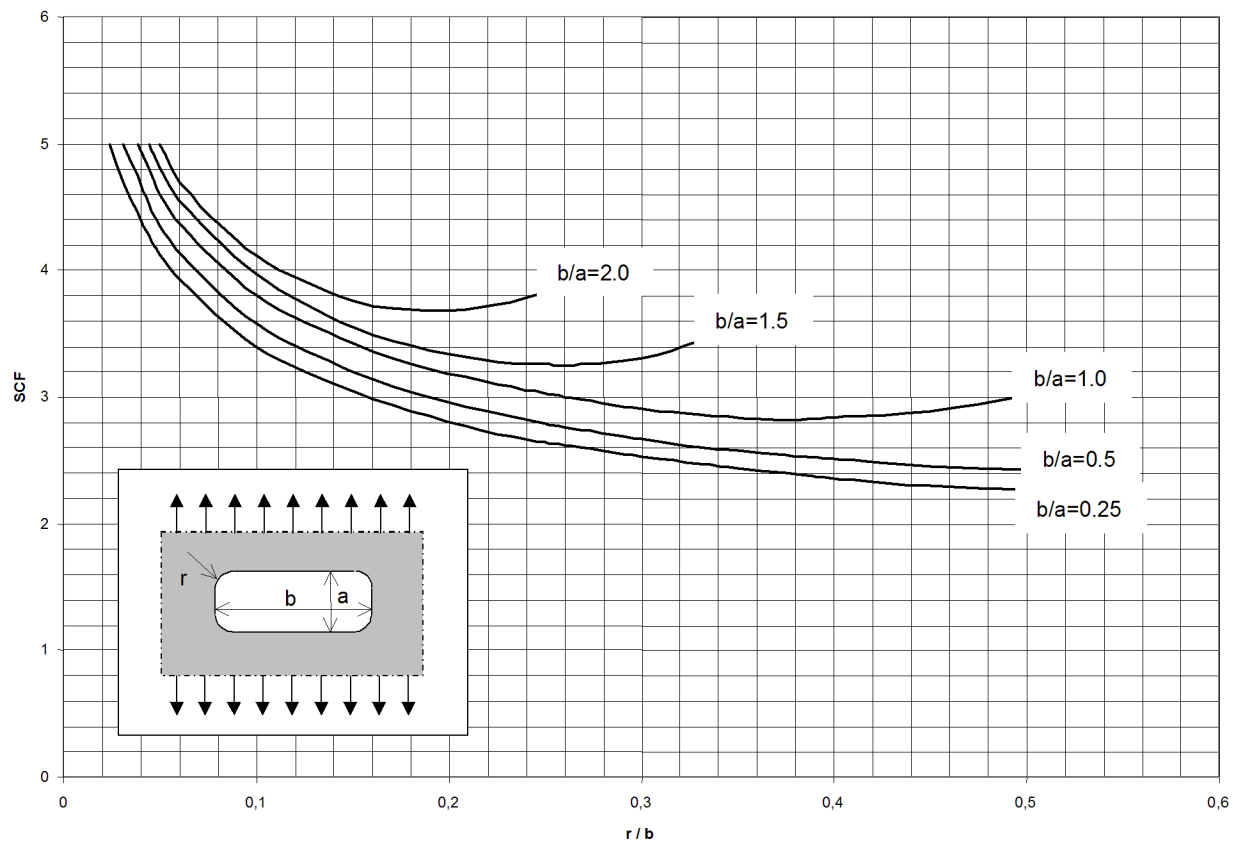


Figure 3-2 Stress concentration factors for rounded rectangular holes

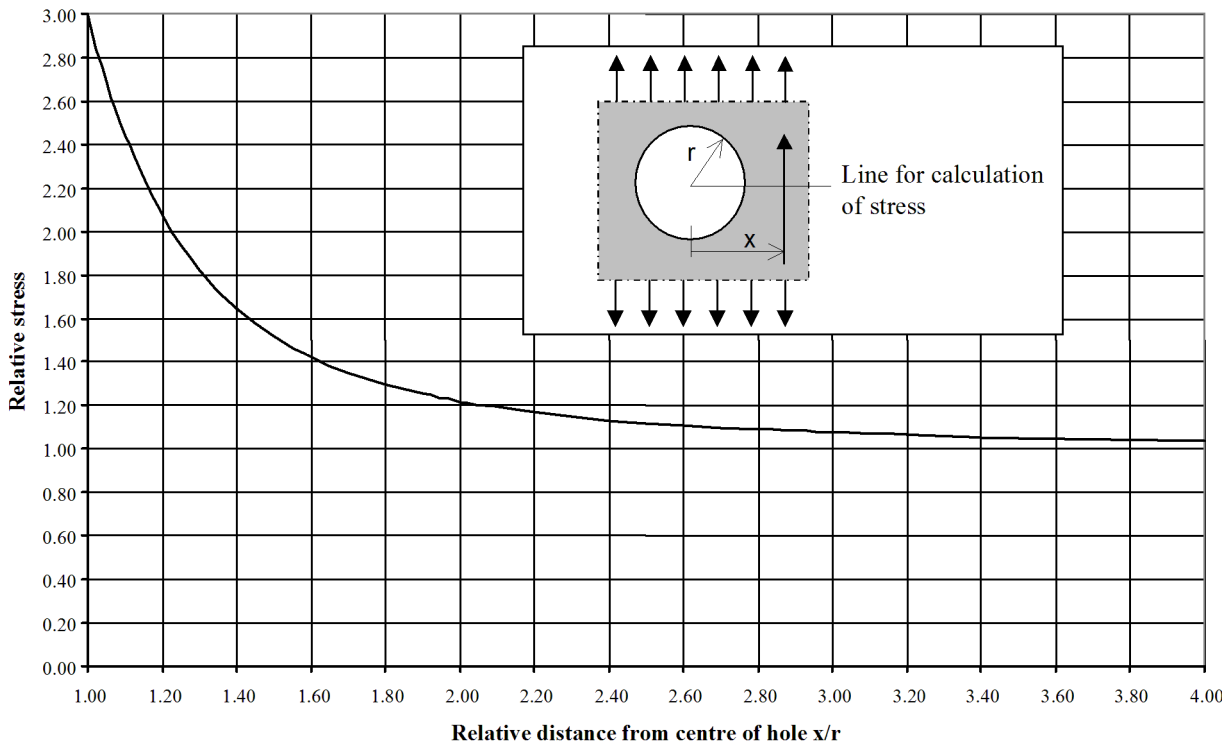


Figure 3-3 Stress distribution at a hole

3.1.5 Stress concentration factors for holes with edge reinforcement

Stress concentration factors for holes with reinforcement are given in [App.C](#).

Fatigue cracking around a circumferential weld may occur at several locations at reinforced rings in plates depending on geometry of ring and weld size.

- 1) Fatigue cracking transverse to the weld toe in a region with a large stress concentration giving large stress parallel to the weld (flexible reinforcement), see [Figure 3-4 a\)](#). Then $\sigma_{\text{hot spot}} = \sigma_p$ which includes the stress concentration due to the detail ($\sigma_p = \text{SCF} \cdot \sigma_n$).
- 2) Fatigue cracking parallel to the weld toe (stiff reinforcement with full penetration weld or large fillet weld size), see [Figure 3-4 b\)](#). Fatigue crack initiating from the weld toe. The principal stress σ_1 is the crack driving stress.

Then $\sigma_{\text{hot spot}} = \sigma_1$.

Also the region at the top position needs to be checked.

Then $\sigma_{\text{hot spot}} = \sigma_n$.

As an alternative to using the principal stress as hot spot stress at 45° position in [Figure 3-4 b\)](#) one may use the concept of effective hot spot stress as described in [\[4.3.4\]](#). See also [\[4.3.9\]](#).

- 3) Fatigue cracking from the weld root (stiff reinforcement with small fillet weld size), see [Figure 3-4 c\)](#).

Fillet welds at positions $\theta = 45^\circ$ and $\theta = 0^\circ$ should be assessed with respect to fatigue.

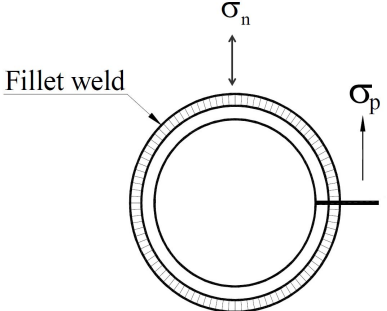
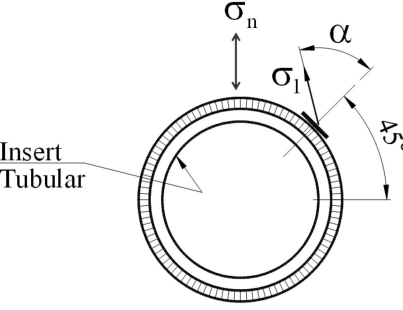
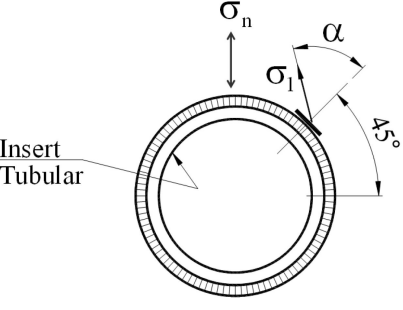
Position of fatigue crack	Comment
<p>a)</p> 	<p>Fatigue crack growing normal to the weld toe due to large stress concentration when insert tubular member is thin.</p> <p>Then $\sigma_{hot\ spot} = \sigma_p$ with stress concentration factor accounted for in σ_p.</p>
<p>b)</p> 	<p>Fatigue crack initiating from the weld toe for thicker inserted tubular member.</p> <p>The principal stress at the weld toe may be considered as the crack driving stress.</p> <p>Then $\sigma_{hot\ spot} = \sigma_1$ with stress concentration factor accounted for in σ_1.</p> <p>The region at the top position should also be checked.</p> <p>Then $\sigma_{hot\ spot} = \sigma_{np}$ where the stress concentration factor is accounted for as $\sigma_{np} = SCF\sigma_n$.</p>
<p>c)</p> 	<p>Fatigue crack initiating from the weld root in fillet welds at a region with large normal stress and shear stress. This failure mode is likely for small fillet welds compared with the thickness of the inserted tubular member or stiffening ring and the main plate.</p> <p>Fatigue failure is observed in fatigue tests at $\theta = 45^\circ$.</p> <p>Fatigue failure may also occur at $\theta = 0^\circ$ for compressive mean load (σ_n) giving tensile stresses at the weld toe.</p>

Figure 3-4 Potential fatigue crack locations at welded penetrations

All these potential regions for fatigue cracking should be assessed in a design with use of appropriate stress concentration factors for holes with reinforcement. For full penetration welds only the first two points shall be assessed.

For stresses to be used together with the different S-N curves see [2.3].

Potential fatigue cracking transverse to the weld toe

For stresses parallel with the weld the local stress to be used together with the C curve is obtained with SCF from [App.C](#) ($\sigma_{\text{hot spot}}$ in [Figure 3-4 a](#)). With start and stop positions at the hot spot region a lower S-N curve should be used, see [Table A-3](#).

Potential fatigue cracking parallel with the weld toe

For stresses normal to the weld the resulting hot spot stress to be used together with the D curve is obtained with SCF from [App.C](#) ($\sigma_{\text{hot spot}}$ in [Figure 3-4 b](#)).

Potential fatigue cracking from the weld root

At some locations of the welds there are stresses in the plate transverse to the fillet weld, σ_{np} , and shear stress in the plate parallel with the weld $\tau_{//p}$ see [Figure 3-4 c](#)). Then the fillet weld is designed for a combined stress obtained as:

$$\Delta\sigma_w = \frac{t}{2a} \sqrt{\Delta\sigma_{np}^2 + 0.2\Delta\tau_{//p}^2} \quad (3.1.5)$$

where:

t = plate thickness

a = throat thickness for a double sided fillet weld.

The total stress range (i.e. maximum compression and maximum tension) should be considered to be transmitted through the welds for fatigue assessments. See also /63/ and [App.C](#) for an example.

Equation (3.1.5) may be deduced from equation (2.3.4) and the resulting stress range should be used together with the W3 curve. The stresses at the hot spots in the plate as shown in [Figure 3-4](#) is derived from [App.C](#).

3.1.6 Stress concentration factors for scallops in plated structures

See [Figure 3-5](#) for stress concentration factors for scallops.

The stress concentration factors are applicable to stiffeners subject to axial loads. For significant dynamic pressure loads on the plate these details are susceptible to fatigue cracking and other design solutions should be considered to achieve a proper fatigue life.

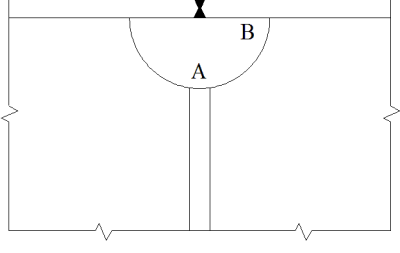
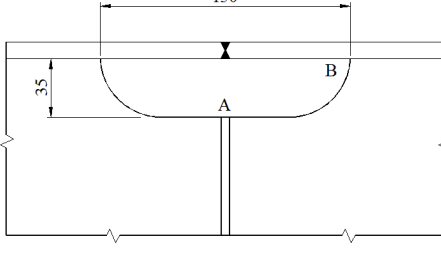
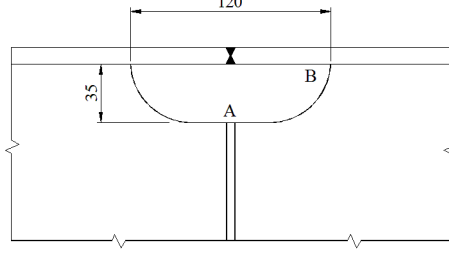
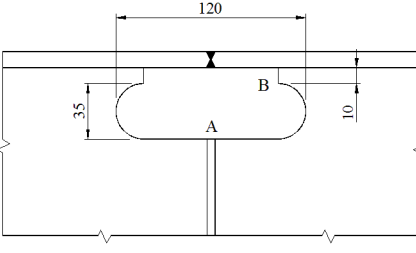
 <p>SCF = 2.4 at point A (misalignment not included) SCF = 1.27 at point B</p>	 <p>SCF = 1.17 at point A (misalignment not included) SCF = 1.27 at point B</p>
 <p>SCF = 1.27 at point A (misalignment not included) SCF = 1.27 at point B</p>	 <p>SCF = 1.17 at point A (misalignment not included) SCF = 1.27 at point B</p>
<p>For scallops without transverse welds, the SCF at point B are governing for the design.</p>	

Figure 3-5 Stress concentration factors for scallops

3.2 Stress concentration factors for ship details

Stress concentration factors for ship details may be found in DNVGL-CG-0129.

3.3 Tubular joints and members

3.3.1 Stress concentration factors for simple tubular joints

Stress concentration factors for simple tubular joints are given in App.B.

3.3.2 Superposition of stresses in tubular joints

The stresses in tubular joints due to brace loads are calculated at the crown and the saddle points, see Figure 3-6. Then the hot spot stress at these points is derived by summation of the single stress components from axial, in-plane and out of plane action. The hot spot stress may be higher for the intermediate points between the saddle and the crown. The hot spot stress at these points is derived by a linear interpolation of the stress due to the axial action at the crown and saddle and a sinusoidal variation of the bending stress resulting from in-plane and out of plane bending. Thus the hot spot stress should be evaluated at 8 spots around the circumference of the intersection, see Figure 3-7.

$$\begin{aligned}
 \sigma_1 &= \text{SCF}_{\text{AC}} \sigma_x + \text{SCF}_{\text{MIP}} \sigma_{my} \\
 \sigma_2 &= \frac{1}{2} (\text{SCF}_{\text{AC}} + \text{SCF}_{\text{AS}}) \sigma_x + \frac{1}{2} \sqrt{2} \text{SCF}_{\text{MIP}} \sigma_{my} - \frac{1}{2} \sqrt{2} \text{SCF}_{\text{MOP}} \sigma_{mz} \\
 \sigma_3 &= \text{SCF}_{\text{AS}} \sigma_x - \text{SCF}_{\text{MOP}} \sigma_{mz} \\
 \sigma_4 &= \frac{1}{2} (\text{SCF}_{\text{AC}} + \text{SCF}_{\text{AS}}) \sigma_x - \frac{1}{2} \sqrt{2} \text{SCF}_{\text{MIP}} \sigma_{my} - \frac{1}{2} \sqrt{2} \text{SCF}_{\text{MOP}} \sigma_{mz} \\
 \sigma_5 &= \text{SCF}_{\text{AC}} \sigma_x - \text{SCF}_{\text{MIP}} \sigma_{my} \\
 \sigma_6 &= \frac{1}{2} (\text{SCF}_{\text{AC}} + \text{SCF}_{\text{AS}}) \sigma_x - \frac{1}{2} \sqrt{2} \text{SCF}_{\text{MIP}} \sigma_{my} + \frac{1}{2} \sqrt{2} \text{SCF}_{\text{MOP}} \sigma_{mz} \\
 \sigma_7 &= \text{SCF}_{\text{AS}} \sigma_x + \text{SCF}_{\text{MOP}} \sigma_{mz} \\
 \sigma_8 &= \frac{1}{2} (\text{SCF}_{\text{AC}} + \text{SCF}_{\text{AS}}) \sigma_x + \frac{1}{2} \sqrt{2} \text{SCF}_{\text{MIP}} \sigma_{my} + \frac{1}{2} \sqrt{2} \text{SCF}_{\text{MOP}} \sigma_{mz}
 \end{aligned} \tag{3.3.1}$$

Here σ_x , σ_{my} and σ_{mz} are the maximum nominal stresses due to axial load and bending in-plane and out-of-plane respectively. SCF_{AS} is the stress concentration factor at the saddle for axial load and the SCF_{AC} is the stress concentration factor at the crown. SCF_{MIP} is the stress concentration factor for in plane moment and SCF_{MOP} is the stress concentration factor for out of plane moment.

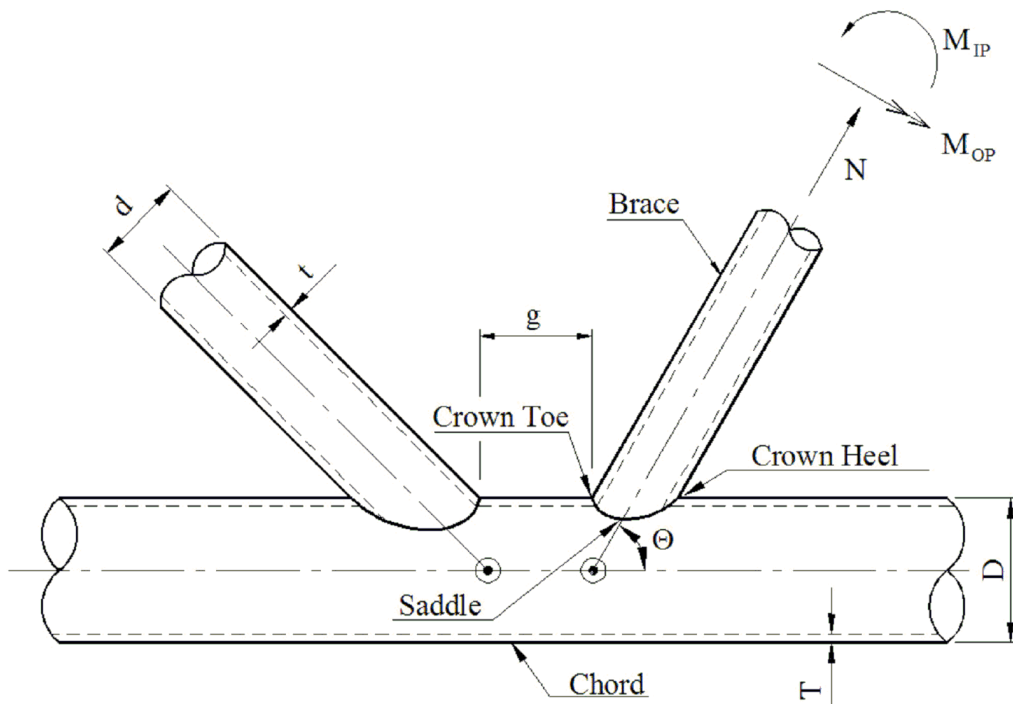


Figure 3-6 Geometrical definitions for tubular joints

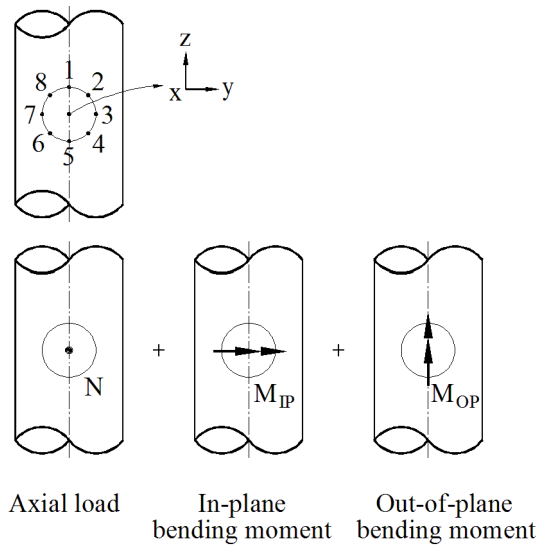


Figure 3-7 Superposition of stresses

Influence functions may be used as an alternative to the procedure given here to calculate hot spot stress. See e.g. *Combined Hot-Spot Stress Procedures for Tubular Joints /24/* and *Development of SCF Formulae and Generalised Influence Functions for use in Fatigue Analysis /2/*.

The stress concentration factors for tubular joints in App.B are due to loads in the braces. For significant dynamic stresses also in the axial direction of the chord, the hot spot stresses at the crown toe and at the crown heel should be added to the corresponding hot spot stresses resulting from the brace loads before the S-N curve is entered for calculation of fatigue damage. The braces can be considered as attachments to the chord for loads in the axial direction of the chord. Due to this the axial stress in the chord should be increased by a SCF = 1.20 for calculation of additional hot spot stress at the crown toe and the crown heel for dynamic loading in the axial direction of the chord.

3.3.3 Tubular joints welded from one side

The root area of single-sided welded tubular joints may be more critical with respect to fatigue cracks than the outside weld connecting the brace to the chord. In such cases, it is recommended that stubs are provided for tubular joints where high fatigue strength is required, such that welding from the backside can be performed.

Failure from the root has been observed at the saddle position of tubular joints where the brace diameter is equal the chord diameter, both in laboratory tests and in service. It is likely that fatigue cracking from the root might occur for rather low stress concentrations. Thus, special attention should be given to joints other than simple joints, such as ring-stiffened joints and joints where weld profiling or grinding on the outside surface is required to achieve sufficient fatigue life. It should be remembered that outside surface improvement does not increase the fatigue life at the root.

Some guidance on fatigue assessment of the root side is given in [F.10].

Due to limited accessibility for in service inspection a higher design fatigue factor should be considered used for the weld root than for the outside weld toe hot spot. See also [F.10].

3.3.4 Stiffened tubular joints

Equations for joints for ring stiffened joints are given in *Stress Concentration Factors for Ring-Stiffened Tubular Joints* /3/. The following points should be noted regarding the equations:

- The derived SCF ratios for the brace/chord intersection and the SCFs for the ring edge are mean values, although the degree of scatter and proposed design factors are given.
- Short chord effects shall be taken into account where relevant.
- For joints with diameter ratio $\beta \geq 0.8$, the effect of stiffening is uncertain. It may even increase the SCF.
- The maximum of the saddle and crown stress concentration factor values should be applied around the whole brace/chord intersection. The T-curve can be used for these hot spots when the stress range is derived from the procedure in /3/. If the hot spot stresses are derived from less conservative finite element analysis following the guidelines in Sec.4, it is recommended to also use the hot spot stress S-N curve described in [4.3.5].
- The following points can be made about the use of ring stiffeners in general:
- Thin shell FE analysis should be avoided for calculating the SCF if the maximum stress is expected to be near the brace-ring crossing point in the fatigue analysis. An alternative is to use a three-dimensional solid element analysis model.
- Ring stiffeners have a marked effect on the circumferential stress in the chord, but have little or no effect on the longitudinal stress.
- Ring stiffeners outside the brace footprint have little effect on the SCF, but may be of help for the static strength.
- Failures in the ring inner edge or brace ring interface occur internally, and will probably only be detected after through thickness cracking, at which the majority of the fatigue life will have been expired. These areas should therefore be considered as non-inspectable unless more sophisticated inspection methods are used. See also /56/. The C-curve can be used for hot spots at the edge of an internal ring stiffener without flange. The C2-curve can be used for hot spots at the circumferential weld between the web and flange of an internal ring stiffener with flange on the ring stiffener.

3.3.5 Grouted tubular joints

3.3.5.1 General

Grouted joints have either the chord completely filled with grout (single skin grouted joints) or the annulus between the chord and an inner member filled with grout (double skin grouted joints). The SCF of a grouted joint depends on load history and loading direction. The SCF is less if the bond between the chord and the grout is unbroken. For model testing of grouted joints the bond should be broken prior to SCF measurements. The tensile and compressive SCF may be different due to the bond.

To achieve a fatigue design that is on the safe side it is recommended to use SCFs derived from tests where the bonds are broken and where the joint is subjected to tensile loading. The bonds can be broken by a significant tension load. This load may be determined during the testing by an evaluation of the force displacement relationship. (When incrementing the loading into a non-linear behaviour.)

3.3.5.2 Chord filled with grout

The grouted joints can be treated as simple joints, except that the chord thickness in the γ term for saddle SCF calculation for brace and chord shall be substituted with an equivalent chord wall thickness given by:

$$T_e = (5D + 134T)/144 \quad (3.3.2)$$

where D and T are chord diameter and thickness respectively. The dimensions shall be given in [mm].

Joints with high β or low γ ratios have little effect from the grout. The benefits of grouting should be neglected for joints with $\beta > 0.9$ or $\gamma \leq 12.0$ unless documented otherwise.

3.3.5.3 Annulus between tubular members filled with grout

For joints where the annulus between tubular members are filled with grout such as joints in legs with insert piles, the grouted joints can be treated as simple joints, except that the chord thickness in SCF calculation for brace and chord shall be substituted with an equivalent chord wall thickness given by:

$$T_e = T + 0.45T_p \quad (3.3.3)$$

where:

T = chord thickness

T_p = thickness of insert pile.

where T is chord thickness and T_p is thickness of insert pile.

3.3.6 Cast nodes

It is recommended that finite element analysis is used to determine the magnitude and location of the maximum stress range in castings sensitive to fatigue. The finite element model should use volume elements at the critical areas and properly model the shape of the joint. Consideration should be given to the inside of the castings. The brace to casting circumferential butt weld (which is designed to an appropriate S-N curve for such connections) may be the most critical location for fatigue.

3.3.7 Tubular butt weld connections

3.3.7.1 Sources to eccentricities

Stress concentrations at tubular butt weld connections are due to eccentricities resulting from different sources. These may be classified as concentricity (difference in tubular diameters), differences in thickness of joined tubulars, out of roundness (ovality) and centre eccentricity, see [Figure 3-9](#) and [Figure 3-10](#). The resulting eccentricity may be conservatively evaluated by a direct summation of the contribution from the different sources. The eccentricity due to out of roundness normally gives the largest contribution to the resulting eccentricity or misalignment.

3.3.7.2 Stress concentration factors for butt welds between members with equal thickness

The following equation may be used for weld toes at butt welds between members with equal plate thickness:

$$SCF = 1 + \frac{3(\delta_m - \delta_0)}{t} e^{-\alpha} \quad (3.3.4)$$

where:

δ_0 = 0.05t is misalignment inherent in the S-N data and analysis procedure for as welded butt welds (not for ground connections)

L = width of weld at surface.

$$\alpha = \frac{0.91L}{\sqrt{Dt}}$$

δ_0 is introduced into the equation to account for statistical scatter of tolerances in combination with the statistical scatter in test data for derivation of S-N curve.

For tethers it is recommended to put $\delta_0 = 0$ due to the many weld connections in one tether that is subjected to a similar loading and that a potential failure will most likely occur from the weakest point.

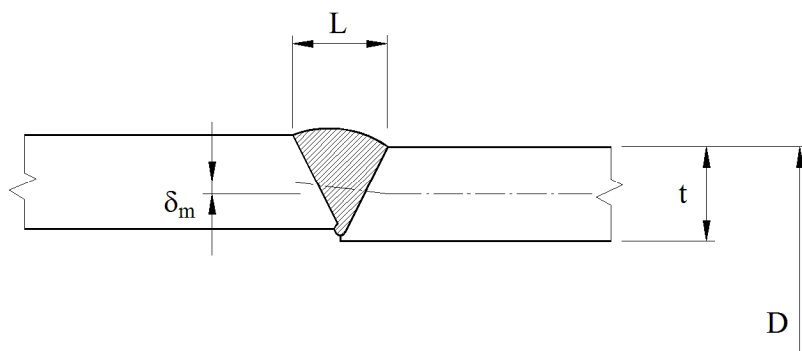


Figure 3-8 Section through weld

3.3.7.3 Stress concentration factors for butt welds at thickness transitions at girth welds in tubulars

The following section is included for purpose of design of structural tubular elements and tethers. Due to less severe S-N curve for the outside weld toe than for the inside weld root, it is strongly recommended that tubular butt weld connections subjected to axial loading are designed such that any thickness transitions are placed on the outside, see [Figure 3-11](#). For this geometry, the SCF for the transition applies to the outside. Thickness transitions shall normally be fabricated with slope 1:4.

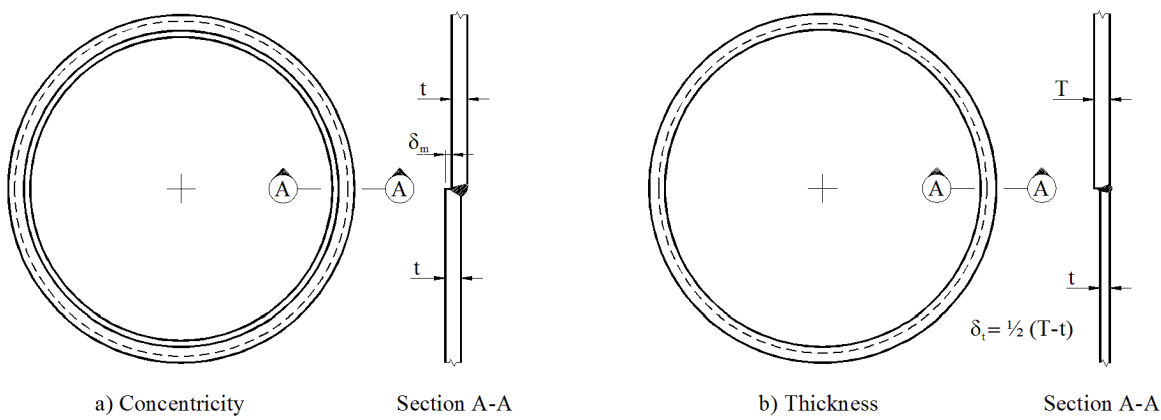


Figure 3-9 Geometric sources of local stress concentrations in tubular butt welds

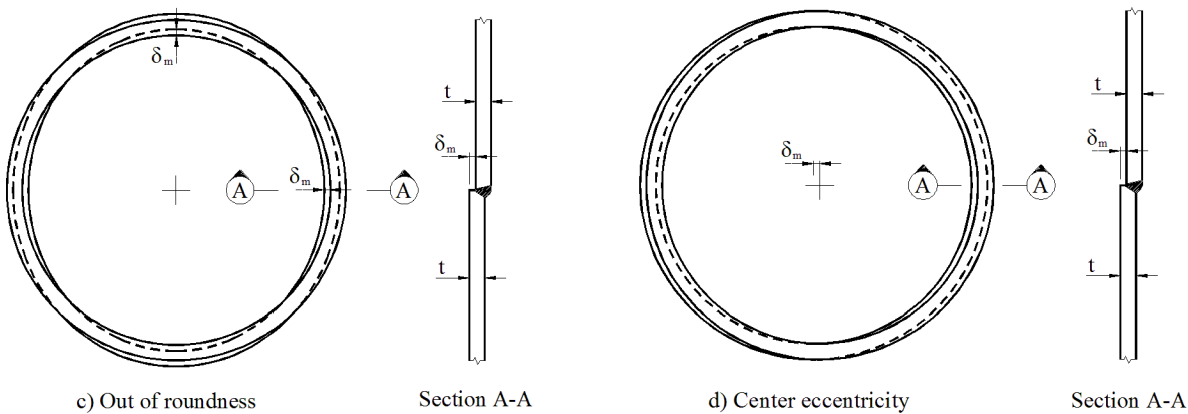


Figure 3-10 Geometric sources of local stress concentrations in tubular butt welds

The following equation for calculation of SCF at tubular butt welds with eccentricities may be used:

$$SCF = 1 + \frac{6(\delta_t + \delta_m - \delta_0)}{t} \cdot \frac{1}{1 + \left(\frac{T}{t}\right)^\beta} e^{-\alpha} \quad (3.3.5)$$

where:

$$\alpha = \frac{1.82L}{\sqrt{Dt}} \cdot \frac{1}{1 + \left(\frac{T}{t}\right)^\beta}$$

$\delta_0 = 0.05t$ is misalignment inherent in the S-N data and analysis procedure for as welded butt welds (not for ground connections)

D = outer tubular diameter as defined in [Figure 3-8](#).

$$\beta = 1.5 - \frac{1.0}{\log\left(\frac{D}{t}\right)} + \frac{3.0}{\left(\log\left(\frac{D}{t}\right)\right)^2}$$

This formula also takes into account the length over which the eccentricity is distributed: L, see [Figure 3-11](#) and [Figure 3-8](#). The stress concentration is reduced as L is increased and or D is reduced. It is noted that for small L and large D the last formula provides stress concentration factors that are close to that of the simpler formula for plates.

The transition of the weld to base material on the outside of the tubular can normally be classified to S-N curve E. If welding is performed in a flat position it can be classified as D. This means that the pipe would have to be rotated during welding.

Where high quality joints are required, the weld may be placed some distance outside the thickness transition as shown in [Figure 3-13](#). This geometry improves the conditions for welding and a reliable NDT.

Equation (3.3.5) applies for calculation of stress concentration factors for the outside tubular side shown in [Figure 3-12 a\)](#) when the thickness transition is on the outside. For the inside of connections with transitions in thickness on the outside as shown in [Figure 3-12 b\)](#) the following equation may be used:

$$SCF = 1 - \frac{6(\delta_t - \delta_m + \delta_0)}{t} \frac{1}{1 + \left(\frac{T}{t}\right)^{\beta}} e^{-\alpha} \quad (3.3.6)$$

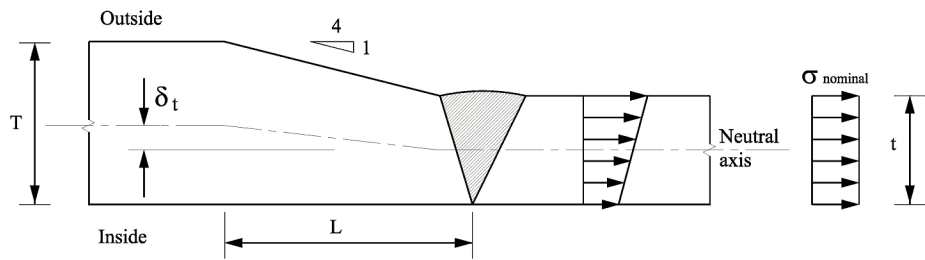
It is here assumed welding from both sides. For welding from the outside only one should put $\delta_0 = 0$ and this equation is used to calculate the stress concentration factor to be used for the weld root.

If the transition in thickness is on the inside of the tubular and the weld is made from both sides, equation (3.3.5) may be applied for the inside weld toe and equation (3.3.6) for the outside weld toe.

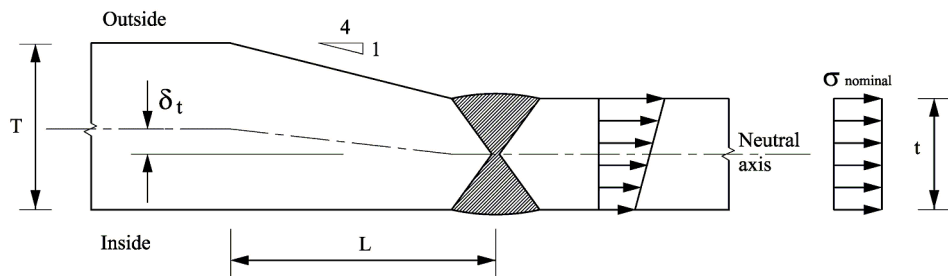
If the transition in thickness is on the inside of the tubular and the weld is made from the outside only, as shown in [Figure 3-12 c\)](#), equation (3.3.6) may be used for calculation of stress concentration for the outside weld toe.

If the transition in thickness is on the inside of the tubular and the weld is made from the outside only, as shown in [Figure 3-12 d\)](#), equation (3.3.5) may be used for calculation of stress concentration for the inside weld root with $\delta_0 = 0$.

Thus, the equations listed for SCFs above may be used both for butt welds made from both sides as shown in [Figure 3-11 b\)](#) and also for welds made from one side only.



- a) Preferred transition in thickness is on outside of tubular butt weld when welding is performed from the outside only.



- b) Transition in thickness at butt weld in tubular made from both sides.

Figure 3-11 Transition in thickness at tubular butt weld

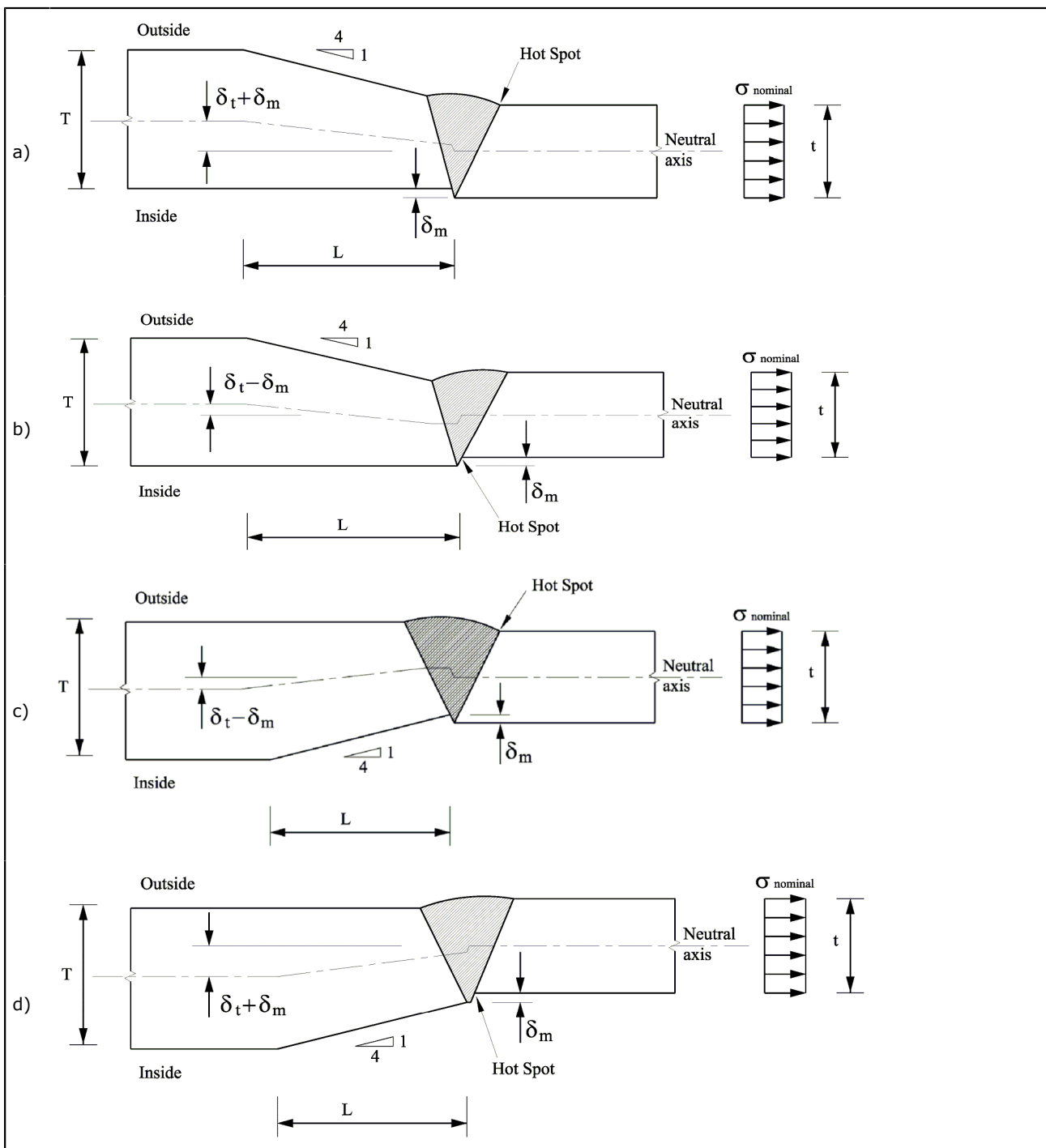


Figure 3-12 Different combinations of geometry and fabrication tolerances for weld in tubulars made from the outside

In tubulars, the root side of welds made from one side is normally classified as F3. This requires good workmanship during construction, in order to ensure full penetration welds, and that work is checked by non-destructive examination. It may be difficult to document a full penetration weld in most cases due to

limitations in the non-destructive examination technique to detect defects in the root area. The F3 curve can be considered to account for some lack of penetration, but it should be noted that a major part of the fatigue life is associated with the initial crack growth while the defects are small. This may be evaluated by fracture mechanics such as described in BS 7910 *Guidance on Methods for Assessing the Acceptability of Flaws in Fusion Welded Structures*, /7/ or DNVGL-RP-C210, /107/. Therefore, if a fabrication method is used where lack of penetration shall be expected, the design S-N curves should be adjusted to account for this by use of fracture mechanics.

The local bending stress over the thickness of a tubular at a welded connection is due to the membrane stress acting over the thickness. Thus the membrane stress shall be used for calculation of the additional stress resulting from a stress concentration at a weld. Stress concentration representative for the outside shall be used for calculation of stress on the outside. Stress concentration representative for the inside shall be used for calculation of stress on the inside. The local bending stress over the thickness is derived as the stress concentration minus 1.0 times the membrane stress (stress due to axial force and global bending moment in the middle of the thickness). Then this local bending stress should be added to that from the global stress in the tubular resulting from axial force and global bending moment. More detailed guidance on this is presented in [F.14]. Also guidance on how to calculate the stress on the inside is presented more in detail in [F.14]. The stress on the outside shall be used for fatigue crack initiation from the outside and the stress on the inside shall be used for fatigue crack initiation from the inside.

More machining of the ends of the tubulars can be performed to separate the geometric effects from thickness transition from that of the fabrication tolerances at the weld as shown in Figure 3-13. The interaction of stresses from these sources is small when the length $L_2 \geq 1.4 l_e$ where:

$$l_e = \frac{\sqrt{rt}}{\sqrt[4]{3(1-\nu^2)}} \quad (3.3.7)$$

where:

- r = radius to mid surface of the pipe
- t = thickness of the pipe
- ν = Poisson's ratio.

With shorter length L_2 one should consider interaction between the bending stress at the notch at thickness transition and the bending stress due to the tolerances at the weld.

For shorter lengths of L_2 with interaction of bending stresses the SCF can be calculated based on superposition of bending stresses. Then the resulting SCFs can be derived as follows. This SCF relates to nominal stresses in the pipe with thickness t .

For hot spot A:

Stress concentration at hot spot A (Figure 3-13):

$$SCF = 1 + \frac{6\delta_t}{t} \frac{1}{1 + \left(\frac{T}{t}\right)^\beta} e^{-\alpha} + \frac{3\delta_m}{t} e^{-\sqrt{t/D}} e^{-\gamma} \cos \gamma \quad (3.3.8)$$

where:

$$\alpha = \frac{1.82L_1}{\sqrt{Dt}} \cdot \frac{1}{1 + \left(\frac{T}{t}\right)^\beta}$$

and:

$$\beta = 1.5 - \frac{1.0}{\log\left(\frac{D}{t}\right)} + \frac{3.0}{\left(\log\left(\frac{D}{t}\right)\right)^2}$$

$$\gamma = \frac{L_2}{l_e}$$

Depending on how the machining of the notch area is performed, one may consider an additional stress concentration due to this notch. This depends on transition radius from the sloped area and the thinner section in relation to the selected S-N curve.

If the highest S-N curve for base material (B1 or the HS curve in [D.1]) is used, one may include an additional SCF depending on transition radius. Guidance can be found in *Petersons Stress Concentration Factors* /15/, or alternative a fine mesh finite element analysis is recommended.

(In a finite element analysis the combined effects of notch and bending due to thickness transition are included.)

For hot spot B:

Stress concentration at hot spot B ([Figure 3-13](#)).

$$SCF = 1 + \frac{6\delta_t}{t} \frac{1}{1 + \left(\frac{T}{t}\right)^\beta} e^{-\alpha} e^{-\gamma} \cos \gamma + \frac{3\delta_m}{t} e^{-\sqrt{t/D}} \quad (3.3.9)$$

For hot spot C:

Stress concentration at hot spot C ([Figure 3-13](#)).

$$SCF = 1 - \frac{6\delta_t}{t} \frac{1}{1 + \left(\frac{T}{t}\right)^\beta} e^{-\alpha} e^{-\gamma} \cos \gamma \quad (3.3.10)$$

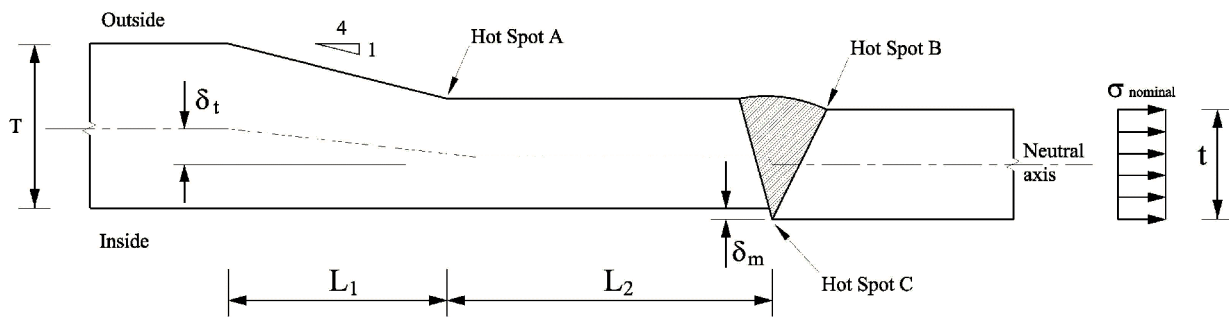


Figure 3-13 Geometry with thickness transition away from the butt weld

3.3.8 Stress concentration factors for stiffened shells

The stress concentration at a ring stiffener can be calculated as

$$\text{SCF} = 1 + \frac{0.54}{\alpha} \text{ for the outside of the shell}$$

$$\text{SCF} = 1 - \frac{0.54}{\alpha} \text{ for the inside of the shell} \quad (3.3.11)$$

$$\alpha = 1 + \frac{1.56t\sqrt{rt}}{A_r}$$

where:

A_r = area of ring stiffener without effective shell

r = radius of shell measured from centre to mean shell thickness

t = thickness of shell plating.

Due to less stress on the inside it is more efficient to place ring stiffeners on the inside of shell, as compared with the outside. In addition, if the shell comprises longitudinal stiffeners that are ended, it is recommended to end the longitudinal stiffeners against ring stiffeners at the inside. The corresponding combination of geometry on the outside gives a considerably larger stress concentration.

The SCF = 1.0 if continuous longitudinal stiffeners are used.

In the case of a bulkhead instead of a ring, A_r is taken as $\frac{rt_b}{(1-v)}$ where t_b is the thickness of the bulkhead.

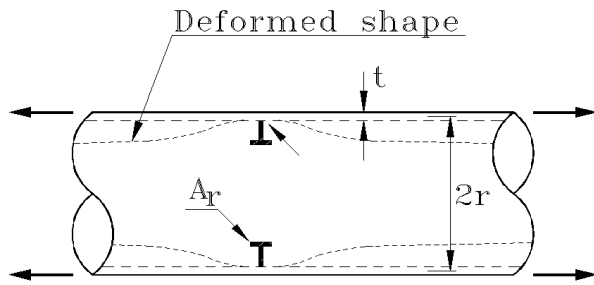


Figure 3-14 Ring stiffened shell

3.3.9 Stress concentration factors for conical transitions

The stress concentration at each side of unstiffened tubular-cone junction can be estimated by the following equations (the SCF shall be used together with the stress in the tubular at the junction for both the tubular and the cone side of the weld):

$$SCF = 1 + \frac{0.6t\sqrt{D_j(t+t_c)}}{t^2} \tan\alpha \quad (3.3.12)$$

for the tubular side.

$$SCF = 1 + \frac{0.6t\sqrt{D_j(t+t_c)}}{t_c^2} \tan\alpha \quad (3.3.13)$$

for the cone side.

where:

D_j = cylinder diameter at junction (D_s, D_L)

t = tubular member wall thickness (t_s, t_L)

t_c = cone thickness

α = the slope angle of the cone, see [Figure 3-15](#).

For conical connection with typical cone angles used in design of jacket structures it is normal practise to place the thickness transition in the cone (with thicker cone than tubular) on the outside of the large diameter junction and on the inside of the smaller diameter junction. Then it is not normal practise to consider the effect of the thickness transition on stress concentration at these junctions.

In design of large diameter structures like monopiles it is observed that in some cases the thickness transition in the cone section has been placed on the inside of the large diameter junction. In such a case the additional stress concentration due to the thickness transition needs to be added to the stress concentration for the conical transition. It is thus recommended to place the thickness transition in the cone (with thicker cone than tubular) on the outside of the large diameter junction and on the inside of the smaller diameter junction, see also /103/ for background. A procedure for calculation of stresses at conical connections where the thickness of the cone is different from the cylinders is presented in [\[F.17\]](#) and [/113/](#).

The stress concentration at a junction with ring stiffener may be calculated as:

$$SCF = 1 + \left(0.54 + \frac{0.91D_j t}{A_r} \tan\alpha \right) \frac{1}{\beta}$$

at the outside smaller diameter junction

$$SCF = 1 - \left(0.54 + \frac{0.91D_j t}{A_r} \tan\alpha \right) \frac{1}{\beta}$$

at the inside smaller diameter junction

$$SCF = 1 + \left(0.54 - \frac{0.91D_j t}{A_r} \tan\alpha \right) \frac{1}{\beta} \quad (3.3.14)$$

at the outside larger diameter junction

$$SCF = 1 - \left(0.54 - \frac{0.91D_j t}{A_r} \tan\alpha \right) \frac{1}{\beta}$$

at the inside larger diameter junction, and

$$\beta = 1 + \frac{1.10t\sqrt{D_j t}}{A_r}$$

where:

A_r = area of ring stiffener without effective shell.

A ring stiffener may be placed centric at the cone junction. Then the butt weld should be ground and NDE examined before the ring stiffener is welded.

If a ring stiffener is placed a distance d_e away from the intersection lines, an additional stress concentration should be included to account for this eccentricity:

$$SCF = 1 + \frac{3\delta_e \tan\alpha}{t} \frac{1}{1 + \frac{68I}{\sqrt{D_j^3(t+t_c)^5}}} \quad (3.3.15)$$

where:

D_j = cylinder diameter at junction (D_s , D_L)

t = tubular member wall thickness (t_s , t_L)

t_c = cone thickness

α = the slope angle of the cone, see [Figure 3-15](#)

I = moment of inertia about the x-x axis in [Figure 3-16](#) calculated as:

$$I = b \frac{t^3}{12} + 0.5 b \left(h + \frac{t}{2} - \bar{y} \right)^2 (t_c + t_s) + t_r h \left(\frac{h^2}{12} + \left(\frac{h}{2} - \bar{y} \right)^2 \right) \quad (3.3.16)$$

where:

$$\bar{y} = \frac{h^2 t_r + \left(h + \frac{t}{2} \right) b (t_c + t_s)}{2 h t_r + (t_c + t_s) b} \quad (3.3.17)$$

where:

h = height of ring stiffener

t_r = thickness of ringstiffener

b = effective flange width calculated as:

$$b = 0.78 \sqrt{D_j (t_c + t_s)} + \delta_e \quad (3.3.18)$$

If a ring stiffener with a flange is used, the effect of the flange should be included when calculating the moment of inertia about the neutral axis x-x shown in [Figure 3-16](#).

The stress concentration factor from equation (3.3.15) minus 1.0 shall be added together with the relevant stress concentration factor from equation (3.3.14).

A full penetration weld connecting the ring stiffener to the tubular is often preferred as potential fatigue cracks from the root of fillet weld into the cylinder can hardly be detected during in service inspection. If improvement methods are used for the weld toe, the requirement of a full penetration weld shall be enhanced.

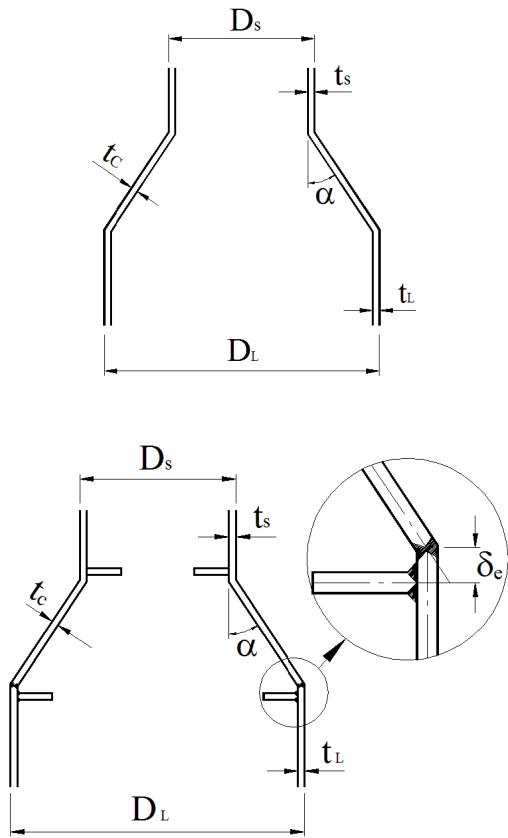


Figure 3-15 Cone geometry

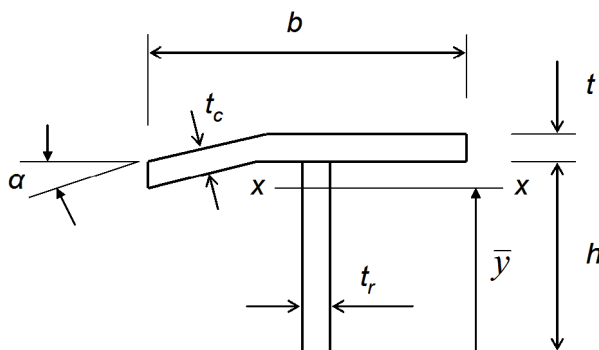


Figure 3-16 Notations for calculation of moment of inertia

3.3.10 Stress concentration factors for tubulars subjected to axial force

This section applies to tubular sections welded together to long strings and subjected to axial tension. Tethers and risers in a TLP are examples of such structures.

The collinearity with small angle deviation between consecutive fabricated tubular segments results in increased stress due to a resulting global bending moment, see [Figure 3-18](#). The eccentricity due to collinearity is a function of axial tension in the tubular and is significantly reduced as the axial force is increased by tension. Assuming that the moment M results from an eccentricity δ_N where pretension is accounted for in the analysis, the following stress is calculated:

$$\sigma = \frac{N}{\pi(D-t)t} SCF \quad (3.3.19)$$

where the stress concentration factor is:

$$SCF = 1 + \frac{4\delta_N}{D-t} \quad (3.3.20)$$

where δ_N is eccentricity as function of the axial force N , D is outer diameter and t is thickness of tubular. The eccentricity for two elements is indicated in [Figure 3-18](#). With zero tension the eccentricity is δ . With an axial tension force N the eccentricity becomes:

$$\delta_N = \delta \frac{\tanh kl}{kl} \quad (3.3.21)$$

where:

$$k = \sqrt{\frac{N}{EI}}$$

l = segment lengths of the tubulars

N = axial force in tubulars

I = moment of inertia of tubulars

E = Young's modulus.

The formula for reduction in eccentricity due to increased axial force can be deduced from differential equation for the deflected shape of the model shown in [Figure 3-18](#). Thus the non-linearity in terms of geometry is included in the formula for the stress concentration factor.

Judgement should be used to evaluate the number of elements to be considered, and whether deviation from a straight line is systematic or random, see [Figure 3-17](#). In the first case, the errors shall be added linearly, in the second case it may be added quadratically.

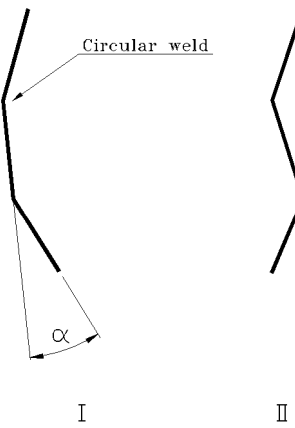


Figure 3-17 Collinearity or angle deviation in pipe segment fabrication, I = systematic deviation, II = random deviation

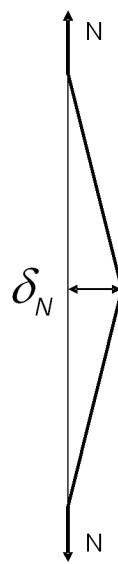


Figure 3-18 Eccentricity due to collinearity

3.3.11 Stress concentration factors for joints with square sections

Stress concentration factors shall be determined for the particular geometries being used in a design. These stress concentration factors may be established from finite element analysis or from parametric equations where these can be found for the joints under consideration.

Stress concentration factors for square to square joints may be found in *Design guide for circular and rectangular hollow section welded joints under fatigue loading*, see /27/. These stress concentration factors may be used together with the D-curve.

The following stress concentration factors may be used for $d/D_w = 1.0$, where d = depth and width of brace, D_w = depth and width of chord:

- axial: 1.90
- in-plane bending: 4.00
- out-of plane bending: 1.35.

These stress concentration factors should be used together with the F-curve.

3.3.12 Stress concentration factors for joints with gusset plates

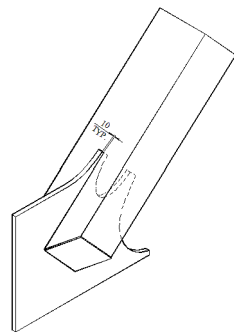
Insert gusset plates are sometimes used in joints in topside structures to connect RHS or tubular members to main girders, see [Figure 3-19](#).

When such connections are subjected to dynamic loading a full penetration weld between the member and the gusset plate is preferred. Otherwise it is considered difficult to document the fatigue capacity for fatigue cracking starting from the weld root. In dynamically loaded structures it is also recommended to shape the gusset plate to smoothen the stress flow from the member into the gusset plate, see [Figure 3-19 a](#)).

Where a reliable fatigue life shall be documented, it is recommended to perform finite element analysis. This is because such joints can create high stress concentrations. Hot spot stresses derived by finite element analysis can be combined with the D-curve. The F3 or the W3 curve should be used for the hot spot on the inside of the tubular if the connection is made without any back weld, as is generally the case. Regarding selection of S-N curve, see [Table A-6](#) as it also depends on amount of inspection performed.

Use of shell elements for such analysis provides conservative stress concentration factors compared to analysis with three-dimensional elements that include modelling of an external fillet weld. (There should normally be a fillet weld on the outside of a full or partial penetration weld that increases the effective area. A fillet weld on the outside effectively reduces the stress in the weld root due to eccentricity, see [\[3.3.7\]](#)).). See also [\[F.16\]](#).

a)



b)

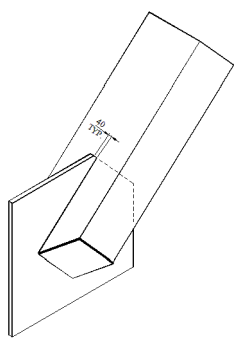


Figure 3-19 Joints with gusset plates, a) favourable geometry and b) simple geometry

SECTION 4 CALCULATION OF HOT SPOT STRESS BY FINITE ELEMENT ANALYSIS

4.1 General

From detailed finite element analysis of structures it may be difficult to evaluate what is 'nominal stress' to be used together with the S-N curves, as some of the local stress due to a detail is accounted for in the S-N curve.

In many cases it may therefore be more convenient to use an alternative approach for calculation of fatigue damage when local stresses are obtained from finite element analysis.

It is realised that it is difficult to calculate the notch stress at a weld due to a significant scatter in local weld geometry and different types of imperfections. This scatter is normally more efficiently accounted for by use of an appropriate S-N curve. In this respect it should also be mentioned that the weld toe region shall be modelled with a radius in order to obtain reliable results for the notch stress.

If a weld corner detail with zero radius is modelled, the calculated stress will approach infinity as the element size is decreased to zero. The modelling of a relevant radius requires a very fine element mesh, increasing the size of the computer model.

The notch stress concept may be used in special cases where other methods are not found appropriate, see [App.E](#).

For design analysis a simplified numerical procedure is used in order to reduce the demand for large fine mesh models for the calculation of hot spot stress and SCF factors:

- the stress concentration or the notch factor due to the weld itself is included in the S-N curve to be used, in general the D-curve. This S-N curve can normally be considered as the hot spot S-N curve, see also [\[4.3.5\]](#)
- the stress concentration due to the geometry effect of the actual detail is calculated by means of a fine mesh model using shell elements (or solid elements), resulting in a geometric SCF factor.

This procedure is denoted the hot spot method.

It is important to have a continuous and not too steep, change in the density of the element mesh in the areas where the hot spot stresses are calculated.

The geometry of the elements should be evaluated carefully in order to avoid errors due to deformed elements (for example corner angles between 60° and 120° and length/breadth ratio less than 5 are recommended).

The size of the model should be so large that the calculated results are not significantly affected by assumptions made for boundary conditions and application of loads.

It should be noted that the hot spot concept cannot be used for fatigue checks of cracks starting from the weld root of fillet/partial penetration welds. A fillet weld should be checked separately considering the stresses in the weld itself, see [\[2.3.5\]](#).

The hot spot stress method may be used for fatigue analysis of crack growth from the inside weld root in tubular joints as explained in [\[F.10\]](#) and in [\[3.3.12\]](#) for gusset plates.

4.2 Tubular joints

4.2.1 Derivation of hot spot stress

The stress concentration factors for tubular joints listed in [App.B](#) are derived from finite element analysis of tubular joints where the welded connection is modelled with solid element /116/. If a less accurate finite element modelling than this is made, the results from the analysis is expected to be correspondingly less accurate.

More reliable results are obtained by including the weld in the model. This implies use of three-dimensional elements.

If simpler analysis models are used, these should be calibrated to the more accurate models or to test data. The hot spot stress or geometric stress at tubular joints may also be obtained by a linear extrapolation of the stresses obtained from analysis at positions a and b from the weld toe as indicated in Figure 4-1. For extrapolation of stress along the brace surface normal to the weld toe:

$$a = 0.2 \sqrt{rt} \quad (4.2.1)$$

$$b = 0.65 \sqrt{rt}$$

For extrapolation of stress along the chord surface normal to the weld toe at the crown position:

$$a = 0.2 \sqrt{rt} \quad (4.2.2)$$

$$b = 0.4 \sqrt{rt RT}$$

For extrapolation of stress along the chord surface normal to the weld toe at the saddle position:

$$a = 0.2 \sqrt{rt} \quad (4.2.3)$$

$$b = 2\pi R \frac{5}{360} = \frac{\pi R}{36}$$

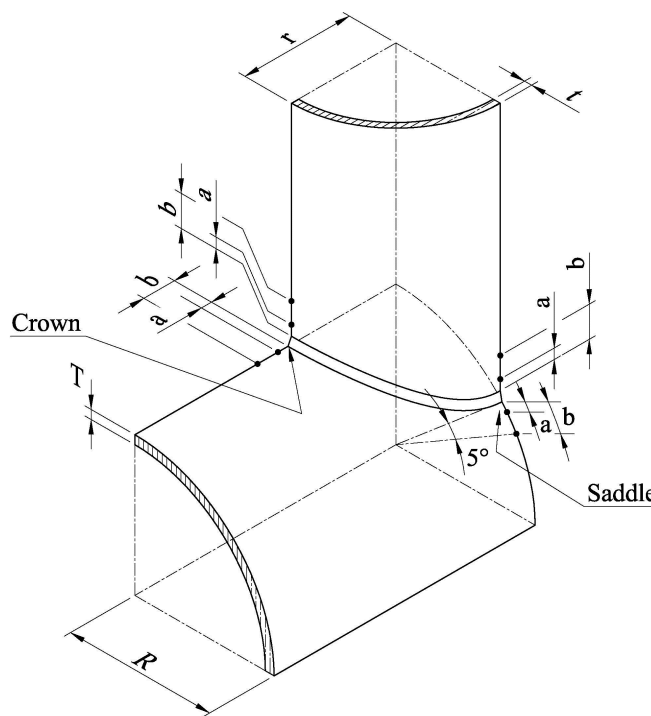


Figure 4-1 Points for read out of stresses for derivation of hot spot stress in tubular joints

An alternative analysis approach is to use the stresses at the Gaussian points if these are placed $0.1\sqrt{rt}$ from the weld toe (r = radius of considered tubular and t = thickness). The stress at this point may be used directly in the fatigue assessment.

Furthermore, it should be noted that the brace thickness at the crown positions of tubular joints can act like that of attachments for stress flow in the axial direction of the chord. The finite element analysis with the hot spot method described in this document does not necessarily provide the correct stress due to such attachments. This is described more in detail in [4.3.5]. This implies also that an additional stress concentration factor equal 1.20 may be needed for stress range calculation for stress fluctuations in the chord, see also comment at end of [Table B-1](#) for tubular T/Y joints. This additional stress concentration may also be needed for stress range calculation for stress fluctuations in the chord for other hot spots at other types of tubular joints such as K joints where the most significant hot spot may be closer to the crown position and away from the saddle position.

The stresses normal to the weld toe have usually been considered governing for the fatigue capacity of tubular joints in jacket structures. However, the derivation of SCF equations in [App.B](#) has been based on maximum principal stresses as has been recommended from some research projects /2/. See also [2.3.4]. These stresses may differ from the stresses normal to the weld toe. The deviations are usually small, especially at the important saddle location, and hence the superposition of hot spot stresses may be approximated by numerical addition of stress values without introducing a significant error. This analysis approach has been considered sufficient for traditional fatigue design of jacket structures for the oil and gas industry.

4.2.2 Tubular joints in wind turbine support structures

It is noted that fatigue analysis of tubular joints in support structures for wind turbines normally requires use of detailed finite element models and time history analysis of the load response. This implies simultaneous calculated load fluctuations in the chord and the braces. In traditional fatigue analysis of jacket structures, it has not been common practice to account for the force fluctuation in the chord at the same time as the force fluctuation in the brace. The combined load effect at hot spots from these loads during a load cycle may result in a maximum principal stress direction that is no longer normal to the weld toe. The maximum principal stress direction may also change during a time series for a constant global load direction. This makes the analysis more challenging as a substantiated analysis procedure for this multidirectional type of fatigue of tubular joints cannot be found in the literature. See also [4.3.4].

It should be noted that the design recommendations in most fabrication standards with respect to required stub length and chord lengths such as in NORSO N-004, /115/, do not in general imply that the stress at the girth welds at the connections to the braces or the chord is equal the nominal stress as calculated by simple beam theory for the elements between the tubular joints in frame structures. There may be some interaction effect between the stress in the tubular joint and the stress at the girth weld which implies a stress increase at the hot spots (at the tubular joint and at the girth weld). Where optimization of the fatigue life is required, the effect of this interaction may be calculated by a finite element analysis using shell elements for modelling of the considered structure.

4.2.3 S-N curves for tubular joints

The stress range at the hot spot of simple tubular joints (joints without stiffeners) from [4.2.1] should be combined with the T-curve for calculation of number of cycles to failure. The T-curve applies only to the outside hot spots at the brace and chord weld toes.

The D-curve can be used for fatigue assessment of hot spots at the outside of ring stiffened tubular joints. See also [4.3.5] for selection of S-N curves for other hot spots. For ring stiffened tubular joints the hot spot stresses may be derived similar to that of plated structures in [4.3].

4.3 Welded connections in plated structures

4.3.1 Stress field at a welded detail

Due to the nature of the stress field at a hot spot region there are questions on how to establish the hot spot stress, see [Figure 4-2](#). The notch effect due to the weld is included in the S-N curve and the hot spot stress is derived by extrapolation of the structural stress to the weld toe as indicated in [Figure 4-2](#). It is observed that the stress used as basis for such an extrapolation should be outside that affected by the weld notch, but close enough to pick up the stress due to local geometry.

4.3.2 Finite element modelling

The following guidance is made to the computation of hot spot stresses with potential fatigue cracking from the weld toe with local models using the finite element method.

Hot spot stresses are calculated assuming linear material behaviour and using an idealized structural model with no fabrication-related misalignment. The extent of the local model shall be chosen such that effects due to the boundaries on the considered structural detail are sufficiently small and reasonable boundary conditions may be formulated.

In plate structures, three types of hot spots at weld toes are identified as exemplified in [Figure 4-4](#):

- at the weld toe on the plate surface at an ending attachment
- at the weld toe around the plate edge of an ending attachment
- along the weld of an attached plate (weld toes on both the plate and attachment surface).

Models with thin plate or shell elements or alternatively with solid elements are normally used. It should be noted that on the one hand the arrangement and type of elements shall allow for steep stress gradients as well as plate bending, and on the other hand, only the linear stress distribution in the plate thickness direction should be evaluated with respect to the definition of hot spot stress.

The following methods of modelling are recommended.

The simplest way of modelling is offered by thin plate and shell elements which shall be arranged in the mid-plane of the structural components, see also [Figure 4-5](#).

8-noded elements are recommended particularly in case of steep stress gradients. Care should be given to possible stress underestimation, especially at weld toes of type b) in [Figure 4-4](#). Use of 4-noded elements with improved in-plane bending modes is a good alternative.

The welds are usually not modelled except for special cases where the results are affected by high local bending, e. g. due to an offset between plates or due to a small free plate length between adjacent welds such as at lug (or collar) plates. Here, the weld may be included by transverse plate elements having appropriate stiffness or by introducing constrained equations for coupled node displacements.

A thickness equal 2 times the thickness of the plates may be used for modelling of the welds by transverse plates.

For 4-node shell elements with additional internal degrees of freedom for improved in plane behaviour and for 8-node shell elements a mesh size from $t \times t$ up to $2t \times 2t$ may be used. Larger mesh sizes at the hot spot region may provide non-conservative results. (For efficient read out of element stresses and hot spot stress derivation a mesh txt is in general preferred at the hot spot region.) The calculated stresses using a $t \times t$ mesh does not necessarily provide converged stresses at the hot spot area. This means that a reduced stress may be calculated with a refined mesh leading to a lower calculated hot spot stress than by following the recommended $t \times t$ mesh. This is especially the situation when using higher order elements /31,40/. This information is given to the analyst to avoid a non-conservative fatigue assessment when using the hot spot analysis methodology. It should be noted that this methodology is based on calibration with analyses of different details such as shown in [\[F.11\]](#).

An alternative particularly for complex cases is offered by solid elements which shall have a displacement function allowing steep stress gradients as well as plate bending with linear stress distribution in the plate

thickness direction. This is offered, e.g., by isoparametric 20-node elements (with mid-side nodes at the edges) which mean that only one element in plate thickness direction is required. An easy evaluation of the membrane and bending stress components is then possible if a reduced integration order with only two integration points in the thickness direction is chosen. A finer mesh sub-division is necessary particularly if 8-noded solid elements are selected. Here, at least four elements are recommended in thickness direction. Modelling of the welds by solid elements is generally recommended and may be performed as shown in [Figure 4-6](#).

For modelling with three dimensional elements the dimensions of the first two or three elements in front of the weld toe should be chosen as follows. The element length may be selected to correspond to the plate thickness. In the transverse direction, the plate thickness may be chosen again for the breadth of the plate elements. However, the breadth should not exceed the attachment width, i. e. the thickness of the attached plate plus $2 \times$ the weld leg length (in case of type c: the thickness of the web plate behind plus $2 \times$ weld leg length). The length of the elements should be limited to $2 t$.

In cases where three-dimensional elements are used for the FE modelling it is recommended that also the fillet weld is modelled to achieve proper local stiffness and geometry.

In order to capture the properties of bulb sections with respect to St Venant torsion it is recommended to use several three-dimensional elements for modelling of a bulb section. If in addition the weld from stiffeners in the transverse frames is modelled, the requirements with respect to element shape will likely govern the FE model at the hot spot region.

4.3.3 Derivation of stress at read out points $0.5 t$ and $1.5 t$

The stress components on the plate surface should be evaluated along the paths shown in [Figure 4-5](#) and [Figure 4-6](#) and extrapolated to the hot spot. The average stress components between adjacent elements are used for the extrapolation.

Recommended stress evaluation points are typically located at distances $0.5 t$ and $1.5 t$ away from the hot spot, where t is the plate thickness at the weld toe. These locations are also denoted as stress read out points. t and $1.5t$ away from the hot spot, where t is the plate thickness at the weld toe. These locations are also denoted as stress read out points.

If the element size at a hot spot region of size $t \times t$ is used, the stresses may be evaluated as follows:

- In case of plate or shell elements the surface stress may be evaluated at the corresponding mid-side points. Thus the stresses at mid side nodes along line A-B in [Figure 4-3](#) may be used directly as stress at read out points $0.5 t$ and $1.5 t$.
- In case of solid elements the stress may first be extrapolated from the Gaussian points to the surface. Then these stresses may be interpolated linearly to the surface centre or extrapolated to the edge of the elements if this is the line for hot spot stress derivation.

For meshes with 4-node shell elements larger than $t \times t$ it is recommended to fit a second order polynomial to the element stresses in the three first elements and derive stresses for extrapolation from the $0.5 t$ and $1.5 t$ points. An example of this is shown schematically in [Figure 4-7](#). This procedure may be used to establish stress values at the $0.5 t$ and $1.5 t$ points. For 8-node elements a second order polynomial may be fitted to the stress results at the mid-side nodes of the three first elements and the stress at the read out points $0.5 t$ and $1.5 t$ can be derived.

4.3.4 Derivation of hot spot stress

4.3.4.1 Typical plated structures

Two alternative methods may be used for hot spot stress derivation where the stress direction does not change significantly during a load cycle: method A and method B.

These methods are based on calibration of the analysis methodology for hot spots in typical plated structures such as shown in [\[F.11\]](#). Thus, for hot spots in significantly thicker plates and at hot spots with steep stress gradients more refined methods are recommended as described in [\[4.3.4.2\]](#).

Method A

For modelling with shell elements without any weld included in the model a linear extrapolation of the stresses to the intersection line from the read out points at 0.5 t and 1.5 t from the intersection line can be performed to derive hot spot stress.

For modelling with three-dimensional elements with the weld included in the model a linear extrapolation of the stresses to the weld toe from the read out points at 0.5 t and 1.5 t from the weld toe can be performed to derive hot spot stress.

The notations for stress components are shown in [Figure 2-3](#) and [Figure 2-4](#).

The effective hot spot stress range to be used together with the hot spot S-N curve is derived as

$$\Delta\sigma_{\text{Eff}} = \max \begin{cases} \sqrt{\Delta\sigma_{\perp}^2 + 0.81\Delta\tau_{\parallel}^2} \\ \alpha|\Delta\sigma_1| \\ \alpha|\Delta\sigma_2| \end{cases} \quad (4.3.1)$$

where:

$\alpha = 0.90$ if the detail is classified as C2 with stress parallel to the weld at the hot spot, see [Table A-3](#)

$\alpha = 0.80$ if the detail is classified as C1 with stress parallel to the weld at the hot spot, see [Table A-3](#)

$\alpha = 0.72$ if the detail is classified as C with stress parallel to the weld at the hot spot, see [Table A-3](#).

The first principal stress is calculated as:

$$\Delta\sigma_1 = \frac{\Delta\sigma_{\perp} + \Delta\sigma_{\parallel}}{2} + \frac{1}{2}\sqrt{(\Delta\sigma_{\perp} - \Delta\sigma_{\parallel})^2 + 4\Delta\tau_{\parallel}^2} \quad (4.3.2)$$

and:

$$\Delta\sigma_2 = \frac{\Delta\sigma_{\perp} + \Delta\sigma_{\parallel}}{2} - \frac{1}{2}\sqrt{(\Delta\sigma_{\perp} - \Delta\sigma_{\parallel})^2 + 4\Delta\tau_{\parallel}^2} \quad (4.3.3)$$

It is not always obvious which of these equations will result in the largest calculated fatigue damage for example from a time domain simulation of stress ranges. Therefore, it is recommended to calculate the fatigue damage based on all three equations and select the largest of the damages as being representative for the calculated fatigue damage at the considered hot spot.

$\Delta\sigma_1$ and $\Delta\sigma_2$ may first be calculated without use of absolute sign to achieve correct stress ranges. This means that the stress range in the second equation in equation (4.3.1) is derived as:

$$\Delta\sigma_1 = \sigma_{1,\text{max}} - \sigma_{\text{min}} \quad (4.3.4)$$

where σ_{min} is calculated in the same direction as the principal stress with $\sigma_{1,\text{max}}$. The same procedure may be used to derive the stress range in the third equation in equation (4.3.1).

The equation for effective stress is made to account for the situation with fatigue cracking along a weld toe as shown in [Figure 2-3](#) and fatigue cracking when the principal stress direction is more parallel with the weld toe as shown in [Figure 2-4](#).

Method B

For modelling with shell elements without any weld included in the model the hot spot stress is taken as the stress at the read out point 0.5 t away from the intersection line.

For modelling with three-dimensional elements with the weld included in the model the hot spot stress is taken as the stress at the read out point 0.5 t away from the weld toe.

The effective hot spot stress range is derived as:

$$\Delta\sigma_{Eff} = \max \begin{cases} 1.12\sqrt{\Delta\sigma_{\perp}^2 + 0.81\Delta\tau_{//}^2} \\ 1.12\alpha|\Delta\sigma_1| \\ 1.12\alpha|\Delta\sigma_2| \end{cases} \quad (4.3.5)$$

where:

α , $\Delta\sigma_1$ and $\Delta\sigma_2$ are explained under method A.

The equation for effective stress is made to account for the situation with fatigue cracking along a weld toe as shown in [Figure 2-3](#) and fatigue cracking when the principal stress direction is more parallel with the weld toe as shown in [Figure 2-4](#).

A numerical analysis procedure for fatigue assessment using rainflow counting is wanted. It is understood that the main principal stress direction may change even if the main global load direction is kept constant during the considered time interval. Some guidance on this is included in [\[F.12\]](#).

The stress direction should be considered constant within each time series that is analysis. However, the fatigue damages from different time series with different stress directions may be added for calculation of total fatigue damage.

4.3.4.2 Hot spot stress derivation at connections with steep stress gradients

The linear extrapolation technique for approximation of the structural stress at the hot spot may sometimes under-estimate the structural hot spot stress. Examples of this can be welded attachments to thick plates and plates with attachments placed symmetrically on each side of the plate. This may also include the stress at hot spot type b in [Figure 4-4](#) where the calculated hot spot stress should not depend on the plate thickness. When the plate thickness is increased, the extrapolation points using linearization are moved away from the hot spot and the calculated hot spot stress becomes reduced. Therefore, more accurate techniques for stress determination at these details are recommended for critical components that requires a high safety margin.

Multi-grid strip gauges are sometimes used in fatigue testing of structural details with a pronounced non-linear structural stress increase towards the hot spot. Then the strains at positions 0.4 t, 0.9 t and 1.4 t can be used together with a quadratic extrapolation to derive the hot spot strain at the weld toe. The same procedure can also be used to derive the hot spot stress from fine element models of type a in [Figure 4-4](#). The stresses should be derived from different elements at positions 0.4 t, 0.9 t and 1.4 t from the weld toe. This method is recommended for cases of pronounced non-linear structural stress increase towards the hot spot and for thick-walled structures.

$$\sigma_{hot\ spot} = 2.52 \cdot \sigma_{0.4t} - 2.24 \cdot \sigma_{0.9t} + 0.72 \cdot \sigma_{1.4t} \quad (4.3.6)$$

For fine mesh models with element length not more than 4 mm of type b in [Figure 4-4](#) the hot spot stress may be derived from stress points 4 mm, 8 mm and 12 mm using quadratic extrapolation. It is recommended to include the weld in the model when using this methodology with so small elements.

$$\sigma_{hot\ spot} = 3 \cdot \sigma_{4\ mm} - 3 \cdot \sigma_{8\ mm} + \sigma_{12\ mm} \quad (4.3.7)$$

This hot spot stress calculation for type b hot spot is made independent of the plate thickness. Therefore, a thickness correction on the calculated hot spot stress is not needed. Normally one element through the thickness of the plate is recommended. However, if a solid model with more than one element through

the plate is used, the mean stress through the plate at each stress point should be used in the quadratic extrapolation.

4.3.5 Hot spot S-N curve

It is generally recommended to link the hot spot stress derived from finite element analysis to the D-curve. It should be noted that the definition of the stress field through the plate thickness in [4.3.1] implies that the hot spot stress methodology is not recommended for simple cruciform joints, simple T-joints in plated structures or simple butt joints that are welded from one side only. This is because analysis of such connections with shell elements would result in a hot spot stress equal the nominal stress.

This is illustrated by the shell model shown in [Figure 4-8](#). For stresses in the direction normal to the shell (direction I) there will be no stress flow into the transverse shell plating which is represented only by one plane in the shell model. However, it attracts stresses for in-plane (direction II) shown in [Figure 4-8](#). The described hot spot concept linked with the D-curve gives acceptable results when there is a bracket behind the transverse plate as shown in [Figure 4-4](#) acting with its stiffness in the direction of I ([Figure 4-8](#)).

As the nominal stress S-N curve for direction I is lower than that of the D-curve, it would be non-conservative to use hot spot stresses extracted from finite element analysis for this connection for direction I, whereas it would be acceptable for direction II at position 'a'. Therefore, the nominal stress approach is recommended for use for direction I at position 'c'. This nominal stress can be easily derived from the analysis of these connections, and is recommended to be used with the appropriate detail S-N class as given in [App.A](#). Thus, the calculation can simply be performed by using these nominal S-N curves as hot spot S-N curves for this detail.

For simple cruciform joints, simple T-joints in plated structures or simple butt welds that are welded from one side only it is recommended to use the calculated hot spot stress from finite element analysis together with the representative nominal S-N curves presented for these details as presented in [App.A](#). Thus the relevant nominal S-N curve is defined as the relevant hot spot S-N curve also for these details. This is because analysis of such connections with shell and solid elements would result in a hot spot stress equal the nominal stress.

It should also be noted that fabrication tolerances are most important just for these joints (butt welds and cruciform joints) and hence shall be considered in a fatigue assessment. When misalignments exceed the values explicitly included in the S-N curve, it is recommended that appropriate stress concentration factors are applied to the analysis results, or the analysis should explicitly model misalignments in a conservative way.

A similar situation occurs when a brace with a simple ring stiffener is analysed. The hot spot stress will include the effect of decreased stress on the inside and increased stress on the outside due to the circumferential stiffness of the ring. However, the ring will not attract stress normal to its plane. Therefore, a lower S-N curve than D shall be used from the tables of S-N classification in [App.A](#) (this typically results in an E or F- curve depending on the thickness of the stiffener). From a finite element analysis using shell elements the largest stress at the node at the shell-ring stiffener interface should be used as nominal stress. This is important at an outside ring stiffener in order to include the bending stress in the shell due to its deformed shape, see [Figure 3-14](#). See the example fatigue analysis of the drum in [\[F.13\]](#). However, the S-N curve D is appropriate where a longitudinal stiffener ends at a circumferential ring stiffener.

These considerations also apply to the assessment of fillet welds, and for connections such as gusset joints analysed by finite element methods, see [\[3.3.12\]](#). See also the example calculation in [\[F.16\]](#).

4.3.6 Derivation of effective hot spot stress from finite element analysis

At hot spots with significant plate bending one might derive an effective hot spot stress for fatigue assessment based on the following equation:

$$\Delta\sigma_{e,\text{hot spot}} = \Delta\sigma_{a,\text{hot spot}} + 0.60\Delta\sigma_{b,\text{hot spot}} \quad (4.3.8)$$

where:

$\Delta\sigma_{a,\text{hot spot}}$ = membrane stress

$\Delta\sigma_{b,\text{hot spot}}$ = bending stress.

The reduction factor on the bending stress can be explained by redistribution of loads to other areas during crack growth while the crack tip is growing into a region with reduced stress. The effect is limited to areas with a localised stress concentration, which occurs for example at a hopper corner in a ship shaped structure. However, in a case where the stress variation along the weld is small, the difference in fatigue life between axial loading and pure bending is much smaller. Therefore it should be noted that it is not correct to generally reduce the bending part of the stress to 60%. This shall be restricted to cases with a pronounced stress concentration (where the stress distribution under fatigue crack development is more similar to a displacement controlled situation than that of a load controlled development). Thus, it should be noted that its use in practise is considered to be rather limited.

The hot spot stress at a longitudinal stiffener between transverse frames in a floating structure subjected to varying transverse pressure is an example where redistribution of stress during crack growth will not occur and where a reduction factor on the bending stress cannot be used. Furthermore, fatigue testing of tubular joints implies that the actual stress field through the thickness is already included in the fatigue test data and the S-N curve for tubular joints, thus, this reduction factor should not be used together with this S-N curve even if the hot spot stress is derived from a finite element analysis.

The use of this reduction factor may be documented by fracture mechanics analysis as shown in /41/, /103/. It is important to use realistic initial defect sizes for such calculation in order to derive results that are on the safe side, see guidance in [DNVGL-RP-C210](#), /107/.

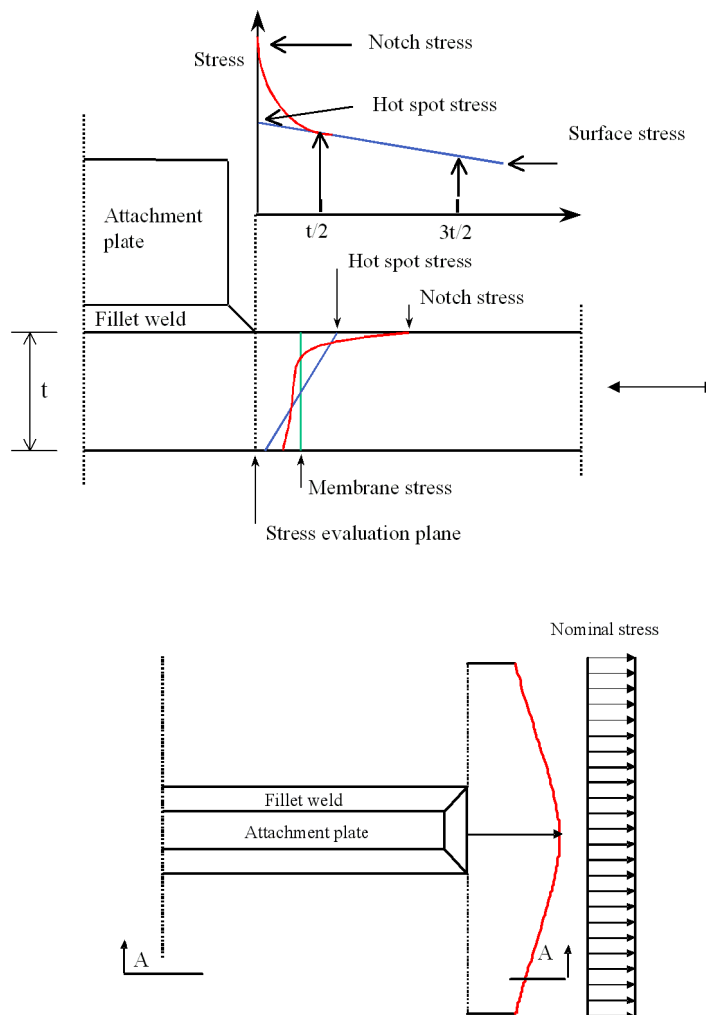


Figure 4-2 Schematic stress distribution at a hot spot

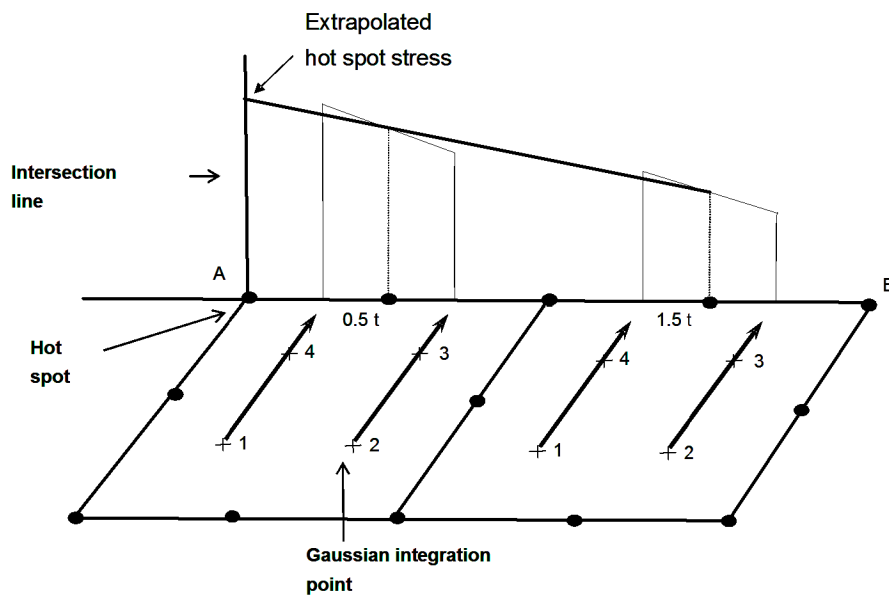


Figure 4-3 Example of derivation of hot spot stress

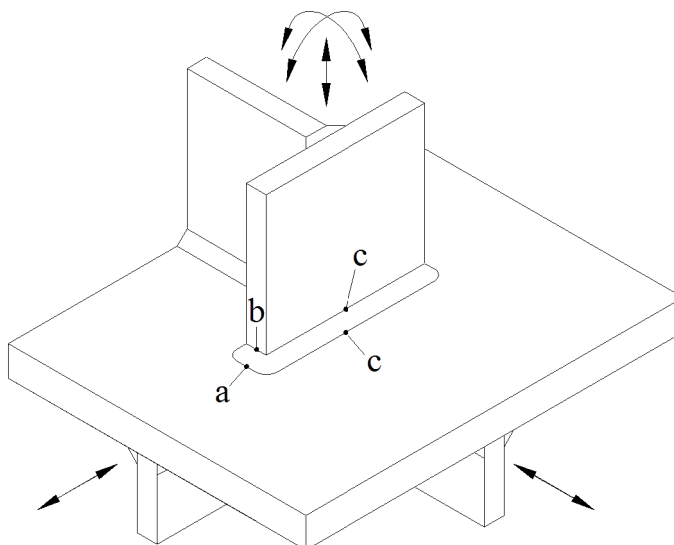


Figure 4-4 Different hot spot positions

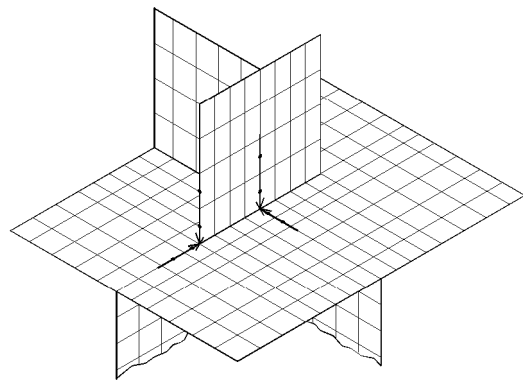


Figure 4-5 Stress extrapolation in a three-dimensional finite element shell model to the weld toe

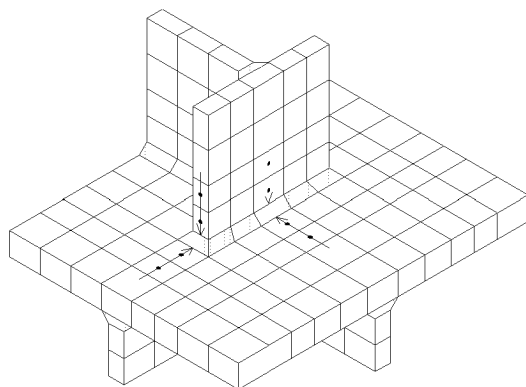


Figure 4-6 Stress extrapolation in a three-dimensional finite element solid model to the weld toe

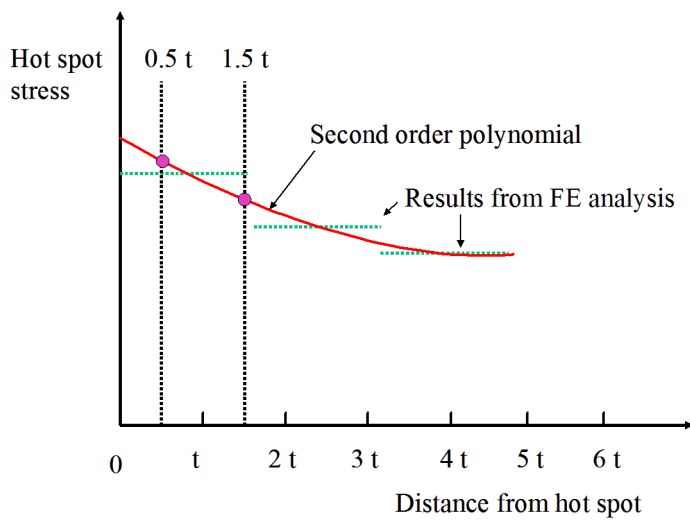


Figure 4-7 Derivation of hot spot stress for element size different from $t \times t$

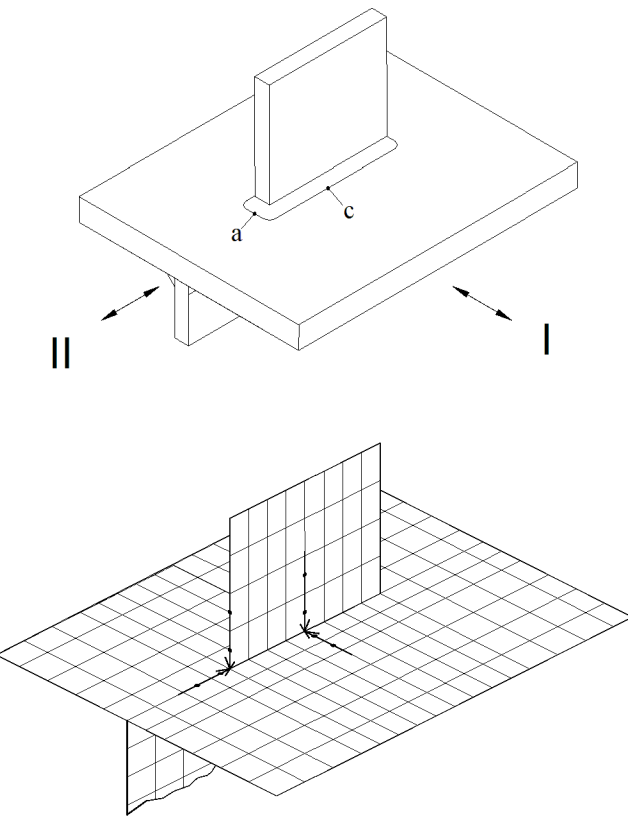


Figure 4-8 Different stress flow normal to and in plane of a shell element model which implies use of different hot spot S-N curves for hot spot c as compared with hot spot a

4.3.7 Verification of analysis methodology

The analysis methodology may be verified based on analysis of details with derived target hot spot stress. Such details with target hot spot stress are shown in [F.11].

4.3.8 Procedure for analysis of web stiffened cruciform connections

A number of FE analyses using models with three-dimensional elements and models with shell elements have been performed of web stiffened cruciform joints such as typical found at hopper connections, at stringer heels and at joints connecting deck structures to vertical members in ship structures using shell elements, see Figure 4-9. The weld leg length is a parameter that has been included in these analyses. Based on the result from these analyses a methodology for derivation of hot spot stress at welded connections using shell finite element models has been developed.

It should be noted that the procedure described in the following is limited to the plate flange connection. Other hot spots as indicated in Figure 4-9 should be checked according to the general procedure given in [4.3].

This procedure is described as follows:

It is assumed that the weld is not included in the shell finite element analysis. The procedure is calibrated such that surface stress can be read out from read out points shifted away from the intersection line at a position of the actual weld toe. The distance from the intersection line to the weld toe is obtained as:

$$x_{shift} = \frac{t_1}{2} + x_{wt} \quad (4.3.9)$$

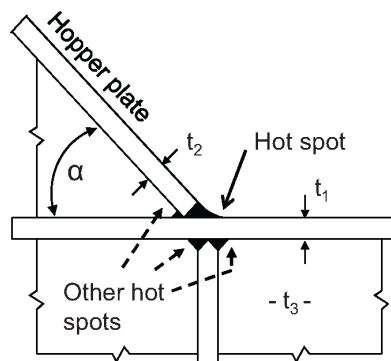
where:

t_1 = plate thickness of plate welded to the plate number 1 in Figure 4-10. See also [F.11]

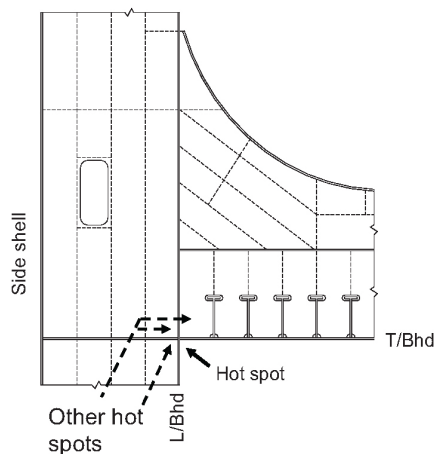
x_{wt} = fillet weld leg length.

The stress at the shift position is derived directly from the analysis (without any extrapolation of stresses). The surface stress (including membrane and bending stress) is denoted $\sigma_{surface}(x_{shift})$. The membrane stress and the bending stress are denoted $\sigma_{membrane}(x_{shift})$ and $\sigma_{bending}(x_{shift})$ respectively.

a) Hopper knuckle in tanker:



b) Heel of stringer in tanker:



c) Connection between deck web frame and side web frame in vehicle carrier:

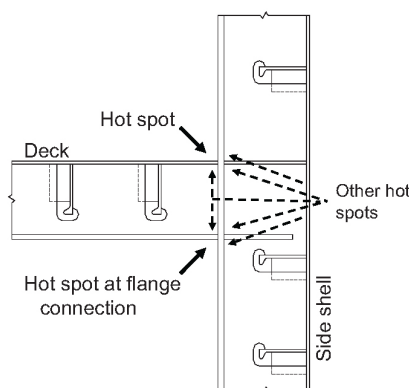


Figure 4-9 Example of web stiffened cruciform joints

The hot spot stress is derived as:

$$\sigma_{\text{hot spot}} = (\sigma_{\text{membrane}}(x_{\text{shift}}) + \sigma_{\text{bending}}(x_{\text{shift}}) * 0.60) * \beta \quad (4.3.10)$$

where:

$$\sigma_{\text{bending}}(x_{\text{shift}}) = \sigma_{\text{surface}}(x_{\text{shift}}) - \sigma_{\text{membrane}}(x_{\text{shift}}) \quad (4.3.11)$$

For $\alpha = 45^\circ$ connections a correction factor is derived as:

$$\beta = 1.07 - 0.15 \frac{x_{\text{wt}}}{t_1} + 0.22 \left(\frac{x_{\text{wt}}}{t_1} \right)^2 \quad (4.3.12)$$

For $\alpha = 60^\circ$ connections a correction factor is derived as:

$$\beta = 1.09 - 0.16 \frac{x_{\text{wt}}}{t_1} + 0.36 \left(\frac{x_{\text{wt}}}{t_1} \right)^2 \quad (4.3.13)$$

For $\alpha = 90^\circ$ connections a correction factor is derived as:

$$\beta = 1.20 + 0.04 \frac{x_{\text{wt}}}{t_1} + 0.30 \left(\frac{x_{\text{wt}}}{t_1} \right)^2 \quad (4.3.14)$$

The procedure is calibrated for $0 \leq x_{\text{wt}}/t_1 \leq 1.0$.

The derived hot spot stress shall be entered the hot spot S-N curve for welded connections.

The analysis procedure is illustrated in [Figure 4-11](#).

Other hot spots located in way of the web as indicated in [Figure 4-9](#) can be checked by the following procedure: the maximum principal surface stress defined at a distance $x_h = t_3/2 + x_{\text{wt}}$ (where t_3 is web thickness and x_{wt} is the smallest value for the two welds meeting in the corner) from the crossing intersection lines to the hot spot and not closer to the intersection lines than $t_3/2$, see [Figure 4-12](#), should be used for fatigue evaluation. This stress should be combined with nominal stress S-N curves E or F for cruciform joints as presented in [Table A-7](#) details 8-10.

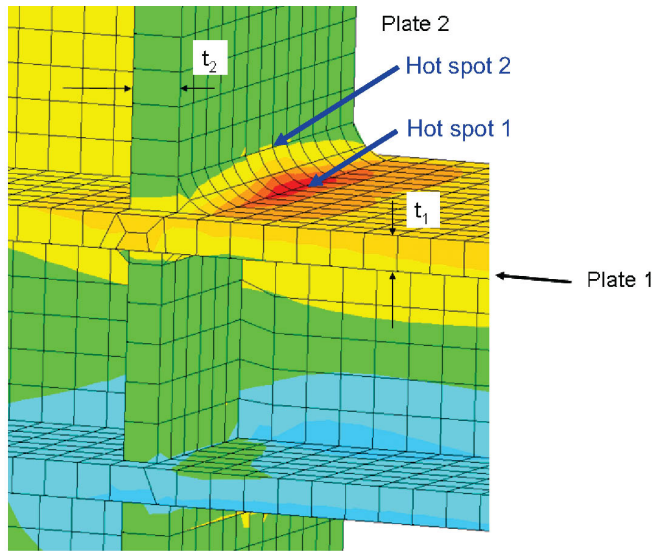


Figure 4-10 Three dimensional model used for calibration of analysis procedure

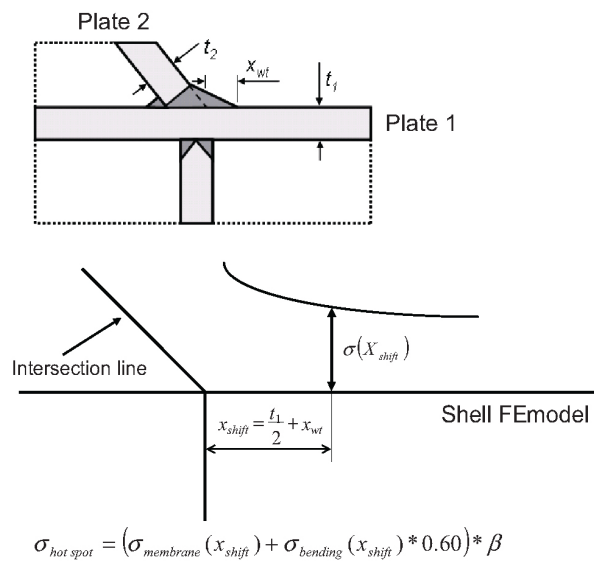


Figure 4-11 Illustration of procedure for derivation of hot spot stress using shell finite element model

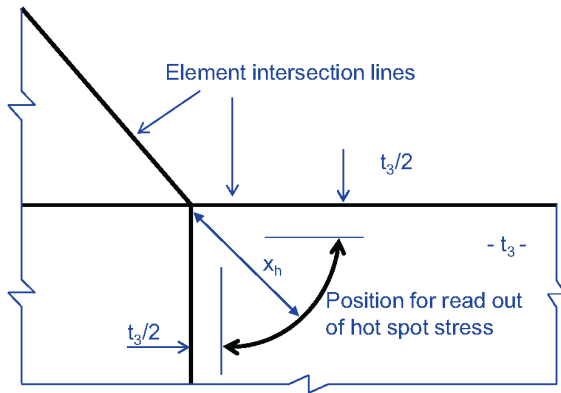


Figure 4-12 Read out of hot spot stress for other hot spots in Figure 4-9

4.3.9 Analysis of welded penetrations

Finite element analysis is normally used to analyse plated structures in floating offshore structures. The welded penetrations are normally not included in the analysis models due to modelling time and analysis capacity. At a position of a penetration a two-dimensional stress field is calculated using shell elements for modelling of the plated structures. This implies stresses in x- and y-direction in the coordinate system of the element and a shear stress. From these stresses the principal stresses can be calculated as:

$$\Delta\sigma_1 = \frac{\Delta\sigma_x + \Delta\sigma_y}{2} + \frac{1}{2}\sqrt{(\Delta\sigma_x - \Delta\sigma_y)^2 + 4\Delta\tau_{xy}^2} \quad (4.3.15)$$

$$\Delta\sigma_2 = \frac{\Delta\sigma_x + \Delta\sigma_y}{2} - \frac{1}{2}\sqrt{(\Delta\sigma_x - \Delta\sigma_y)^2 + 4\Delta\tau_{xy}^2}$$

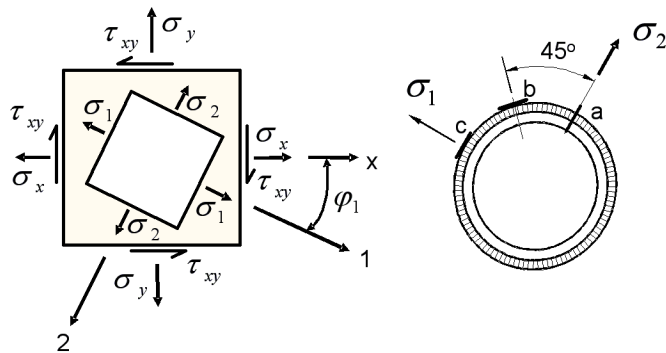


Figure 4-13 Hot spot locations around penetration relative to principal stress direction

Stresses for fatigue design at position a in Figure 4-13

For a single stress state the hot spot stress at position a in Figure 4-13 can be derived from the graphs in Figure C-3 and Figure C-4 in App.C for hot spot position shown in left part of Figure 4-14. These graphs can be used to calculate the stress range due to the first principal stress.

This principal stress will also create a parallel stress at position c in Figure 4-13 as shown in Figure 4-14. The graph in Figure C-15 can be used to calculate the hot spot stress at position a (Figure 4-13) for the second principal stress (shown to the right in Figure 4-14).

Then the resulting hot spot stress due to the first and the second principal stresses are derived by summation of derived hot spot stresses. Finally this hot spot stress can be entered into the curve C for calculation of fatigue damage.

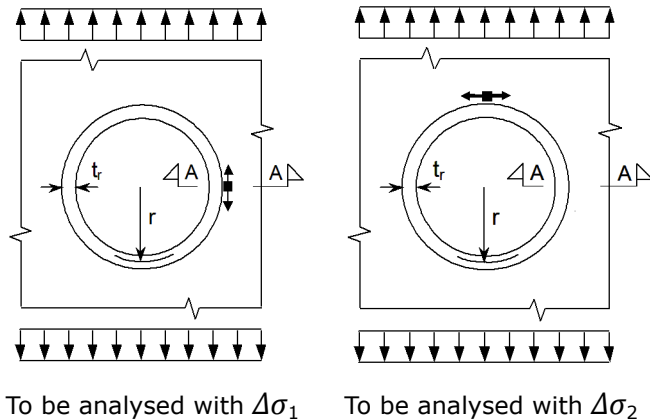


Figure 4-14 Stresses required for derivation of hot spot stress at position a in Figure 4-13

Stresses for fatigue design at position b) in Figure 4-13

The stress components normal to and parallel with the weld toe and the shear stress (see Figure 3-4 c for notations) are evaluated for first principal stress and for the second principal stress shown in Figure 4-13 separately. Then these stress components are added together before they are inserted into equation (4.3.14) and equation (4.3.15).

Then the principal stresses at position b in Figure 4-13 can be calculated as:

$$\Delta\sigma_{1b} = \frac{\Delta\sigma_n + \Delta\sigma_{\parallel p}}{2} + \frac{1}{2}\sqrt{(\Delta\sigma_n - \Delta\sigma_{\parallel p})^2 + 4\Delta\tau_{\parallel p}^2} \quad (4.3.16)$$

$$\Delta\sigma_{2b} = \frac{\Delta\sigma_n + \Delta\sigma_{\parallel p}}{2} - \frac{1}{2}\sqrt{(\Delta\sigma_n - \Delta\sigma_{\parallel p})^2 + 4\Delta\tau_{\parallel p}^2}$$

Finally the effective hot spot stress at position b is calculated as:

$$\Delta\sigma_{Eff} = \max \begin{cases} \sqrt{\Delta\sigma_\perp^2 + 0.81\Delta\tau_\parallel^2} \\ 0.90|\Delta\sigma_1| \\ 0.90|\Delta\sigma_2| \end{cases} \quad (4.3.17)$$

Then this stress range is entered the hot spot stress curve D.

Stresses for fatigue design at position c) in Figure 4-13

Graphs for stress concentration factors for the conditions shown in Figure 4-15 are required for calculation of hot spot stress at position c in Figure 4-13. One set of stress concentration factors is combined with the first principal stress and another set of stress concentration factors is combined with the second principal stress, see graphs in App.C. Then these hot spot stresses are added together before the D-curve is entered for calculation of fatigue damage.

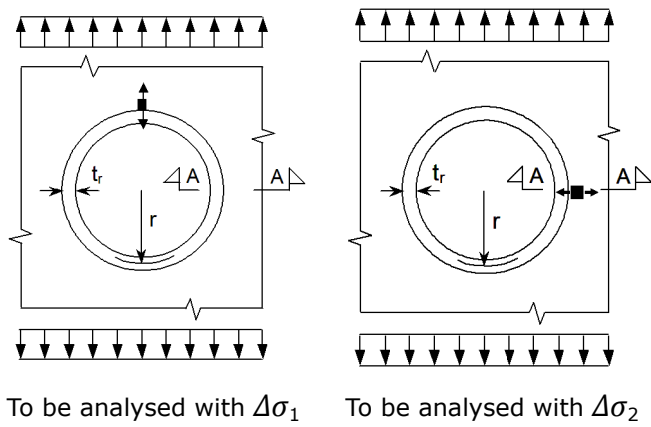


Figure 4-15 Stresses required for derivation of hot spot stress at position c in Figure 4-13

SECTION 5 SIMPLIFIED FATIGUE ANALYSIS

5.1 General

The long term stress range distribution may be presented as a two-parameter Weibull distribution:

$$Q(\Delta\sigma) = \exp\left[-\left(\frac{\Delta\sigma}{q}\right)^h\right] \quad (5.1.1)$$

where:

Q = probability for exceedance of the stress range $\Delta\sigma$

h = Weibull shape parameter

q = Weibull scale parameter is defined from the stress range level, $\Delta\sigma_0$, as:

$$q = \frac{\Delta\sigma_0}{(\ln n_0)^{1/h}} \quad (5.1.2)$$

$\Delta\sigma_0$ is the largest stress range out of n_0 cycles.

When the long-term stress range distribution is defined applying Weibull distributions for the different load conditions, and a one-slope S-N curve is used, the fatigue damage is given by:

$$D = \frac{v_0 T_d}{\bar{a}} q^m \Gamma(1 + \frac{m}{h}) \leq \eta \quad (5.1.3)$$

where:

T_d = design life in seconds

h = Weibull stress range shape distribution parameter

q = Weibull stress range scale distribution parameter

v_0 = average zero up-crossing frequency

$\Gamma(1 + \frac{m}{h})$ = gamma function. Values of the gamma function are listed in [Table 5-1](#).

Use of one slope S-N curves leads to results on the safe side for calculated fatigue lives (with slope of curve at $N < 10^6 - 10^7$ cycles).

For expressions for calculation of fatigue damage using bi-linear S-N curves see [\[F.13\]](#).

Table 5-1 Numerical values for $\Gamma(1+m/h)$

h	$m = 3.0$	h	$m = 3.0$	h	$m = 3.0$
0.60	120.000	0.77	20.548	0.94	7.671
0.61	104.403	0.78	19.087	0.95	7.342
0.62	91.350	0.79	17.772	0.96	7.035
0.63	80.358	0.80	16.586	0.97	6.750
0.64	71.048	0.81	15.514	0.98	6.483
0.65	63.119	0.82	14.542	0.99	6.234
0.66	56.331	0.83	13.658	1.00	6.000
0.67	50.491	0.84	12.853	1.01	5.781
0.68	45.442	0.85	12.118	1.02	5.575
0.69	41.058	0.86	11.446	1.03	5.382
0.70	37.234	0.87	10.829	1.04	5.200
0.71	33.886	0.88	10.263	1.05	5.029
0.72	30.942	0.89	9.741	1.06	4.868
0.73	28.344	0.90	9.261	1.07	4.715
0.74	26.044	0.91	8.816	1.08	4.571
0.75	24.000	0.92	8.405	1.09	4.435
0.76	22.178	0.93	8.024	1.10	4.306

5.2 Fatigue design charts

Design charts for steel components in air and in seawater with cathodic protection are shown in [Figure 5-1](#) and [Figure 5-2](#) respectively. These charts have been derived based on the two slopes S-N curves given in this RP and calculated fatigue damage using equation (F.12.1). The corresponding numerical values are given in [Table 5-2](#) and [Table 5-3](#).

These design charts have been derived based on an assumption of an allowable fatigue damage $\eta = 1.0$ during 10^8 cycles (20 years service life which corresponds to an average cycling period of 6.3 sec.). For design with other allowable fatigue damages, η , the allowable stress from the design charts should be reduced by factors derived from [Table 5-4](#) and [Table 5-5](#) for conditions in air and [Table 5-6](#) and [Table 5-7](#) for conditions in seawater with cathodic protection.

The fatigue utilisation factor h as a function of design life and design fatigue factor (DFF) is given in [Table 5-8](#).

The stresses derived here correspond to the reference thickness. For thickness larger than the reference thickness, an allowable extreme stress range during 10^8 cycles may be obtained as:

$$\sigma_{0,t} = \sigma_{0,\text{tref}} \left(\frac{t_{\text{ref}}}{t} \right)^k \quad (5.2.1)$$

where:

k = thickness exponent, see [\[2.4\]](#) and [Table 2-1](#), [Table 2-2](#) and [Table 2-3](#)

$\sigma_{0,\text{tref}}$ = allowable stress as derived from [Table 5-2](#) and [Table 5-3](#).

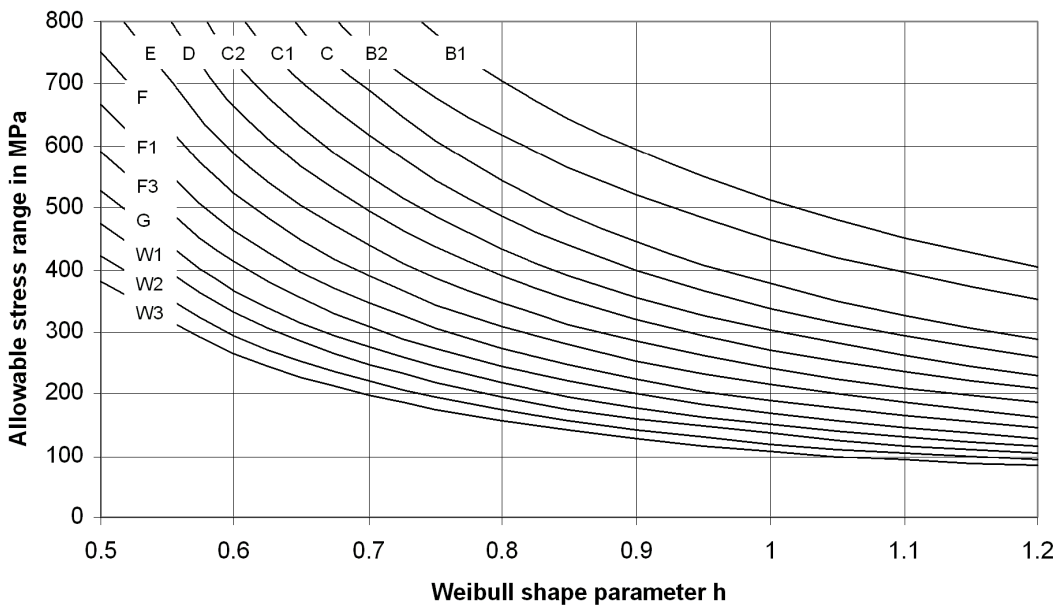


Figure 5-1 Allowable extreme stress range during 10^8 cycles for components in air

Table 5-2 Allowable extreme stress range in [MPa] during 10^8 cycles for components in air

S-N curves	Weibull shape parameter h							
	0.50	0.60	0.70	0.80	0.90	1.00	1.10	1.20
B1	1449.3	1092.2	861.2	704.7	594.1	512.9	451.4	403.6
B2	1268.1	955.7	753.6	616.6	519.7	448.7	394.9	353.1
C	1319.3	919.6	688.1	542.8	445.5	377.2	326.9	289.0
C1	1182.0	824.0	616.5	486.2	399.2	337.8	292.9	258.9
C2	1055.3	735.6	550.3	434.1	356.3	301.6	261.5	231.1
D	949.9	662.1	495.4	390.7	320.8	271.5	235.4	208.1
E	843.9	588.3	440.2	347.2	284.9	241.2	209.2	184.9
F	749.2	522.3	390.8	308.2	253.0	214.1	185.6	164.1
F1	664.8	463.4	346.7	273.5	224.5	190.0	164.7	145.6
F3	591.1	412.0	308.3	243.2	199.6	169.0	146.5	129.4
G	527.6	367.8	275.2	217.1	178.2	150.8	130.8	115.6
W1	475.0	331.0	247.8	195.4	160.4	135.8	117.7	104.0
W2	422.1	294.1	220.1	173.6	142.5	120.6	104.6	92.5
W3	379.9	264.8	198.2	156.0	128.2	108.6	94.2	83.2
T	1210.3	843.6	631.2	497.8	408.5	345.8	299.8	264.9

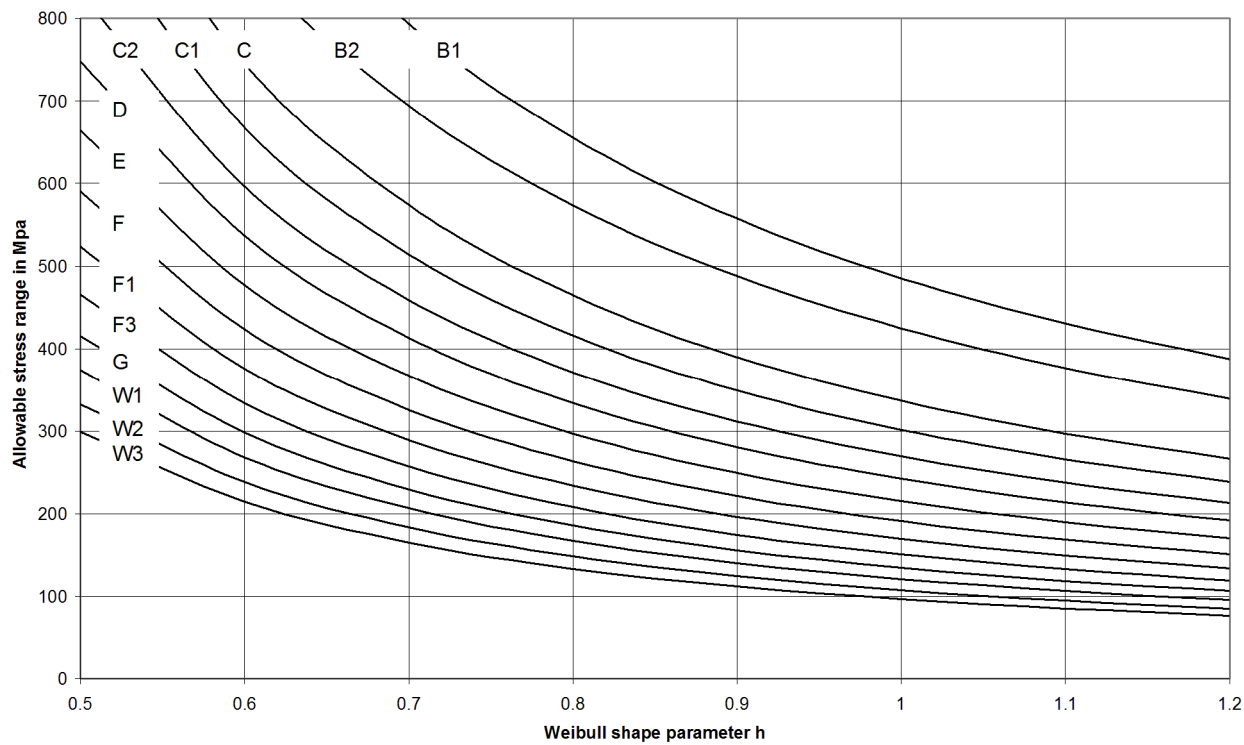


Figure 5-2 Allowable extreme stress range during 10^8 cycles for components in seawater with cathodic protection

Table 5-3 Allowable extreme stress range in [MPa] during 10^8 cycles for components in seawater with cathodic protection

S-N curves	Weibull shape parameter h							
	0.50	0.60	0.70	0.80	0.90	1.00	1.10	1.20
B1	1309.8	996.0	793.0	655.2	557.4	485.3	430.5	387.6
B2	1146.0	871.5	693.9	573.3	487.7	424.7	376.6	339.1
C	1038.5	745.5	573.6	464.3	389.8	336.7	297.0	266.5
C1	930.5	668.0	513.9	415.8	349.3	301.5	266.1	238.7
C2	830.7	596.3	458.7	371.3	311.7	269.2	237.6	213.1
D	747.8	536.7	413.0	334.2	280.7	242.4	213.9	191.9
E	664.3	476.9	367.0	297.0	249.3	215.3	190.1	170.5
F	589.8	423.4	325.8	263.6	221.4	191.1	168.6	151.3
F1	523.3	375.7	289.0	233.9	196.4	169.6	149.6	134.3
F3	465.3	334.0	257.0	208.0	174.6	150.9	133.1	119.3

S-N curves	Weibull shape parameter h							
	0.50	0.60	0.70	0.80	0.90	1.00	1.10	1.20
G	415.3	298.2	229.4	185.7	155.9	134.6	118.8	106.6
W1	373.9	268.3	206.6	167.1	140.3	121.2	106.9	95.9
W2	332.3	238.4	183.5	148.5	124.7	107.7	95.0	85.3
W3	299.1	214.7	165.2	133.4	112.2	96.9	85.6	76.7
T	1004.9	714.7	545.4	438.1	365.6	314.1	275.9	246.7

Table 5-4 Reduction factor on stress to correspond with utilisation factor η for B1 and B2 curves in air environment

Fatigue damage utilisation η	Weibull shape parameter h							
	0.50	0.60	0.70	0.80	0.90	1.00	1.10	1.20
0.10	0.570	0.575	0.581	0.587	0.592	0.597	0.602	0.603
0.20	0.674	0.678	0.682	0.686	0.690	0.694	0.698	0.701
0.22	0.690	0.693	0.697	0.701	0.705	0.709	0.712	0.715
0.27	0.725	0.728	0.731	0.735	0.738	0.742	0.745	0.748
0.30	0.744	0.747	0.750	0.753	0.756	0.759	0.762	0.765
0.33	0.762	0.764	0.767	0.770	0.773	0.776	0.778	0.781
0.40	0.798	0.800	0.803	0.805	0.808	0.810	0.812	0.815
0.50	0.843	0.845	0.846	0.848	0.850	0.852	0.854	0.856
0.60	0.882	0.883	0.884	0.886	0.887	0.888	0.890	0.891
0.67	0.906	0.907	0.908	0.909	0.910	0.911	0.912	0.913
0.70	0.916	0.917	0.917	0.919	0.920	0.920	0.921	0.922
0.80	0.946	0.947	0.947	0.948	0.949	0.949	0.950	0.950
1.00	1.000	1.000	1.000	1.000	1.000	1.000	1.000	1.000

Table 5-5 Reduction factor on stress to correspond with utilisation factor η for C - W3 curves in air environment

Fatigue damage utilisation η	Weibull shape parameter h							
	0.50	0.60	0.70	0.80	0.90	1.00	1.10	1.20
0.10	0.497	0.511	0.526	0.540	0.552	0.563	0.573	0.582
0.20	0.609	0.620	0.632	0.642	0.652	0.661	0.670	0.677
0.22	0.627	0.638	0.648	0.659	0.668	0.677	0.685	0.692
0.27	0.661	0.676	0.686	0.695	0.703	0.711	0.719	0.725

Fatigue damage utilisation η	Weibull shape parameter h							
	0.50	0.60	0.70	0.80	0.90	1.00	1.10	1.20
0.30	0.688	0.697	0.706	0.715	0.723	0.730	0.737	0.743
0.33	0.708	0.717	0.725	0.733	0.741	0.748	0.754	0.760
0.40	0.751	0.758	0.765	0.772	0.779	0.785	0.790	0.795
0.50	0.805	0.810	0.816	0.821	0.826	0.831	0.835	0.839
0.60	0.852	0.856	0.860	0.864	0.868	0.871	0.875	0.878
0.67	0.882	0.885	0.888	0.891	0.894	0.897	0.900	0.902
0.70	0.894	0.897	0.900	0.902	0.905	0.908	0.910	0.912
0.80	0.932	0.934	0.936	0.938	0.939	0.941	0.942	0.944
1.00	1.000	1.000	1.000	1.000	1.000	1.000	1.000	1.000

Table 5-6 Reduction factor on stress to correspond with utilisation factor η for B1 and B2 curves in seawater with cathodic protection

Fatigue damage utilisation η	Weibull shape parameter h							
	0.50	0.60	0.70	0.80	0.90	1.00	1.10	1.20
0.10	0.583	0.593	0.602	0.610	0.617	0.621	0.625	0.627
0.20	0.684	0.691	0.699	0.705	0.711	0.715	0.718	0.720
0.22	0.699	0.706	0.714	0.720	0.725	0.729	0.732	0.735
0.27	0.733	0.740	0.746	0.752	0.757	0.760	0.763	0.766
0.30	0.751	0.758	0.764	0.769	0.773	0.777	0.780	0.782
0.33	0.768	0.774	0.780	0.785	0.789	0.792	0.795	0.792
0.40	0.804	0.809	0.814	0.818	0.822	0.825	0.827	0.829
0.50	0.848	0.851	0.855	0.858	0.861	0.864	0.866	0.867
0.60	0.885	0.888	0.891	0.893	0.896	0.897	0.899	0.900
0.67	0.909	0.911	0.913	0.915	0.917	0.919	0.920	0.921
0.70	0.918	0.920	0.922	0.924	0.926	0.927	0.928	0.929
0.80	0.948	0.949	0.950	0.952	0.953	0.954	0.955	0.955
1.00	1.000	1.000	1.000	1.000	1.000	1.000	1.000	1.000

Table 5-7 Reduction factor on stress to correspond with utilisation factor η for C - W3 curves in seawater with cathodic protection

Fatigue damage utilisation η	Weibull shape parameter h							
	0.50	0.60	0.70	0.80	0.90	1.00	1.10	1.20
0.10	0.535	0.558	0.577	0.593	0.605	0.613	0.619	0.623
0.20	0.640	0.659	0.676	0.689	0.699	0.707	0.713	0.717
0.22	0.657	0.675	0.691	0.703	0.713	0.721	0.727	0.731
0.27	0.694	0.710	0.725	0.736	0.745	0.752	0.758	0.762
0.30	0.714	0.729	0.743	0.754	0.763	0.769	0.775	0.779
0.33	0.732	0.747	0.760	0.770	0.779	0.785	0.790	0.794
0.40	0.772	0.785	0.796	0.805	0.812	0.818	0.822	0.825
0.50	0.821	0.831	0.840	0.847	0.853	0.858	0.862	0.864
0.60	0.864	0.872	0.879	0.885	0.889	0.893	0.896	0.898
0.67	0.892	0.898	0.903	0.908	0.912	0.915	0.917	0.919
0.70	0.903	0.908	0.913	0.917	0.921	0.924	0.926	0.927
0.80	0.938	0.941	0.945	0.947	0.949	0.951	0.953	0.954
1.00	1.000	1.000	1.000	1.000	1.000	1.000	1.000	1.000

Table 5-8 Utilisation factors η as function of design life and design fatigue factor

Design fatigue factor	Design life in years						
	5	10	15	20	25	30	50
1	4.0	2.0	1.33	1.00	0.80	0.67	0.40
2	2.0	1.0	0.67	0.50	0.40	0.33	0.20
3	1.33	0.67	0.44	0.33	0.27	0.22	0.13
5	0.80	0.40	0.27	0.20	0.16	0.13	0.08
10	0.40	0.20	0.13	0.10	0.08	0.07	0.04

5.3 Example of use of design charts

The allowable stress range in a deck structure of a FPSO shall be determined.

The maximum thickness of the steel plates is 35.0 mm. From DNVGL-CG-0129 a Weibull shape parameter equal 0.97 is determined. It is assumed that details corresponding to a classification F3 is going to be welded to the deck structure.

The design life of the FPSO is 25 years and the operator would like to use a design fatigue factor equal 2.

The detail is in air environment. The following allowable stress range is derived by a linear interpolation of stress ranges for h-values 0.90 and 1.0 in Table 5-2 for S-N curve F3 is obtained:

$$199.6 - (199.6 - 169.0) ((0.97 - 0.90)/(1.0 - 0.90)) = 178.18 \text{ MPa.}$$

This corresponds to an allowable stress for 20 years design life and a DFF equal 1. Then from [Table 5-8](#) an utilisation factor η equal 0.40 is obtained for 25 years service life and a DFF equal 2.0.

Then from [Table 5-5](#) a reduction factor is obtained by linear interpolation between the factors for h-values 0.90 and 1.0 for $\eta = 0.40$. The following reduction factor is obtained:

$$0.779 + (0.785-0.779) ((0.97 - 0.90)/(1.0 - 0.90)) = 0.783.$$

Thus the allowable stress range for a 25 mm thick plate is obtained as $178.18 \cdot 0.783 = 139.55$.

The thickness exponent for a F3 detail is $k = 0.25$ from [Table 2-1](#).

Then the allowable stress range for the 35 mm thick plate is obtained as: $139.55 \cdot (25/35)^{0.25} = 128.29$ MPa.

5.4 Fatigue capacity of connectors

5.4.1 General

This section provides guidance for determining a S-N based fatigue capacity (safe life design) for preloaded connectors. This includes threaded, clamped, collet and dog connectors. Some of these connectors may be remotely operated. Wellhead connectors for XTs and BOPs are included. In many cases, the primary cyclic load for these connectors is cyclic bending. For such cases, the fatigue capacity is conveniently presented in terms of a M-N curve (bending moment range versus cycles to failure). This guidance is limited to establishing the connector design fatigue capacity (M-N curve) for fatigue hot spots (notches) in base materials of connectors subjected to cyclic bending moments.

One of the following methods can be used for determining the connector design fatigue capacity:

- 1) Method 1, by analysis
 - a. Fatigue capacity by analysis, see [\[5.4.4.2\]](#).
- 2) Method 2, by analysis and testing
 - a. Fatigue capacity by analysis validated by strain measurements, see [\[5.4.4.3\]](#)
 - b. Fatigue capacity by analysis in combination with full-scale connector fatigue testing, see [\[5.4.4.4\]](#).
- 3) Method 3, by full-scale connector fatigue testing
 - a. Full-scale connector fatigue tests assessed in accordance with [\[F.7\]](#).

The following terminology is used in this section:

- Analysis based mean M-N curve: established based on analysis only with use of a mean S-N curve for the test environment in accordance with [\[5.4.3\]](#).
- Analysis based design M-N curve: established based on analysis only with use of a design S-N curve (mean - $2s_{\log N}$ curve) for the actual in-service environment in accordance with [\[5.4.3\]](#).
- Connector design fatigue capacity: resultant M-N curve for the actual in-service environment established in accordance with [\[5.4.4\]](#).

5.4.2 Finite element model

The finite element model of the connector can be created based on nominal geometry and use of nominal connector preload. A three-dimensional model should be used for analyses with bending moments, unless it can be documented that an axisymmetric model can be used. The analysis should be performed with large deformations (nonlinear geometry). The calculated stress ranges for fatigue analysis should not be influenced by boundary conditions. Contact surfaces should be included where they influence the stiffness of the connector and the calculated stress ranges for fatigue analysis. Analyses should be performed with friction coefficients based on relevant test data (e.g. material, coating, lubricants and environment). The effect of corrosion should be considered for connector design where corrosion is expected. The effects of pressure should be included in the analysis. Weld overlay and cladding should be included with nominal

dimensions to ensure a realistic load distribution within the connector. Realistic mechanical properties should be used.

The analysis may be performed assuming linear elastic material behaviour. Elastic-plastic analysis may be performed using a true stress-strain curve with a yield strength and tensile strength of 1.15 times its specified minimum values (i.e. 1.15·SMYS and 1.15·SMTS). Actual stress-strain curves or stress-strain curves constructed based on actual yield and tensile strength may be used if available. The true stress-strain curve may be established in accordance with Annex 3-D ASME Section VIII Division 2:2017 /119/. Isotropic hardening should be used. The use of elastic-plastic analysis will allow for local yielding during make-up, pressure testing and for simulating any local yielding that might occur in the first load cycle.

The fatigue analysis of full-scale fatigue tested connectors should be performed using expected friction and expected connector preload. All loads included in the test should be applied to the analysis model (e.g. internal pressure, effective tension and bending moment). For elastic-plastic analysis actual stress-strain curves or stress-strain curves constructed based on actual yield and tensile strength should be used.

A fine mesh should be used in areas of stress concentrations. The use of submodels may be needed. Mesh convergence should be documented.

It is recommended to perform a sensitivity check of essential parameters, e.g., coefficient of friction.

5.4.3 Fatigue analysis

The analysis based mean and/or the design M-N curve should be established according to the following procedure using a finite element model of the connector as described in [5.4.2]:

- 1) Select an S-N curve based on the actual environment and conditions, tensile strength and surface roughness. BM S-N curve in [D.2] is recommended if the fatigue hot spot is not subjected to free corrosion or not likely to be damaged during make-up/break-out or during handling.
- 2) For elastic-plastic analysis include relevant assembly and factory acceptance tests in the sequence they occur (e.g. preload, pressure test). Static service loads such as tension and internal pressure should be included if they reduce the fatigue capacity.
- 3) Apply fully reversed bending moment cycles, i.e. $R = -M_i / +M_i = -1$, until a steady (converged) stress state is achieved (this may require several cycles). For elastic-plastic analysis each bending moment range should be applied independently. This to avoid load sequence effects in the determination of the fatigue capacity. Increasing or decreasing bending moment ranges may be applied if load sequence effects are demonstrated not to be present.
- 4) Calculate the cyclic stresses as:
 - a. Calculate the stress range, $\Delta\sigma$, in accordance with equation (D.2.4) for monotonically increasing bending moment to stress curves.
 - b. If a BM S-N curve for $R = 0$ is used, calculate the mean stress, σ_m , in accordance with equation (D.2.5).
 - c. Calculate the fatigue stress $\Delta\bar{\sigma}$, in accordance with equation (D.2.1):
 - i. The mean stress adjustment factor, f_m , is calculated in accordance with equation (D.2.2) if a BM S-N curve for $R = 0$ is used, else $f_m = 1$.
 - ii. Calculate the notch support factor, f_χ , in accordance with equation (D.2.3) if a BM S-N curve is used, else $f_\chi = 1$.
 - iii. Report the maximum fatigue stress $\Delta\bar{\sigma}$ in each fatigue hot spot.
- 5) Calculate and report the fatigue life for the bending moment range $\Delta M_i = |2M_i|$ using the fatigue stress calculated in step 4c.
- 6) Repeat steps 3 to 5 to establish a M-N curve covering fatigue lives in the range of 10^4 to 10^8 cycles for all hot spots in the connector.

- 7) Construct the M-N curve as a lower bound curve for all fatigue hot spots in the connector (i.e. curve passing through or below the minimum of all M-N data points).
- 8) Report the M-N curve together with the fatigue load capacity, ΔM_c , at 10^6 cycles.

The analysis based M-N curve (in step 8) represents the presence of a through wall fatigue crack due to fatigue crack initiation and subsequent fatigue crack growth from a notch.

5.4.4 Connector fatigue capacity

5.4.4.1 General

The connector design fatigue capacity is determined based on the analysis based design M-N curve in accordance with [5.4.3] and use of a fatigue life reduction factor:

$$\log N = \begin{cases} \log \bar{a}_{\Delta M, 1} - m_1 \log \Delta M = \log \bar{a}_1 - \log RF - m_1 \log \Delta M, & \text{for } \Delta M \geq \Delta M_{1,2} \\ \log \bar{a}_{\Delta M, 2} - m_2 \log \Delta M = \log \bar{a}_2 - \log RF - m_2 \log \Delta M, & \text{for } \Delta M < \Delta M_{1,2} \end{cases} \quad (5.4.1)$$

where:

- N = number of cycles to fatigue failure
- ΔM = applied bending moment range
- $\Delta M_{1,2}$ = bending moment range at change of slope in M-N curve
- $\log \bar{a}_{\Delta M}$ = intercept of the connector fatigue capacity curve with the N axis
- $\log \bar{a}$ = intercept of the analysis based design M-N curve with the N axis
- m = negative inverse slope of the M-N curve
- RF = Fatigue life reduction factor that depends on validation, see [5.4.4.2], [5.4.4.3] and [5.4.4.4].

A single or a multilinear slope M-N curve can be used. The connector design fatigue capacity curve has the same slope(s) as the analysis based M-N curve.

5.4.4.2 Fatigue capacity by analysis (method 1)

The connector design fatigue capacity is established based on the analysis based design M-N curve and use of a fatigue life reduction factor of $RF = 4$ in accordance with equation (5.4.1). This is illustrated in Figure 5-3.

5.4.4.3 Fatigue capacity by analysis validated by strain measurements (method 2a)

A fatigue life reduction factor of $RF = 2$ can be used (as illustrated in Figure 5-3) in equation (5.4.1) when the stress analysis (load to stress curve) has been validated with strain measurements of a full-scale bend test of the connector.

The comparison should cover bending moment loads giving a fatigue life of 10^4 cycles or less as determined by the analysis based design M-N curve. Both the mean stress and the stress range should be compared. This will require that the connector is subjected to a number of quasi-static load cycles. The number of load cycles should be sufficient to obtain a steady state strain behaviour.

The strain measurements should be taken near the identified fatigue hot spots, if possible, and at a selected number of locations away. The cyclic stresses, mean and range, in the full-scale bend test and in the finite element analysis should be within an expected range as to be determined by considering the accuracy of the strain measurement and strain gradients.

5.4.4.4 Fatigue capacity by analysis in combination with full-scale connector testing (method 2b)

A fatigue life reduction of $RF = 1$ can be used in equation (5.4.1) when the analysis based mean M-N curve has been validated to be conservative compared to full-scale connector fatigue test results. Guidance on fatigue test load selection is given in [Table 5-9](#). The connectors should be tested to fatigue failure (i.e. the test load should preferably be above the constant amplitude fatigue limit). It is recommended to establish the analysis based mean M-N curve for the test environment using a log-log linear M-N curve.

Table 5-9 Recommended fatigue test loads

<i>Number of connector fatigue tests</i>	<i>Fatigue test loads</i>
1	Medium
2	Medium and low
3	High, medium and low
4	High, 2 x medium and low
5	High, 2 x medium and 2 x low
6	2 x high, 2 x medium and 2 x low
9	3 x high, 3 x medium and 3 x low
High fatigue load with target fatigue life of $10^5 - 5 \cdot 10^5$	
Medium fatigue load with target fatigue life of $5 \cdot 10^5 - 2 \cdot 10^6$	
Low fatigue load with target fatigue life of $2 \cdot 10^6 - 5 \cdot 10^6$	

The following validation steps applies:

- 1) Establish a target fatigue test curve as

$$\log N_{\text{target}} = \log a + \log F - m \log \Delta M \quad (5.4.2)$$

where:

N_{target} = fatigue life for the target fatigue test curve

$\log a$ = intercept of log N axis for the mean M-N curve for the test environment (e.g. air)

F = fatigue test factor whose value depends on the number of fatigue tests, see [Table 5-10](#).

- 2) Establish the mean M-N curve for the c fatigue test data using the same slope m as the target fatigue test curve as:

$$\log N_{\text{test}} = \log a_{\text{test}} - m \log \Delta M \quad (5.4.3)$$

where:

$$\log a_{\text{test}} = \frac{1}{c} \sum_{i=1}^c \log N_i + \frac{m}{c} \sum_{i=1}^c \log \Delta M_i \quad (5.4.4)$$

- 3) Compare the mean M-N curve for the fatigue test data (step 2) with the target fatigue test curve (step 1). A fatigue life reduction factor of $RF = 1$ may be used in equation (5.4.1) if the mean M-N curve for the test data has a fatigue life in excess of the target fatigue test curve, i.e. $N_{\text{test}} > N_{\text{target}}$.

If the mean M-N curve for the fatigue test data has a fatigue life less than the target fatigue test curve, i.e. $N_{\text{test}} < N_{\text{target}}$, then either of the following is recommended:

- 1) Fatigue analysis should be revised to be more representative of the test results.
- 2) Establish the connector design fatigue capacity in accordance with [F.7] based on full-scale connector fatigue test data.

The use of the target fatigue test curve to validate the use of $RF = 1$ in equation (5.4.1) is illustrated in Figure 5-3.

Table 5-10 Recommended fatigue test factors

<i>Number of connector fatigue tests, c</i>	<i>Fatigue test factor F^a</i>
1	2.13
2	1.71
3	1.55
4	1.46
5	1.40
6	1.36
9	1.29

^a Based on [F.7] $(\log F = x_c s_{\log N} / \sqrt{c})$ using a standard deviation of $s_{\log N} = 0.20$ and 95% confidence level ($x_c = 1.645$).

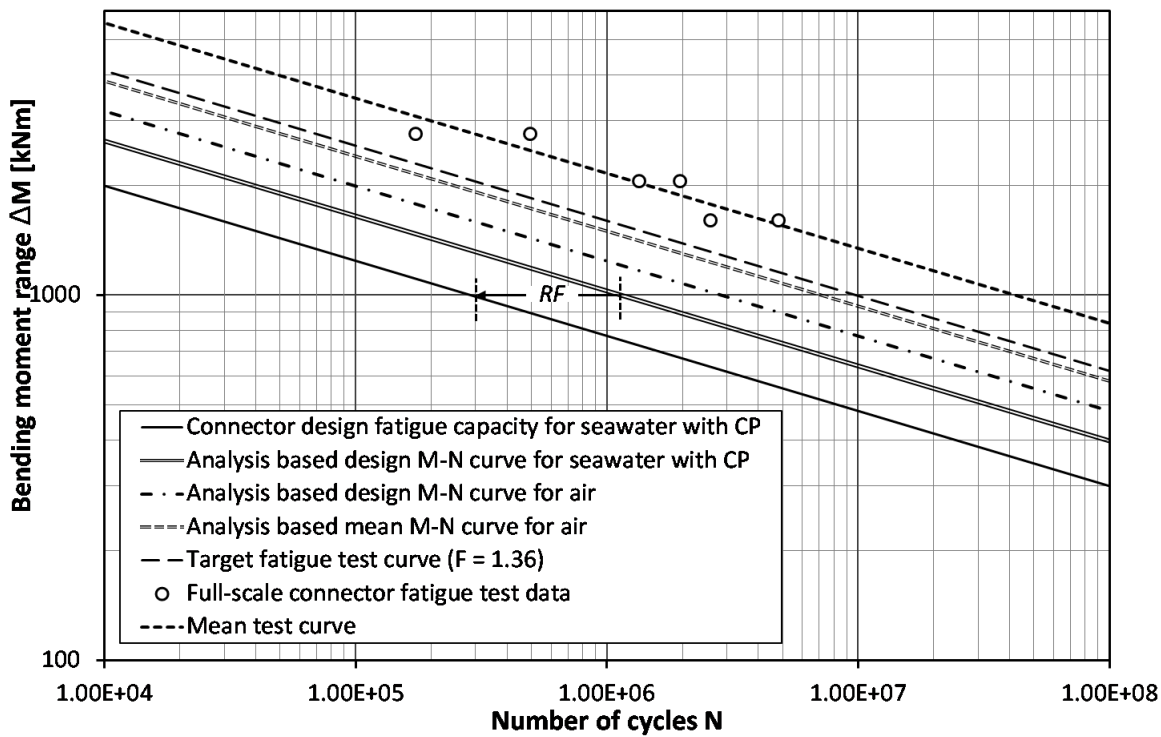


Figure 5-3 Determination of the connector design fatigue capacity for seawater with CP

SECTION 6 FATIGUE ANALYSIS BASED ON FRACTURE MECHANICS

6.1 General on analysis methodology

Fracture mechanics may be used for fatigue analyses as supplement to S-N data, see also [1.4].

Fracture mechanics is recommended for use in assessment of acceptable defects, evaluation of acceptance criteria for fabrication and for planning in-service inspection.

The purpose of such analysis is to document, by means of calculations, that fatigue cracks, which might occur during service life, will not exceed the crack size corresponding to unstable fracture. The calculations should be performed such that the structural reliability by use of fracture mechanics will not be less than that achieved by use of S-N data. This can be achieved by performing the analysis according to the following procedure:

- crack growth parameter C determined as mean plus 2 standard deviation
- a careful evaluation of initial defects that might be present in the structure when taking into account the actual NDE inspection method used to detect cracks during fabrication
- use of geometry functions that are on the safe side
- use of utilisation factors or design fatigue factors (DFFs) similar to those used when the fatigue analysis is based on S-N data.

As crack initiation is not included in the fracture mechanics approach, shorter fatigue life is normally derived from fracture mechanics than by S-N data.

In a case that the results from fracture mechanics analyses cannot be directly compared with S-N data it might be recommended to perform a comparison for a detail where S-N data are available, in order to verify that the assumptions made for the fracture mechanics analyses are acceptable.

The initial crack size to be used in the calculation should be considered in each case, taking account of experienced imperfection or defect sizes for various weldments, geometries, access and reliability of the inspection method. For surface cracks starting from transitions between weld/base material, a crack depth of 0.5 mm (e.g. due to undercuts and micro-cracks at bottom of the undercuts) may be assumed if other documented information about crack depth is not available. See also [DNVGL-RP-C210 /107/](#).

It is normally, assumed that compressive stresses do not contribute to crack propagation. However, for welded connections containing residual stresses, the whole stress range should be applied. Only stress components normal to the propagation plane need to be considered.

The Paris' equation may be used to predict the crack propagation or the fatigue life:

$$\frac{da}{dN} = C(\Delta K)^m \quad (6.1.1)$$

where:

ΔK = $K_{\max} - K_{\min}$

N = number of cycles to failure

a = crack depth. It is here assumed that the crack depth/length ratio is low (less than 1:5)
Otherwise crack growth analysis along two axes is recommended.

C, m = material parameters, see [DNVGL-RP-C210, /107/](#) and BS 7910, /7/.

The stress intensity factor K may be expressed as:

$$K = \sigma g \sqrt{\pi a} \quad (6.1.2)$$

where:

σ = nominal stress in the member normal to the crack

g = factor depending on the geometry of the member, the weld and the crack geometry.

See [DNVGL-RP-C210](#) /107/ and BS 7910 /7/, for further guidelines related to fatigue assessment based on fracture mechanics.

SECTION 7 IMPROVEMENT OF FATIGUE LIFE BY FABRICATION

7.1 General

It should be noted that improvement of the weld toe will not improve the fatigue life if fatigue cracking from the weld root is the most likely failure mode. The considerations made in the following are for conditions where the weld root is not considered to be a critical initiation point. Except for weld profiling ([7.2]) the effect from different improvement methods as given in the following cannot be added.

See *IIW Recommendations /16/, on post weld improvement with respect to tools and execution of the improvement.*

7.2 Weld profiling by machining and grinding

By weld profiling in this section is understood profiling by machining or grinding as profiling by welding only is not considered to be an efficient mean to improve fatigue lives.

In design calculations, the thickness effect may be reduced to an exponent 0.15 provided that the weld is profiled by either machining or grinding to a radius of approximately half the plate thickness, ($T/2$ with stress direction as shown in [Figure 7-2 B](#)).

Where weld profiling is used, the calculated fatigue life can be increased taking account of a reduced local stress concentration factor. A reduced local stress due to weld profiling can be obtained as follows.

When weld profiling is performed, a reduced hot spot stress can be calculated as:

$$\sigma_{Local\ reduced} = \sigma_{Membrane} \alpha + \sigma_{Bending} \beta \quad (7.2.1)$$

where α and β are derived from equation (7.2.2) and equation (7.2.3) respectively.

$$\alpha = 0.47 + 0.17(\tan\phi)^{0.25}(T/R)^{0.5} \quad (7.2.2)$$

$$\beta = 0.60 + 0.13(\tan\phi)^{0.25}(T/R)^{0.5} \quad (7.2.3)$$

For description of geometric parameters see [Figure 7-1](#).

The membrane part and the bending part of the stress shall be separated from the local stress as:

$$\sigma_{Local} = \sigma_{Membrane} + \sigma_{Bending} \quad (7.2.4)$$

where:

$\sigma_{Membrane}$ = membrane stress

$\sigma_{Bending}$ = bending stress.

If a finite element analysis of the considered connection has been performed, the results from this can be used directly to derive membrane stress and bending stress.

For cruciform joints and heavy stiffened tubular joints it may be assumed that the hot spot stress is mainly due to membrane stress.

For simple tubular joints it may be assumed that the hot spot stress in the chord is due to bending only.

However, for X-joints with a large β -ratio there is mainly membrane stress at the hot spot.

The reduced local stress in equation (7.2.1) shall be used together with the same S-N curves as the detail is classified for without weld profiling. (It is assumed that $R/T = 0.1$ without weld profiling for a plate thickness $T = 25 \text{ mm}$.)

In addition the fatigue life can be increased taking account of local toe grinding, see [7.3]. However, the maximum improvement factor from grinding only should then be limited to a factor 2 on fatigue life.

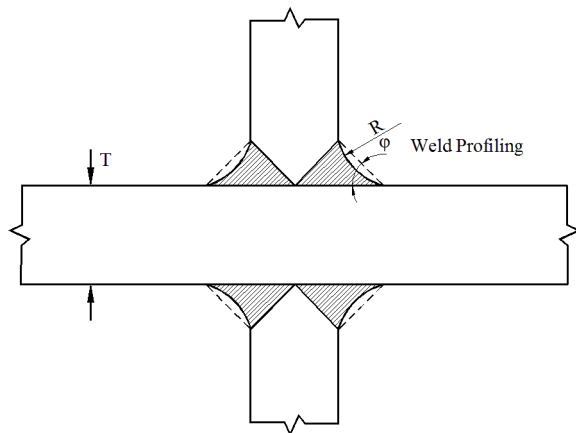


Figure 7-1 Weld profiling of cruciform joint

7.3 Weld toe grinding

Where local grinding of the weld toes below any visible undercuts is performed the fatigue life may be increased by a factor given in [Table 7-1](#). In addition the thickness effect may be reduced to an exponent $k = 0.20$ for S-N curves with $k = 0.25$ (for S-N curves F to W3 and T) and is reduced to an exponent $k = 0.15$ for S-N curves D and E. See [Figure 7-2](#). Grinding a weld toe tangentially to the plate surface, as at A, will produce only little improvement in fatigue strength. To be efficient, grinding should extend below the plate surface, as at B, in order to remove weld toe defects. Grinding is normally carried out by a rotary burr. The treatment should produce a smooth concave profile at the weld toe with the depth of the depression penetrating into the plate surface to at least 0.5 mm below the bottom of any visible undercut, see [Figure 7-2](#). The grinding depth should not exceed 2 mm or 7% of the plate thickness, whichever is smaller.

Grinding has been used as an efficient method for reliable fatigue life improvement after fabrication. Grinding also improves the reliability of inspection after fabrication and during service life. However, experience indicates that it may be a good design practice to exclude this factor at the design stage. The designer is advised to improve the details locally by other means, or to reduce the stress range through design and keep the possibility of fatigue life improvement as a reserve to allow for possible increase in fatigue loading during the design and fabrication process, see also [DNVGL-OS-C101 Ch.2 Sec.1 \[2\]](#) *General safety principles*.

It should also be noted that if grinding is required to achieve a specified fatigue life, the hot spot stress is rather high. Due to grinding a larger fraction of the fatigue life is spent during the initiation of fatigue cracks, and the crack grows faster after initiation (due to the higher stress range). This implies use of shorter inspection intervals during service life in order to detect the cracks before they become dangerous for the integrity of the structure.

For grinding of weld toes it is recommended to use a rotary ball shaped burr with typical diameter of 12 mm.

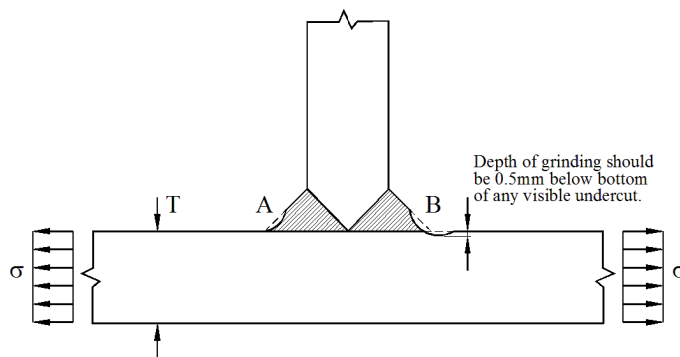


Figure 7-2 Grinding of welds

In some structures the welds are machined or ground flush to achieve a high S-N class, see [Table A-5](#). It shall be documented that weld overfill has been removed by grinding and that the surface has been proven free from defects. The weld overfill may be removed by a coarse grinder tool such as a coarse grit flapper disk, grit size 40-60. The final surface should be achieved by fine grit grinding below that of weld toe defects. The surface should show a smooth or polished finish with no visible score marks. The roughness should correspond to $R_a = 3.2 \mu\text{m}$ or better to achieve a full improvement. The surface should be checked by magnetic particle inspection. It is assumed that grinding is performed until all indications of defects are removed. Then possible presence of internal defects in the weld may be a limitation for use of a high S-N class and it is important to perform a reliable non-destructive examination and use acceptance criteria that are in correspondence with the S-N classification that is used. See also the [\[F.5\]](#).

In design standards such as NORSOK M-101 (2011) grit blasting of the surfaces is recommended prior to coating to $Sa 2 \frac{1}{2}$ in order to achieve a surface roughness, $R_{y5} = 50-85 \mu\text{m}$. This corresponds to Grade G in ISO8501: 2012, Part 1. R_{y5} has the same definition as R_z which is also used in standards to characterize surface roughness. The definition of the R_a parameter used to describe the acceptance criterion for grinding differs from that of R_{y5} . This means that it is difficult to make a direct comparison of requirements for surface finish as a well-defined ratio between R_a and R_{y5} is lacking. Some measurements on steel surfaces indicate that $R_z/R_a = R_{y5}/R_a \approx 6$ may be used as an approximate value. However, a somewhat smaller value has also been reported from measurements of machined surfaces. Thus, $R_{y5} = 50 - 85 \mu\text{m}$ corresponds approximately to $R_a = 8 - 14 \mu\text{m}$. This means that where surface preparation for coating is specified according to NORSOK M-501 (2012), the benefits from grinding that are obtained in laboratory testing with specimens ground to $R_a = 3.2 \mu\text{m}$ are unlikely to be achieved. The reduction in fatigue strength for surfaces with R_a values larger than $3.2 \mu\text{m}$ can be included in the design analysis by increasing the stress range at the considered hot spot by the following factor:

$$\psi = \frac{1 - 0.28 \log(R_m / 200)}{1 - 0.221 \log(6R_a) \log(R_m / 200)} \quad (7.3.1)$$

where R_m = material tensile strength in [MPa]. Then the S-N curves in [Table F-9](#) may be used for fatigue assessment. See [/103/](#) for a detailed background and definitions of the different parameters used to characterize the surface roughness.

Equation (7.3.1) can be used for fatigue assessment of surfaces where grit blasting is used to achieve a typical surface roughness of $R_a = 12.8 \mu\text{m}$ together with information in [Table 7-1](#) and [\[F.15\]](#). For typical normalised steels with tensile strength around 550 MPa this corresponds to a reduction factor on fatigue life of 1.3. This factor can then be used to reduce the improvement factors in [Table 7-1](#) for this material and this

surface roughness for all improvement methods. For high strength steel with tensile strength around 800 MPa the corresponding reduction factor on fatigue life increases to 1.5.

Table 7-1 Improvement on fatigue life by different methods⁴⁾

<i>Improvement method</i>	<i>Minimum specified yield strength</i>	<i>Increase in fatigue life (factor on life)¹⁾</i>
Grinding	Less than 350 MPa	$0.01f_y^{2)}$
	Higher than 350 MPa	3.5
TIG dressing	Less than 350 MPa	$0.01f_y$
	Higher than 350 MPa	3.5
Hammer peening ³⁾	Less than 350 MPa	$0.011f_y$
	Higher than 350 MPa	4.0

1) The maximum S-N class that can be claimed by weld improvement is C1 or C depending on NDE and quality assurance for execution see [Table A-5](#).

2) f_y = characteristic yield strength for the actual material.

3) The improvement effect is dependent on tool used and workmanship. Therefore, if the fabricator is without experience with respect to hammer peening, it is recommended to perform fatigue testing of relevant detail (with and without hammer peening) before a factor on improvement is decided.

4) Improvement of welded connections provides S-N data that shows increased improvement in the high cycle region of the S-N curve as compared with that of low cycle region. Thus the slope factor m is increased by improvement. The factor on fatigue life after improvement in this table is based on a typical long term stress range distribution that corresponds to wave environment for a service life of 20 years or more. Thus the factor on improvement may be lower than this for low cycle fatigue in the region $N < 10^6$ cycles. In the high cycle region an alternative way of calculating fatigue life after improvement is by analysis of fatigue damage by using S-N curves representing better the improved state. Such SN curves can be found in [\[F.15\]](#).

The full benefit of potential grinding of welds cannot be expected when the S-N curves for free corrosion are applied in design. The effect of free corrosion on a ground weld may be accounted for by downgrading the S-N curve by one class and applying the S-N curves for free corrosion in [\[2.4.9\]](#).

7.4 TIG dressing

The fatigue life may be improved by TIG dressing by a factor given in [Table 7-1](#).

Due to uncertainties regarding quality assurance of this process, this method may not be recommended for general use at the design stage. See also [\[7.3\]](#) for effect of surface roughness due to grit blasting.

7.5 Hammer peening

The fatigue life may be improved by means of hammer peening by a factor given in [Table 7-1](#).

However, the following limitations apply:

- Hammer peening should only be used on members where failure will be without substantial consequences, see [DNVGL-OS-C101 Ch.2 Sec.1 \[2\] General safety principles](#).
- Overload in compression shall be avoided, because the residual stress set up by hammer peening will be destroyed.
- It is recommended to grind a steering groove by means of a rotary burr of a diameter suitable for the hammer head to be used for the peening. The peening tip shall be small enough to reach the weld toe.

Due to uncertainties regarding workmanship and quality assurance of the process, this method may not be recommendable for general use at the design stage.

See also [7.3] for effect of surface roughness due to grit blasting.

SECTION 8 EXTENDED FATIGUE LIFE

8.1 Methodology

An extended fatigue life is considered to be acceptable and within normal design criteria if the calculated fatigue life is longer than the total design life times the fatigue design factor.

Otherwise an extended life may be based on results from performed inspections throughout the prior service life. Such an evaluation should be based on:

- 1) Calculated crack growth.

Crack growth characteristics, i.e. crack length/depth as function of time/number of cycles (this depends on type of joint, type of loading, and possibility for redistribution of stress).

- 2) Reliability of inspection method used.

Elapsed time from last inspection performed.

It is recommended to use Eddy current or magnetic particle inspection for inspection of surface cracks starting at hot spots.

For welded connections that are ground and inspected for fatigue cracks the following procedure may be used for calculation of an elongated fatigue life. Provided that grinding below the surface to a depth of approximately 1.0 mm is performed and that fatigue cracks are not found by a detailed magnetic particle inspection of the considered hot spot region at the weld toe, the fatigue damage at this hot spot may be considered to start again at zero. If a fatigue crack is found, a further grinding should be performed to remove any indication of this crack. If more than 7% of the thickness is removed by grinding, the effect of this on increased stress should be included when a new fatigue life is assessed. In some cases as much as 30% of the plate thickness may be removed by grinding before a weld repair needs to be performed. This depends on type of joint, loading condition and accessibility for a repair.

It should be noted that fatigue cracks growing from the weld root of fillet welds can hardly be detected by NDE. Also, the fatigue life of such regions cannot be improved by grinding of the surface.

It should also be remembered that if renewal of one hot spot area is performed by local grinding, there are likely other areas close to the considered hot spot region that are not ground and that also experience a significant dynamic loading. The fatigue damage at this region is the same as earlier. However, also this fatigue damage may be reassessed taking into account:

- the correlation with a ground neighbour hot spot region that has not cracked
- an updated reliability taking the reliability of performed in-service inspections into account as discussed above.

See also [DNVGL-RP-C210 /107/](#).

SECTION 9 UNCERTAINTIES IN FATIGUE LIFE PREDICTION

9.1 Calculated probabilities of fatigue failures

Large uncertainties are normally associated with fatigue life assessments. Reliability methods may be used to illustrate the effect of uncertainties on probability of a fatigue failure. An example of this is shown in [Figure 9-1](#) based on mean expected uncertainties for a jacket design from *Reliability of Calculated Fatigue Lives of Offshore Structures*, /17/.

From [Figure 9-1](#) it might be concluded that a design modification to achieve a longer calculated fatigue life is an efficient mean to reduce probability of a fatigue failure.

The effect of scatter in S-N data may be illustrated by [Figure 9-2](#) where the difference between calculated life is shown for mean S-N data and design S-N data (which is determined as mean minus 2 standard deviations).

The effect of using design fatigue factors (DFFs) larger than 1.0 is shown in [Figure 9-3](#). This figure shows the calculated probability of a fatigue failure the last year in service when a structure is designed for 20 years design life. Uncertainties on the most important parameters in the fatigue design procedure are accounted for when probability of fatigue failure is calculated. This figure is derived by probabilistic analysis where the uncertainty in loading is included in addition to uncertainties in S-N data and the Palmgren-Miner damage accumulation rule. (The loading including all analyses of stress is assumed normal distributed with CoV = 25%, standard deviation = 0.20 in S-N data that is assumed normal distributed in logarithmic scale and the Palmgren-Miner is assumed log normal distributed with median 1.0 and CoV = 0.3.)

The same figure also shows the calculated accumulated probability of failure during the service life as function of DFF. The accumulated probability of failure is independent of design life and need not be linked to 20 years' service life.

An expected long term stress range is aimed for in the design response analysis. A design fatigue factor equal 1.0 implies a probability of a fatigue crack during service life equal 2.3% due to the safety in the S-N curve if uncertainties in other parameters are neglected.

[Figure 9-4](#) shows the calculated accumulated probability of a fatigue failure as function of years in service for different assumptions of uncertainty in the input parameters. This figure shows the results for DFF = 1.0. The left part of this figure corresponding to the first 20 years service life is shown in [Figure 9-5](#).

One may achieve results for other values of DFFs by multiplication of the time scale on the abscissa axis by the actual DFF that is considered used.

[Figure 9-4](#) and [Figure 9-5](#) shows the calculated accumulated probability of fatigue failure for uncertainty in S-N data corresponding to a standard deviation of 0.20 in log N scale. A normal distribution in logarithmic scale is assumed. The uncertainty in Miner summation is described as log normal with median 1.0 and CoV equal 0.30. Other uncertainties on load and response are assumed as normal distributed with CoV 15-20% and the hot spot stress derivation is also assumed as normal distributed with CoV equal 5-10%.

Calculated fatigue life forms the basis for assessment of probability of fatigue cracking during service life. Thus, it implicitly forms the basis for requirement to in-service inspection, see also [\[9.2\]](#). For details showing a short fatigue life at an early design stage, it is recommended that the considered details are evaluated in terms of improvement of local geometry to reduce its stress concentration. At an early design stage it is considered more cost efficient to prepare for minor geometric modifications than to rely on methods for fatigue improvement under fabrication and construction, such as grinding and hammer peening.

Design fatigue factors for different areas should be defined in company specifications to be used as a contract document for construction as factors defined by classification societies are mainly intended to assure structural integrity.

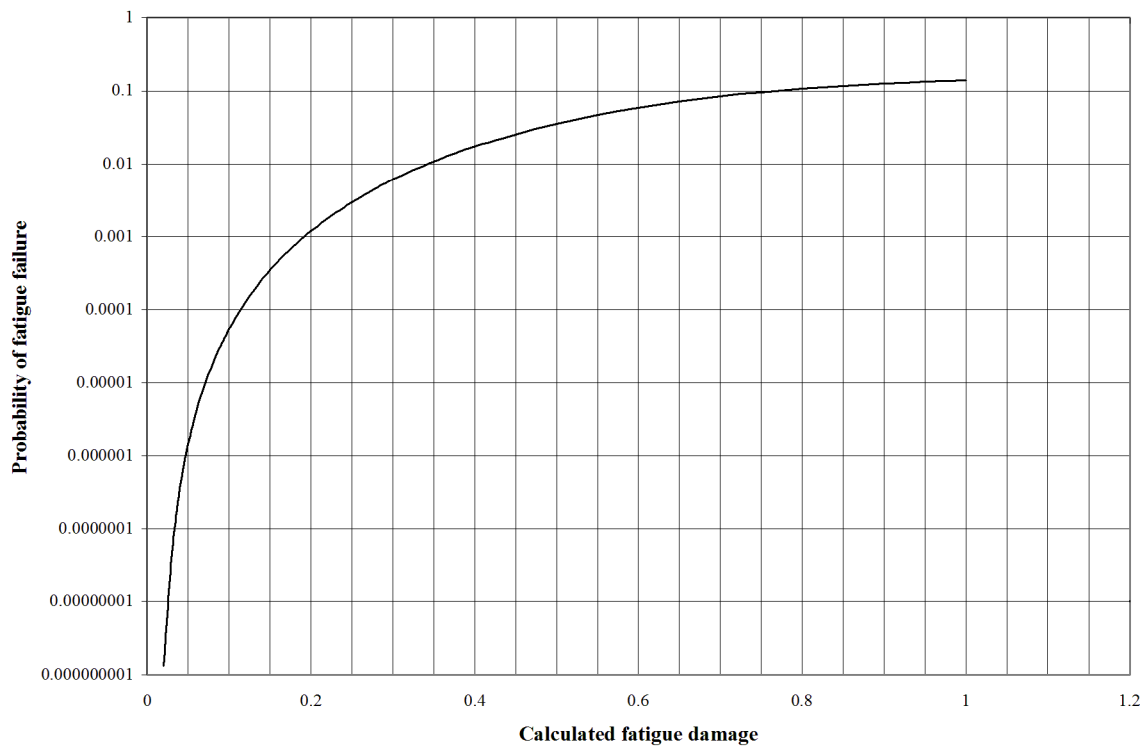


Figure 9-1 Calculated probability of fatigue failure as function of calculated damage

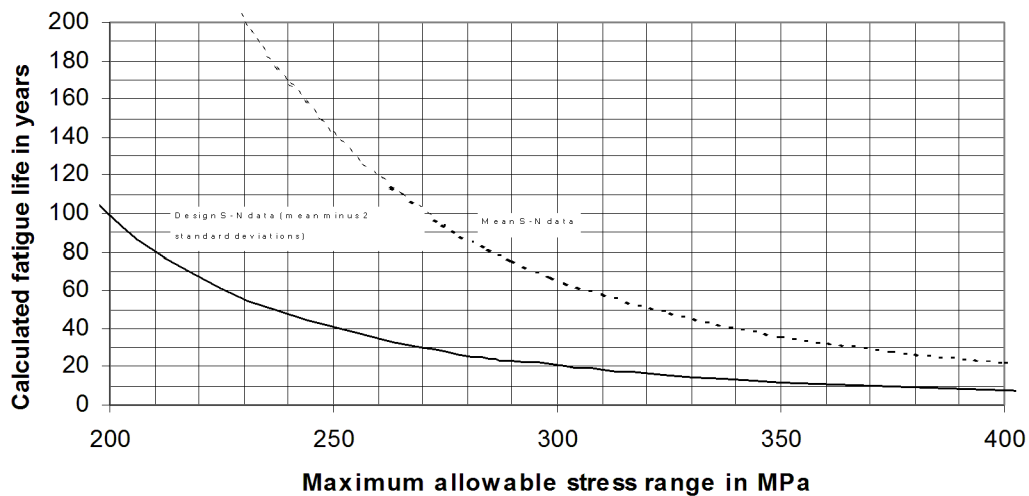


Figure 9-2 Effect of scatter in S-N data on calculated fatigue life

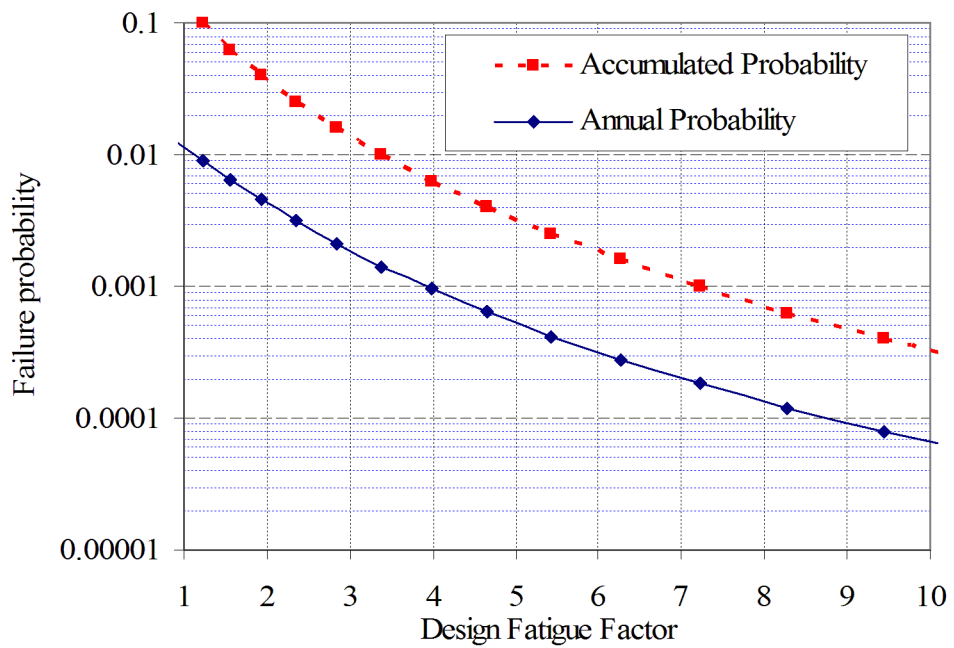


Figure 9-3 Fatigue failure probability as function of design fatigue factor (the annual probability of failure is shown for a design life equal 20 years)

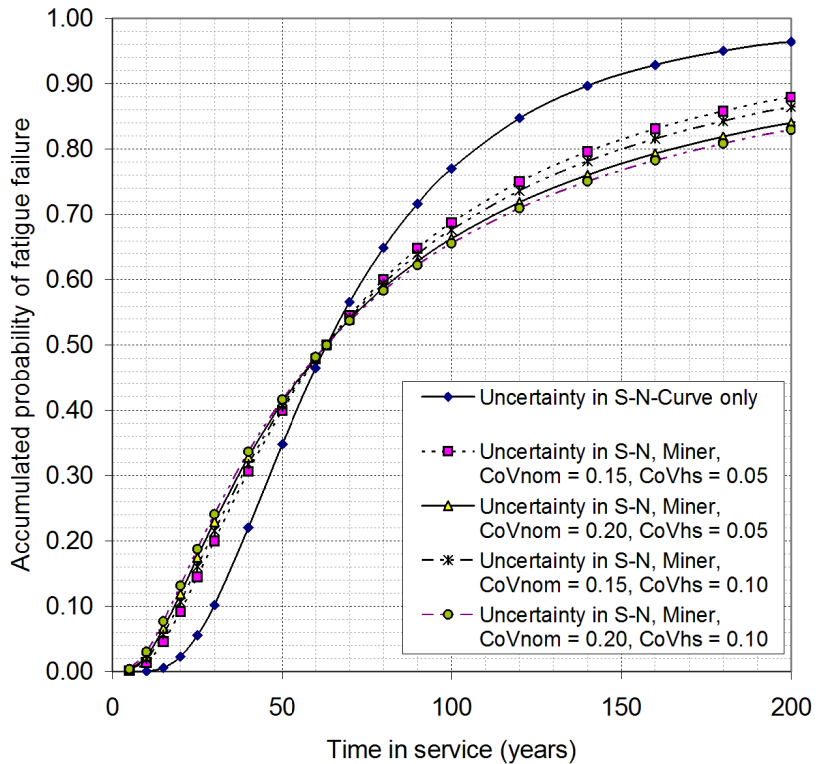


Figure 9-4 Accumulated probability of fatigue failure (through thickness crack) as function of service life for 20 years design life

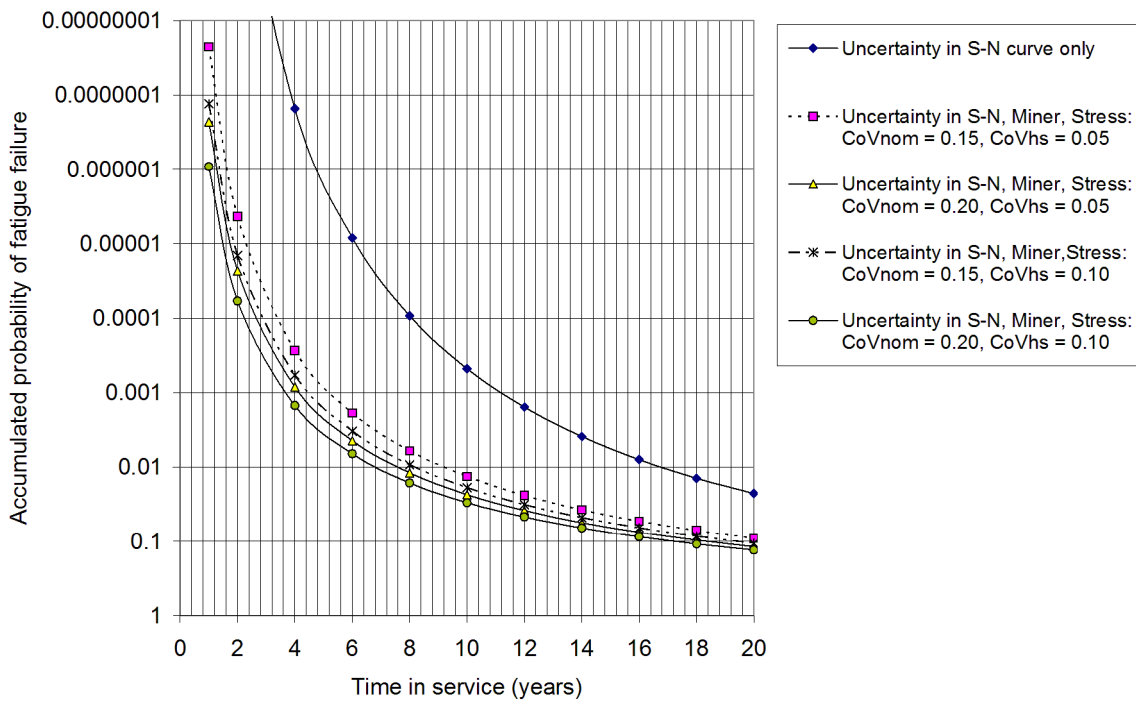


Figure 9-5 Accumulated probability of through wall fatigue crack as function of service life for 20 years calculated fatigue life (left part from Figure 9-4)

9.2 Requirements to in-service inspection for fatigue cracks

Uncertainties associated with fatigue life calculation normally imply that some in-service inspection for fatigue cracks will be required during service life depending on consequence of a fatigue failure and calculated fatigue life. Figure 9-5 may be used for a first estimate of time to a first inspection based on the lower graph in this figure if normal uncertainties are associated with the fatigue life calculation. Figure 9-5 is derived for a calculated fatigue life equal 20 years. For other calculated fatigue lives (L_{calc}) the numbers on the abscissa axis can be scaled by a factor $f = L_{\text{calc}}/20$ for estimate of time to first required inspection. If a fatigue crack is without substantial consequences, an accumulated probability of 10^{-2} may be considered acceptable and from Figure 9-5 it is not required inspection the first 6 years. If the consequence of a fatigue crack is substantial, the accumulated probability of a fatigue failure should be less than 10^{-4} and from Figure 9-5 an inspection would be required after 2 years.

(Normally a calculated fatigue life significantly longer than 20 years would be required for a large consequence connection during design.)

After a first inspection the time interval to the next inspection can be estimated based on fracture mechanics and probabilistic analysis taking the uncertainty in the inspection method into account.

See DNVGL-RP-C210, /107/.

SECTION 10 REFERENCES

10.1 List of references

- /1/ DNVGL-CG-0129 *Fatigue Assessment of Ship Structures*, DNV GL, Oslo.
- /2/ Efthymiou, M.: *Development of SCF Formulae and Generalised Influence Functions for use in Fatigue Analysis*. Recent Developments in Tubular Joint Technology, OTJ'88, October 1988, London.
- /3/ Smedley, S. and Fischer, P.: *Stress Concentration Factors for Ring-Stiffened Tubular Joints*. Fourth Int. Symp. on Tubular Structures, Delft 1991. pp. 239-250.
- /4/ Lotsberg, I., Cramer, E., Holtsmark, G., Løseth, R., Olaisen, K. and Valsgård, S.: *Fatigue Assessment of Floating Production Vessels*. BOSS'97, July 1997.
- /5/ Eurocode: *Design of steel structures. Part 1-1: General rules and rules for buildings*, February 1993.
- /6/ *Guidance on Design, Construction and Certification*, Third Amendment to Fourth Edition HSE, London. February 1995.
- /7/ BS7910:2013. *Guidance on Methods for Assessing the Acceptability of Flaws in Metallic Structures*, BSI, 2013.
- /8/ Van Wingerde, A. M. Parker, J. A. and Wardenier, J.: *IIW Fatigue Rules for Tubular Joints*. Int. conf. on Performance of Dynamic Loaded Welded Structures, San Francisco, July 1997.
- /9/ Gulati, K. C., Wang, W. J. and Kan, K. Y.: *An Analytical study of Stress Concentration Effects in Multibrace Joints under Combined Loading*. OTC paper no 4407, Houston, May 1982.
- /10/ Gurney, T.R.: *Fatigue Design Rules for welded Steel Joints*, the Welding Institute Research Bulletin. Volume 17, number 5, May 1976.
- /11/ Gurney, T. R.: *The Basis for the Revised Fatigue Design Rules in the Department of Energy Offshore Guidance Notes*. Paper No 55.
- /12/ Berge, S.: *Effect of Plate Thickness in Fatigue Design of Welded Structures*. OTC Paper no 4829, Houston, May 1984.
- /13/ Buitrago, J. and Zettlemoyer, N.: *Fatigue of Welded Joints Peened Underwater*. 1997 OMAE, ASME 1997.
- /14/ Stacey, A., Sharp, J. V. and Nichols, N. W.: *Fatigue Performance of Single-sided Circumferential and Closure Welds in Offshore Jacket Structures*, 1997 OMAE, ASME.
- /15/ Pilkey, W. D.: *Peterson's Stress Concentration Factors*. Second Edition. John Wiley & Sons, 1997.
- /16/ Haagensen, P. and S. J. Maddox (2013). *IIW Recommendations on Post Weld Fatigue Life Improvement of Steel and Aluminium Structures*, Woodhead Publishing Ltd., Cambridge, UK.
- /17/ Lotsberg, I., Fines, S. and Foss, G.: *Reliability of Calculated Fatigue Lives of Offshore Structures*, Fatigue 84, 2nd Int. Conf. on Fatigue and Fatigue Thresholds, 3-7 September 1984. Birmingham.
- /18/ Haagensen, P. J., Slind, T. and Ørjasæter, O.: *Scale Effects in Fatigue Design Data for Welded and Unwelded Components*. Proc. Ninth Int. Conf. On Offshore Mechanics and Arctic Engineering. Houston, February 1990.
- /19/ Berge, S., Eide, O., Astrup, O. C., Palm, S., Wästberg, S., Gunleiksrud, Å. and Lian, B.: *Effect of Plate Thickness in Fatigue of Welded Joints in Air and in Sea Water*. Steel in Marine Structures, edited by C. Noorhook and J. deBack Elsevier Science Publishers B.V., Amsterdam, 1987, pp. 799-810.

- /20/ Razmjoo, G. R.: *Design Guidance on Fatigue of Welded Stainless Steel Joints*, OMAE 1995. Vol. III, Materials Engineering ASME 1995.
- /21/ Madsen, H. O., Krenk, S. and Lind, N. C. (1986) *Methods of Structural Safety*, Prentice-Hall, Inc., NJ.
- /22/ Marshall, P. W.: *API Provisions for SCF, S-N, and Size-Profile Effects*. OTC Paper no 7155. Houston, May 1993.
- /23/ Waløen, Å. Ø.: *Maskindeler 2*, Tapir, NTNU (in Norwegian).
- /24/ Buitrago, J., Zettlemoyer, N. and Kahlish, J. L.: *Combined Hot-Spot Stress Procedures for Tubular Joints*. OTC Paper No. 4775. Houston, May 1984.
- /25/ Lotsberg, I.: *Stress Concentration Factors at Circumferential Welds in Tubulars*. Journal of Marine Structures, Vol. II. 1998, pp. 207-230.
- /26/ VDI 2230. *Systmatic calculation of high duty bolted joints. Joints with one cylindrical bolt*. Part 1. Beuth Verlag GmbH, 10772 Berlin, 2003.
- /27/ Zhao X-L, Herion S, Packer J A, Puthli R S, Sedlacek G, Wardenier J, Weynand K, van Wingerde A M & Yeomans N F (2000) *Design guide for circular and rectangular hollow section welded joints under fatigue loading*, published by TÜV-Verlag for Comité International pour le Développement et l'Etude de la Construction Tubulaire.
- /28/ DNVGL-OS-C101 *Design of offshore steel structures, general LRFD Method*.
- /29/ Lotsberg, I., and Rove, H.: *Stress Concentration Factors for Butt Welds in Stiffened Plates*, OMAE2014-23316. OMAE 2014.
- /30/ IIW. *Recommendations for Fatigue Design of Welded Joints and Components*. Edited by Hobacker, A. Springer, 2016.
- /31/ Fricke, W. (2001), *Recommended Hot Spot Analysis Procedure for Structural Details of FPSOs and Ships Based on Round-Robin FE Analyses*. Proc. 11th ISOPE, Stavanger. Also Int. J. of Offshore and Polar Engineering. Vol. 12, No. 1, March 2002.
- /32/ Lotsberg, I. (2004), *Recommended Methodology for Analysis of Structural Stress for Fatigue Assessment of Plated Structures*. OMAE-FPSO'04-0013, Int. Conf. Houston.
- /33/ Lotsberg, I. and Larsen, P. K.: *Developments in Fatigue Design Standards for Offshore Structures*. ISOPE, Stavanger, June 2001.
- /34/ Bergan, P. G., Lotsberg, I.: *Advances in Fatigue Assessment of FPSOs*. OMAE-FPSO'04-0012, Int. Conf. Houston 2004.
- /35/ Sigurdsson, S., Landet, E. and Lotsberg, I. , *Inspection Planning of a Critical Block Weld in an FPSO*. OMAE-FPSO'04-0032, Int. Conf. Houston, 2004.
- /36/ Storsul, R., Landet, E. and Lotsberg, I. , *Convergence Analysis for Welded Details in Ship Shaped Structures*. OMAE-FPSO'04-0016, Int. Conf. Houston 2004.
- /37/ Storsul, R., Landet, E. and Lotsberg, I., *Calculated and Measured Stress at Welded Connections between Side Longitudinals and Transverse Frames in Ship Shaped Structures*. OMAE-FPSO'04-0017, Int. Conf. Houston 2004.
- /38/ Lotsberg, I., *Fatigue Design of Welded Pipe Penetrations in Plated Structures*. Marine Structures, Vol 17/1 pp. 29-51, 2004.
- /39/ ISO 19902 *Fixed Steel Structures*, 2007.
- /40/ Lotsberg, I., *Recommended Methodology for Analysis of Structural Stress for Fatigue Assessment of Plated Structures*. OMAE-FPSO'04-0013, Int. Conf. Houston 2004.

- /41/ Lotsberg, I. and Sigurdsson, G., *Hot Spot S-N Curve for Fatigue Analysis of Plated Structures*. OMAE-FPSO'04-0014, Int. Conf. Houston 2004. Journal of Offshore and Arctic Engineering, Vol. 128, pp. 330-336.
- /42/ Lindemark, T., Lotsberg, I., Kang, J-K., Kim, K-S. and Oma, N.: *Fatigue Capacity of Stiffener to Web Frame Connections*. OMAE2009-79061, OMAE 2009.
- /43/ Urm, H. S., Yoo, I. S., Heo, J. H., Kim, S. C. and Lotsberg, I.: *Low Cycle Fatigue Strength Assessment for Ship Structures*, PRADS 2004.
- /44/ Kim, W.S. and Lotsberg, I., *Fatigue Test Data for Welded Connections in Ship Shaped Structures* OMAE-FPSO'04-0018, Int. Conf. Houston 2004.
- /45/ Maddox, S. J. *Key Development in the Fatigue Design of Welded Constructions*, Portewin Lecture IIW Int. Conf. Bucharest, 2003.
- /46/ Kristoffersen, S. and Haagensen, P. J.: *Fatigue Design Criteria for Small Super Duplex Steel Pipes*, Proceedings OMAE Vancouver, 2004.
- /47/ Berge, S., Kihl, D., Lotsberg, I., Maherault, S., Mikkola, T. P. J., Nielsen, L. P., Paetzold, H., Shin, C. -H., Sun, H. -H and Tomita, Y.: *Special Task Committee VI.2 Fatigue Strength Assessment*. 15th ISSC, San Diego, 2003.
- /48/ Chen, W. and Landet, E. (2001), *Stress Analysis of Cut-outs with and without Reinforcement*. OMAE Rio de Janeiro.
- /49/ Choo, Y.S. and Zahidul Hasan, M. (2004), *Hot Spot Stress Evaluation for Selected Connection Details*. OMAE-FPSO'04-0028. Int. Conf. Houston.
- /50/ Fricke, W., Doerk, O. and Gruenitz, L. (2004), *Fatigue Strength Investigation and Assessment of Fillet-Welds around Toes of Stiffeners and Brackets*. OMAE-FPSO'04-0010. Int. Conf. Houston.
- /51/ Radaj, D., Sonsino, C. M. and Fricke, W.: (2006): *Fatigue Assessment of Welded Joints by Local Approaches*. Woodhead Publishing in Materials.
- /52/ Ranestad Kaase, G. O.: *Finite Element Analysis of SCF in Stiffener to Plate Connections*, Pre-Project Thesis, Marine Structures NTNU 2002.
- /53/ [DNVGL-ST-F201 Dynamic risers](#), January 2018.
- /54/ [DNVGL-ST-F101 Submarine pipeline systems](#), October 2017.
- /55/ Schneider, C. R. A. and Maddox, S. J.: *Best Practice Guide on Statistical Analysis of Fatigue Data*. Doc. IIW-XIII-2138-06.
- /56/ Slater, G. and P. J. Tubby, P. J. (1996). *Fatigue behaviour of internally ring stiffened tubular joints*. OMAE 1996. Volume III, Material Engineering ASME, 483-492.
- /57/ ASME B.31.4, *Code for Pressure Piping*, Chapter IX.
- /58/ Lotsberg, I., Background for Revision of [DNV-RP-C203 Fatigue Analysis of Offshore Steel Structures](#). OMAE 2005-67549. Int. Conf. Halkidiki, Greece, June 2005.
- /59/ Wästberg, S., Salama, M.: *Fatigue Testing and Analysis of Full Scale Girth weld Tubulars*. OMAE2007-29399, OMAE 2007.
- /60/ [DNVGL-OS-C401 Fabrication and testing of offshore structures](#), July 2015.
- /61/ Lotsberg, I.: *Fatigue Design of Plated Structures using Finite Element Analysis*. Journal of Ships and Offshore Structures. 2006 Vol. 1 No 1 pp. 45-54.
- /62/ Lotsberg, I and Landet, E., *Fatigue Capacity of Side Longitudinals in Floating Structures*. Marine Structures, Vol 18, 2005, pp. 25-42.

- /63/ Lotsberg, I., *Fatigue Capacity of Fillet Welded Connections subjected to Axial and Shear Loading*. Presented at OMAE in Hamburg, 4 - 9 June 2006. OMAE paper no 2006 - 92086. Also in Journal of Offshore and Arctic Engineering.
- /64/ Lotsberg, I. *Recent Advances on Fatigue Limit State Design for FPSOs*, Journal of Ships and Offshore Structures, 2007 Vol. 2 No. 1 pp. 49-68.
- /65/ Lotsberg, I. and Holth, P. A.: *Stress Concentration Factors at Welds in Tubular Sections and Pipelines*. Presented at OMAE 2007. OMAE paper no 2007-29571. 26th International Conference on Offshore Mechanics and Arctic Engineering, San Diego, California, June 2007.
- /66/ Lotsberg, I., Rundhaug, T. A., Thorkildsen, H., Bøe, Å. and Lindemark, T.: *Fatigue Design of Web Stiffened Cruciform Connections*. Presented at PRADS 2007.
- /67/ Lotsberg, I.: *Stress Concentration Factors at Welds in Pipelines and Tanks subjected to Internal Pressure*. In Journal of Marine Engineering 2008.
- /68/ Sele, A., Collberg, L., Lauersen, H.: *Double Skin Grout Reinforced Joints, Part Project One and Two*. Fatigue Tests on Grouted Joints. DNV-Report No 83-0119.
- /69/ Lotsberg, I.: *Fatigue Design Criteria as Function of the Principal Stress Direction Relative to the Weld Toe*. OMAE 2008-57249. OMAE 2008 Estoril, Portugal.
- /70/ Lotsberg, I., Wästberg, S., Ulle, H., Haagensen, P. and Hall, M. E.: *Fatigue Testing and S-N data for Fatigue Analysis of Piles*. OMAE 2008-57250. OMAE 2008 Estoril, Portugal. Journal of Offshore and Arctic Engineering, Vol. 132, Issue 4, pp. 041602-1-7.
- /71/ Lotsberg, I., Sigurdsson, G. Arnesen, K. and Hall, M. E.: *Recommended Design Fatigue Factors for Reassessment of Piles subjected to Dynamic Actions from Pile Driving*. OMAE 2008-57251. OMAE 2008 Estoril, Portugal. Journal of Offshore and Arctic Engineering, Vol. 132, Issue 4, pp. 041603-1-8.
- /72/ Lotsberg, I.: *Stress Concentrations at Butt Welds in Pipelines*. Marine Structures 22 (2009), pp. 335-337.
- /73/ Solland, G., Lotsberg, I., Bjørheim, L. G., Ersdal, G., Gjerstad, V.- A., and Smedley, P.: *New Standard for Assessment of Structural Integrity for Existing Load-Bearing Structures – NORSO N-006*, OMAE 2009-79379.
- /74/ Lotsberg, I. and Fredheim, S.: *Assessment of Design S-N curve for Umbilical Tubes*. OMAE2009-79201, OMAE 2009.
- /75/ ISO 2394 *General principles on reliability of structures*, 1998.
- /76/ Ronold, K.O., and Echtermeyer, A.: *Estimation of fatigue curves for design of composite laminates, Composites*, Part A: Applied Science and Manufacturing, Elsevier, Vol. 27A, No. 6, 485-491, 1996.
- /77/ Lotsberg, I.: *Stress Concentration due to Misalignment at Butt Welds in Plated Structures and at Girth Welds in Tubulars*. International Journal of Fatigue 31 (2009), pp. 1337-1345 DOI information: 10.1016/j.ijfatigue.2009.03.005.
- /78/ Lotsberg, I., Rundhaug, T. A. and Andersen, Ø.: *Fatigue Design Methodology for Welded Pipe Penetrations in Plated Structures*. IIW paper XIII-2289-09 Presented at IIW in Singapore July 2009.
- /79/ Lotsberg, I., Mørk, K., Valsgård, S. and Sigurdsson, G.: *System effects in Fatigue Design of Long Pipes and Pipelines*. OME2010-20647. OMAE 2010, Shanghai, China.
- /80/ Lotsberg, I.: *Background for Revision of DNV-RP-C203 Fatigue Design of Offshore Steel Structures*. OME2010-20649. OMAE 2010, Shanghai, China.
- /81/ NORSO N-006 *Assessment of structural integrity for existing offshore load-bearing structures*. Revision 02, 2015.

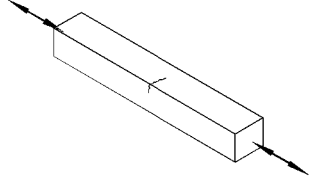
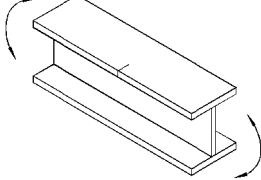
- /82/ Ang, A. H-S. and Tang, W. H.: *Probability Concepts in Engineering Planning and Design*, Volume I - Basic Principles, John Wiley and Sons, New York, N.Y., 1975.
- /83/ DNVGL-RP-C207 *Statistical representation of soil data*, April 2007.
- /84/ Sørensen, J. D., Tychsen, J., Andersen, J. U. and Brandstrup, R. D.: *Fatigue Analysis of Load-carrying Fillet Welds*, Journal of Offshore Mechanics and Arctic Engineering, February 2006, Vol. 128, pp. 65 - 74.
- /85/ Lotsberg, I.: *On Stress Concentration Factors for Tubular Y- and T-joints*. Journal of Marine Structures (20) 2011, pp. 60-69. doi:10.1016/j.marstruc.2011.01.002.
- /86/ Lotsberg, I. and Ronold, K.: *On the Derivation of Design S-N Curves based on Limited Fatigue Test Data*. OMAE 2011, June 2011.
- /87/ Yildirim, H. C. and Marquis, G. M.: *Overview of Fatigue Data for High Frequency Treated Welded Joints*, IIW Paper no XIII-2362-11. IIW 2011.
- /88/ Lotsberg, I., Fjeldstad, A., Ro Helsem, M. and Oma, N.: *Fatigue Life Improvement of Welded Doubling Plates*. OMAE, Rio de Janeiro, July 2012.
- /89/ Ronold, K. and Lotsberg, I.: *On the Estimation of Characteristic S-N curves with Confidence*. Marine Structures, vol. 27, 2012, pp. 29-44.
- /90/ DNVGL-OS-C102 *Structural design of offshore ship-shaped units*, DNV GL, Oslo.
- /91/ ISO 5817:2014 *Welding – Fusion-welded joints in steel, nickel, titanium and their alloys (beam welding excluded) Quality levels for imperfections*.
- /92/ NORSO standard M-101 *Structural steel fabrication*. Edition 5, December 2011.
- /93/ Lotsberg, I., Rundhaug, T. A., Thorkildsen, H., Bøe, Å. and Lindemark, T.: *A Procedure Fatigue Design of Web Stiffened Cruciform Connections*. Journal of Ships and Offshore Structures, 2008, Vol. 3, Issue 2, pp. 113-126.
- /94/ Lotsberg, I.: *Assessment of Design Criteria for Fatigue Cracking from Weld Toes subjected to Proportional Loading*. Journal of Ships and Offshore Structures, Volume 4, Issue 2, June 2009.
- /95/ Lotsberg, I., A. Fjeldstad, A., M. Ro Helsem and N. Oma (2014): *Fatigue Life Improvement of Welded Doubling Plates by Grinding and Ultrasonic Peening, Welding in the World*. Volume 58, Issue 6 (2014), 819-830.
- /96/ Lotsberg, I. (2014): *Assessment of the size effect for use in design standards for fatigue analysis*. Journal of Fatigue, 66 (2014), pp. 86-100.
- /97/ Maddox, S.: *Recommended Hot-Spot Stress Design S-N Curves for Fatigue Assessment of FPSOs*. Proceedings of the Eleventh International Offshore and Polar Engineering Conference, Stavanger, Norway, June 2001.
- /98/ Lotsberg, I. and Sigurdsson, G.: *A New recommended practice for Inspection Planning of Fatigue Cracks in Offshore Structures based on Probabilistic Methods*. OMAE2014-23188.
- /99/ Lee, M. M. K.: *Estimation of stress concentrations in single-sided welds in offshore tubular joints*. International Journal of Fatigue 21, 1999, pp. 895-908.
- /100/ Wormsen A., Avice, M. Fjeldstad, A. Reinås, L. Macdonald, K. A. Berg, E. and Muff, A. D.: *Fatigue Testing and Analysis of Notched Specimens with Typical Subsea Design Features*. Int. Journal of Fatigue. 2015.
- /101/ DNVGL-RP-E104 *Wellhead fatigue analysis*, DNV GL, Oslo.
- /102/ DNVGL-RP-0034 *Steel forgings for subsea applications*, DNV GL, Oslo.
- /103/ Lotsberg, I.: *Fatigue Design of Marine Structures*. Cambridge University Press, New York, 2016.

- /104/ NORSOK M-501 (2012). *Surface preparation and protective coating*, Edition 6.
- /105/ ISO 8501:2012 *Preparation of steel substrates before application of paints and related products – visual assessment of surface cleanliness – Part 1: Rust grades and preparation grades of uncoated steel substrates and of steel substrates after overall removal of previous coatings*.
Informative supplements to part 1: Representative photographic examples of the change of the appearance imparted to steel when blast-cleaned with different abrasives.
- /106/ Roark, R. J. and W. C. Young (1975): *Formulas for Stress and Strain*. International Student Edition, McGraw-Hill.
- /107/ [DNVGL-RP-C210 Probabilistic methods for planning of inspection for fatigue cracks in offshore structures](#). DNV GL, Oslo.
- /108/ Lotsberg, I.: (2019) *Development of Fatigue Design Standards for Marine Structures*, Journal of Offshore Mechanics and Arctic Engineering, Vol. 141, pp. 011604-1-7.
- /109/ [DNVGL-RP-F108 Methods for determining allowable flaw sizes in pipelines and risers girth welds](#), DNV GL, Oslo.
- /110/ Wormsen, A., Kirkemo, F., Macdonald, K. A., Reinås, L., Muff, A. D. and Fjeldstad, A. (2016): *Fatigue testing and analysis of notched specimens in seawater with cathodic protection*. Int. Journal of Fatigue.
- /111/ Lotsberg, I., Fjeldstad, A. and Ronold, K. O.: Background for the revision of the DNVGL-RP-C203 Fatigue Design of Offshore Steel Structures in 2016. Proceedings of the ASME 2016 35th International Conference on Ocean, Offshore and Arctic Engineering, Busan, South Korea.
- /112/ Toor, K. K. and Lotsberg, I. (2017): *Assessment of Fatigue Strength of Welded Connections on Thick Plates*. OMAE2017-61143. Proceedings of the 36th Int. Conf. on Ocean, Offshore and Arctic Engineering, Trondheim.
- /113/ Lotsberg, I. (2019): *Design Recommendations for Conical Connections in Tubular Structures*, Journal of Offshore and Arctic Engineering. ASME, Vol. 141, pp. 031301-1-10.
- /114/ Manteghi, S., Gibson, D. and Johnston, C. (2017): *Fatigue performance of friction welds manufactured both in air and underwater*. OMAE2017-62495. Proceedings of the 36th Int. Conf. on Ocean, Offshore and Arctic Engineering, Trondheim.
- /115/ NORSOK N-004 *Design of steel structures* (2013).
- /116/ Efthymiou, M. and Durkan, S. (1985): *Stress concentrations in T/Y and gap/overlap K-joints. Behaviour of Offshore Structures*, Amsterdam, The Netherlands.
- /117/ ISO 965-1:2013 ISO general purpose metric screw threads -- Tolerances -- Part 1: Principles and basic data.
- /118/ BS 7608:2014 *Guide to fatigue design and assessment of steel products*. BSI, London.
- /119/ *ASME Boiler and Pressure Vessel Code Section VIII Division 2:2017 Annex 3-D*
- /120/ Horn, A. M., Lotsberg, I. and Ørjasæter, O. (2018): *The Rationale for Update of S-N curves for Single Sided Girth Welds for Risers and Pipelines in DNVGL-RP-C203 based on Fatigue Performance of more than 1700 Full Scale Fatigue Test Results*. OMAE2018-78408. Proceedings of the ASME 2018 37th International Conference on Ocean, Offshore and Arctic Engineering OMAE 2018 Madrid, Spain June 17-22, 2018.

APPENDIX A CLASSIFICATION OF STRUCTURAL DETAILS

A.1 Non-welded details

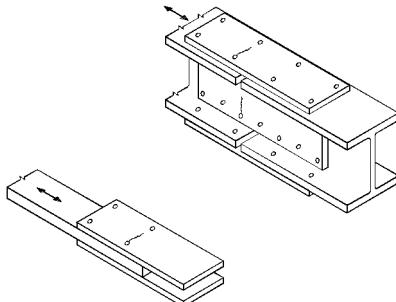
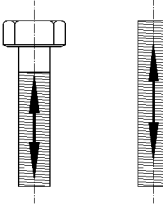
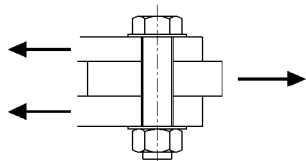
Table A-1 Non-welded details

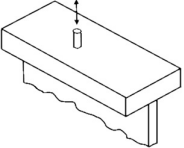
<i>Detail category</i>	<i>Constructional details</i>	<i>Description</i>	<i>Requirement</i>
Notes on potential modes of failure			
<p>In plain steel, fatigue cracks will initiate at the surface, usually either at surface irregularities or at corners of the cross-section. In welded construction, fatigue failure will rarely occur in a region of plain material since the fatigue strength of the welded joints will usually be much lower. In steel with bolt holes or other stress concentrations arising from the shape of the member, failure will usually initiate at the stress concentration. The applied stress range shall include applicable stress concentration factors arising from the shape of the member.</p> <p>See App.D for non-welded components made of high strength steel with a surface finish $R_a = 6.4 \mu\text{m}$ or better. The surface roughness will increase compared to final machining if the component is grit blasted before coating is applied.</p>			
B1	<p>1.</p>  <p>2.</p> 	<p>1.</p> <p>Rolled or extruded plates and flats.</p> <p>2.</p> <p>Rolled sections.</p>	<p>1. to 2.</p> <ul style="list-style-type: none"> — Sharp edges, surface and rolling flaws to be improved by grinding. — For members that can acquire stress concentrations due to rust pitting etc. curve C is required.

<i>Detail category</i>	<i>Constructional details</i>	<i>Description</i>	<i>Requirement</i>
B2	3.	3. Machine gas cut or sheared material with no drag lines.	3. <ul style="list-style-type: none"> — All visible signs of edge discontinuities should be removed. — No repair by weld refill. — Re-entrant corners (slope $<1:4$) or aperture should be improved by grinding for any visible defects. — At apertures the design stress area should be taken as the net cross-section area.
C	4.	4. Manually gas cut material or material with machine gas cut edges with shallow and regular draglines.	4. <ul style="list-style-type: none"> — Subsequently ground to remove all edge discontinuities. — No repair by weld refill. — Re-entrant corners (slope $<1:4$) or aperture should be improved by grinding for any visible defects. — At apertures the design stress area should be taken as the net cross-section area.

A.2 Bolted connections

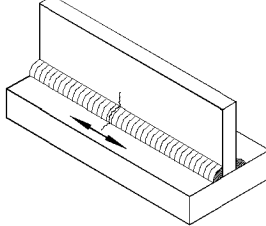
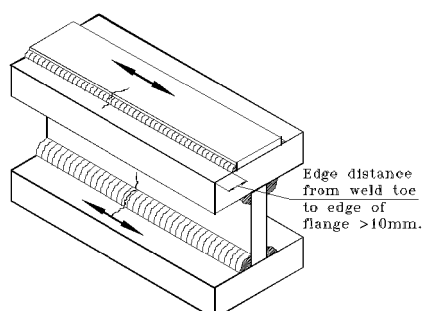
Table A-2 Bolted connections

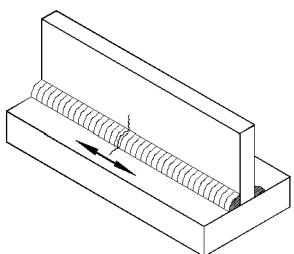
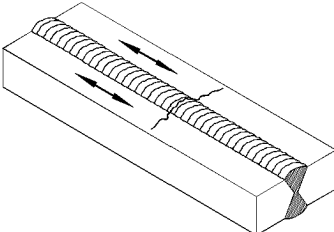
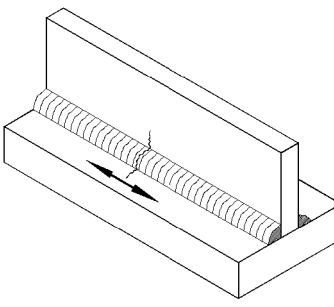
<i>Detail category</i>	<i>Constructional details</i>	<i>Description</i>	<i>Requirement</i>
C1	1. 2. 	1. Unsupported one-sided connections shall be avoided or else effects of eccentricities shall be taken into account when calculating stresses. 2. Beam splices or bolted cover plates.	1. and 2. <ul style="list-style-type: none">— Stresses to be calculated in the gross section.— Bolts subjected to reversal forces in shear shall be designed as a slip resistant connection and only the members shall be checked for fatigue.
F1 G	3. 	3. Bolts and threaded rods in tension. Cold rolled threads with no following heat treatment such as hot galvanising. Cut threads and rolled threads with a following heat treatment such as hot galvanising.	3. <ul style="list-style-type: none">— Tensile stresses to be calculated using the tensile stress area of the bolt.— For preloaded bolts, the stress-range in the bolt depends upon the level of preload and the geometry of the connection, see e.g. <i>Maskindeler 2 /23/</i>.— The bolts to meet the fabrication tolerances in ISO 965-1:2013 /117/.
See [2.9.3]		4. Bolts in single or double shear. Fitted bolts and normal bolts without load reversal.	4. <ul style="list-style-type: none">— Thread not in shear plane.— The shear stress to be calculated on the shank area of the bolt.

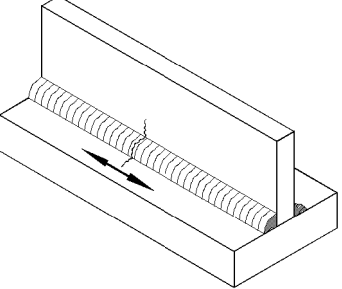
<i>Detail category</i>	<i>Constructional details</i>	<i>Description</i>	<i>Requirement</i>
C1	4. 	4. Friction welded bolt to base material.	4. — Stress range in the axial direction of the bolt.

A.3 Continuous welds essentially parallel to the direction of applied stress

Table A-3 Continuous welds essentially parallel to the direction of applied stress

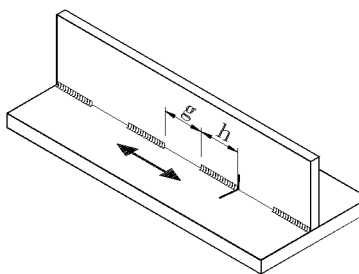
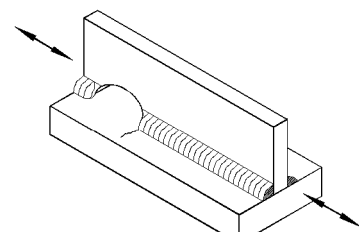
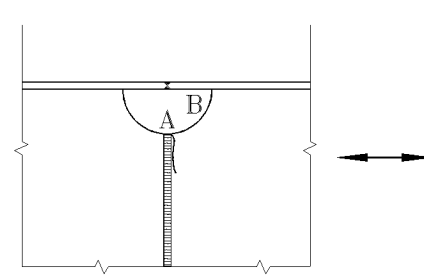
<i>Detail category</i>	<i>Constructional details</i>	<i>Description</i>	<i>Requirement</i>
Notes on potential modes of failure.			
With the excess weld material machined or ground flush, fatigue cracks would be expected to initiate at weld defect locations. In the as welded condition, cracks may initiate at start-stop positions or, if these are not present, at weld surface ripples.			
General comments			
a) Backing strips	If backing strips are used in these joints, they shall be continuous. If they are attached by welding, such welds shall also comply with the relevant joint classification requirements (note particularly that tack welds, unless subsequently ground out or covered by a continuous weld, would reduce the joint to class F)		
b) Edge distance	An edge distance criterion exists to limit the possibility of local stress concentrations occurring at unwelded edges as a result, for example, of undercut, weld spatter, or accidental overweave in manual fillet welding (see also notes in Table A-7). Although an edge distance can be specified only for the width direction of an element, it is equally important to ensure that no accidental undercutting occurs on the unwelded corners of, for example cover plates or box girder flanges. If undercutting occurs it should subsequently be ground smooth.		
C	<p>1.</p>  <p>2.</p> 	<p>1.</p> <p>Automatic welds carried out from both sides.</p> <p>2.</p> <p>Automatic fillet welds. Cover plate ends shall be verified using detail 5. in Table A-8</p>	<p>1. and 2.</p> <ul style="list-style-type: none"> — No start-stop position is permitted except when the repair is performed by a specialist and inspection carried out to verify the proper execution of the repair.

<i>Detail category</i>	<i>Constructional details</i>	<i>Description</i>	<i>Requirement</i>
C1	<p>3.</p>  <p>4.</p> 	<p>3.</p> <p>Automatic fillet or butt welds carried out from both sides but containing stop-start positions.</p> <p>4.</p> <p>Automatic butt welds made from one side only, with a backing bar, but without start-stop positions.</p>	<p>4.</p> <ul style="list-style-type: none"> — When the detail contains start-stop positions use category C2.
C2		<p>5.</p> <p>Manual fillet or butt welds.</p> <p>6.</p> <p>Manual or automatic butt welds carried out from one side only, particularly for box girders.</p>	<p>6.</p> <ul style="list-style-type: none"> — A very good fit between the flange and web plates is essential. Prepare the web edge such that the root face is adequate for the achievement of regular root penetration.

<i>Detail category</i>	<i>Constructional details</i>	<i>Description</i>	<i>Requirement</i>
C2		7. Repaired automatic or manual fillet or butt welds.	7. — Improvement methods that are adequately verified may restore the original category.

A.4 Intermittent welds and welds at cope holes

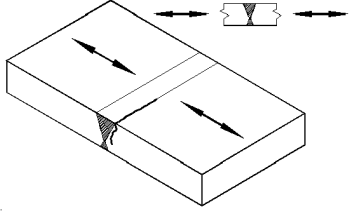
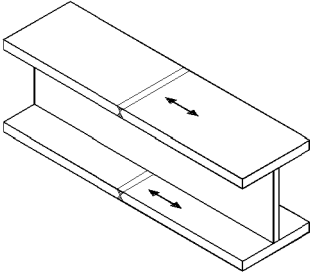
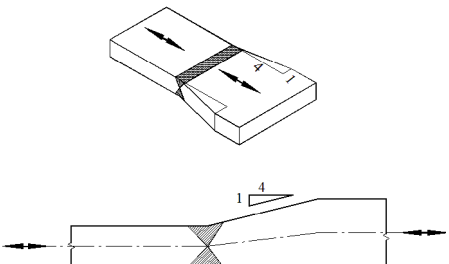
Table A-4 Intermittent welds and welds at cope holes

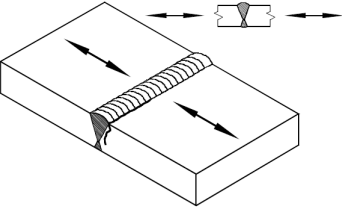
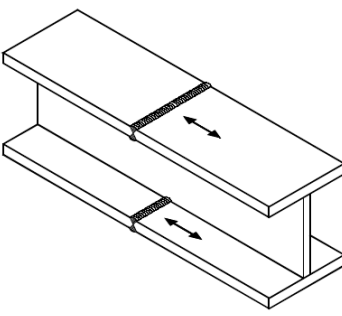
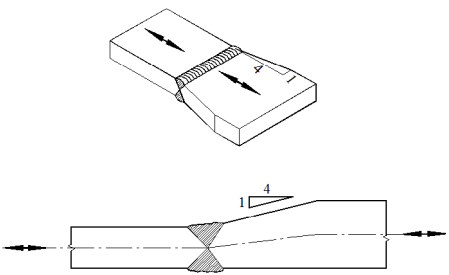
<i>Detail category</i>	<i>Constructional details</i>	<i>Description</i>	<i>Requirement</i>
E	1. 	1. Stitch or tack welds not subsequently covered by a continuous weld.	1. — Intermittent fillet weld with gap ratio $g/h \leq 2.5$.
F	2. 	2. Ends of continuous welds at cope holes. The S-N classification is the same with and without welding through the hole.	2. — Cope hole not to be filled with weld material.
	3. 	3. Cope hole and transverse butt weld.	3. — Advice on fatigue assessment for butt weld in material with cope hole may be found in [3.1.6]. — The SCFs from [3.1.6] may be used together with the D-curve.

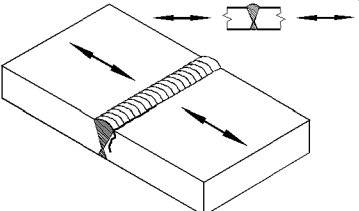
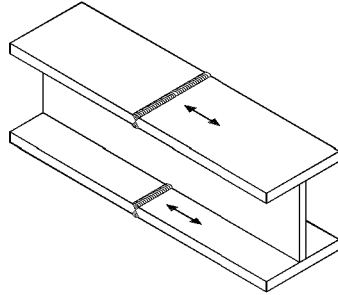
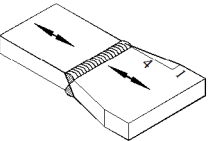
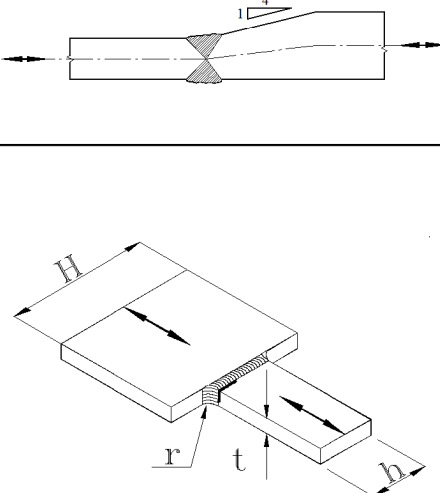
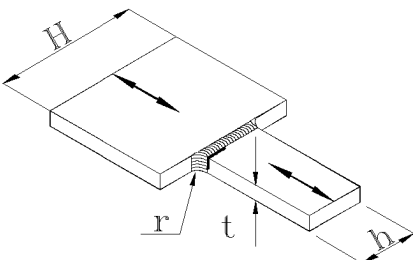
A.5 Transverse butt welds, welded from both sides

Table A-5 Transverse butt welds, welded from both sides

<i>Detail category</i>	<i>Constructional details</i>	<i>Description</i>	<i>Requirement</i>
Notes on potential modes of failure			
With the weld ends machined flush with the plate edges, fatigue cracks in the as-welded condition normally initiate at the weld toe, so that the fatigue strength depends largely upon the shape of the weld overfill. If the overfill is machined or ground flush, the notch stress concentration caused by it is removed, and failure is then associated with weld defects.			
Design stresses			
In the design of butt welds that are not symmetric about the root and are not aligned, the stresses shall include the effect of any eccentricity, see [3.1] and [3.3].			
With connections that are supported laterally, e.g. flanges of a beam that are supported by the web, eccentricity may be neglected. However, this depends on width of flanges, see e.g. /29/.			
Due to use of a high S-N curve for welds machined flush one cannot assume that significant tolerances are accounted for in the S-N curve, and hence, the δ_0 should be put equal to 0 in the equations for stress concentration factors for butt welds for plated structures in [3.1.2] and for tubular girth welds in [3.3.7] when used together with the C/C1 curve.			
For description of machining or grinding the surface flush see [7.3].			

<i>Detail category</i>	<i>Constructional details</i>	<i>Description</i>	<i>Requirement</i>
C1	<p>1.</p>  <p>2.</p>  <p>3.</p> 	<p>1.</p> <p>Transverse splices in plates flats and rolled sections.</p> <p>2.</p> <p>Flange splices in plate girders.</p> <p>3.</p> <p>Transverse splices in plates or flats tapered in width or in thickness where the slope is not greater than 1:4.</p>	<p>1. and 2.</p> <ul style="list-style-type: none"> — Details 1. and 2. may be increased to category C when high quality welding is achieved with a qualified welding procedure and the weld proved free from significant defects by non-destructive examination. <p>Note that special consideration with respect to NDT and acceptance criteria are required for butt welds where a higher classification than D is used. See commentary section.</p> <p>1., 2. and 3.</p> <ul style="list-style-type: none"> — All welds ground flush to plate surface parallel to direction of the arrow. — Weld run-off pieces to be used and subsequently removed. Plate edges to be ground flush in direction of stress. — All welds welded in flat position in shop.

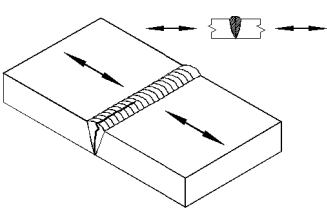
<i>Detail category</i>	<i>Constructional details</i>	<i>Description</i>	<i>Requirement</i>
D	<p>4.</p>  <p>5</p>  <p>6.</p> 	<p>4.</p> <p>Transverse splices in plates and flats.</p> <p>5.</p> <p>Transverse splices in rolled sections or welded plate girders.</p> <p>6.</p> <p>Transverse splices in plates or flats tapered in width or in thickness where the slope is not greater than 1:4.</p>	<p>4., 5. and 6.</p> <ul style="list-style-type: none"> — The height of the weld convexity not to be greater than 10% of the weld width, with smooth transitions to the plate surface. — Welds made in flat position in shop. — Weld run-off pieces to be used and subsequently removed. Plate edges to be ground flush in direction of stress.

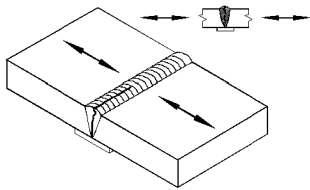
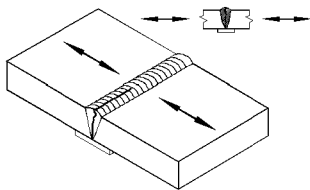
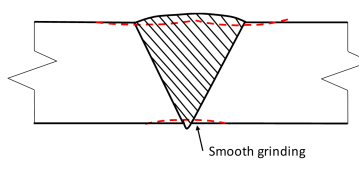
<i>Detail category</i>	<i>Constructional details</i>	<i>Description</i>	<i>Requirement</i>
E	7.    	7. Transverse splices in plates, flats, rolled sections or plate girders made at site. (Detail category D may be used for welds made in flat position at site meeting the requirements under 4., 5. and 6 and when 100% MPI of the weld is performed.)	7. — The height of the weld convexity not to be greater than 20% of the weld width. — Weld run-off pieces to be used and subsequently removed. Plate edges to be ground flush in direction of stress.
	8. 	8. Transverse splice between plates of unequal width, with the weld ends ground to a radius.	8. — The stress concentration has been accounted for in the joint classification. — The width ratio H/h should be less than 2.

<i>Detail category</i>	<i>Constructional details</i>	<i>Description</i>	<i>Requirement</i>
F1	$\frac{r}{h} \geq 0.16$		
F3	$\frac{r}{h} \geq 0.11$		

A.6 Transverse butt welds, welded from one side

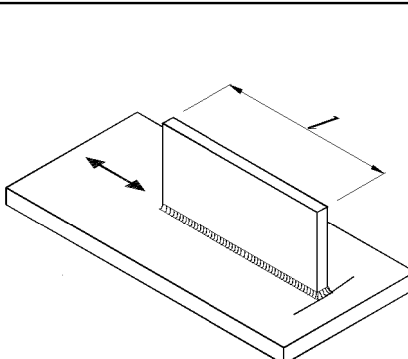
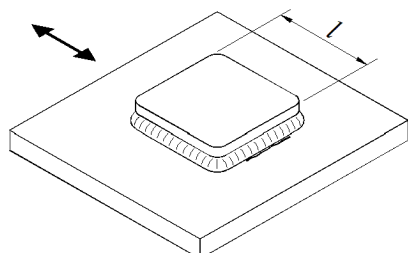
Table A-6 Transverse butt welds, welded from one side

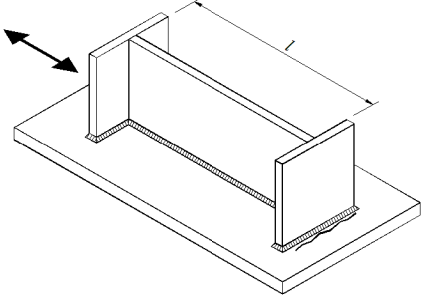
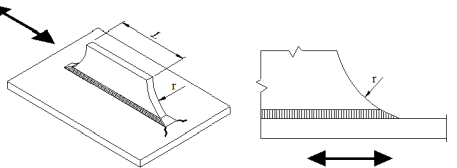
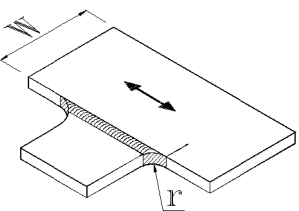
<i>Detail category</i>	<i>Constructional details</i>	<i>Description</i>	<i>Requirement</i>
Notes on potential modes of failure			
<p>With the weld ends machined or ground flush with the plate edges, fatigue cracks in the as-welded condition normally initiate at the weld toe, so that the fatigue strength depends largely upon the shape of the weld overfill. If the overfill is machined flush, the notch stress concentration caused by it is removed, and failure is then associated with weld defects. In welds made on permanent backing strip, fatigue cracks most likely initiate at the weld metal/strip junction.</p> <p>The weld root is normally the most likely initiation point for fatigue cracks in butt welds in structural members made from one side. In girth welds in pipes or tubular sections it can be difficult to get access for welding from the inside, and welding is performed from the outside only. If there is access for grinding/machining of the inside weld root area and access to perform a good NDT, it may still be possible to achieve a fatigue capacity of such connections like that of girth welds made from both sides as described in Table A-5. To use the highest S-N classification for welded connections, such as C1 or C, it is recommended to calculate the nominal stress based on the actual section area left after grinding for purposes of a reliable fatigue analysis.</p>			
Design stresses			
<p>In the design of butt welds that are not symmetric about the root and are not aligned, the stresses shall include the effect of any eccentricity, see [3.1] and [3.3].</p> <p>With connections that are supported laterally, e.g. flanges of a beam that are supported by the web, eccentricity may be neglected. However, this depends on width of flanges, see e.g. /29/.</p>			
W3	<p>1.</p> 	<p>1.</p> <p>Butt weld made from one side only and without backing strip.</p>	<p>1.</p> <ul style="list-style-type: none"> With the root proved free from defects larger than 1-2 mm (in the thickness direction) by non-destructive testing, detail 1 may be categorised to F3 (it is assumed that this is fulfilled by inspection category I). See also commentary section. If it is likely that larger defects may be present after the inspection the detail may be downgraded from F3 based on fatigue life calculation using fracture mechanics. The analysis should then be based on a relevant defect size.

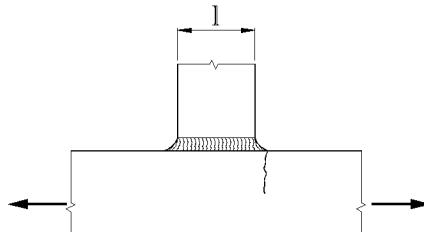
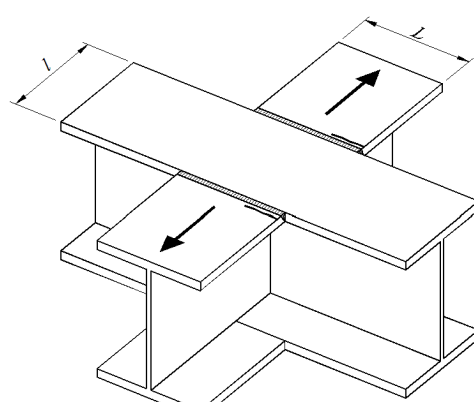
<i>Detail category</i>	<i>Constructional details</i>	<i>Description</i>	<i>Requirement</i>
F	2. 	2. Transverse butt weld on a temporary or a permanent backing strip without fillet welds.	
G	3. 	3. Transverse butt weld on a backing strip fillet welded to the plate.	
C1		4. Transverse butt weld where the weld toes and weld root is ground or machined to a smooth transition from the weld to the base material. The grinding should be minimum 0.2 mm below any imperfection both for weld toes and the weld root. A typical maximum grinding depth is 1.0 mm, however, the planned actual grinding depth should be used for calculation of nominal stress range at the connection. 	4. — The detail classification may be increased to category C when high quality welding is performed using a qualified welding procedure and the weld proved free from defects by non-destructive testing. Note that special consideration with respect to NDT and acceptance criteria are required for butt welds where a higher classification than D is used. See App.F.

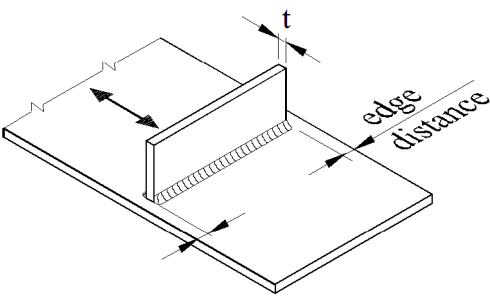
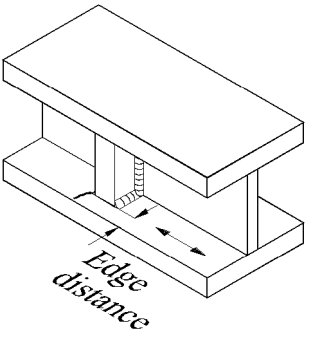
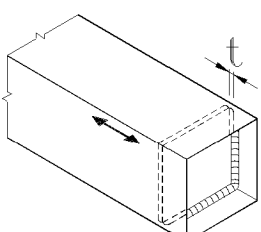
A.7 Welded attachments on the surface or the edge of a stressed member

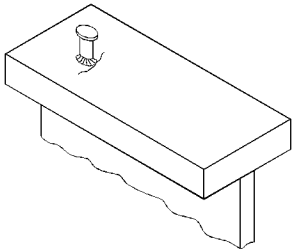
Table A-7 Welded attachments on the surface or the edge of a stressed member

<i>Detail category</i>	<i>Constructional details</i>	<i>Description</i>	<i>Requirement</i>
Notes on potential modes of failure			
	<p>When the weld is parallel to the direction of the applied stress, fatigue cracks normally initiate at the weld ends. When the weld is transverse to the stress direction, cracks usually initiate at the weld toe, however, weld cracks may also initiate at the weld root in fillet welded connections. (Construction detail no 1 is assumed made with a full penetration weld and detail 2 with a fillet weld.) Potential cracks from the weld root may then propagate into the stressed member. When the welds are on or adjacent to the edge of the stressed member, the stress concentration is increased and the fatigue strength is reduced, this is the reason for specifying an 'edge distance' in some of these joints (see also note on edge distance in Table A-3).</p>		
	 	<p>1.</p> <p>Welded longitudinal attachment.</p> <p>2.</p> <p>Doubling plate welded to a plate.</p>	<p>1. and 2.</p> <p>The detail category is given for:</p> <ul style="list-style-type: none"> — Edge distance ≥ 10 mm. — For edge distance < 10 mm the detail category shall be downgraded with one S-N curve.
E	$l \leq 50$ mm		
F	$50 < l \leq 120$ mm		
F1	$120 < l \leq 300$ mm		
F3	$l > 300$ mm		

<i>Detail category</i>	<i>Constructional details</i>	<i>Description</i>	<i>Requirement</i>
	3.	 <p>3. Longitudinal attachment welded to transverse stiffener.</p>	
E	$l \leq 120 \text{ mm}$		
F	$120 < l \leq 300 \text{ mm}$		
F1	$l > 300 \text{ mm}$		
E	4. $r > 150 \text{ mm}$	 <p>4. Longitudinal fillet welded gusset with radius transition to plate or tube, end of fillet weld reinforcement (full penetration), length of reinforcement weld $> r$.</p>	<p>4.</p> <ul style="list-style-type: none"> Smooth transition radius r formed by initially machining or gas cutting the gusset plate before welding. Then subsequently grinding the weld area parallel to the direction of the arrow so that the transverse weld toe is fully removed.
	5.	 <p>5. Gusset plate with a radius welded to the edge of a plate or beam flange.</p>	<p>5.</p> <ul style="list-style-type: none"> The specified radius to be achieved by grinding.
E	$\frac{1}{3} \leq \frac{r}{W}, r \geq 150 \text{ mm}$		

<i>Detail category</i>	<i>Constructional details</i>	<i>Description</i>	<i>Requirement</i>
F	$\frac{1}{6} \leq \frac{r}{W} < \frac{1}{3}$		
F1	$\frac{1}{10} \leq \frac{r}{W} < \frac{1}{6}$		
F3	$\frac{1}{16} \leq \frac{r}{W} < \frac{1}{10}$		
G	$\frac{1}{25} \leq \frac{r}{W} < \frac{1}{16}$		
	<p>6.</p>  <p>7.</p> 	<p>6.</p> <p>Gusset plate welded to the edge of a plate or beam flange.</p> <p>7.</p> <p>Flange welded to another flange at crossing joints.</p> <p>6. and 7.</p> <ul style="list-style-type: none"> — The distance l is governing the detail category for the stress direction shown in sketch. The distance L will govern detail category for main stress in the other beam. 	

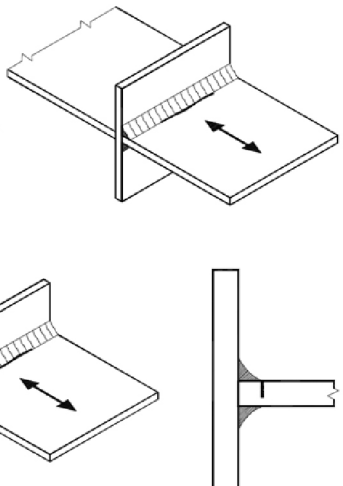
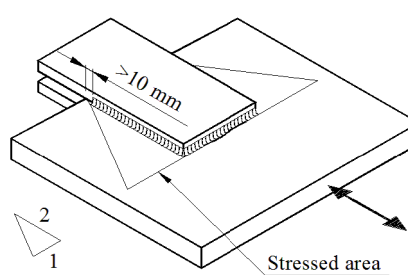
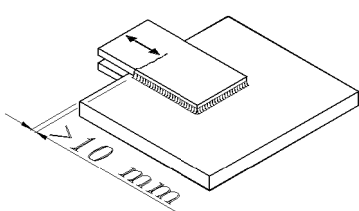
<i>Detail category</i>	<i>Constructional details</i>	<i>Description</i>	<i>Requirement</i>
G	$l \leq 150 \text{ mm}$		
W1	$150 < l \leq 300 \text{ mm}$		
W2	$l > 300 \text{ mm}$		
	8.  9.  10. 	8. Transverse attachments with edge distance $\geq 10 \text{ mm}$ 9. Vertical stiffener welded to a beam or a plate girder. 10. Diaphragms of box girders welded to the flange or web. 8., 9. and 10. The detail category is given for: <ul style="list-style-type: none"> – Edge distance $\geq 10 \text{ mm}$. – For edge distance $< 10 \text{ mm}$ the detail category shall be downgraded with one S-N curve. 	
E	$t \leq 25 \text{ mm}$		
F	$t > 25 \text{ mm}$		

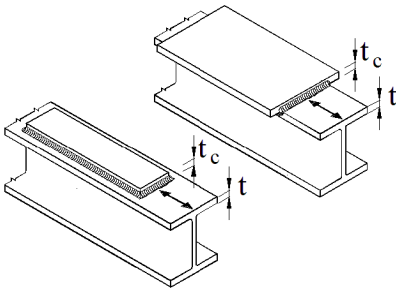
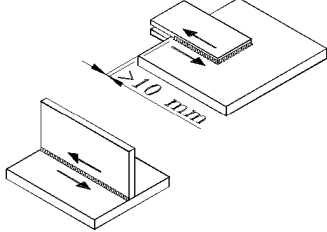
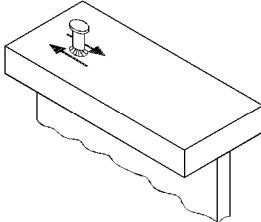
<i>Detail category</i>	<i>Constructional details</i>	<i>Description</i>	<i>Requirement</i>
	11. 	11. Welded shear connector to base material.	
E	Edge distance $\geq 10 \text{ mm}$		
G	Edge distance $< 10 \text{ mm}$		

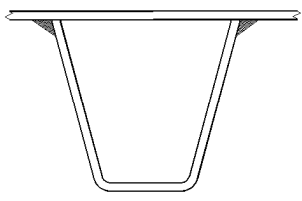
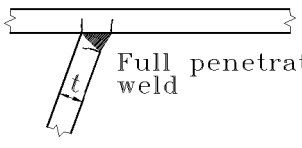
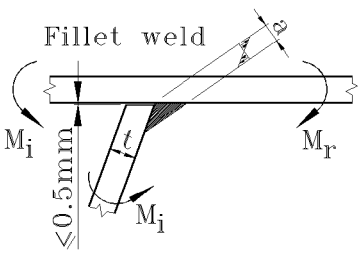
A.8 Welded joints with load carrying welds

Table A-8 Welded joints with load carrying welds

<i>Detail category</i>	<i>Constructional details</i>	<i>Description</i>	<i>Requirement</i>
Notes on potential modes of failure			
Failure in cruciform or T joints with full penetration welds will normally initiate at the weld toe. In joints made with load-carrying fillet or partial penetration butt welds, cracking may initiate either at the weld toe and propagate into the plate, or at the weld root and propagate through the weld. In welds parallel to the direction of the applied stress, however, weld failure is uncommon. In this case, cracks normally initiate at the weld end and propagate into the plate perpendicular to the direction of applied stress. The stress concentration is increased, and the fatigue strength is therefore reduced, if the weld end is located on or adjacent to the edge of a stressed member rather than on its surface.			
Design stresses			
In the design of cruciform joints, which are not aligned the stresses, shall include the effect of any eccentricity. The maximum value of the eccentricity may normally be taken from the fabrication tolerances. The design stress may be obtained as the nominal stress multiplied by the stress concentration factor due to the eccentricity.			
		1. Full penetration butt welded cruciform joint.	1. <ul style="list-style-type: none"> — Inspected and found free from significant defects. <p>The detail category is given for:</p> <ul style="list-style-type: none"> — Edge distance ≥ 10 mm. — For edge distance < 10 mm the detail category shall be downgraded with one S-N curve.
$E t \leq 25$ mm			
$F t > 25$ mm			

Detail category	Constructional details	Description	Requirement
W3	<p>2.</p> 	<p>2.</p> <p>Partial penetration tee-butt joint or fillet welded joint and partial penetration in butt joint. See also [2.8].</p>	<p>2.</p> <ul style="list-style-type: none"> Two fatigue assessments are required. Firstly, root cracking is evaluated taking category W3 for σ_w. σ_w is defined in [2.3.5]. Secondly, toe cracking is evaluated by determining the stress range in the load-carrying plates and use category G. If the requirement in [2.8] that toe cracking is the most likely failure mode is fulfilled and the edge distance ≥ 10 mm, category F1 may be used for partial penetration welds and F3 for fillet welds.
F1	<p>3.</p> 	<p>3.</p> <p>Fillet welded overlap joint. Crack in main plate.</p>	<p>3.</p> <ul style="list-style-type: none"> Stress in the main plate to be calculated on the basis of area shown in the sketch. Weld termination more than 10 mm from plate edge. Shear cracking in the weld should be verified using detail 7.
W1	<p>4.</p> 	<p>4.</p> <p>Fillet welded overlap joint. Crack in overlapping plate.</p>	<p>4.</p> <ul style="list-style-type: none"> Stress to be calculated in the overlapping plate elements. Weld termination more than 10 mm from plate edge. Shear cracking in the weld should be verified using detail 7.

<i>Detail category</i>	<i>Constructional details</i>	<i>Description</i>	<i>Requirement</i>
	5.	 <p>5.</p> <p>End zones of single or multiple welded cover plates in beams and plate girders. Cover plates with or without frontal weld.</p>	<p>5.</p> <ul style="list-style-type: none"> — When the cover plate is wider than the flange, a frontal weld, carefully ground to remove undercut, is necessary.
G	$t \text{ and } t_c \leq 20 \text{ mm}$		
W3	$t \text{ and } t_c > 20 \text{ mm}$		
E	6. and 7.	 <p>6.</p> <p>Continuous fillet welds transmitting a shear flow, such as web to flange welds in plate girders. For continuous full penetration butt weld in shear use category C2.</p> <p>7.</p> <p>Fillet welded lap joint.</p>	<p>6.</p> <ul style="list-style-type: none"> — Stress range to be calculated from the weld throat area. <p>7.</p> <ul style="list-style-type: none"> — Stress range to be calculated from the weld throat area considering the total length of the weld. — Weld terminations more than 10 mm from the plate edge.
E	8.	 <p>8.</p> <p>Stud connectors (failure in the weld or heat affected zone).</p>	<p>8.</p> <ul style="list-style-type: none"> — The shear stress to be calculated on the nominal cross-section of the stud.

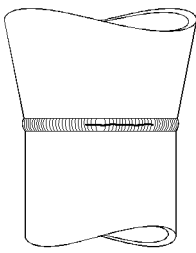
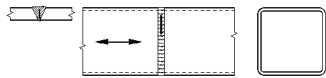
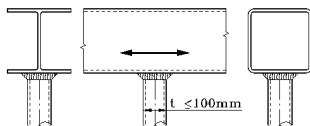
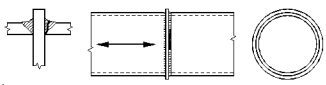
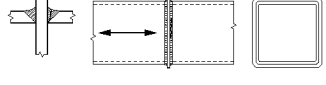
Detail category	Constructional details	Description	Requirement
9.			9.
F	 Full penetration weld	9. Trapezoidal stiffener welded to deck plate with fillet weld or full or partial penetration butt weld.	9. <ul style="list-style-type: none"> — For a full penetration butt weld, the bending stress range shall be calculated on the basis of the thickness of the stiffener. — For a fillet weld or a partial penetration butt weld, the bending stress range shall be calculated on the basis of the throat thickness of the weld, or the thickness of the stiffener if smaller.
G	 Fillet weld M_i M_r		

A.9 Hollow sections

Table A-9 Hollow sections

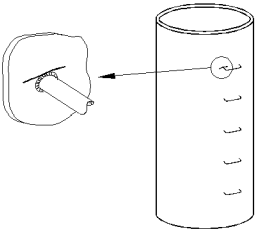
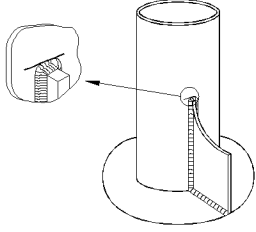
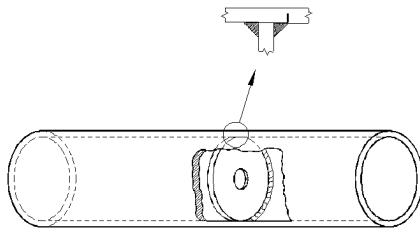
Detail category	Constructional details	Description	Requirement
B1	1.	1. Non-welded sections.	1. — Sharp edges and surface flaws to be improved by grinding.
C	2.	2. Automatic longitudinal seam welds (for all other cases, see Table A-3).	2. — No stop/start positions, and free from defects outside the tolerances of DNVGL-OS-C401 Fabrication and testing of offshore structures .
C1		3. Circumferential butt weld made from both sides machined or ground flush.	3., 4., 5. and 6.
D		4. Circumferential butt weld made from both sides.	— The applied stress shall include the stress concentration factor to allow for any thickness change and for fabrication tolerances, see [3.3.7] .
E		5. Circumferential butt weld made from both sides made at site.	— The requirements to the corresponding detail category in Table A-5 apply.
F		6. Circumferential butt weld made from one side on a backing bar.	

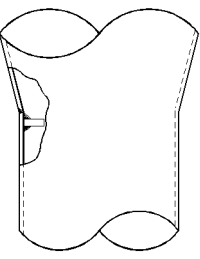
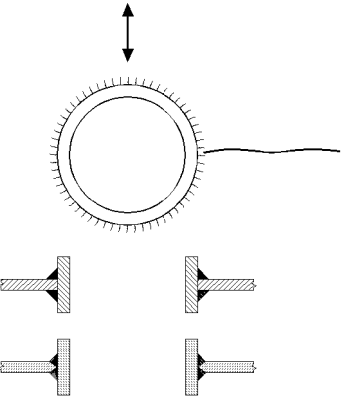
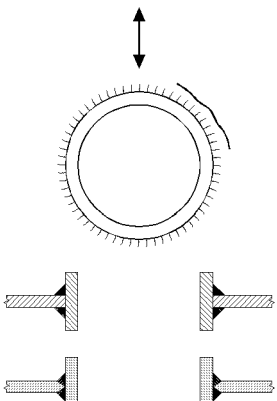
<i>Detail category</i>	<i>Constructional details</i>	<i>Description</i>	<i>Requirement</i>
F3	7.	7. Circumferential butt weld made from one side without a backing bar.	<p>7.</p> <ul style="list-style-type: none"> — The applied stress should include the stress concentration factor to allow for any thickness change and for fabrication tolerances, see [3.3.7]. — The weld root proved free from defects larger than 1-2 mm.
C1	8., 9., 10 and 11.	8. Circumferential butt welds made from one side that are machined or ground flush to remove defects and weld overfill.	<p>8.</p> <ul style="list-style-type: none"> — A machining of the surfaces will reduce the thickness. Specially on the root side material shall be removed. A reduced thickness should be used for calculation of stress. The weld should be proved free from defects by non-destructive examination. It is assumed that this is fulfilled by category I using NORSOK documents, otherwise see [F.5]. Category C may be achieved, see Table A-5.
C1		8. Circumferential butt welds between tubular and conical sections, weld made from both sides machined or ground flush.	
D		9. Circumferential butt welds between tubular and conical sections, weld made from both sides.	<p>8., 9., 10., and 11.</p> <ul style="list-style-type: none"> — The applied stress shall also include the stress concentration factor due to the overall form of the joint, see [3.3.9]. — The requirements to the corresponding detail category in Table A-5 apply.
E		10. Circumferential butt welds between tubular and conical sections, weld made from both sides made at site.	
F		11. Circumferential butt welds between tubular and conical sections, weld made from one side on a backing bar.	

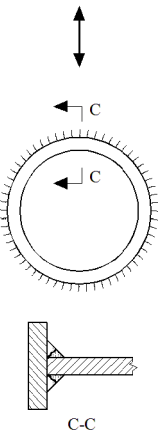
Detail category	Constructional details	Description	Requirement
F3	12.	 <p>12. Circumferential butt welds between tubular and conical sections, weld made from one side without a backing bar. (This classification is for the root. For the outside weld toe see 8-11.)</p>	<p>12.</p> <ul style="list-style-type: none"> The applied stress shall also include the stress concentration factor due to the overall form of the joint. The weld root proved free from defects larger than 1-2 mm.
F3	13.	 <p>13. Butt welded end to end connection of rectangular hollow sections.</p>	<p>13.</p> <ul style="list-style-type: none"> With the weld root proved free from defects larger than 1-2 mm
F	14.	 <p>14. Circular or rectangular hollow section, fillet welded to another section.</p>	<p>14.</p> <ul style="list-style-type: none"> Non load carrying welds. Section width parallel to stress direction ≤ 100 mm. All other cases, see Table A-7.
G	15.	 <p>15. Circular hollow section butt welded end to end with an intermediate plate.</p>	<p>15.</p> <ul style="list-style-type: none"> Load carrying welds. Welds inspected and found free from defects outside the tolerances of DNVGL-OS-C401 Fabrication and testing of offshore structures. See also App.F. Details with wall thickness greater than 8 mm may be classified category F3.
W1	16.	 <p>16. Rectangular hollow section butt welded end to end with an intermediate plate.</p>	<p>16.</p> <ul style="list-style-type: none"> Load carrying welds. Welds inspected and found free from defects outside the tolerances of DNVGL-OS-C401 Fabrication and testing of offshore structures. See also App.F. Details with wall thickness greater than 8 mm may be classified as category G.

A.10 Details relating to tubular members

Table A-10 Details relating to tubular members

<i>Detail category</i>	<i>Constructional details</i>	<i>Description</i>	<i>Requirement</i>
T		1. Parent material adjacent to the toes of full penetration welded tubular joints.	1. — The design should be based on the hot spot stress.
F1	2. 	2. Welded rungs.	
D	3. and 4. 	3. Gusseted connections made with full penetration welds.	3. — The design stress shall include the stress concentration factor due to the overall form of the joint.
F		4. Gusseted connections made with fillet welds.	4. — The design stress shall include the stress concentration factor due to the overall form of the joint.
	5. 	5. Parent material at the toe of a weld attaching a diaphragm to a tubular member.	5. — The nominal design stress for the inside may be determined from [3.3.8].
E	$t \leq 25 \text{ mm}$		
F	$t > 25 \text{ mm}$		

Detail category	Constructional details	Description	Requirement
E to G, see Table A-7	6. 	6. Parent material (of the stressed member) adjacent to the toes of a bevel butt or fillet welded attachments in region of stress concentration.	6. — Class depends on attachment length (see Table A-7) but stress shall include the stress concentration factor due to the overall shape of adjoining structure.
C	7. 	7. Parent material at the weld toe, or weld metal in welds around a penetration through a wall of a member (on a plane essentially perpendicular to the direction of stress).	7. — The relevant stress shall include the stress concentration factor due to the overall geometry of the detail. Without start and stop at hot spot region. See also [3.1.5].
D	8. 	8. At fillet weld toe in parent metal around a penetration in a plate.	8. — The stress in the plate should include the stress concentration factor due to the overall geometry of the detail. See also [3.1.5].

Detail category	Constructional details	Description	Requirement
W3		<p>9.</p> <p>Weld metal in partial penetration or fillet welded joints around a penetration through the wall of a member (on a plane essentially parallel to the plane of stress).</p>	<p>9.</p> <ul style="list-style-type: none"> — The stress in the weld should include an appropriate stress concentration factor to allow for the overall joint geometry. See also App.C. See also [3.1.5].

APPENDIX B STRESS CONCENTRATION FACTORS FOR TUBULAR JOINTS

B.1 Stress concentration factors for simple tubular joints and overlap joints

Stress concentration factors for tubular joints for joint types T/Y are given in [Table B-1](#), for joint types X in [Table B-2](#), for joint types K in [Table B-3](#) and [Table B-4](#) and for joint types KT in [Table B-5](#). Stress concentration factors are based on *Development of SCF Formulae and Generalised Influence Functions for use in Fatigue Analysis /2/*.

Joint classification is the process whereby the axial force in a given brace is subdivided into K, X and Y components of actions corresponding to the three joint types for which stress concentration equations exists. Such subdivision normally considers all of the members in one plane at a joint. For purposes of this provision, brace planes within $\pm 15^\circ$ of each other may be considered as being in a common plane. Each brace in the plane may have a unique classification that could vary with action condition. The classification may be a mixture between the above three joint types.

[Figure B-1](#) provides some simple examples of joint classification. For a brace to be considered as K-joint classification, the axial force in the brace should be balanced to within 10% by forces in other braces in the same plane and on the same side of the joint. For Y-joint classification, the axial force in the brace is reacted as beam shear in the chord. For X-joint classification, the axial force in the brace is carried through the chord to braces on the opposite side. [Figure B-1 c\), e\) and h\)](#) shows joints with a combination of classifications. In c) 50% of the diagonal force is balanced with a force in the horizontal in a K-joint and 50% of the diagonal force is balanced with a beam shear force in the chord in a Y-joint. In e) 33% of the incoming diagonal force is balanced with a force in the horizontal in a K-joint with gap 1 and 67% of the incoming diagonal force is balanced with a force in the other diagonal in a K-joint with gap 2. In h) 50% of the diagonal force is balanced with a force in the horizontal on the same side of the chord in a K-joint and 50% of the diagonal force is balanced with a force in the horizontal on the opposite side of the chord in a X-joint.

Definitions of geometrical parameters can be found in [Figure B-2](#).

A classification of joints can be based on a deterministic analysis using a wave height corresponding to that with the largest contribution to fatigue damage. A conservative classification may be used keeping in mind that:

SCFX > SCFY > SCFK.

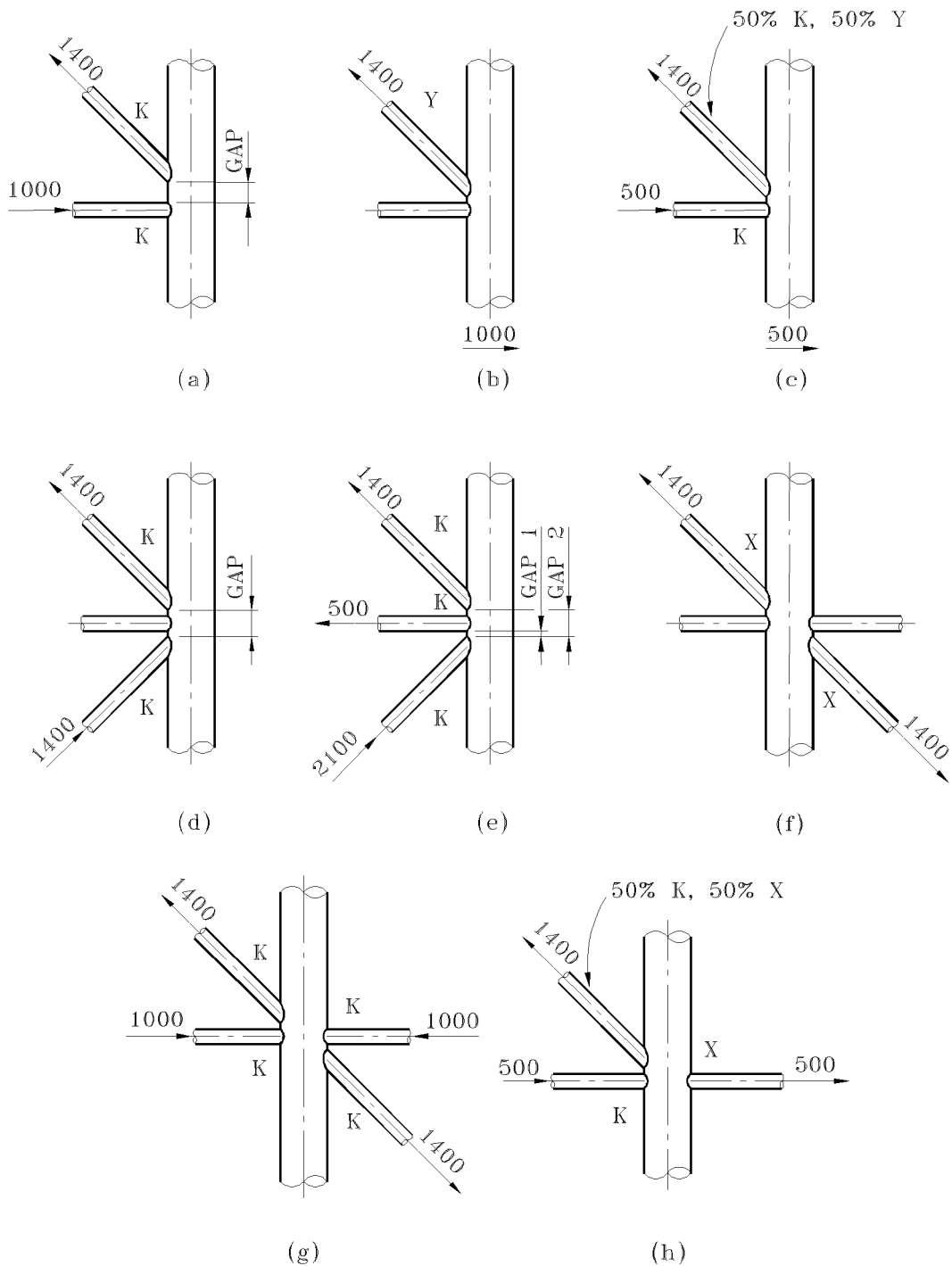
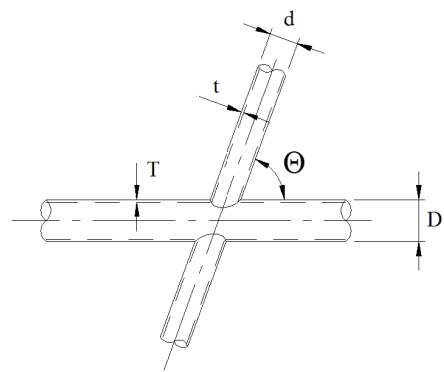
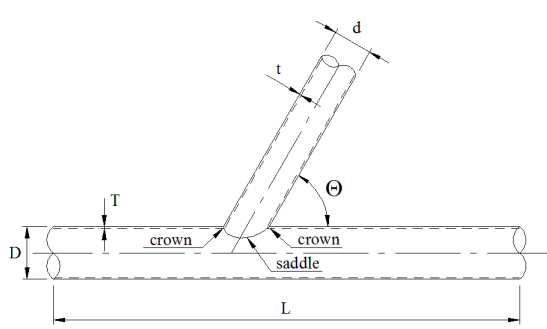


Figure B-1 Classification of simple joints

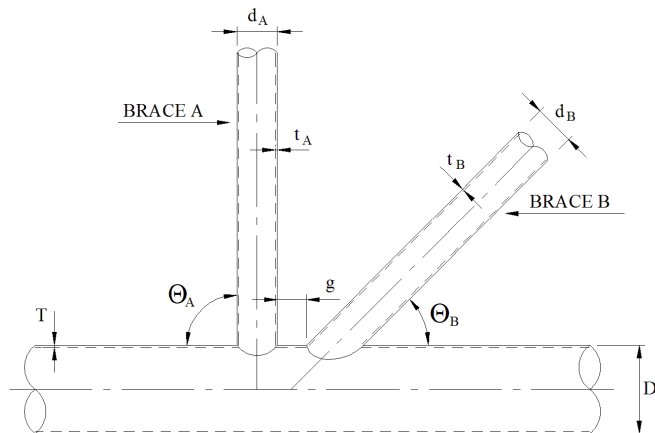


$$\beta = \frac{d}{D}$$

$$\alpha = \frac{2L}{D}$$

$$\gamma = \frac{D}{2T}$$

$$\tau = \frac{t}{T}$$



$$\beta_A = \frac{d_A}{D} \quad \beta_B = \frac{d_B}{D}$$

$$\tau_A = \frac{t_A}{T} \quad \tau_B = \frac{t_B}{T}$$

$$\gamma = \frac{D}{2T} \quad \zeta = \frac{g}{D}$$

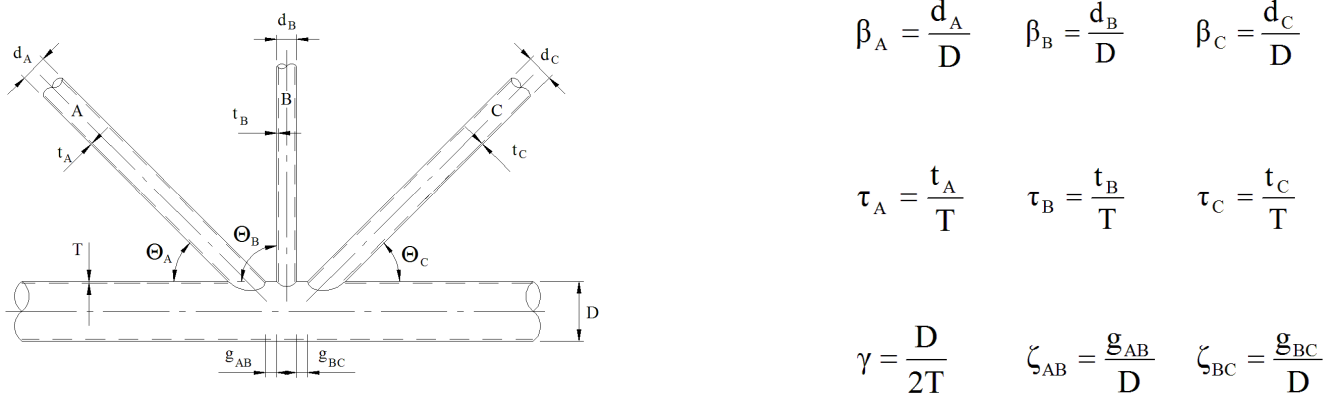


Figure B-2 Definition of geometrical parameters

The validity range for the equations in [Table B-1](#) to [Table B-5](#) is as follows:

$$0.2 \leq \beta \leq 1.0$$

$$0.2 \leq \tau \leq 1.0$$

$$8 \leq \gamma \leq 32$$

$$4 \leq \alpha \leq 40$$

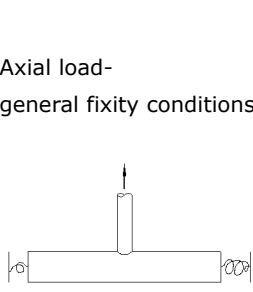
$$20^\circ \leq \theta \leq 90^\circ$$

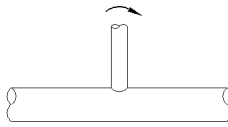
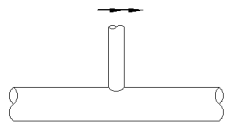
$$\frac{-0.6\beta}{\sin\theta} \leq \zeta \leq 1.0$$

See [\[4.2\]](#) if actual geometry is outside validity range.

Table B-1 Stress concentration factors for simple tubular T/Y joints

Load type and fixity conditions	Stress concentration factor equations	Eqn. no.	Short chord correction
Axial load-chord ends fixed 	Chord saddle: $\gamma \tau^{1.1} (1.11 - 3(\beta - 0.52)^2) (\sin \theta)^{1.6}$ Chord crown: $\gamma^{0.2} \tau (2.65 + 5(\beta - 0.65)^2) + \tau \beta (0.25\alpha - 3) \sin \theta$ Brace saddle: $1.3 + \gamma \tau^{0.52} \alpha^{0.1} (0.187 - 1.25\beta^{1.1}(\beta - 0.96)) (\sin \theta)^{(2.7-0.01\alpha)}$	(1) (2) (3)	F1 None F1

Load type and fixity conditions	Stress concentration factor equations	Eqn. no.	Short chord correction
	Brace crown: $3 + \gamma^{1.2} \left(0.12 \exp(-4\beta) + 0.011\beta^2 - 0.045 \right) + \beta \tau (0.1\alpha - 1.2)$	(4)	None
Axial load- general fixity conditions 	<p>Chord saddle: $(Eqn.(1)) + C_1 (0.8\alpha - 6) \tau \beta^2 (1 - \beta^2)^{0.5} (\sin 2\theta)^2$</p> <p>Chord crown: $\gamma^{0.2} \tau (2.65 + 5(\beta - 0.65)^2) + \tau \beta (C_2 \alpha - 3) \sin \theta$</p> <p>Alternatively: $SCF_{Cc} = \gamma^{0.2} \tau (2.65 + 5(\beta - 0.65)^2) - 3\tau \beta \sin \theta$ $+ \frac{\sigma_{BendingChord}}{\sigma_{AxialBrace}} \sin \theta \ SCF_{att}$</p> <p>where:</p> <ul style="list-style-type: none"> $\sigma_{BendingChord}$ = nominal bending stress in the chord $\sigma_{AxialBrace}$ = nominal axial stress in the brace. SCF_{att} = stress concentration factor for an attachment = 1.20. <p>Brace saddle: $(Eqn. (3))$</p> <p>Brace crown: $3 + \gamma^{1.2} \left(0.12 \exp(-4\beta) + 0.011\beta^2 - 0.045 \right) + \beta \tau (C_3 \alpha - 1.2)$</p> <p>Alternatively: $SCF_{Bc} = 3 + \gamma^{1.2} \left(0.12 \exp(-4\beta) + 0.011\beta^2 - 0.045 \right)$ $- 1.2\beta \tau + \frac{0.4\sigma_{BendingChord}}{\sigma_{AxialBrace}} \frac{1}{\sin \theta}$</p>	(5) (6a) (6b) (7a) (7b)	F2 None F2 None

Load type and fixity conditions	Stress concentration factor equations	Eqn. no.	Short chord correction
In-plane bending 	<p>Chord crown:</p> $1.45\beta \tau^{0.85} \gamma^{(1-0.68\beta)} (\sin \theta)^{0.7}$ <p>Brace crown:</p> $1 + 0.65\beta \tau^{0.4} \gamma^{(1.09 - 0.77\beta)} (\sin \theta)^{(0.06\gamma - 1.16)}$	(8)	None
Out-of-plane bending 	<p>Chord saddle:</p> $\gamma \tau \beta (1.7 - 1.05\beta^3) (\sin \theta)^{1.6}$ <p>Brace saddle:</p> $\tau^{-0.54} \gamma^{-0.05} (0.99 - 0.47\beta + 0.08\beta^4). (\text{Eqn.10}))$	(10)	F3
Short chord correction factors ($\alpha < 12$)			<p>$F1 = 1 - (0.83\beta - 0.56\beta^2 - 0.02) \gamma^{0.23} \exp(-0.21 \gamma^{-1.16} \alpha^{2.5})$</p> <p>$F2 = 1 - (1.43\beta - 0.97\beta^2 - 0.03) \gamma^{0.04} \exp(-0.71 \gamma^{-1.38} \alpha^{2.5})$</p> <p>$F3 = 1 - 0.55 \beta^{1.8} \gamma^{0.16} \exp(-0.49 \gamma^{-0.89} \alpha^{1.8})$</p> <p>where $\exp(x) = e^x$</p> <p>Chord-end fixity parameter: $C1 = 2(C-0.5)$ $C2 = C/2$ $C3 = C/5$ $C = \text{chord end fixity parameter}$ $0.5 \leq C \leq 1.0$, Typically $C = 0.7$.</p>

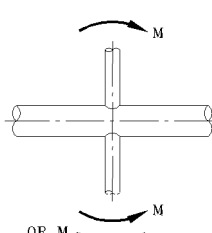
It should be noted that equation (6b) and equation (7b) will for general load conditions and moments in the chord member provide correct hot spot stresses at the crown points while equation (6a) and equation (7a) only provides correct hot spot stress due to a single action load in the considered brace. equation (6b) and equation (7b) are also more general in that a chord-fixation parameter need not be defined. In principle it can account for joint flexibility at the joints when these are included in the structural analysis. Also the upper limit for the α -parameter is removed with respect to validity of the SCF equations. Thus, these equations are in general recommended used.

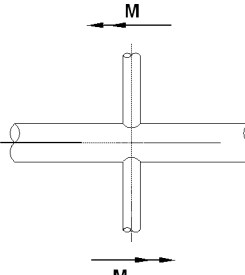
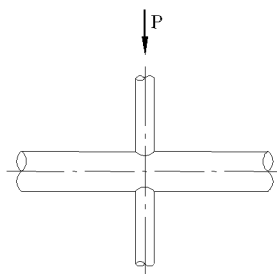
Equation (6a) and equation (6b) will provide the same result only for the special case with a single action load in the considered brace and $SCF_{att} = 1.0$. For long chords the brace may be considered as an attachment to the chord with respect to axial stress at the crown points. This would give detail category F from [Table A-7](#) (for thick braces and E-curve for thinner) which corresponds to $SCF_{att} = 1.27$ from [Table](#)

2-1. However, based on detailed finite element analysis of similar connections without need for fabrication tolerance it is assessed that $SCF_{att} = 1.20$ can be used.

The hot spot stress in the chord at the crown position due to dynamic axial force in the chord should be added to the hot spot stress range due to the bending moment including SCF_{att} .

Table B-2 Stress concentration factors for simple X tubular joints

Load type and fixity conditions	Stress concentration factor equation	Eqn. no.
Axial load (balanced)	<p>Chord saddle:</p> $3.87 \gamma \tau \beta (1.10 - \beta^{1.8}) (\sin \theta)^{1.7} \quad (12)$ <p>Chord crown:</p> $\gamma^{0.2} \tau (2.65 + 5(\beta - 0.65)^2) - 3 \tau \beta \sin \theta \quad (13)$ <p>Brace saddle:</p> $1 + 1.9 \gamma \tau^{0.5} \beta^{0.9} (1.09 - \beta^{1.7}) (\sin \theta)^{2.5} \quad (14)$ <p>Brace crown:</p> $3 + \gamma^{1.2} (0.12 \exp(-4\beta) + 0.011 \beta^2 - 0.045) \quad (15)$ <p>In joints with short cords ($\alpha < 12$) the saddle SCF can be reduced by the factor F1 (fixed chord ends) or F2 (pinned chord ends) where:</p> $F1 = 1 - (0.83 \beta - 0.56 \beta^2 - 0.02) \gamma^{0.23} \exp(-0.21 \gamma^{-1.16} \alpha^{2.5})$ $F2 = 1 - (1.43 \beta - 0.97 \beta^2 - 0.03) \gamma^{0.04} \exp(-0.71 \gamma^{-1.38} \alpha^{2.5})$	
In plane bending	<p>Chord crown: (Eqn. (8))</p> <p>Brace crown: (Eqn. (9))</p> 	

Load type and fixity conditions	Stress concentration factor equation	Eqn. no.
Out of plane bending (balanced) 	Chord saddle: $\gamma \tau \beta (1.56 - 1.34\beta^4)(\sin \theta)^{1.6}$ Brace saddle: $\tau^{-0.54} \gamma^{-0.05} (0.99 - 0.47 \beta + 0.08 \beta^4) \cdot (\text{Eqn.(16)})$ In joints with short chords ($\alpha < 12$) eqns. (16) and (17) can be reduced by the factor F3 where: $F3 = 1 - 0.55 \beta^{1.8} \gamma^{0.16} \exp(-0.49 \gamma^{-0.89} \alpha^{1.8})$	(16) (17)
Axial load in one brace only 	Chord saddle: $(1 - 0.26\beta^3) \cdot (\text{Eqn.(5)})$ Chord crown: (Eqn.6)) Brace saddle: $(1 - 0.26\beta^3) \cdot (\text{Eqn. (3)})$ Brace crown: (Eqn. (7)) In joints with short chords ($\alpha < 12$) the saddle SCFs can be reduced by the factor F1 (fixed chord ends) or F2 (pinned chord ends) where: $F1 = 1 - (0.83\beta - 0.56\beta^2 - 0.02) \gamma^{0.23} \exp(-0.21 \gamma^{-1.16} \alpha^{2.5})$ $F2 = 1 - (1.43\beta - 0.97\beta^2 - 0.03) \gamma^{0.04} \exp(-0.71 \gamma^{-1.38} \alpha^{2.5})$	(18) (19)

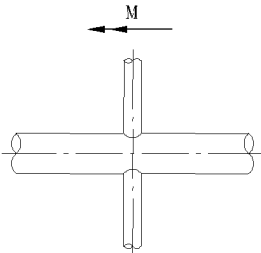
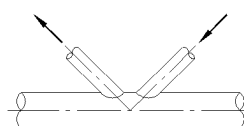
Load type and fixity conditions	Stress concentration factor equation	Eqn. no.
Out-of-plane bending on one brace only 	<p>Chord saddle: (Eqn. (10)) Brace saddle: (Eqn. (11)) In joints with short chords ($\alpha < 12$) eqns. (10) and (11) can be reduced by the factor F3 where:</p> $F3 = 1 - 0.55 \beta^{1.8} \gamma^{0.16} \exp(-0.49 \gamma^{-0.89} \alpha^{1.8})$	

Table B-3 Stress concentration factors for simple tubular K joints and overlap K joints

Load type and fixity conditions	Stress concentration factor equation	Eqn. no.	Short chord correction
Balanced axial load 	<p>Chord:</p> $\tau^{0.9} \gamma^{0.5} \left(0.67 - \beta^2 + 1.16 \beta \right) \sin \theta \left(\frac{\sin \theta_{\max}}{\sin \theta_{\min}} \right)^{0.30} \cdot \left(\frac{\beta_{\max}}{\beta_{\min}} \right)^{0.30} \left(1.64 + 0.29 \beta^{-0.38} \text{ATAN}(8\zeta) \right)$ <p>Brace:</p> $1 + \left(1.97 - 1.57 \beta^{0.25} \right) \tau^{-0.14} (\sin \theta)^{0.7} \cdot (\text{Eqn. (20)}) + \sin^{1.8}(\theta_{\max} + \theta_{\min}) \cdot (0.131 - 0.084 \text{ATAN}(14\zeta + 4.2\beta)) \cdot C \beta^{1.5} \gamma^{0.5} \tau^{-1.22}$ <p>where: $C = 0$ for gap joints $C = 1$ for the through brace $C = 0.5$ for the overlapping brace. Note that τ, β, θ and the nominal stress relate to the brace under consideration. ATAN is arctangent evaluated in radians.</p>	(20) (21)	None None

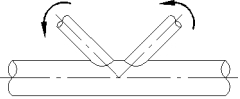
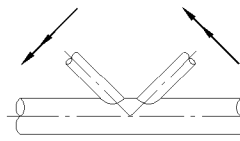
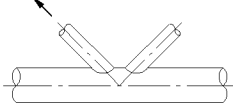
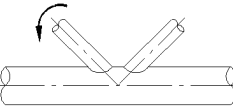
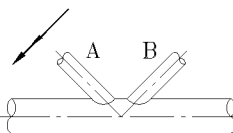
Load type and fixity conditions	Stress concentration factor equation	Eqn. no.	Short chord correction
Unbalanced in plane bending 	Chord crown: (Eqn. (8)) (for overlaps exceeding 30% of contact length use $1.2 \cdot$ (Eqn. (8))) Gap joint brace crown: (Eqn. (9)) Overlap joint brace crown: (Eqn. (9)) $\cdot (0.9 + 0.4\beta)$	(22)	
Unbalanced out-of-plane bending 	Chord saddle SCF adjacent to brace A: $(Eqn.(10))_A \cdot \left(1 - 0.08(\beta_B \gamma)^{0.5} \exp(-0.8x)\right) + (Eqn.(10))_B \cdot \left(1 - 0.08(\beta_A \gamma)^{0.5} \exp(-0.8x)\right) \left(2.05 \beta_{max}^{0.5} \exp(-1.3x)\right)$ where: $x = 1 + \frac{\zeta \sin \theta_A}{\beta_A}$ Brace A saddle SCF: $\tau^{-0.54} \gamma^{-0.05} (0.99 - 0.47 \beta + 0.08 \beta^4) \cdot (Eqn. (23))$	(23)	F4
$F4 = 1 - 1.07 \beta^{1.88} \exp(-0.16 \gamma^{-1.06} \alpha^{2.4})$			
(Eqn. (10)) _A is the chord SCF adjacent to brace A as estimated from Eqn. (10). Note that the designation of braces A and B is not geometry dependent. It is nominated by the user.			

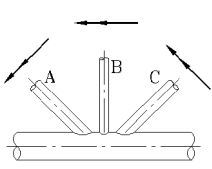
Table B-4 Stress concentration factors for simple tubular K joints and overlap K joints

Load type and fixity conditions	Stress concentration factor equations	Eqn. no.	Short chord correction
Axial load on one brace only 	Chord saddle: (Eqn. (5)) Chord crown: (Eqn. (6)) Brace saddle: (Eqn.(3)) Brace crown: (Eqn. (7)) Note that all geometric parameters and the resulting SCFs relate to the loaded brace.		F1 - F1 -
In-plane-bending on one brace only 	Chord crown: (Eqn. (8)) Brace crown: (Eqn. (9)) Note that all geometric parameters and the resulting SCFs relate to the loaded brace.		
Out-of-plane bending on one brace only 	Chord saddle: $(Eqn.(10))A \cdot \left(1 - 0.08(\beta_B \gamma)^{0.5} \exp(-0.8x)\right)$ where: $x = 1 + \frac{\zeta \sin \theta_A}{\beta_A}$ Brace saddle: $\tau^{-0.54} \gamma^{-0.05} (0.99 - 0.47\beta + 0.08\beta^4) \cdot (Eqn.(25))$	(25)	F3 F3

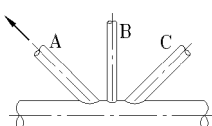
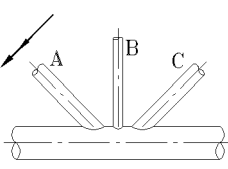
<i>Load type and fixity conditions</i>	<i>Stress concentration factor equations</i>	<i>Eqn. no.</i>	<i>Short chord correction</i>
Short chord correction factors:			
	$F_1 = 1 - (0.83\beta - 0.56\beta^2 - 0.02)\gamma^{0.23} \exp(-0.21\gamma^{-1.16}\alpha^{2.5})$		
	$F_3 = 1 - 0.55\beta^{1.8}\gamma^{0.16} \exp(-0.49\gamma^{-0.89}\alpha^{1.8})$		

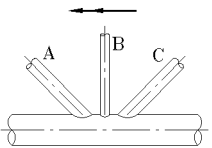
Table B-5 Stress concentration factors for simple KT tubular joints and overlap KT joints

<i>Load type</i>	<i>Stress concentration factor equation</i>	<i>Eqn. no.</i>
Balanced axial load	Chord: (Eqn. (20)) Brace: (Eqn. (21)) For the diagonal braces A and C use $\zeta = \zeta_{AB} + \zeta_{BC} + \beta_B$. For the central brace, B, use $\zeta = \text{maximum of } \zeta_{AB}, \zeta_{BC}$.	
In-plane bending	Chord crown: (Eqn. (8)) Brace crown: (Eqn. (9))	

Load type	Stress concentration factor equation	Eqn. no.
Unbalanced out-of-plane bending 	<p>Chord saddle SCF adjacent to diagonal brace A:</p> $(Eqn.(10))_A \cdot (1 - 0.08(\beta_B \gamma)^{0.5} \exp(-0.8x_{AB})) (1 - 0.08(\beta_C \gamma)^{0.5} \exp(-0.8x_{AC})) +$ $(Eqn(10))_B \cdot (1 - 0.08(\beta_A \gamma)^{0.5} \exp(-0.8x_{AB})) (2.05\beta_{\max}^{0.5} \exp(-1.3x_{AB})) +$ $(Eqn(10))_C \cdot (1 - 0.08(\beta_A \gamma)^{0.5} \exp(-0.8x_{AC})) (2.05\beta_{\max}^{0.5} \exp(-1.3x_{AC}))$ <p>where:</p> $x_{AB} = 1 + \frac{\zeta_{AB} \sin \theta_A}{\beta_A}$ $x_{AC} = 1 + \frac{(\zeta_{AB} + \zeta_{BC} + \beta_B) \sin \theta_A}{\beta_A}$	(27)

Load type	Stress concentration factor equation	Eqn. no.
	<p>Chord saddle SCF adjacent to central brace B:</p> $(Eqn.(10))_B \cdot \left(1 - 0.08(\beta_A \gamma)^{0.5} \exp(-0.8x_{AB})\right)^{P_1} \cdot$ $\left(1 - 0.08(\beta_C \gamma)^{0.5} \exp(-0.8x_{BC})\right)^{P_2} +$ $(Eqn.(10))_A \cdot \left(1 - 0.08(\beta_B \gamma)^{0.5} \exp(-0.8x_{AB})\right) \left(2.05 \beta_{\max}^{0.5} \exp(-1.3x_{AB})\right) +$ $(Eqn.(10))_C \cdot \left(1 - 0.08(\beta_B \gamma)^{0.5} \exp(-0.8x_{BC})\right) \left(2.05 \beta_{\max}^{0.5} \exp(-1.3x_{BC})\right)$ <p>where:</p> $x_{AB} = 1 + \frac{\zeta_{AB} \sin \theta_B}{\beta_B} \quad (28)$ $x_{BC} = 1 + \frac{\zeta_{BC} \sin \theta_B}{\beta_B}$ $P_1 = \left(\frac{\beta_A}{\beta_B}\right)^2$ $P_2 = \left(\frac{\beta_C}{\beta_B}\right)^2$	
Out-of-plane bending brace SCFs	<p>Out-of-plane bending brace SCFs are obtained directly from the adjacent chord SCFs using:</p> $\tau^{-0.54} \gamma^{-0.05} (0.99 - 0.47 \beta + 0.08 \beta^4) \cdot SCF_{chord} \quad (29)$ <p>where $SCF_{chord} = (Eqn. 27) \text{ or } (Eqn. (28))$</p>	

Load type	Stress concentration factor equation	Eqn. no.
Axial load on one brace only 	Chord saddle: (Eqn. (5)) Chord crown: (Eqn. (6)) Brace saddle: (Eqn. (3)) Brace crown: (Eqn. (7))	
Out-of-plane bending on one brace only 	Chord SCF adjacent to diagonal brace A: $(Eqn.(10))_A \cdot \left(1 - 0.08(\beta_B \gamma)^{0.5} \exp(-0.8x_{AB})\right) \left(1 - 0.08(\beta_C \gamma)^{0.5} \exp(-0.8x_{AC})\right)$ where: $x_{AB} = 1 + \frac{\zeta_{AB} \sin \theta_A}{\beta_A}$ $x_{AC} = 1 + \frac{(\zeta_{AB} + \zeta_{BC} + \beta_B) \sin \theta_A}{\beta_A}$	(30)

Load type	Stress concentration factor equation	Eqn. no.
	<p>Chord SCF adjacent to central brace B:</p> $(Eqn.(10))_B \cdot \left(1 - 0.08(\beta_A \gamma)^{0.5} \exp(-0.8x_{AB})\right)^{P_1} \cdot \left(1 - 0.08(\beta_C \gamma)^{0.5} \exp(-0.8x_{BC})\right)^{P_2}$ <p>where:</p> $x_{AB} = 1 + \frac{\zeta_{AB} \sin \theta_B}{\beta_B}$ $x_{BC} = 1 + \frac{\zeta_{BC} \sin \theta_B}{\beta_B}$ $P_1 = \left(\frac{\beta_A}{\beta_B}\right)^2$ $P_2 = \left(\frac{\beta_C}{\beta_B}\right)^2$ 	(31)
Out-of-plane brace SCFs	<p>Out-of-plane brace SCFs are obtained directly from the adjacent chord SCFs using:</p> $\tau^{-0.54} \gamma^{-0.05} (0.99 - 0.47\beta + 0.08\beta^4) \cdot SCF_{chord}$	(32)

APPENDIX C STRESS CONCENTRATION FACTORS FOR PENETRATIONS WITH REINFORCEMENTS

C.1 Stress concentration factors for small circular penetrations with reinforcement

C.1.1 General

Stress concentration factors (SCF) at holes in plates with inserted tubulars are given in [Figure C-1](#) to [Figure C-15](#).

Stress concentration factors at holes in plates with ring reinforcement are given in [Figure C-16](#) to [Figure C-20](#).

Stress concentration factors at holes in plates with double ring reinforcement given in [Figure C-21](#) to [Figure C-24](#).

The SCFs in these figures may also be used for fatigue assessments of the welds. The calculated SCFs are considered to be valid also for thicker plates where larger fillet welds are going to be used in design than that shown in these graphs. Where the forces in the main plate is transferred to the ring reinforcement through two fillet welds, both these welds can be assumed effective for transfer of this force for calculation of fatigue damage in these. Stresses in the plate normal to the weld, $\Delta\sigma_{np}$, and stresses parallel to the weld, $\Delta\tau_{//}$, in equation (3.1.4) may be derived from the stresses in the plate. The total stress range, $\Delta\sigma_w$, from equation (3.1.4) (or from equation (2.3.4)) is then used together with the W3 curve to evaluate number of cycles until failure.

C.1.2 Example of fatigue analysis of a welded penetration in plate

A tubular $\Phi 800 \times 15$ is used as a sleeve through a deck plate of thickness 20 mm. The tubular shall be welded to the deck plate by a double sided fillet weld.

Assume Weibull parameter $h = 0.90$ and that the deck has been designed such that S-N class F3 details can be welded to the deck plate and still achieves a fatigue life of 20 years. From [Table 5-2](#) a maximum stress range of 199.6 MPa during 10^8 cycles is derived for the F3 detail.

Questions asked:

- 1) Is the fatigue life of the penetration acceptable with respect to fatigue cracking from the weld toe?
- 2) How large fillet weld is required to avoid fatigue cracking from the weld root?

The following assessment is made: $r/t_p = 20$, $t_r/t_p = 0.75$. It is assumed that $H/t_r = 5$. Then from:

- [Figure C-4](#) SCF = 2.17 applies to position [Figure 3-4 a\)](#).
- [Figure C-7](#) SCF = 0.15 applies to position [Figure 3-4 c\)](#) and weld root.
- [Figure C-10](#) SCF = 1.07 applies to position [Figure 3-4 b\)](#) and weld toe.
- [Figure C-12](#) SCF = 0.46 applies to position [Figure 3-4 b\)](#) and weld root.
- [Figure C-14](#) SCF = -0.75 applies to position [Figure 3-4 b\)](#) and weld toe.

A negative SCF value in some of the figures means that the resulting stress is negative at the hot spot for a positive stress in the plate. Thus for fatigue assessment the absolute value should be used.

The C-curve applies to position [Figure 3-4 a\).](#)

The D-curve applies to weld toes of [Figure 3-4 b\).](#)

The W3-curve applies to weld root of [Figure 3-4 c\).](#)

Check of fatigue cracking at the [Figure 3-4 a\)](#) position:

$\Delta\sigma = \Delta\sigma_0 \times \text{SCF} = 199.6 \times 2.17 = 433.13$ MPa which is just within the acceptable value of 445.5 MPa for a C detail, see [Table 5-2](#).

Check of fatigue cracking at the [Figure 3-4](#) a b position:

$\Delta\sigma = \Delta\sigma_0 \times SCF = 199.6 \times 1.07 = 213.57$ MPa which is well within the acceptable value of 320.8 MPa for a D detail, see [Table 5-2](#).

Thus the fatigue life of weld toe is acceptable.

The required throat thickness is calculated as follows. From [Table 5-2](#) a maximum stress range of 128.2 MPa for a W3 detail (Weibull shape parameter = 0.90).

Then from considerations of equilibrium in direction normal to the weld toe:

$$\Delta\sigma_n = \sigma_{nominal} SCF = 199.6 \cdot 0.15 = 29.94$$

From considerations of equilibrium in direction parallel with the weld toe:

$$\tau_{\parallel p} = \sigma_{nominal} SCF = 199.6 \cdot 0.46 = 91.82$$

Then from equation (3.1.4):

$$128.2 = \frac{20}{2a} \sqrt{(29.94)^2 + 0.2(91.82)^2}$$

From this equation a required throat thickness is $a = 4.0$ mm for both sides of the plate. This is a required weld size that is well below the minimum required weld size specified in ship classification rules.

C.1.3 Stress control factors for small circular penetrations with reinforcements

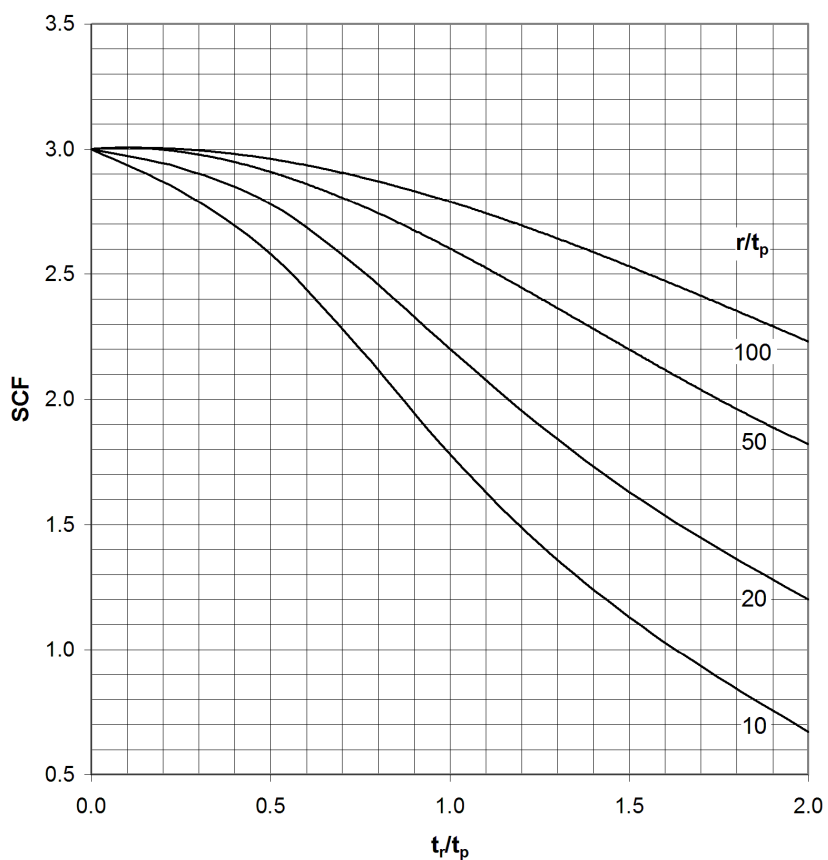
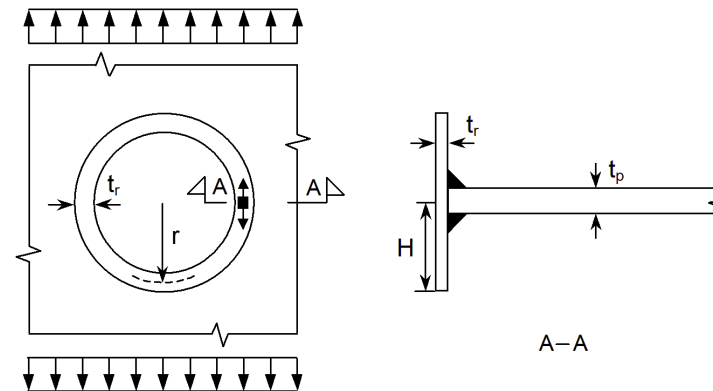


Figure C-1 SCF at hole with inserted tubular. Stress at outer surface of tubular, parallel with weld.
 $H/t_r = 2$

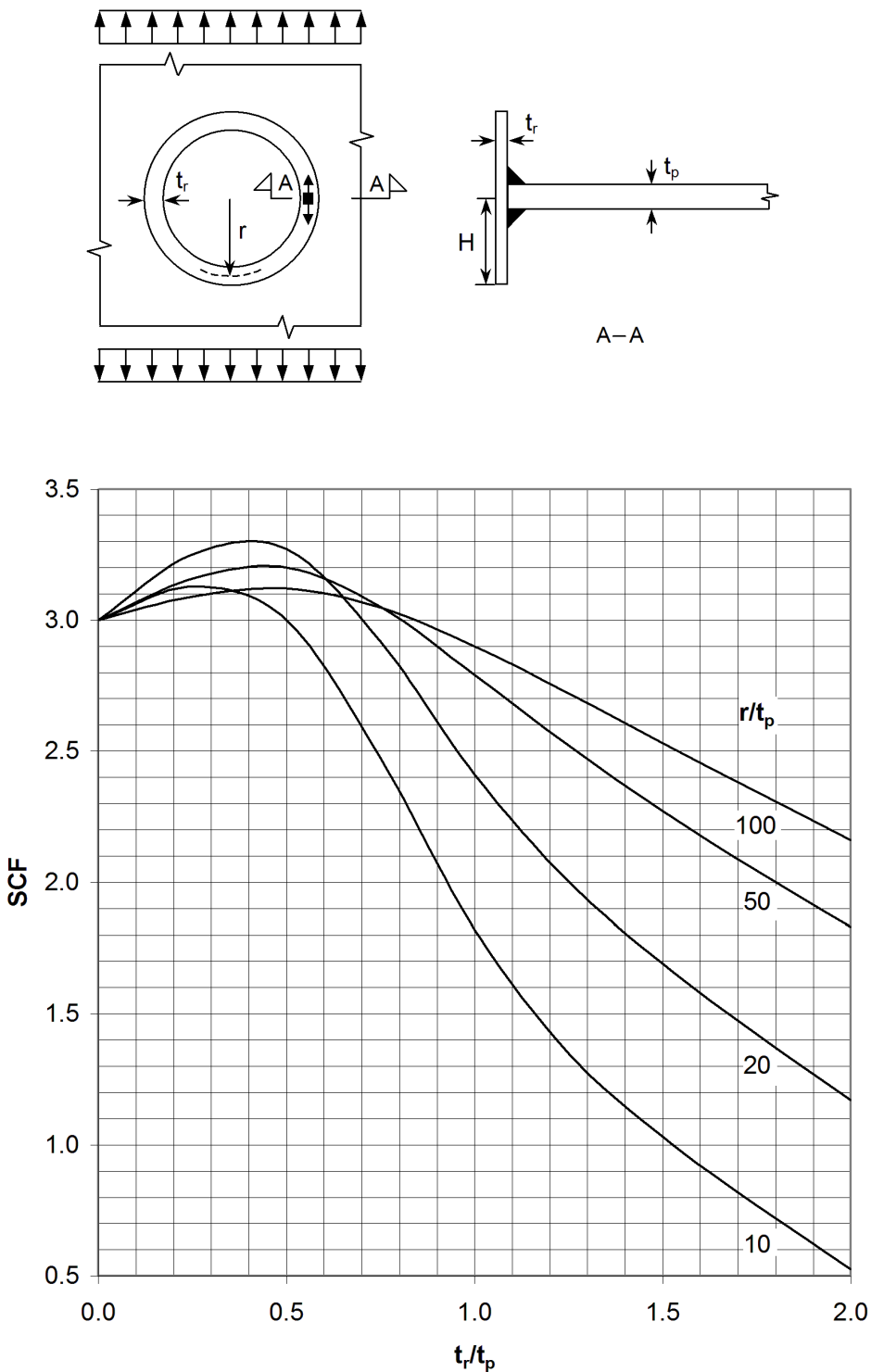


Figure C-2 SCF at hole with inserted tubular. Stress at outer surface of tubular, parallel with weld. $H/t_r = 5$

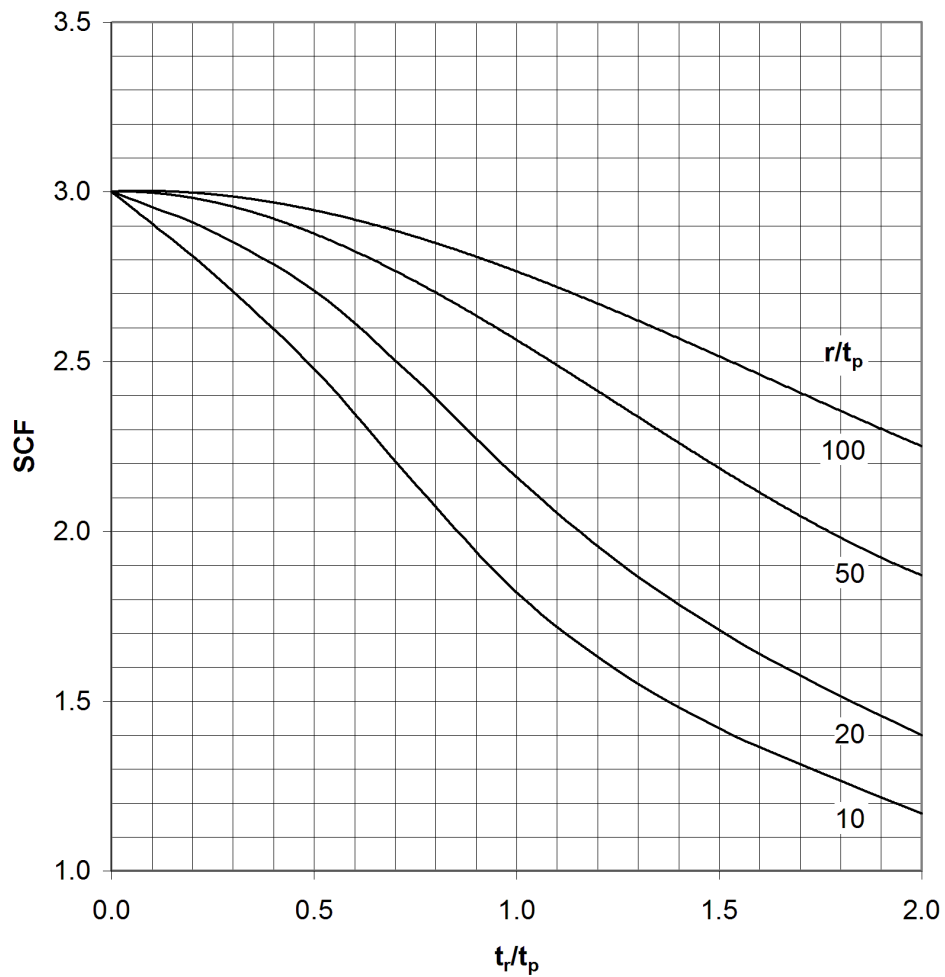
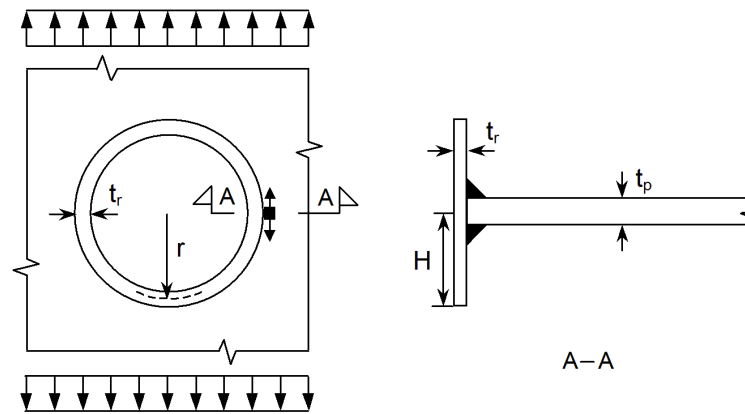


Figure C-3 SCF at hole with inserted tubular. Stress in plate, parallel with weld. $H/t_r = 2$

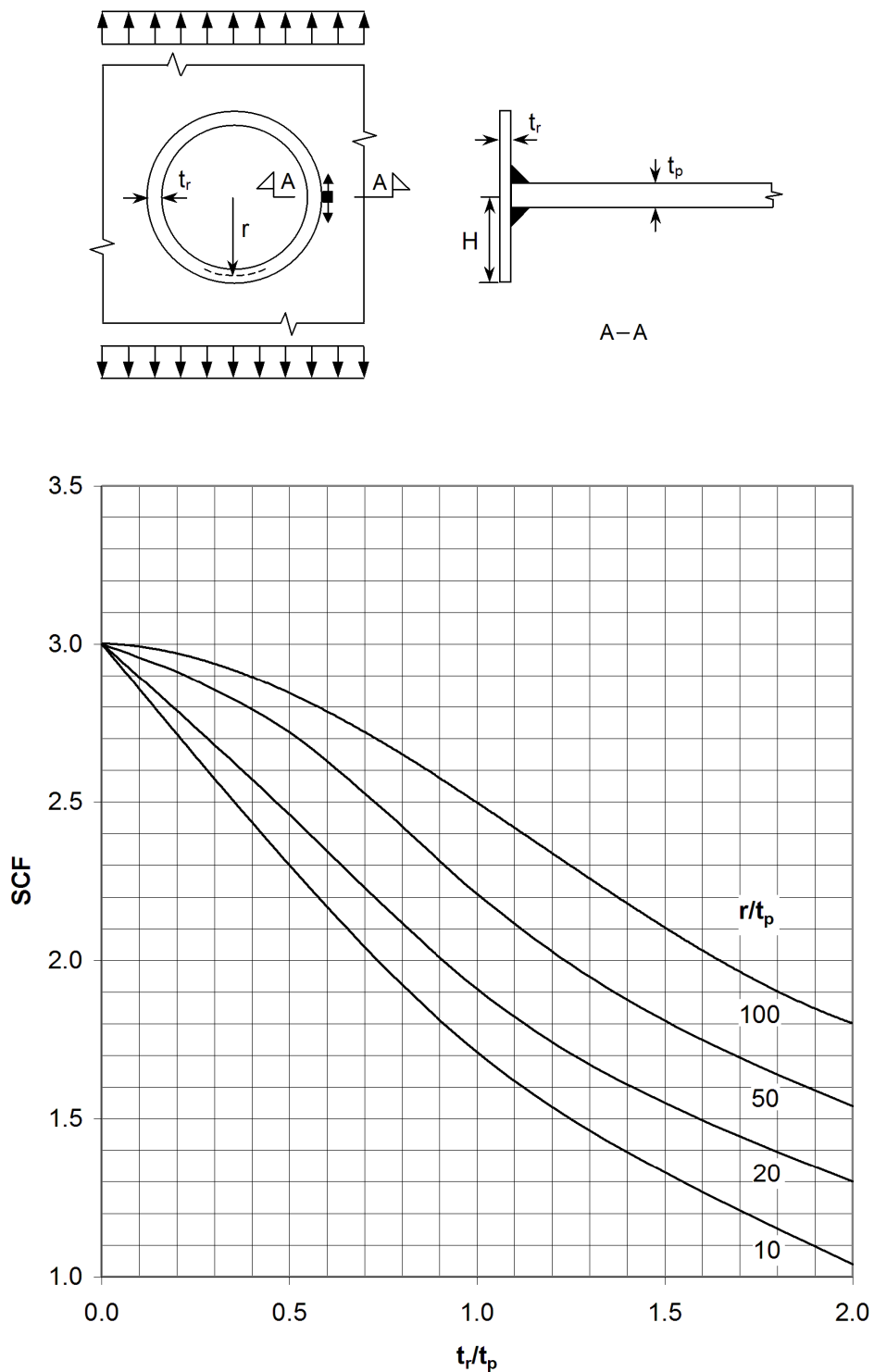


Figure C-4 SCF at hole with inserted tubular. Stress in plate, parallel with weld. $H/t_r = 5$

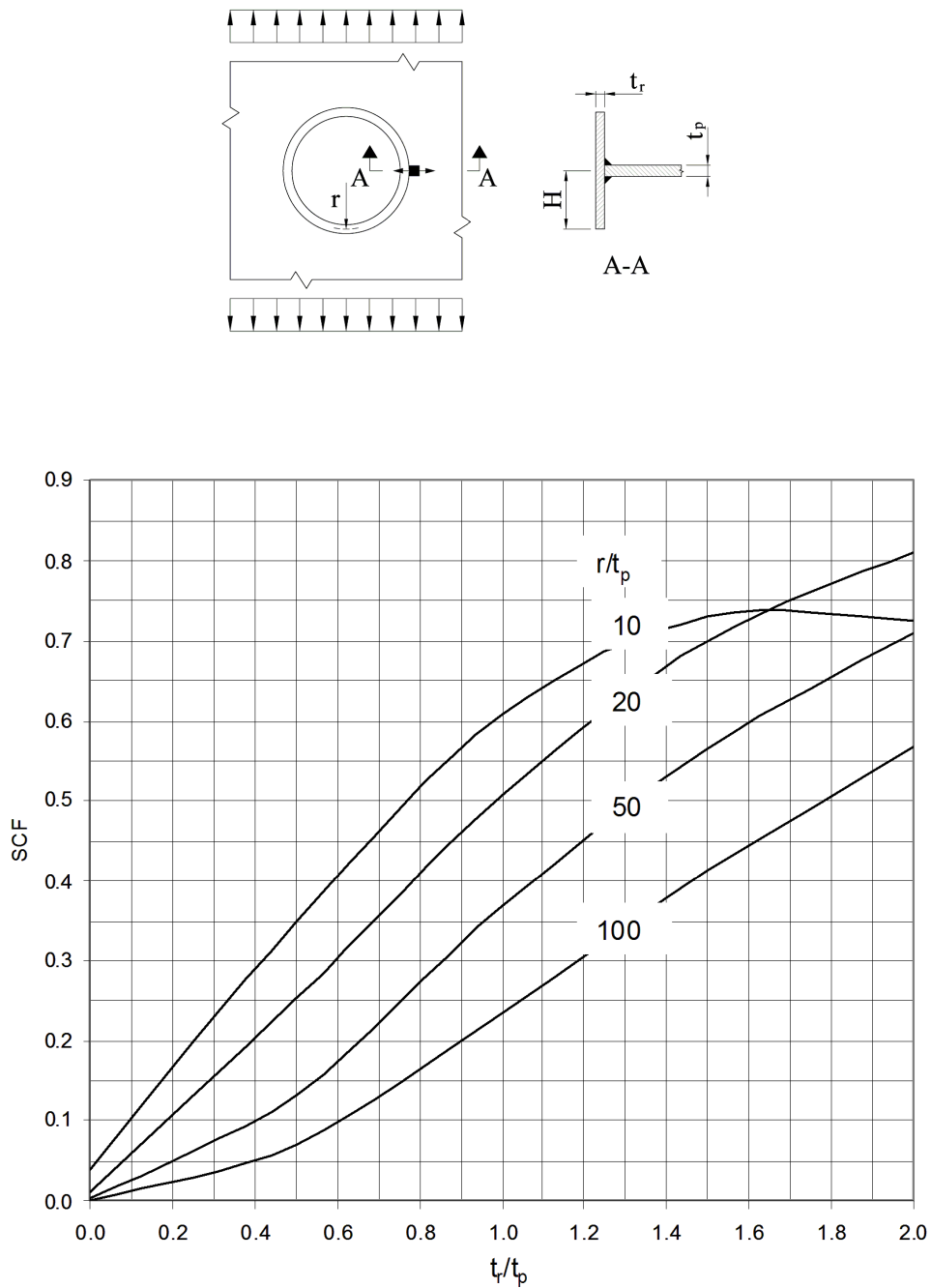


Figure C-5 SCF at hole with inserted tubular. Stress in plate normal to the weld. $H/t_r = 5$

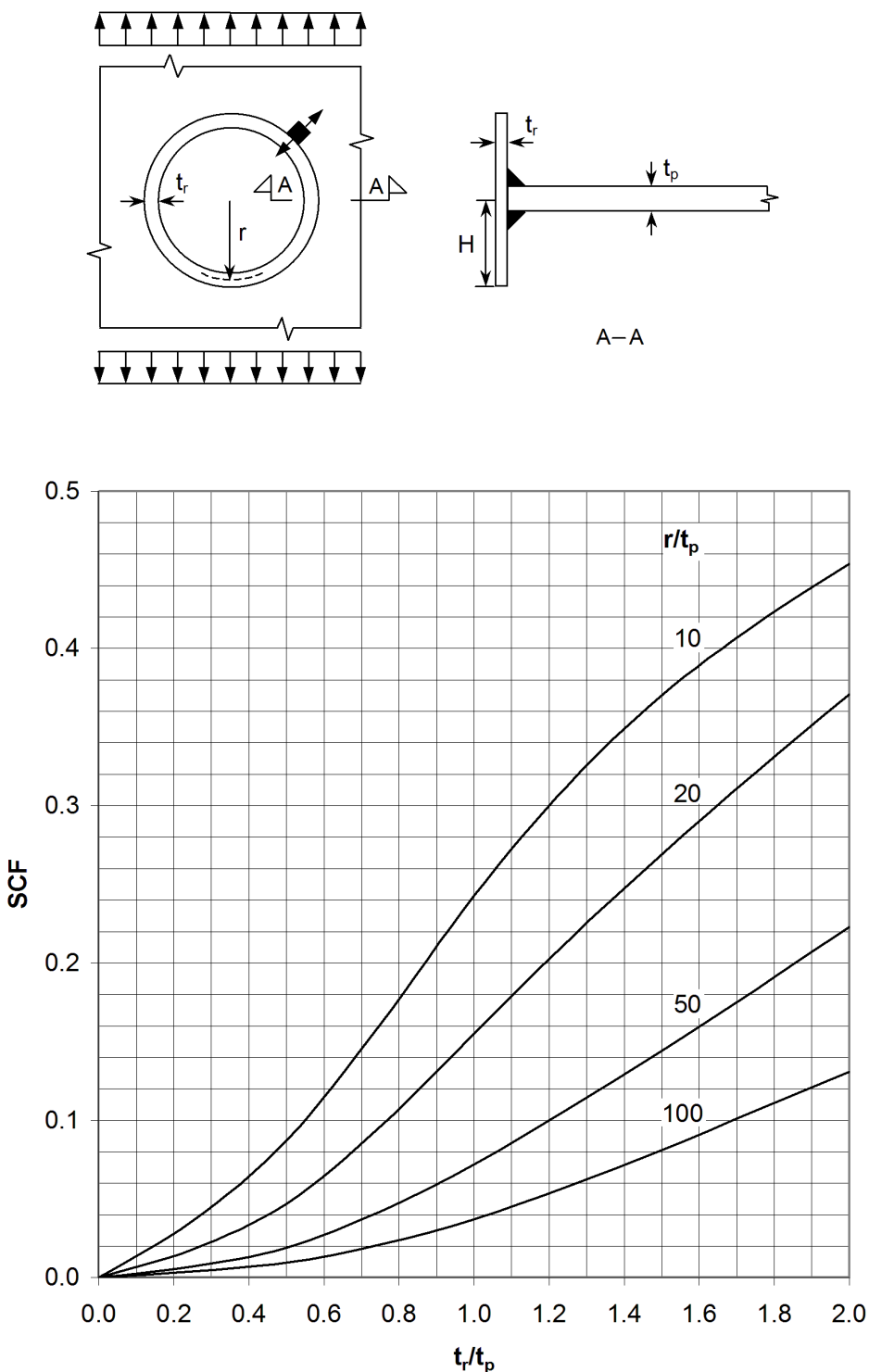


Figure C-6 SCF at hole with inserted tubular. Stress in plate, normal to weld. $H/t_r = 2$

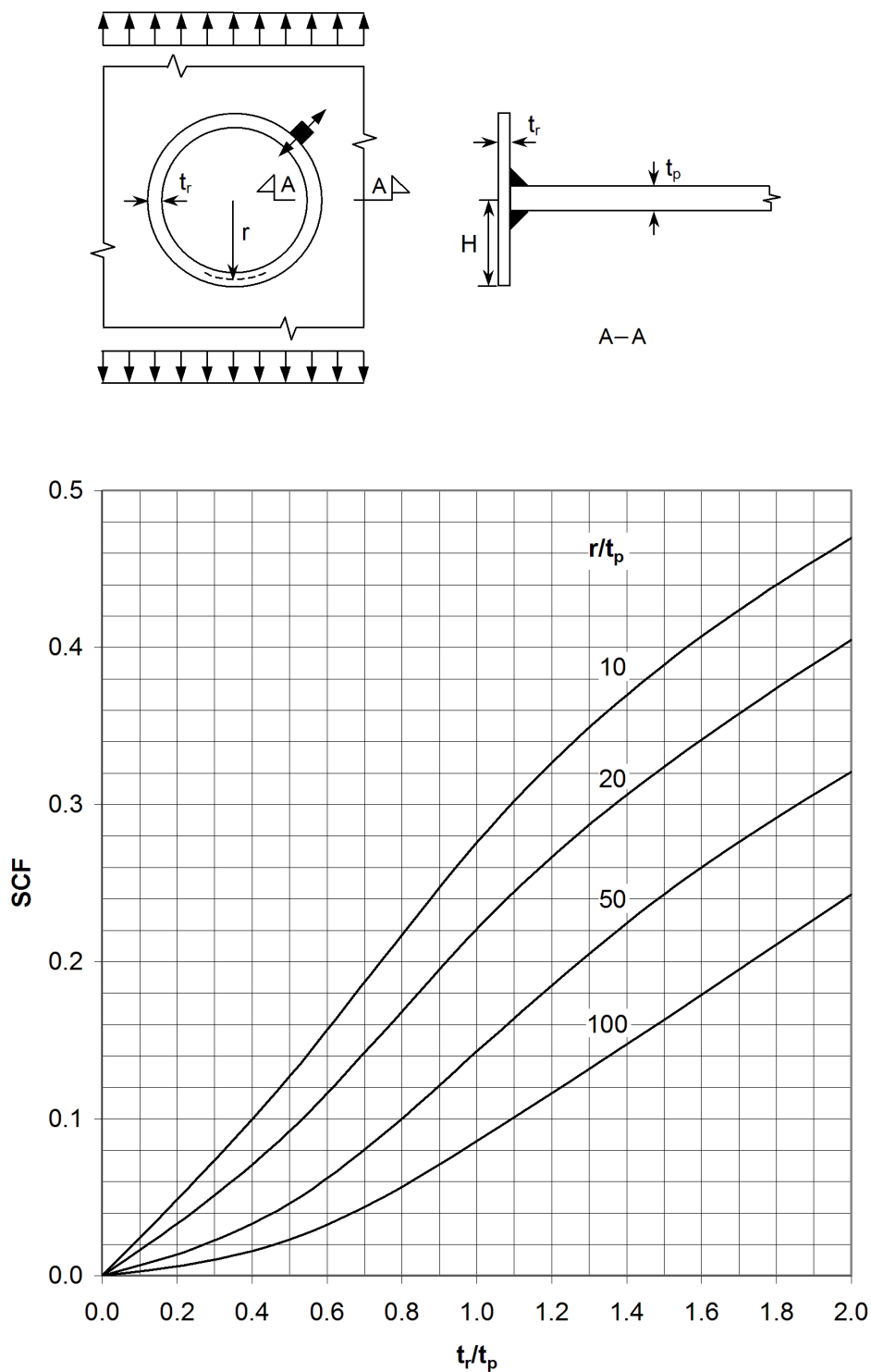


Figure C-7 SCF at hole with inserted tubular. Stress in plate, normal to weld. $H/t_r = 5$

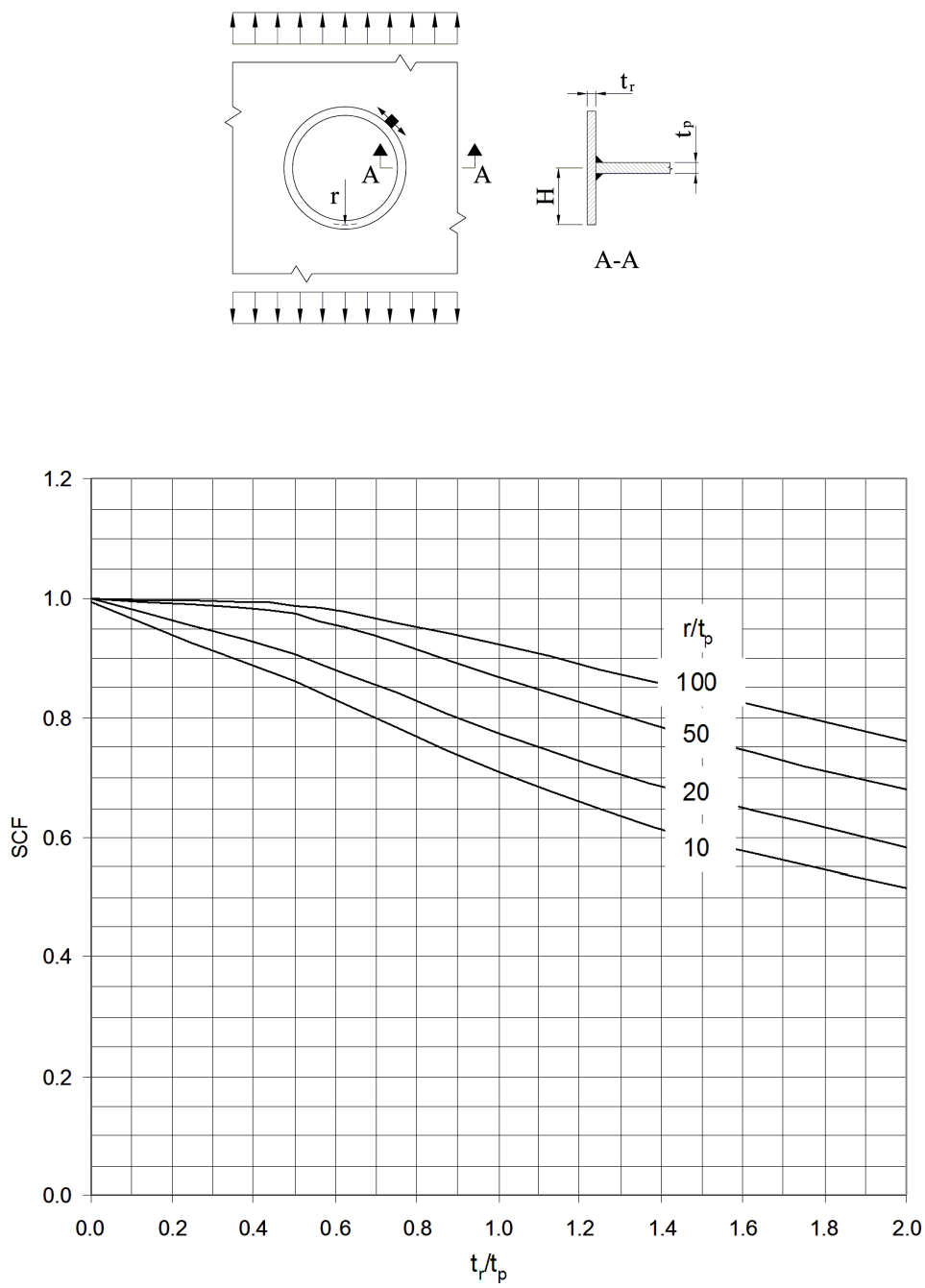


Figure C-8 SCF at hole with inserted tubular. Stress in plate parallel with the weld. $H/t_r = 5$

Table C-1 θ = angle to principal stress. $H/t_r = 2$

t_r/t_p	$r/t_p = 10$	$r/t_p = 20$	$r/t_p = 50$	$r/t_p = 100$
0.0	90	90	90	90
0.5	72	80	86	88
1.0	56	63	75	82
1.5	50	54	64	73
2.0	46	50	57	66

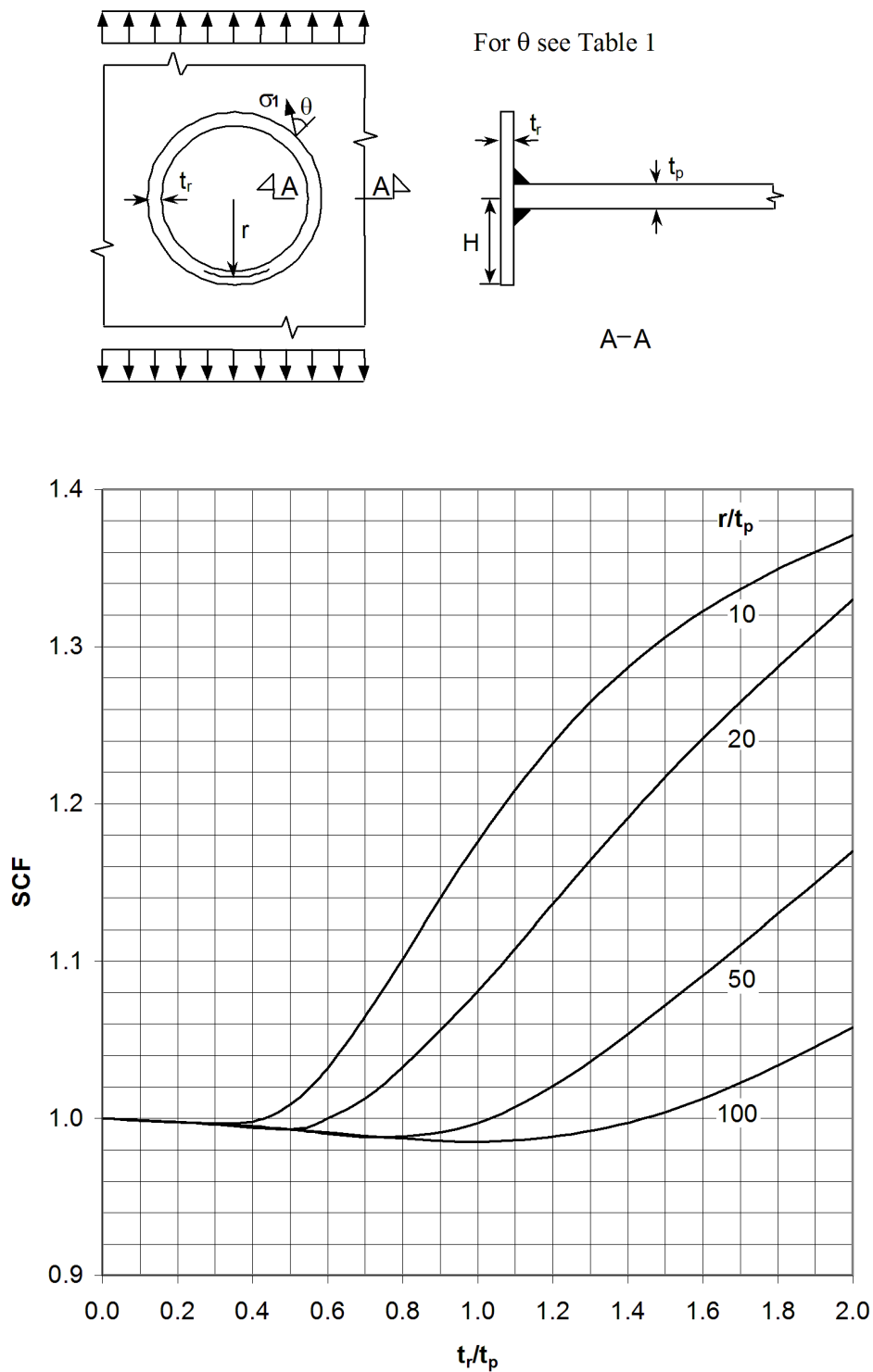


Figure C-9 SCF at hole with inserted tubular. Principal stress in plate. $H/t_r = 2$

Table C-2 θ = angle to principal stress. $H/t_r = 5$

t_r/t_p	$r/t_p = 10$	$r/t_p = 20$	$r/t_p = 50$	$r/t_p = 100$
0.0	90	90	90	90
0.5	66	72	80	85
1.0	54	58	65	72
1.5	49	52	56	62
2.0	46	48	52	56

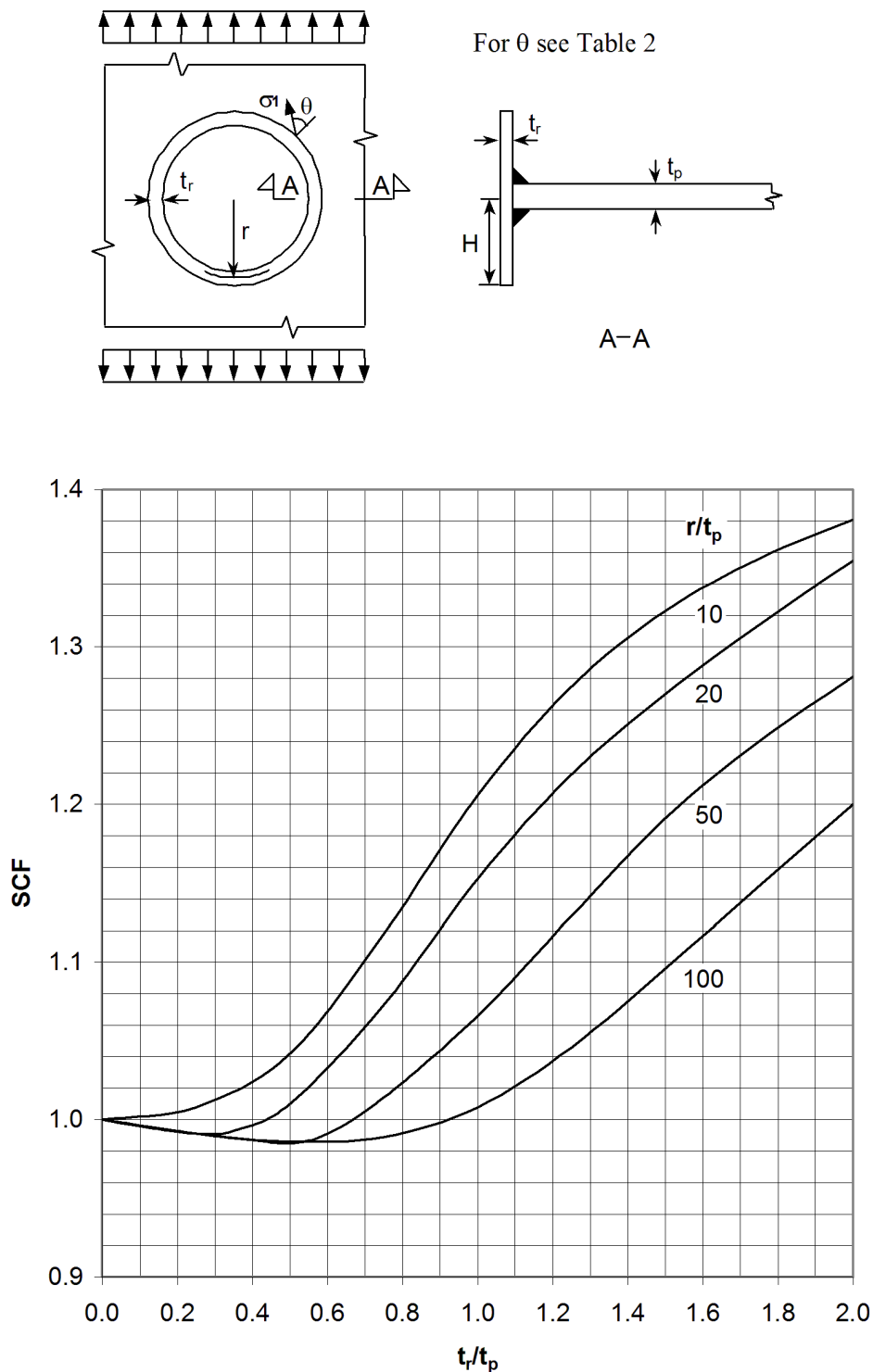


Figure C-10 SCF at hole with inserted tubular. Principal stress in plate. $H/t_r = 5$

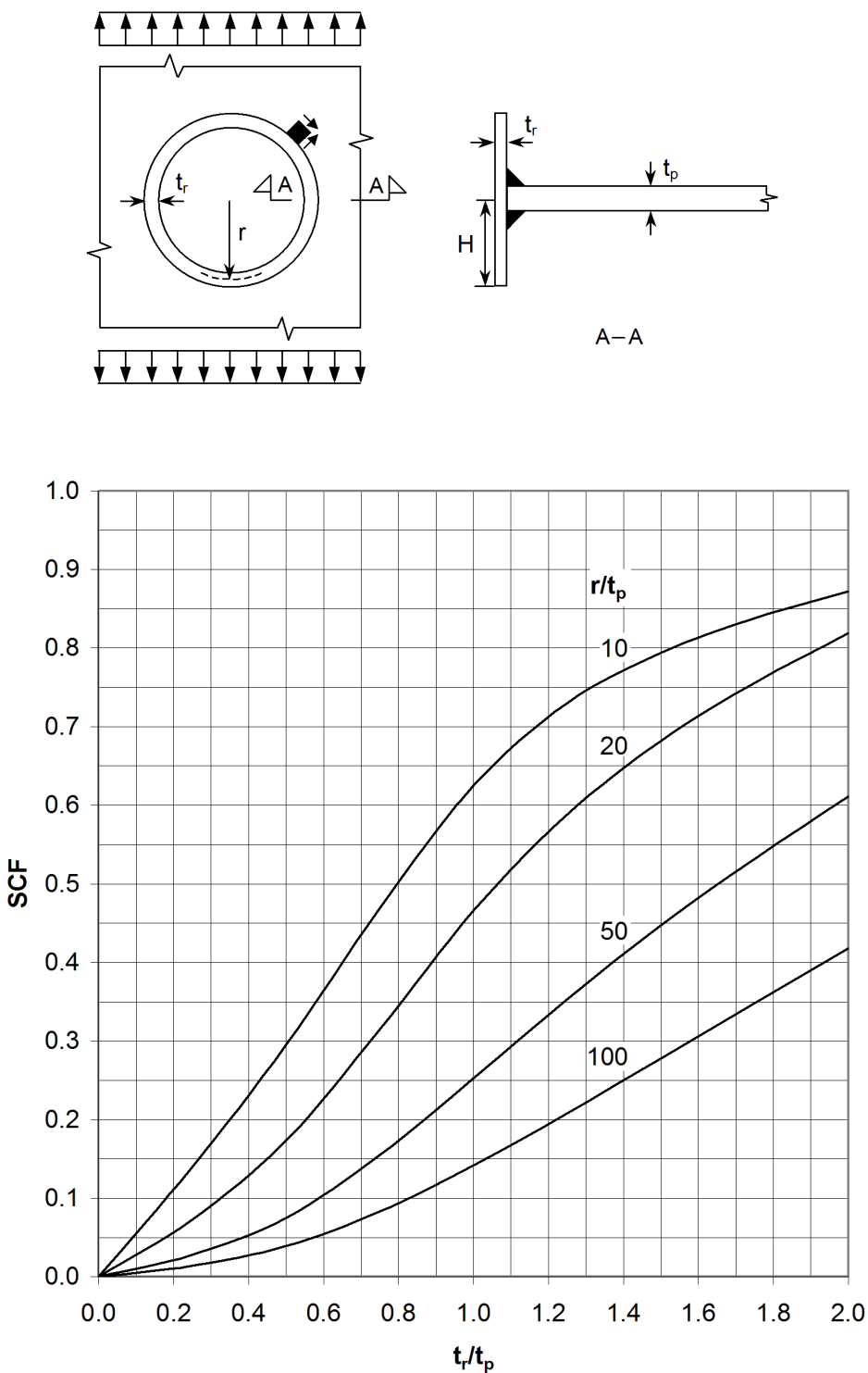


Figure C-11 SCF at hole with inserted tubular. Shear stress in plate. $H/t_r = 2$

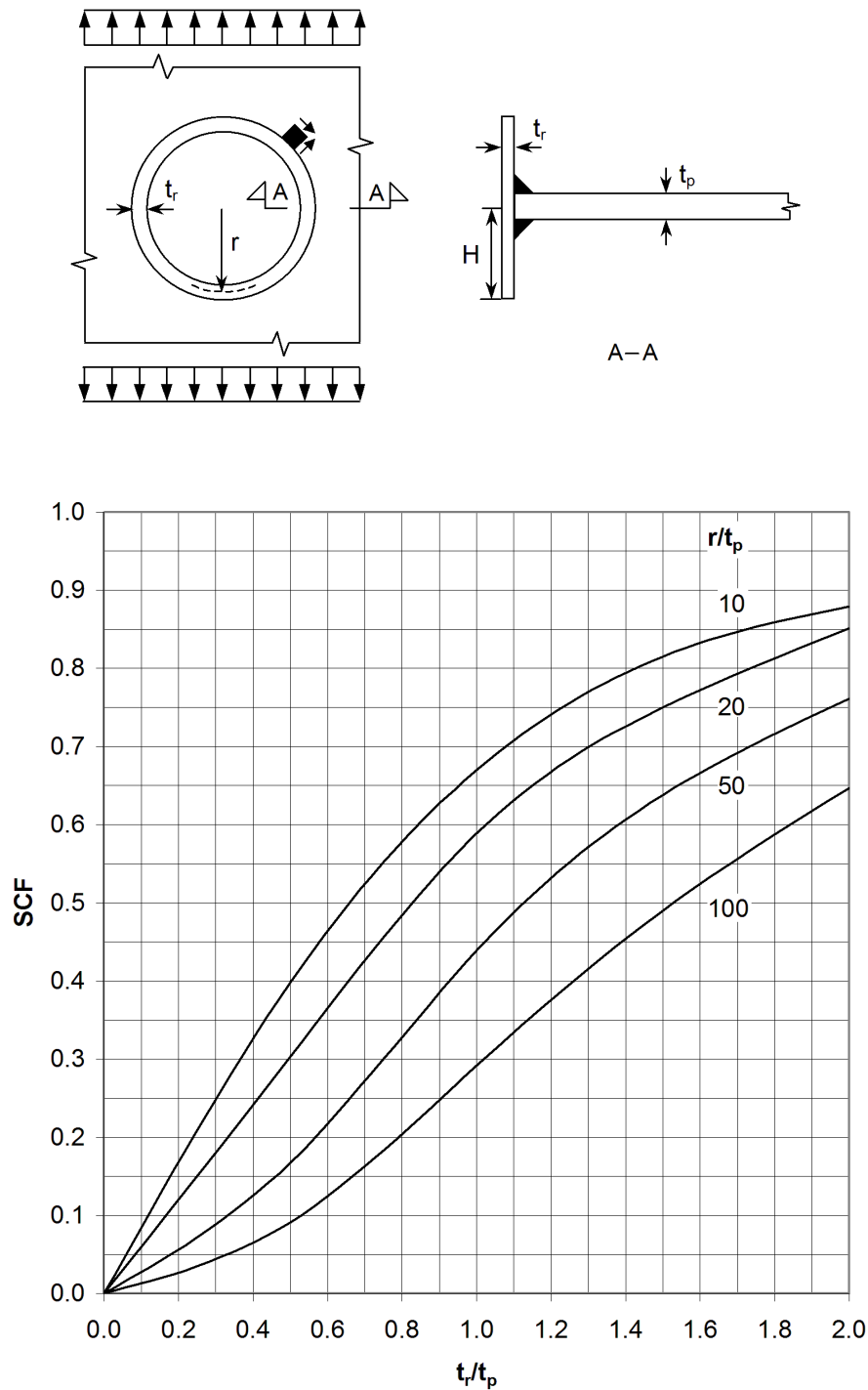


Figure C-12 SCF at hole with inserted tubular. Shear stress in plate. $H/t_r = 5$

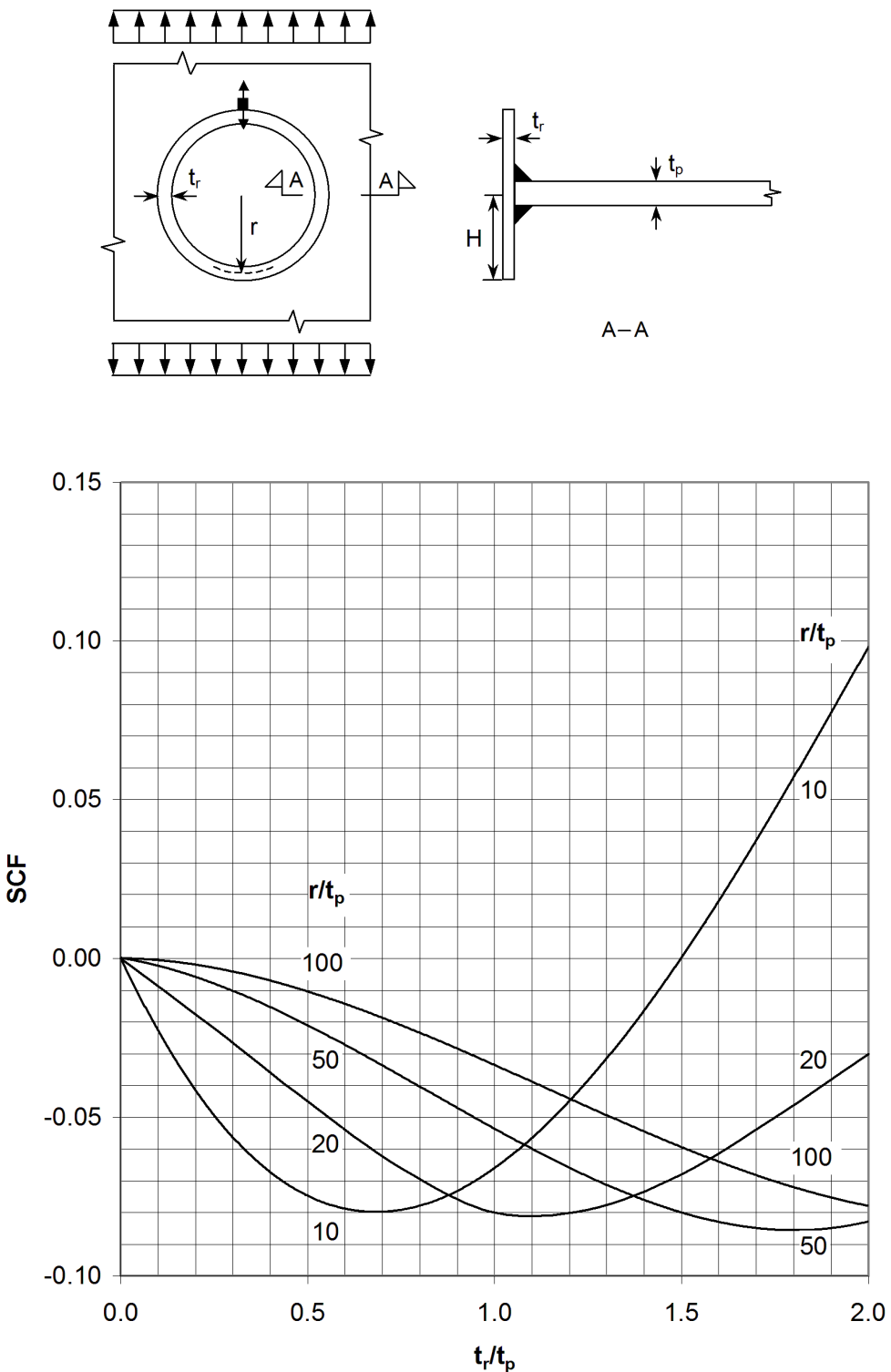


Figure C-13 SCF at hole with inserted tubular. Stress in plate, normal to weld. $H/t_r = 2$

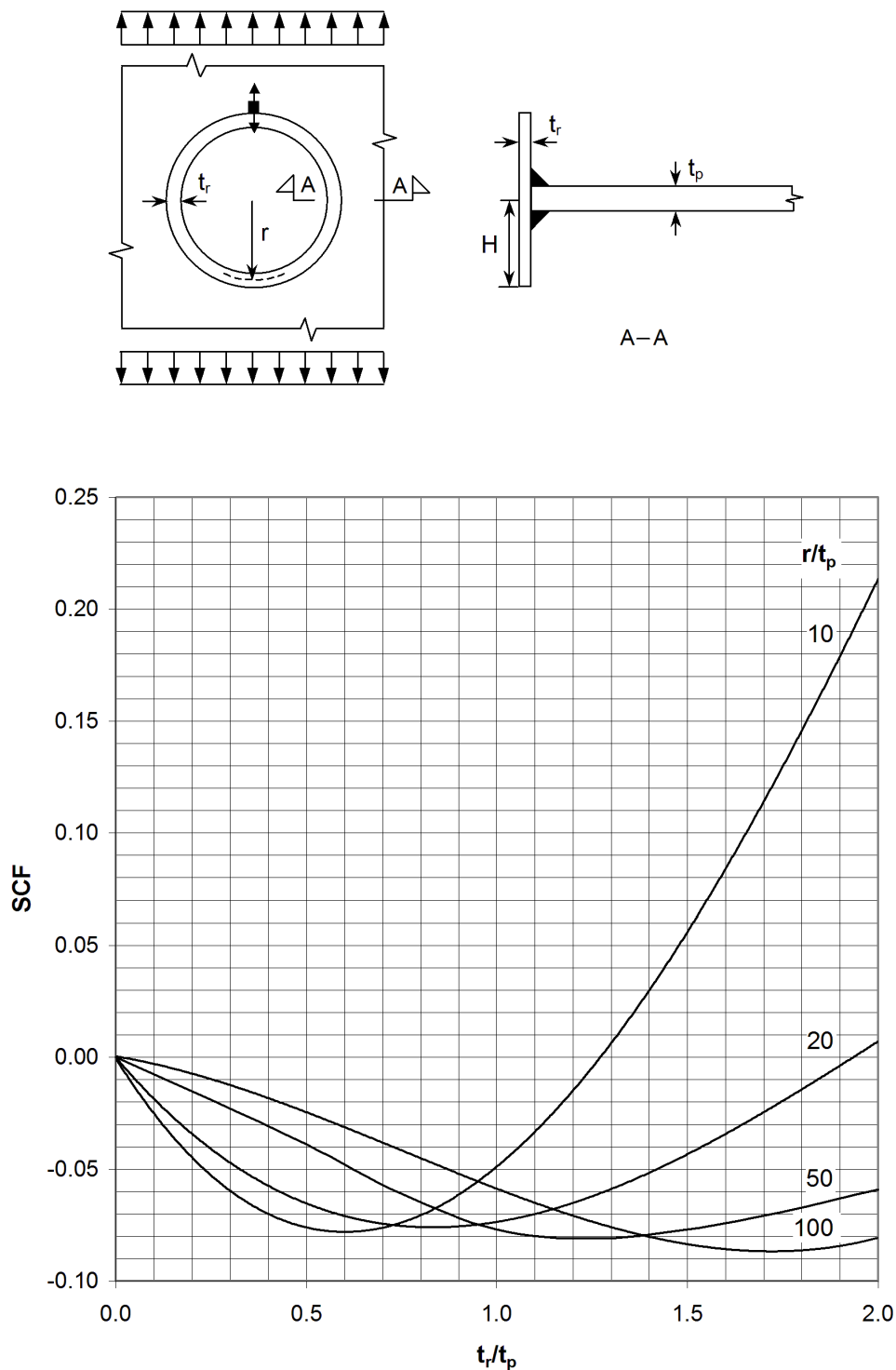


Figure C-14 SCF at hole with inserted tubular. Stress in plate, normal to weld. $H/t_r = 5$

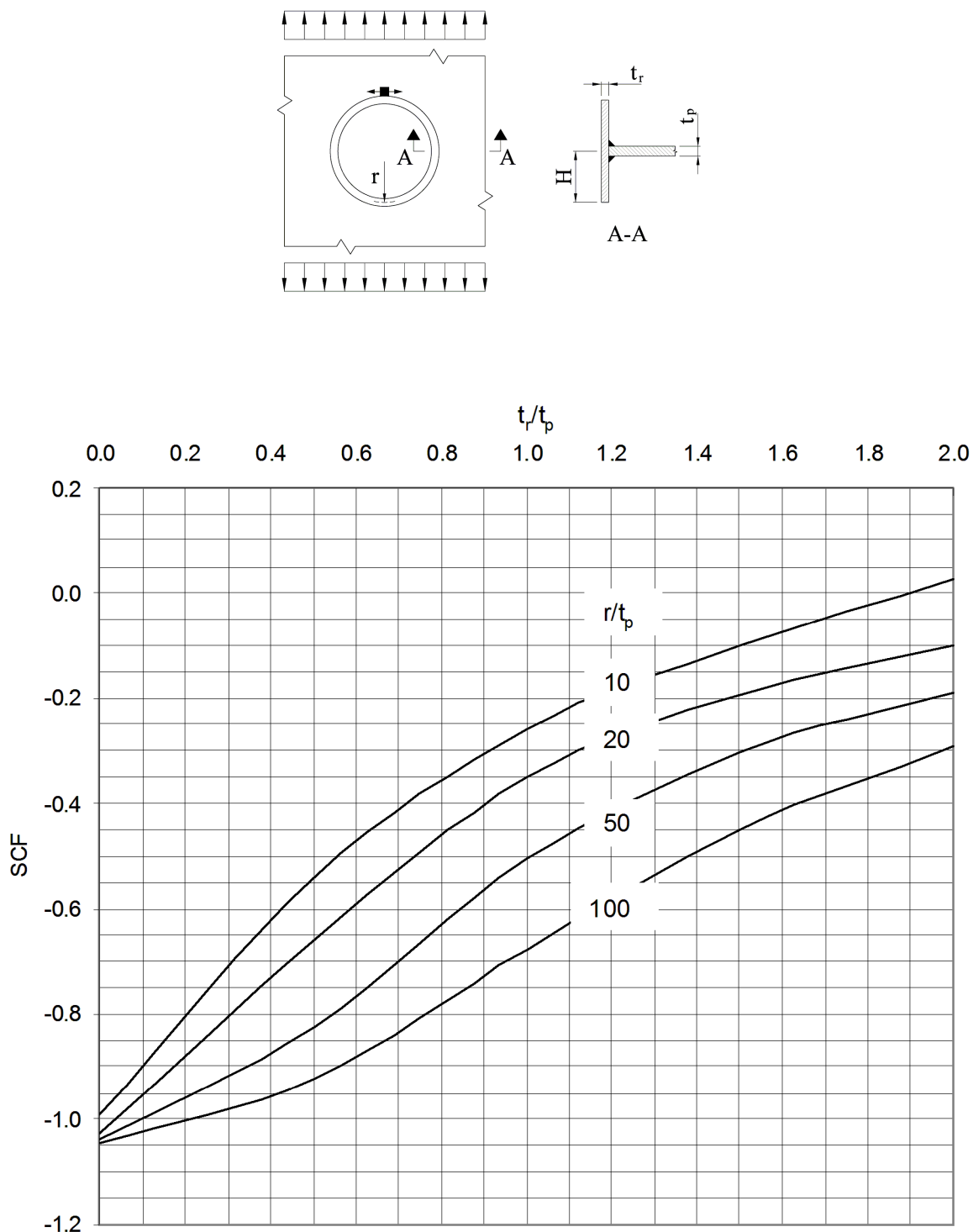


Figure C-15 SCF at hole with inserted tubular. Stress in plate, normal to weld. $H/t_r = 5$

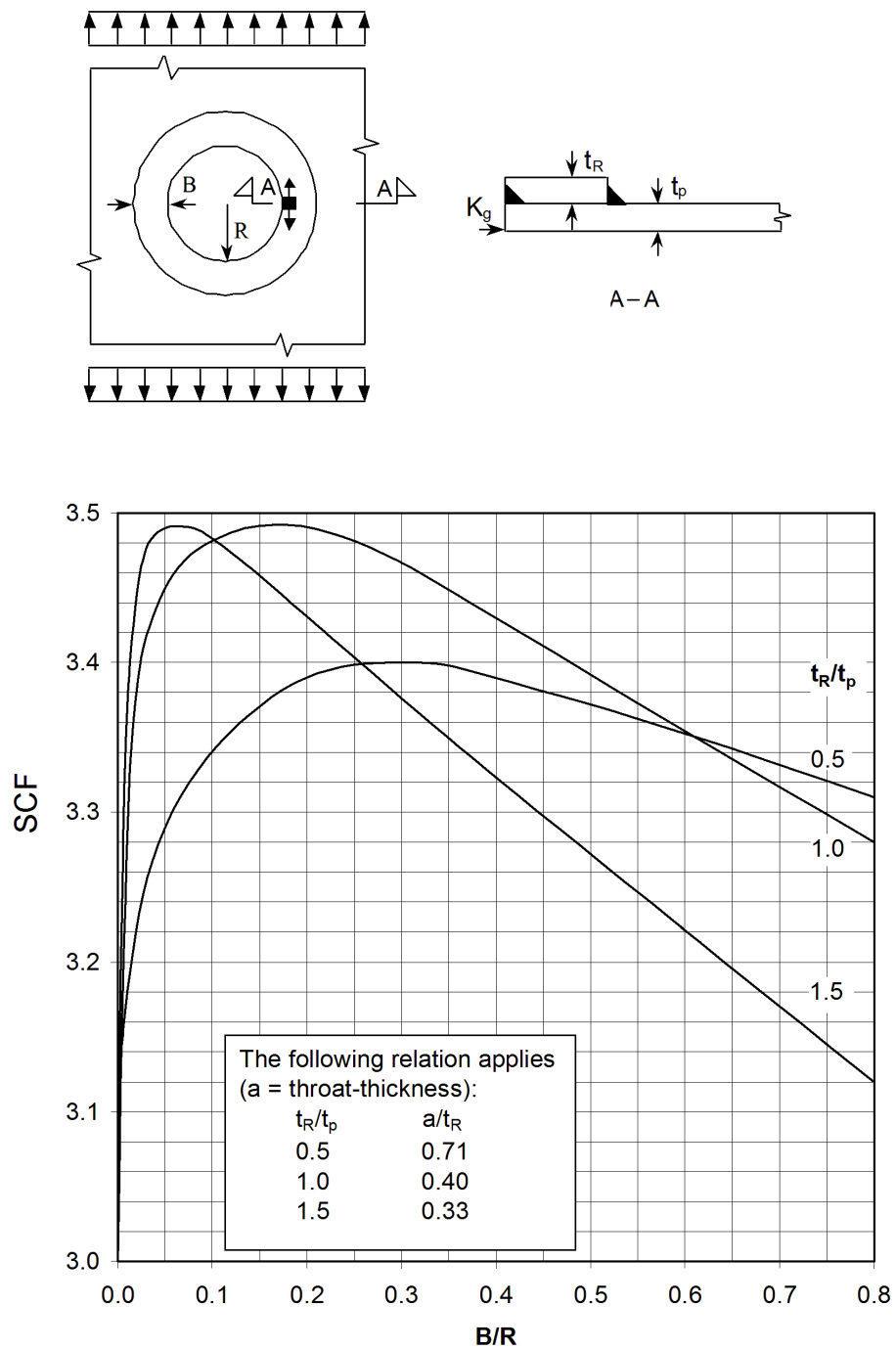


Figure C-16 SCF at hole with ring reinforcement. Max stress concentration

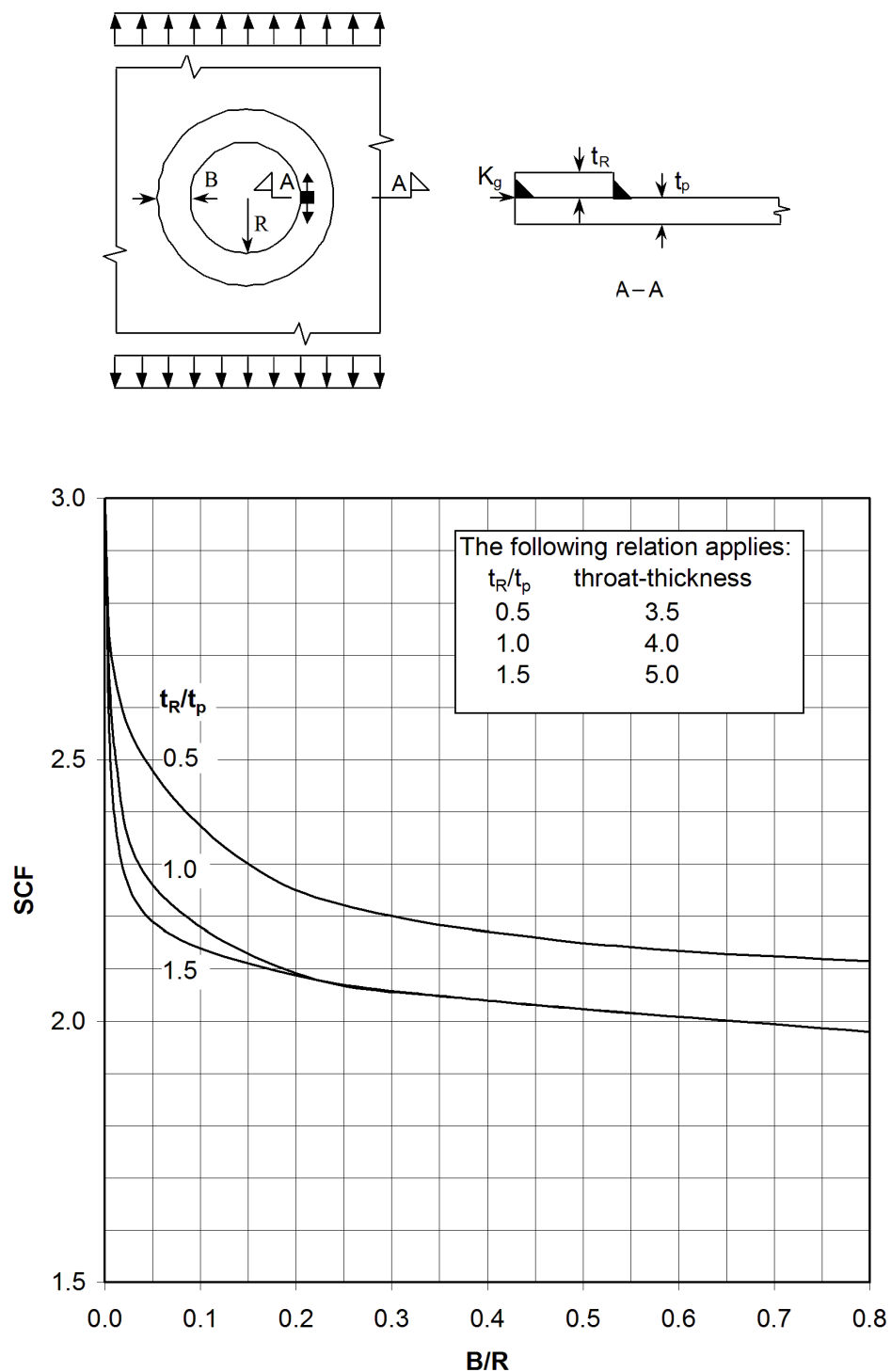


Figure C-17 SCF at hole with ring reinforcement. Stress at inner edge of ring

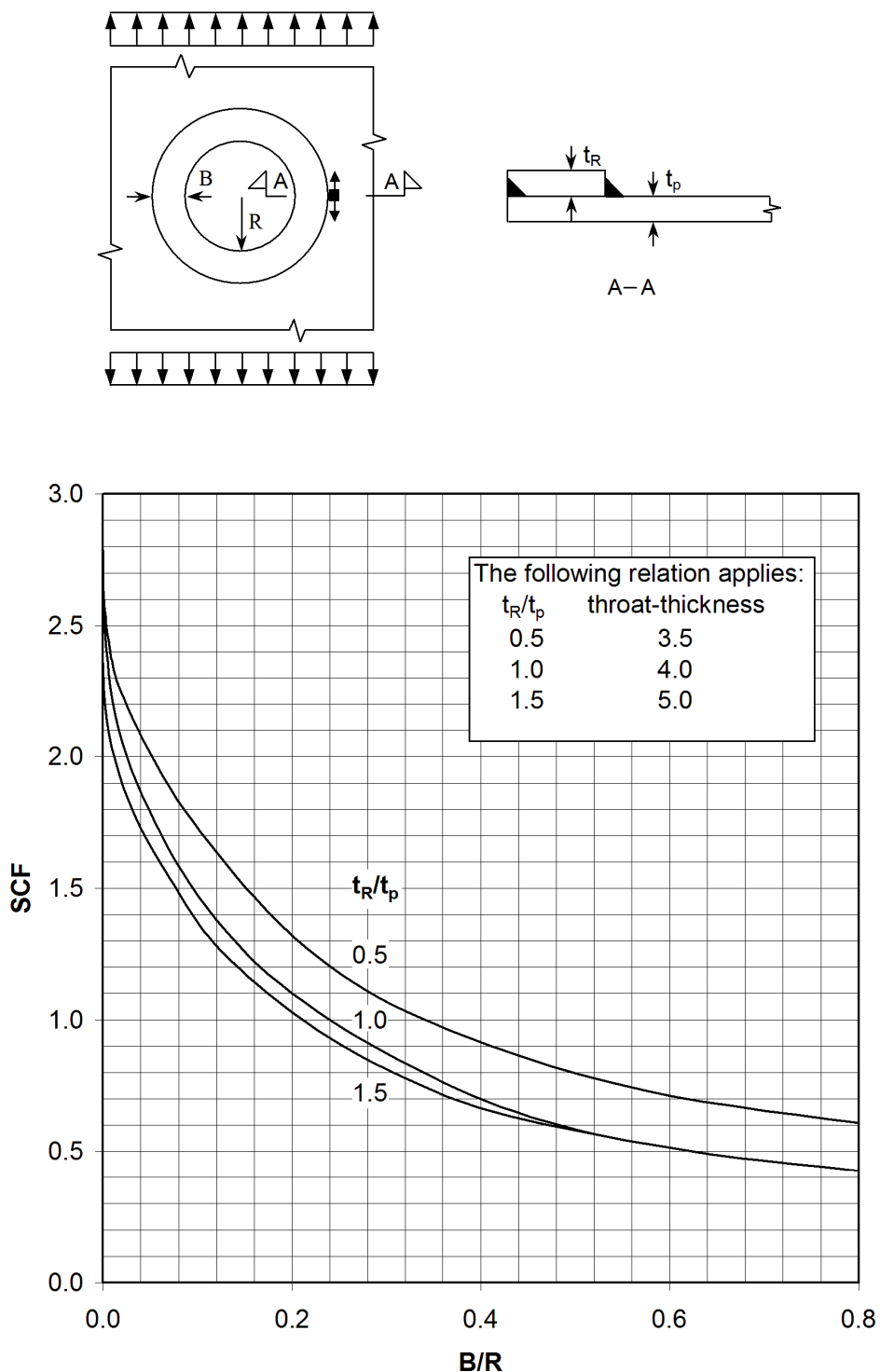


Figure C-18 SCF at hole with ring reinforcement. Stress in plate, parallel with weld

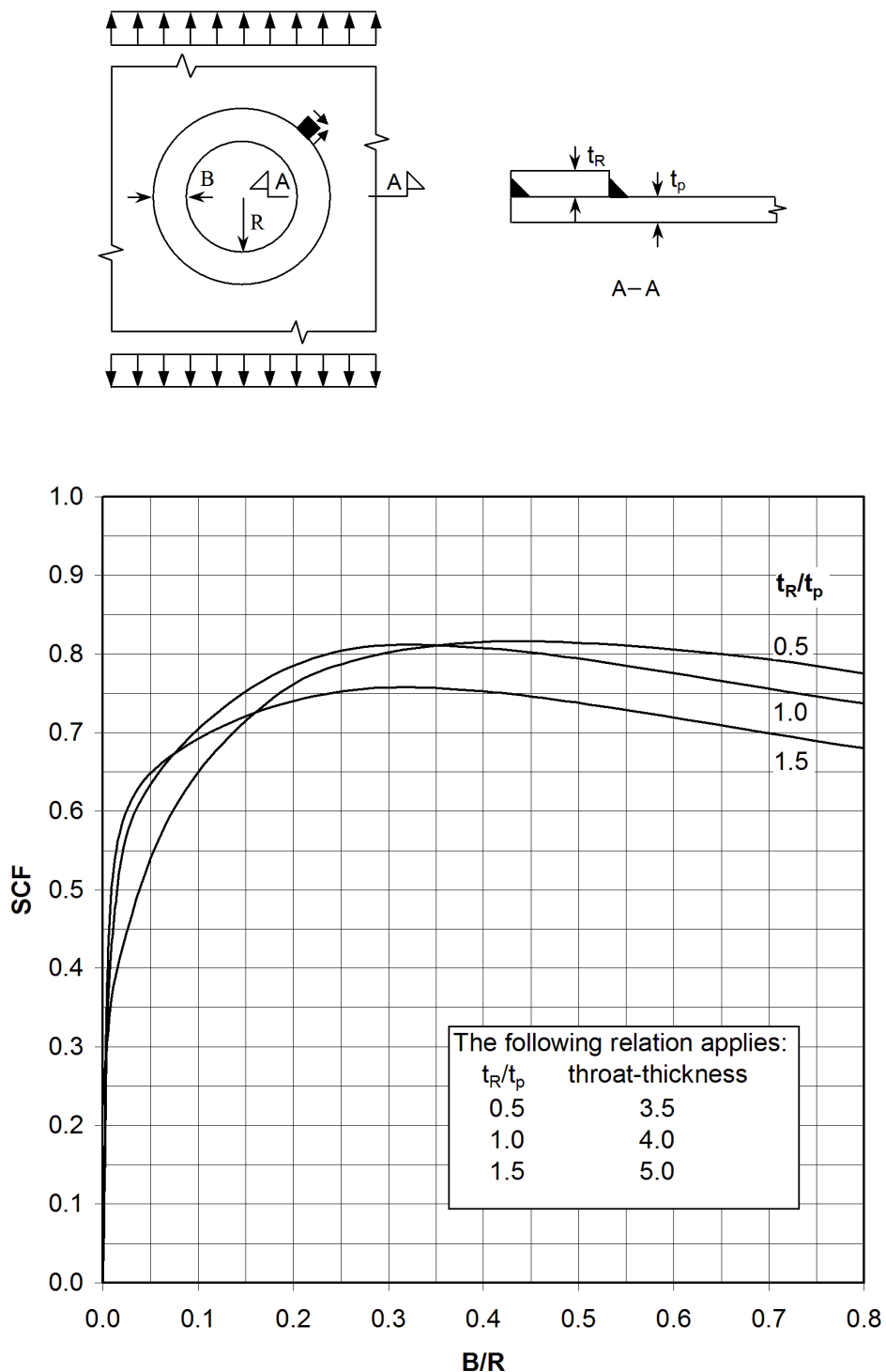


Figure C-19 SCF at hole with ring reinforcement. Shear stress in plate at weld toe

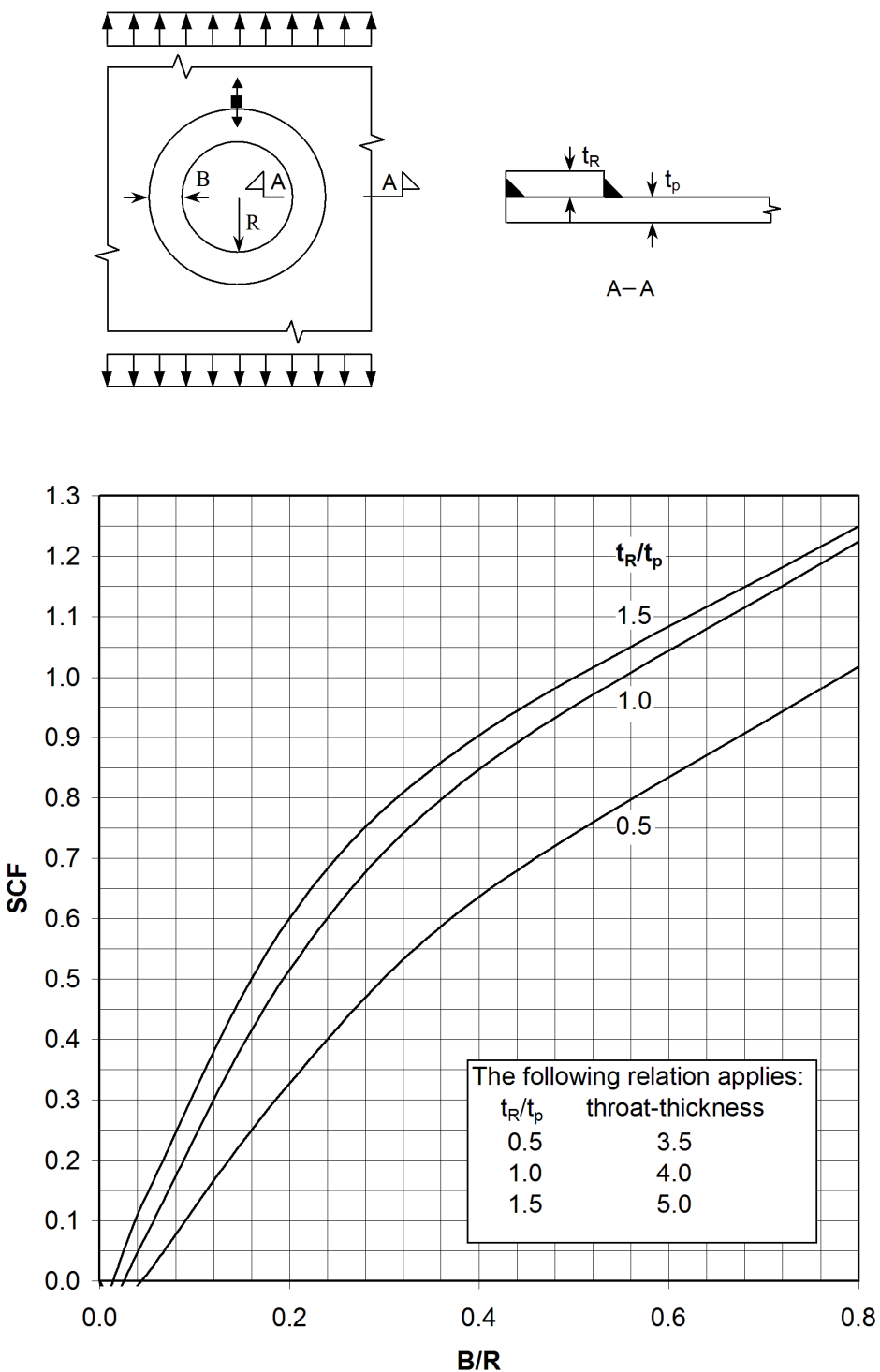


Figure C-20 SCF at hole with ring reinforcement. Stress in plate, normal to weld

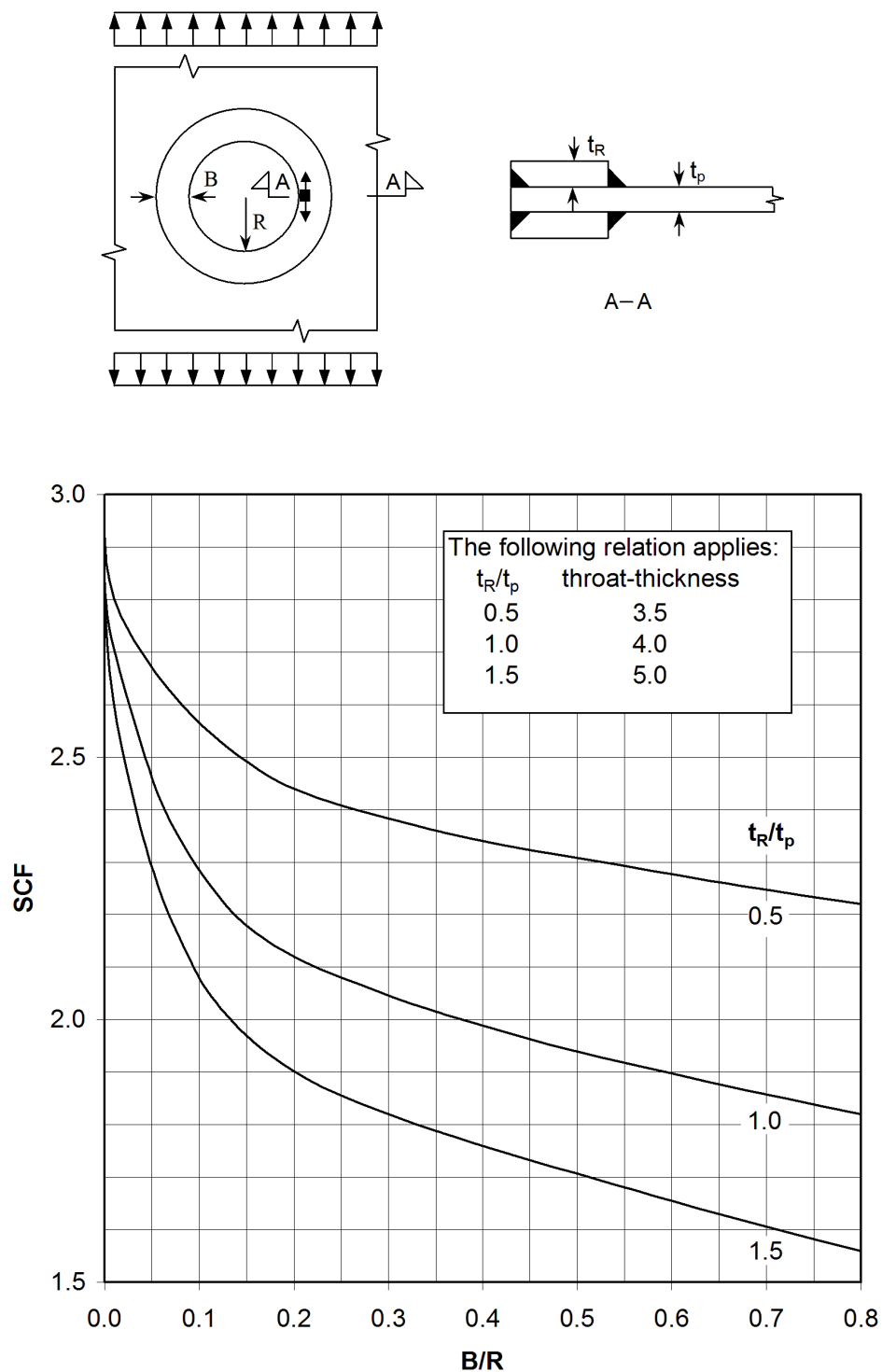


Figure C-21 SCF at hole with double ring reinforcement. Stress at inner edge of ring

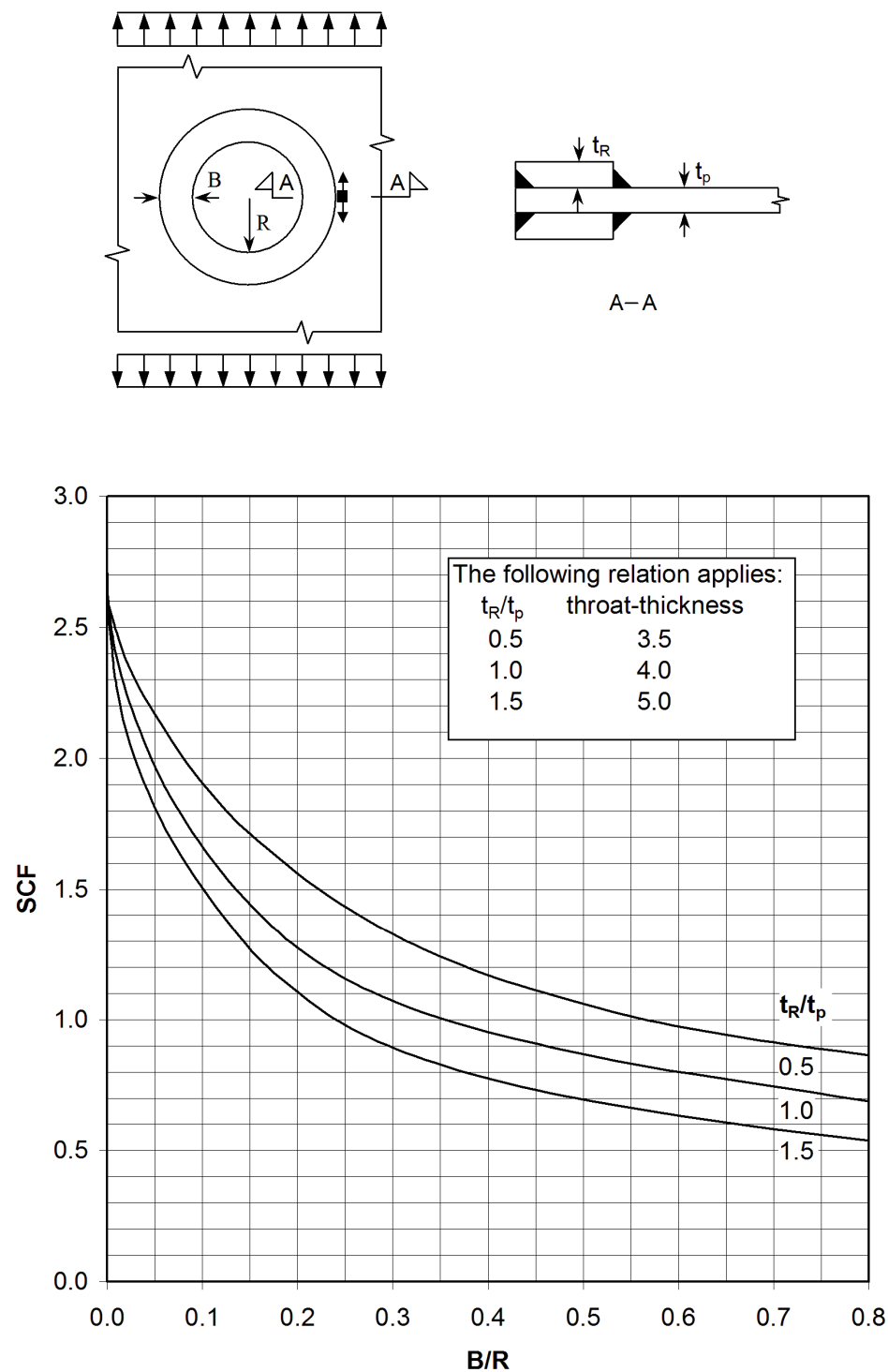


Figure C-22 SCF at hole with double ring reinforcement. Stress in plate, parallel with weld

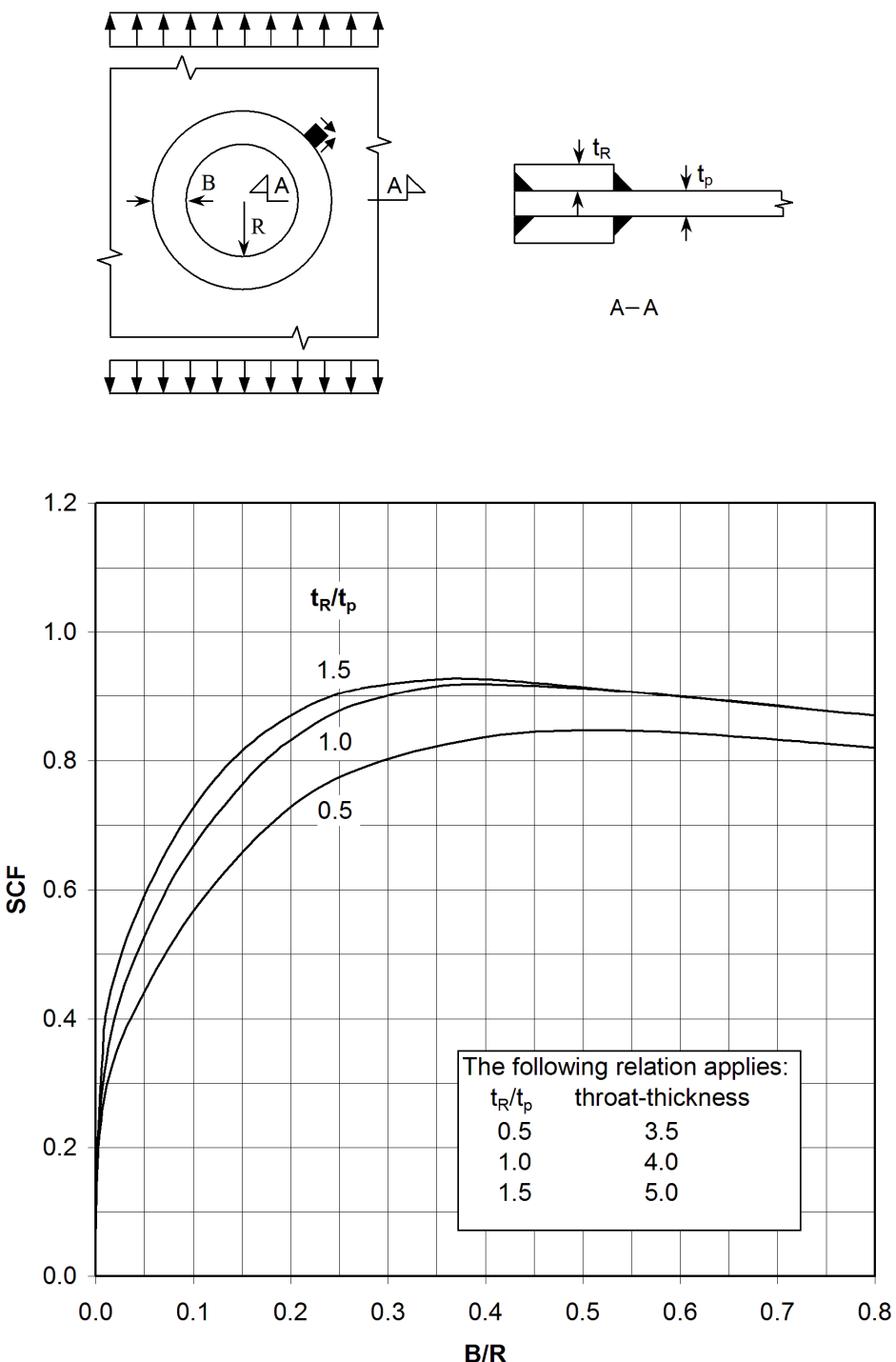


Figure C-23 SCF at hole with double ring reinforcement. Shear stress in plate at weld toe

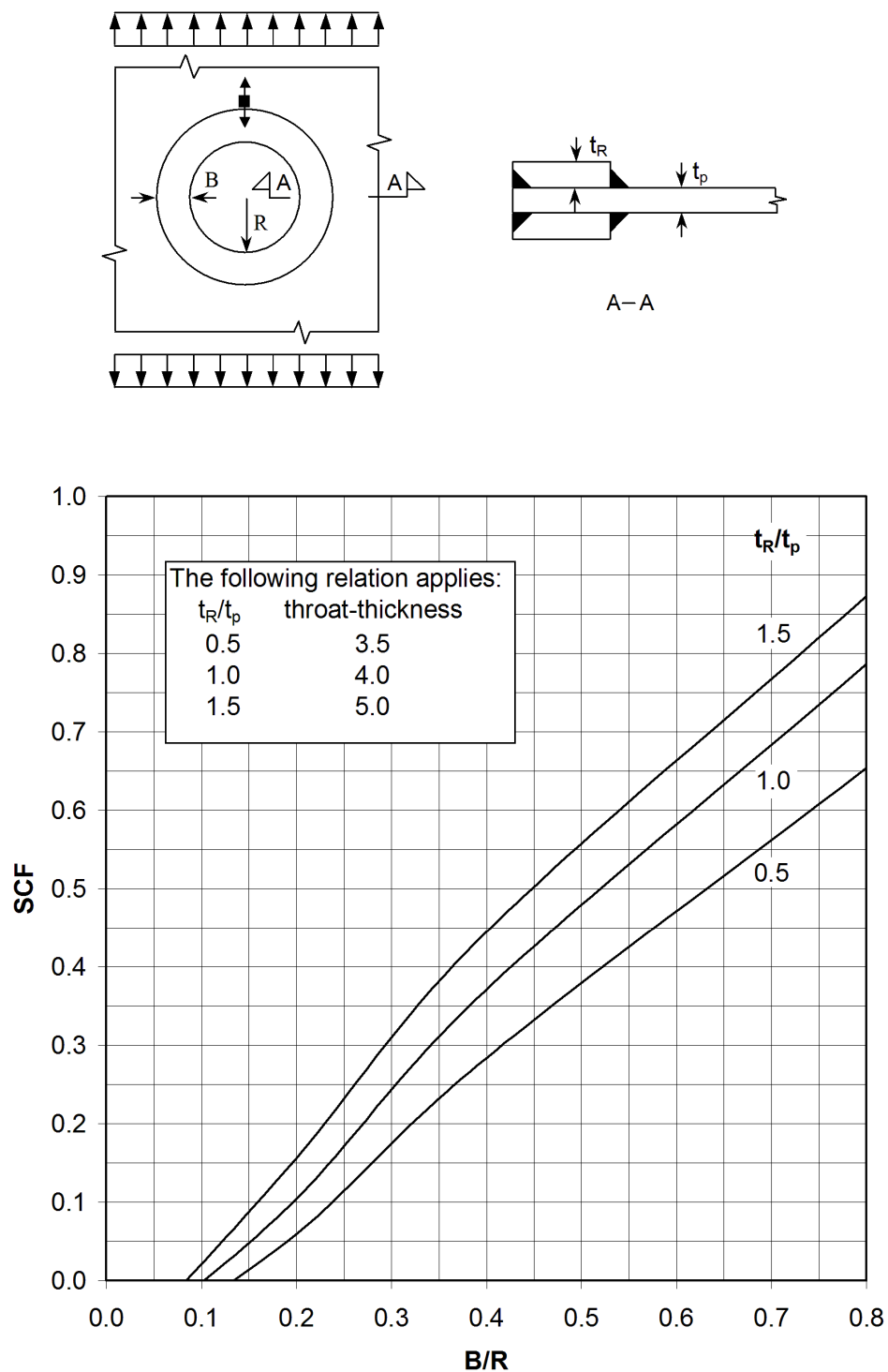


Figure C-24 SCF at hole with double ring reinforcement. Stress in plate, normal to weld

C.2 Stress concentration factors at man-hole penetrations

C.2.1 Geometry

The following hole geometries are considered, see also [Figure C-25](#):

- 1) Circular cut-out with diameter = 600 mm.
- 2) Rectangular cut-out 600 × 800 mm with rounded corner R = 300 mm.
- 3) Rectangular cut-out 600 × 1200 mm with rounded corner R = 300 mm.

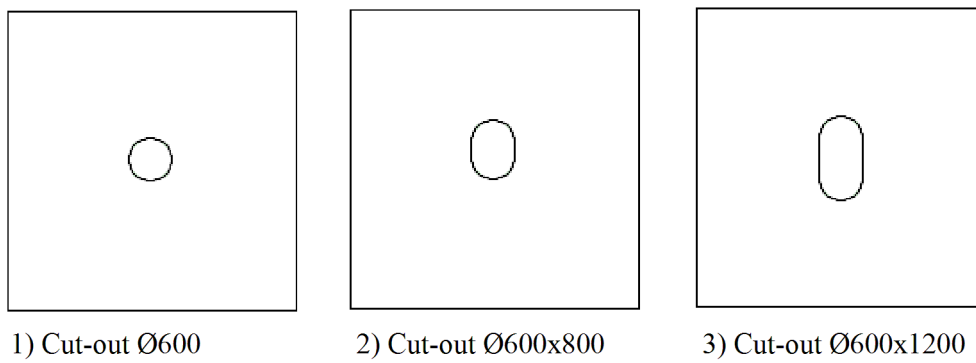


Figure C-25 Cut-out geometry

For the three cut-out geometry six different edge reinforcements are applied, see [Figure C-26](#). The reinforcement details are described below, see also [Figure C-26](#):

- (A) cut-out alone (no reinforcement) ([Figure C-26 \(A\)](#))
- (B) cut-out with inserted plate (15 mm thick, 300 mm wide) around the edge ([Figure C-26 \(B\)](#))
- (C) cut-out with double side reinforcement 50 mm away from the edge ([Figure C-26 \(C\)](#))
- (D) cut-out with single side reinforcement 50 mm away from the edge ([Figure C-26 \(D\)](#))
- (E) cut-out with double side reinforcement 100 mm away from the edge ([Figure C-26 \(E\)](#))
- (F) cut-out with single side reinforcement 100 mm away from the edge ([Figure C-26 \(F\)](#)).

Stress concentrations factors are presented for the hot-spots marked in [Figure C-26](#).

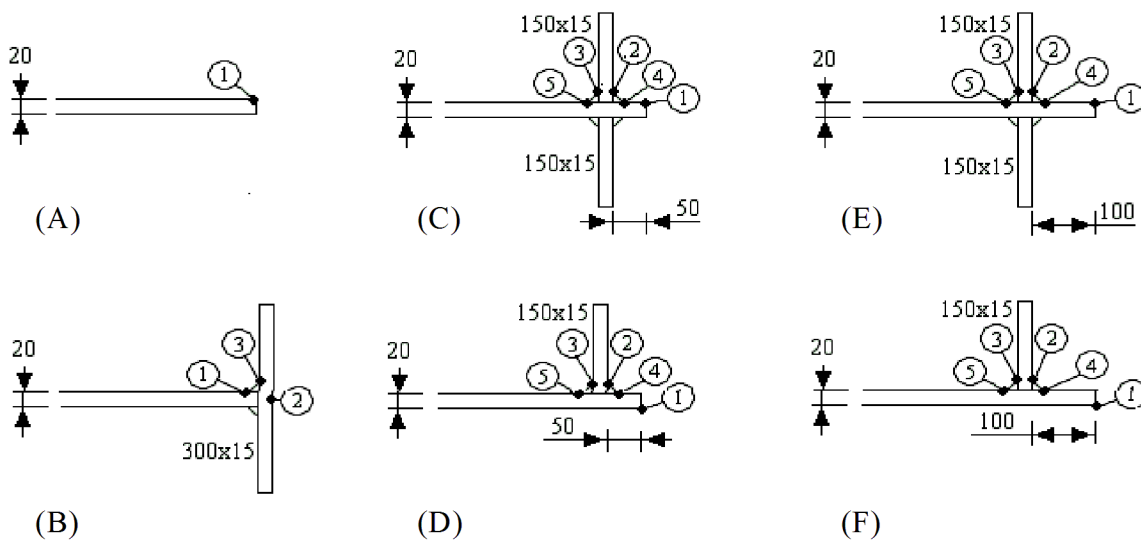


Figure C-26 Cut-out, reinforcement and hot-spot positions

For geometry (D) and (F), the maximum stresses of the bottom or the top surface in the 20 mm plate at the cut-out edge are given in the plots. For the other geometry the stresses are symmetrical about the mid-plane of the plate.

C.2.2 Applied stresses

The following stresses has been considered:

- longitudinal stress, σ_x
- transverse stress, σ_y
- shear stress, τ .

The stresses in the longitudinal and the transverse directions are applied separately but are combined with shear stress. The shear stress is varied between zero and up to the value of the normal stress.

C.2.3 Stress concentration factor definition

The definition of the stress concentration factors presented for cut-outs are the maximum principal stress divided by the nominal normal stress, σ_x or σ_y , (not the nominal principal stress).

The maximum principal stress in the hot-spot is selected as the maximum of $|\sigma_1|$ and $|\sigma_2|$.

The stress concentration factor (K_g) is then:

$$K_{g,x(y)} = \frac{\max(|\sigma_1|; |\sigma_2|)}{\sigma_{x(y)}}$$

C.3 Results

In general, stress concentration factors are given at 5 points (see [Figure C-26](#)) except for the cases shown in [Figure C-26](#) (A) and (B).

The following should be noted:

- Maximum principal stresses are parallel to the weld toe (hot-spots 2 to 5) with only one exception:
for double reinforcement and point 2 (see [Figure C-26](#), (C) and (E)), the maximum principal stress is normal to the weld toe.

C.3.1 Stress concentration factors for point 1, see [Figure C-26](#)

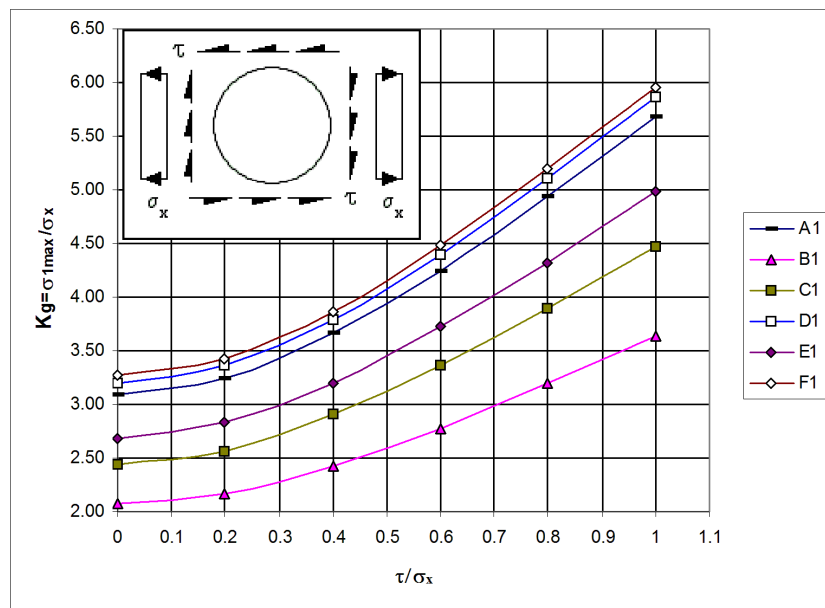


Figure C-27 Circular cut-out $\varnothing = 600$ mm, σ_x and τ

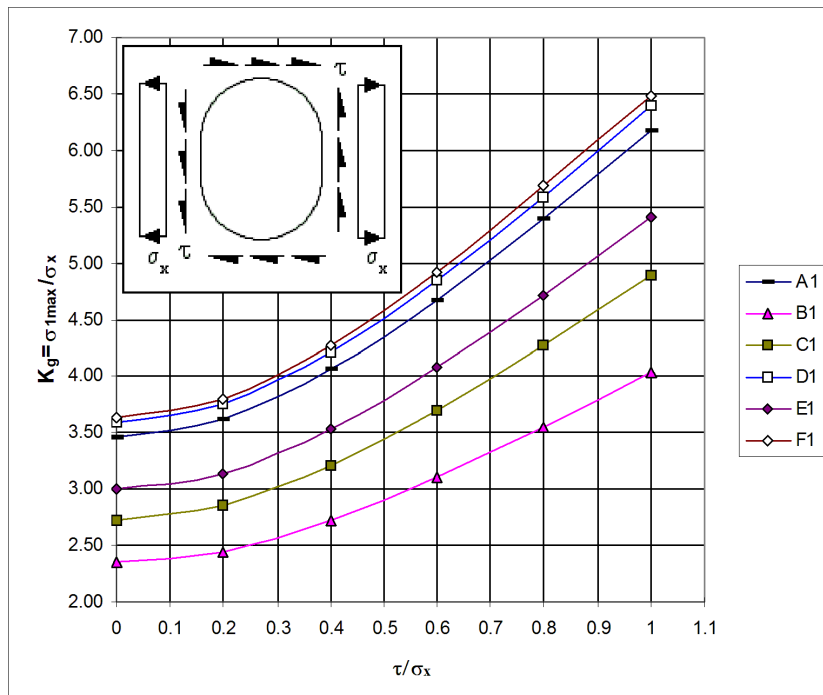


Figure C-28 Rectangular cut-out with rounded corners: 600 x 800 mm, σ_x and τ

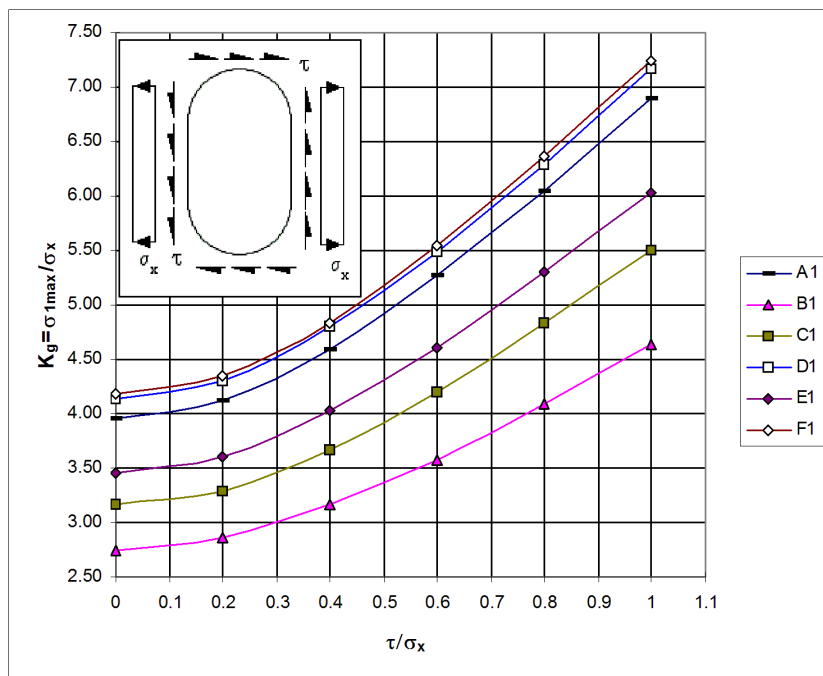


Figure C-29 Rectangular cut-out with rounded corners: 600 x 1200 mm, σ_x and τ

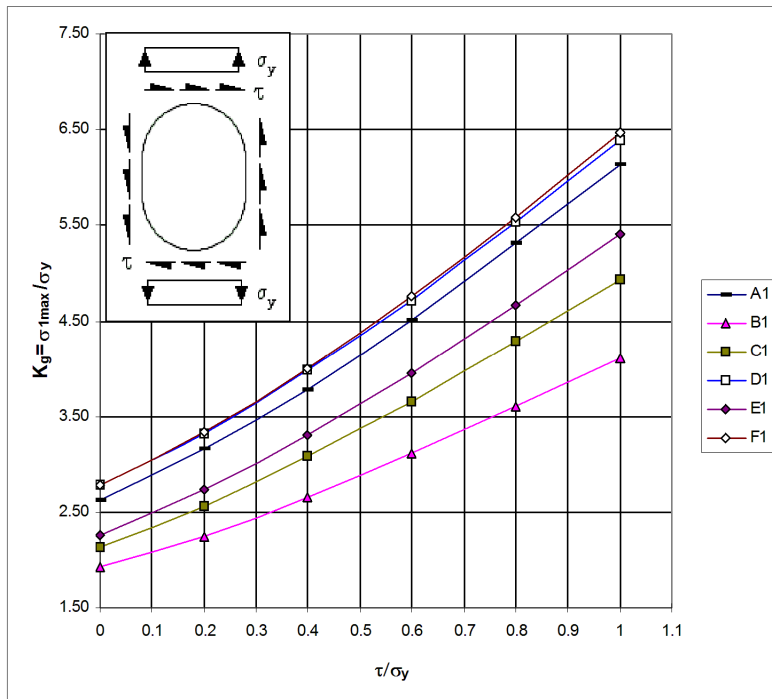


Figure C-30 Rectangular cut-out with rounded corners: 600 × 800 mm, σ_y and τ

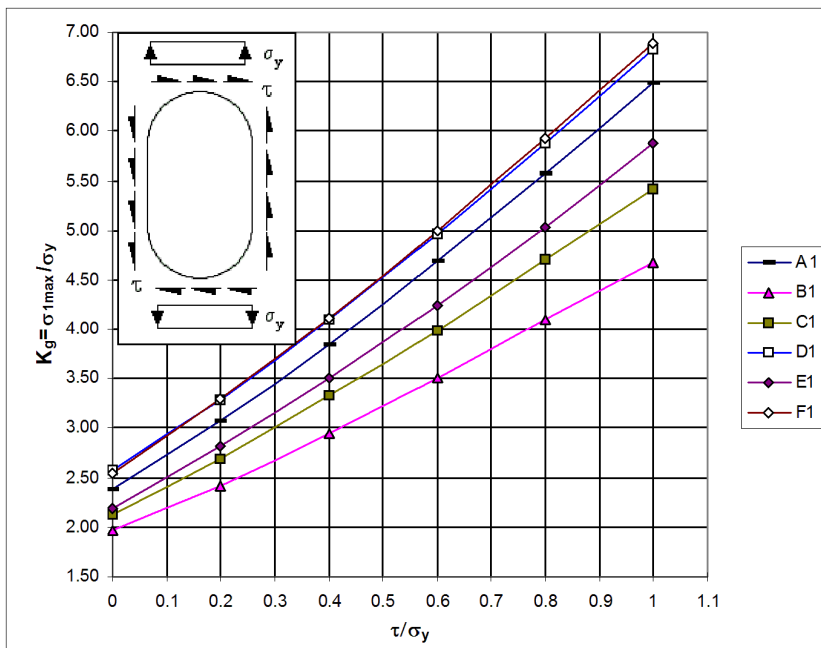


Figure C-31 Rectangular cut-out with rounded corners: 600 × 1200 mm, σ_y and τ

C.3.2 Stress concentration factors for point 2, see Figure C-26

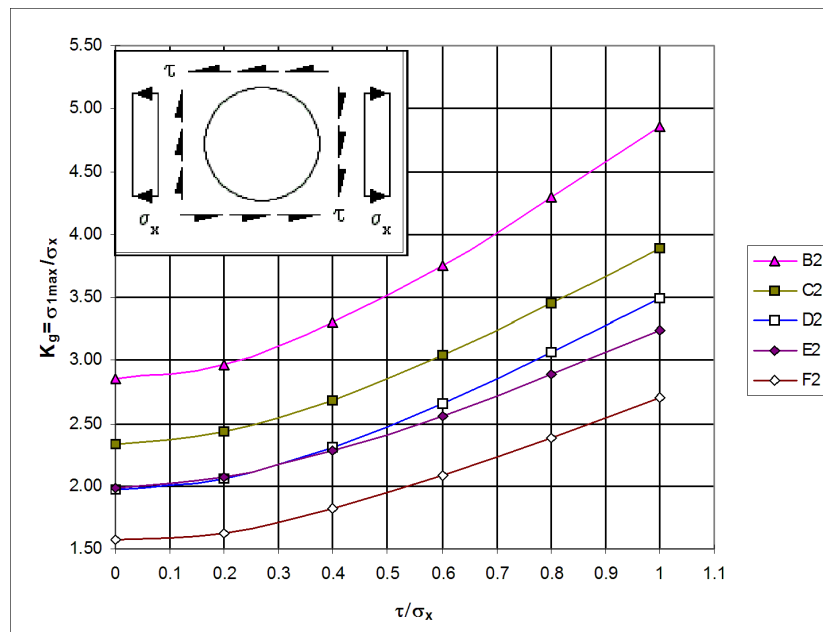


Figure C-32 Circular cut-out $\varnothing = 600$ mm, σ_x and τ stresses for C and E are normal to the weld

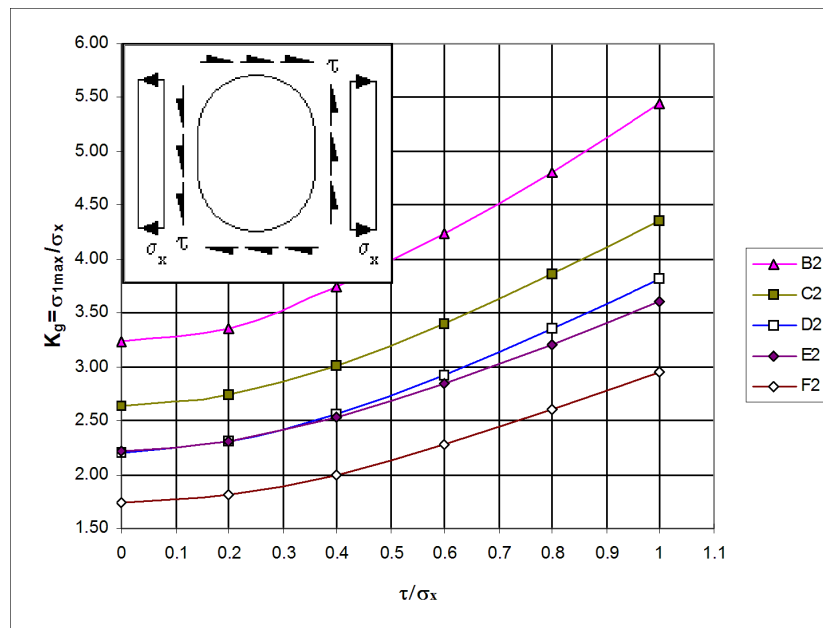


Figure C-33 Rectangular cut-out with rounded corners: 600 x 800 mm, σ_x and τ

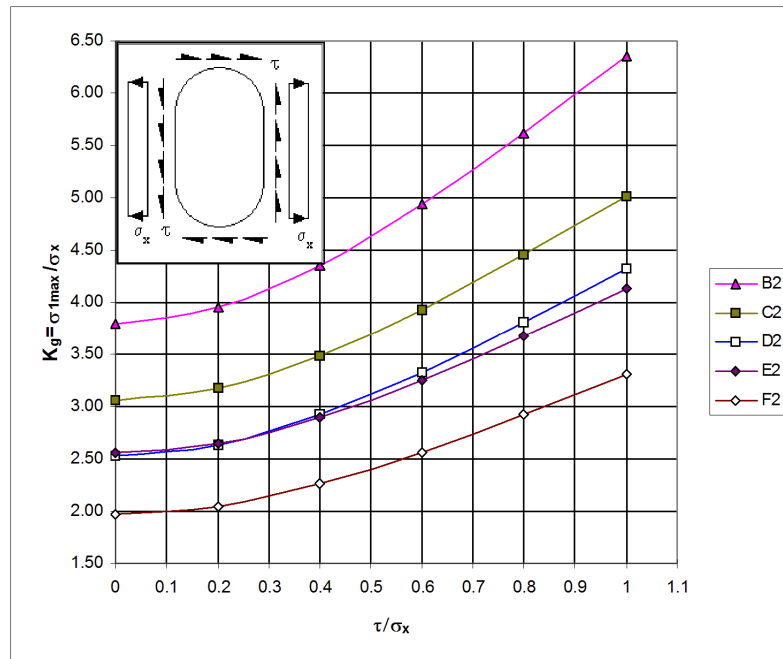


Figure C-34 Rectangular cut-out with rounded corners: 600 × 1200 mm, σ_x and τ

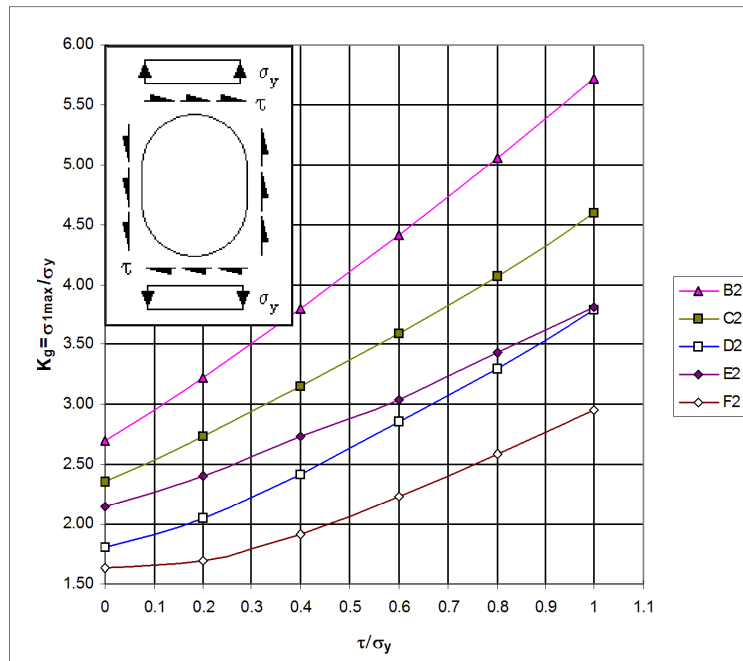


Figure C-35 Rectangular cut-out with rounded corners: 600 × 800 mm, σ_x and τ

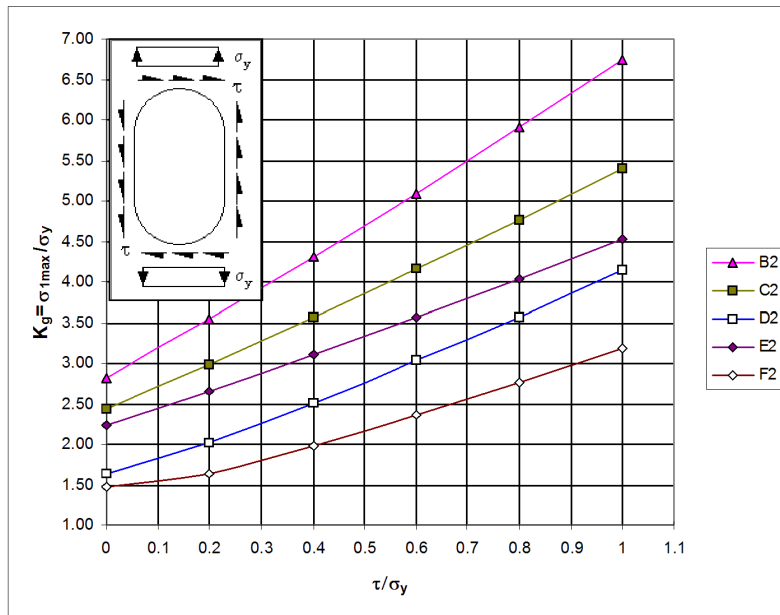


Figure C-36 Rectangular cut-out with rounded corners: 600 x 1200 mm, σ_x and τ

C.3.3 Stress concentration factors for point 3, see Figure C-26

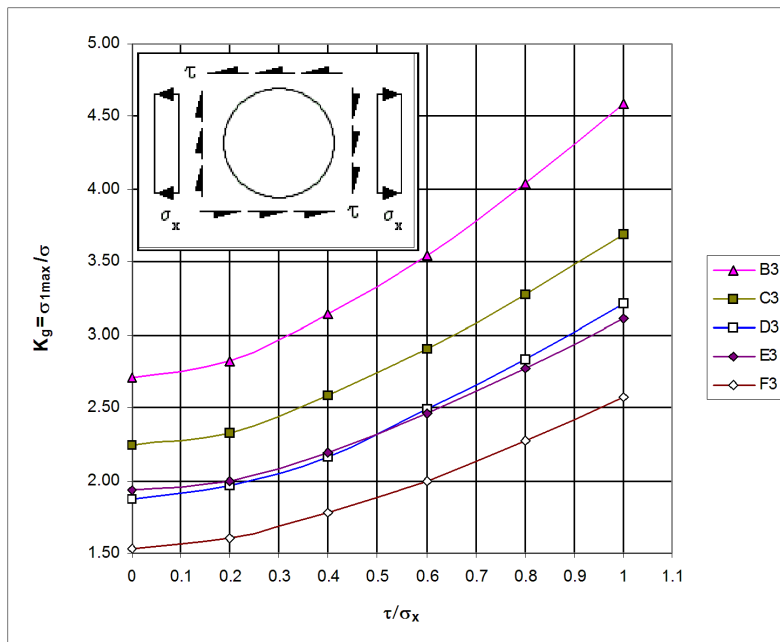


Figure C-37 Circular cut-out Ø = 600 mm, σ_x and τ

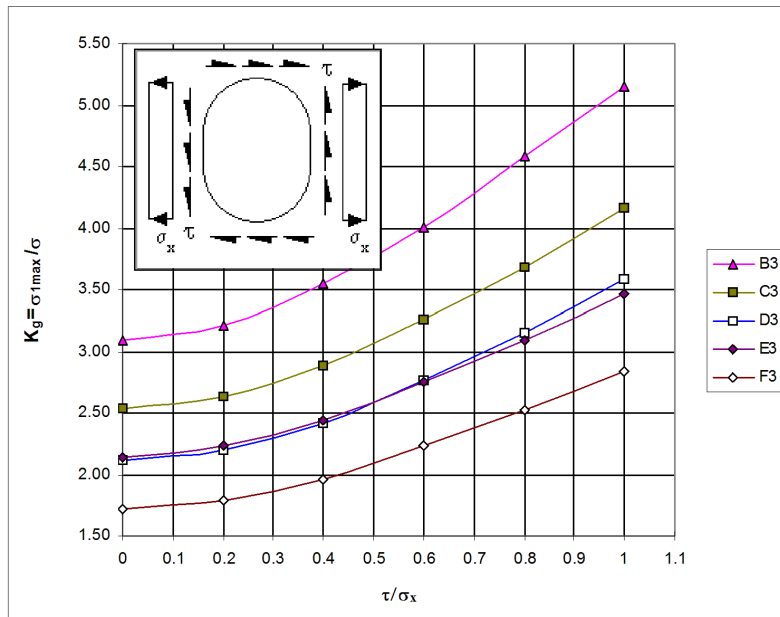


Figure C-38 Rectangular cut-out with rounded corners: 600×800 mm, σ_x and τ

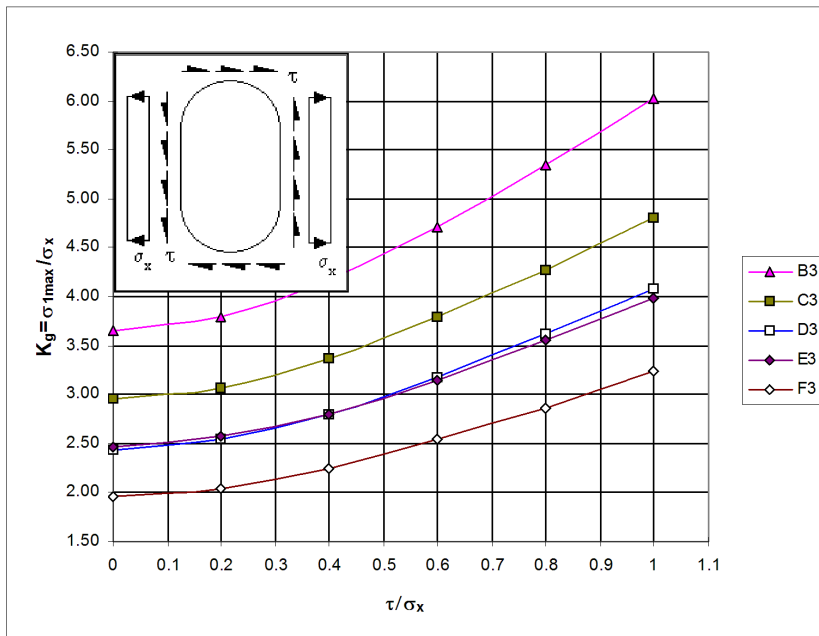


Figure C-39 Rectangular cut-out with rounded corners: 600×1200 mm, σ_x and τ

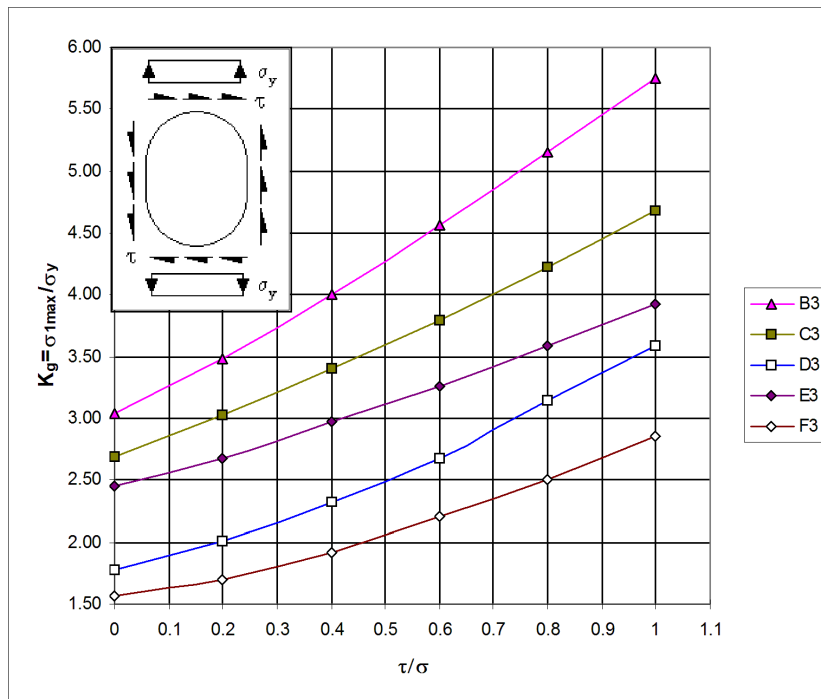


Figure C-40 Rectangular cut-out with rounded corners: 600 × 800 mm, σ_y and τ

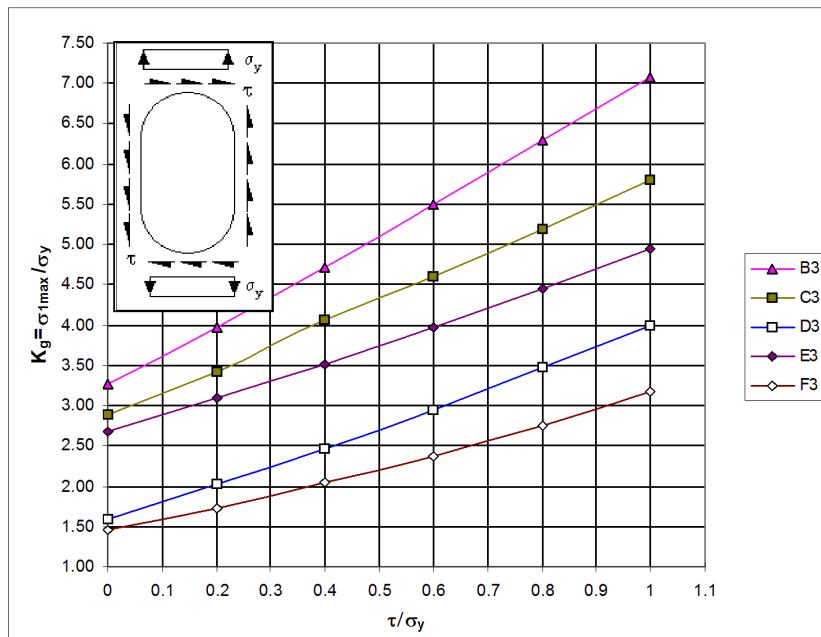


Figure C-41 Rectangular cut-out with rounded corners: 600 × 1200 mm, σ_y and τ

C.3.4 Stress concentration factors for point 4, see Figure C-26

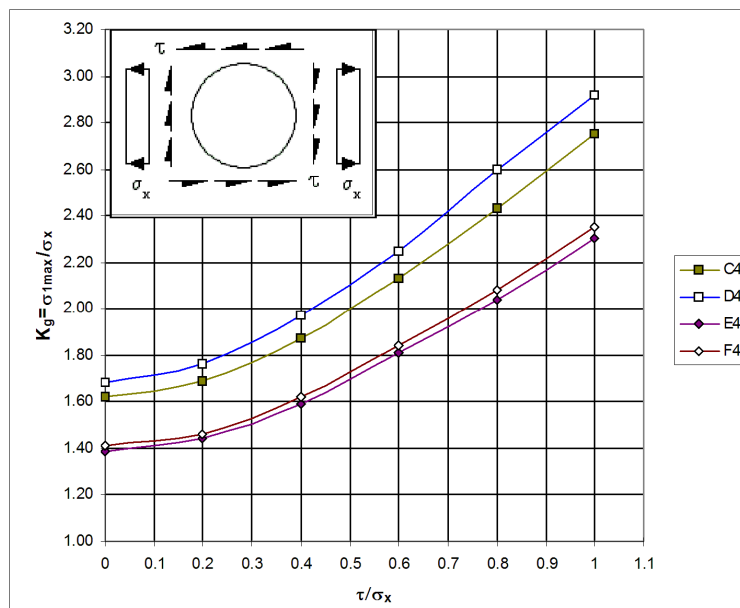


Figure C-42 Circular cut-out $\Ø = 600$ mm, σ_x and τ

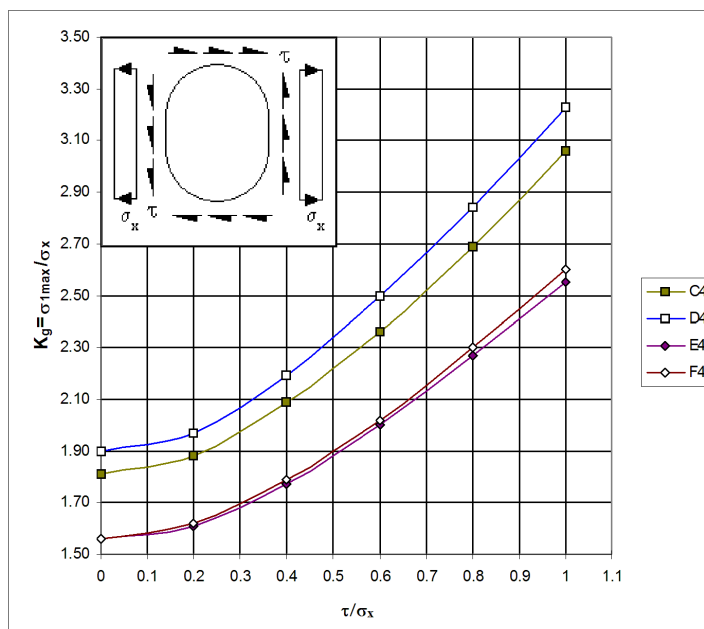


Figure C-43 Rectangular cut-out with rounded corners: 600 x 800 mm, σ_x and τ

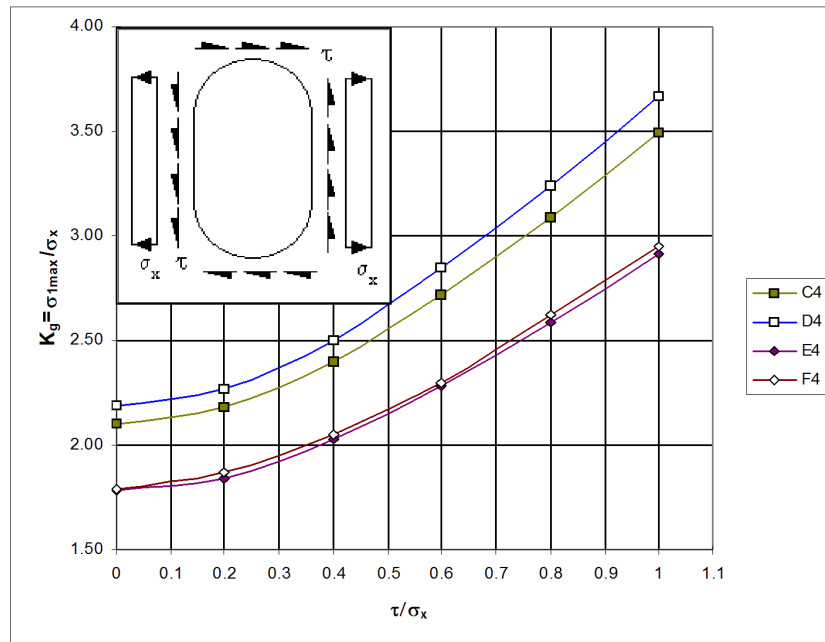


Figure C-44 Rectangular cut-out with rounded corners: 600 × 1200 mm, σ_x and τ

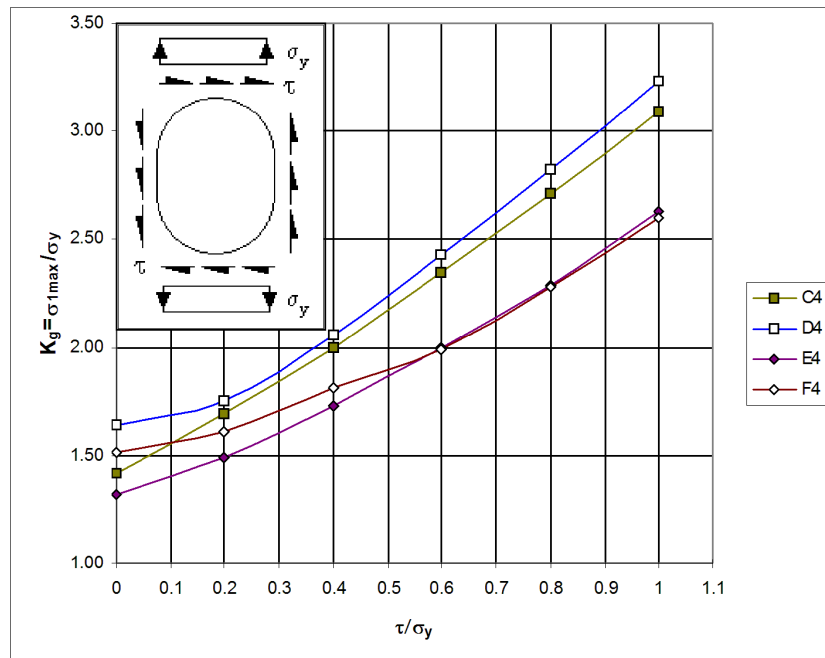


Figure C-45 Rectangular cut-out with rounded corners: 600 × 800 mm, σ_y and τ

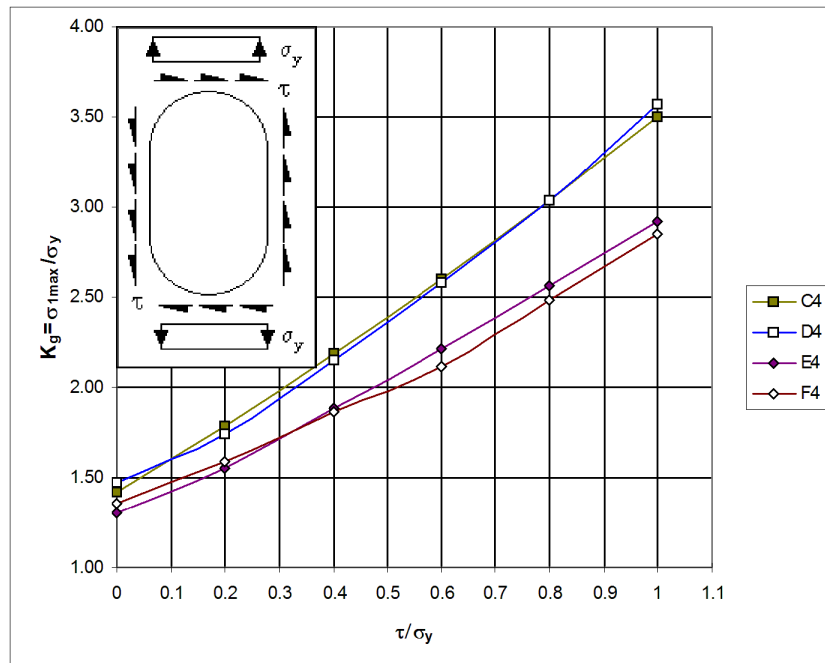


Figure C-46 Rectangular cut-out with rounded corners: 600 x 1200 mm, σ_y and τ

C.3.5 Stress concentration factors for point 5, see Figure C-26

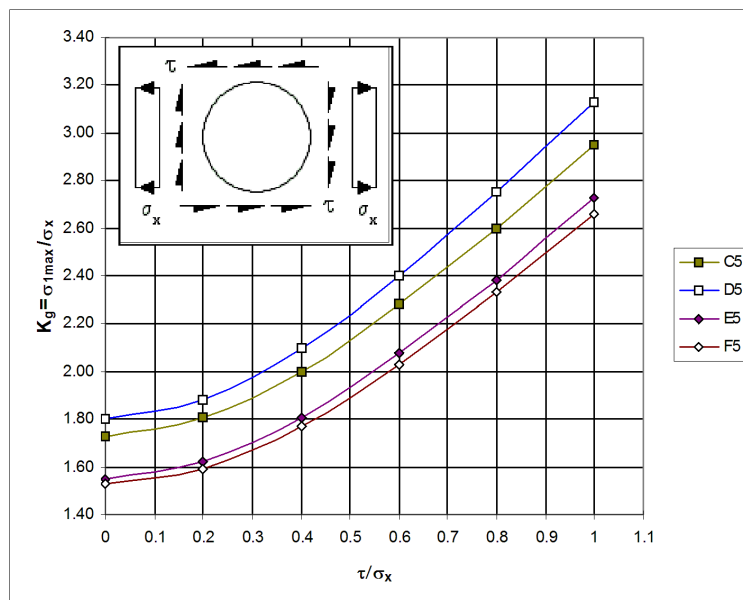


Figure C-47 Circular cut-out $\phi = 600$ mm, σ_x and τ

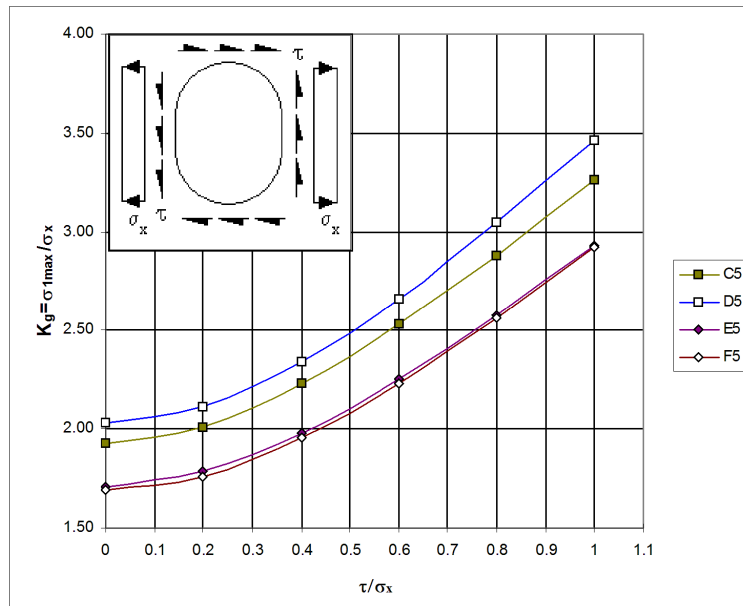


Figure C-48 Rectangular cut-out with rounded corners: 600 x 800 mm, σ_x and τ

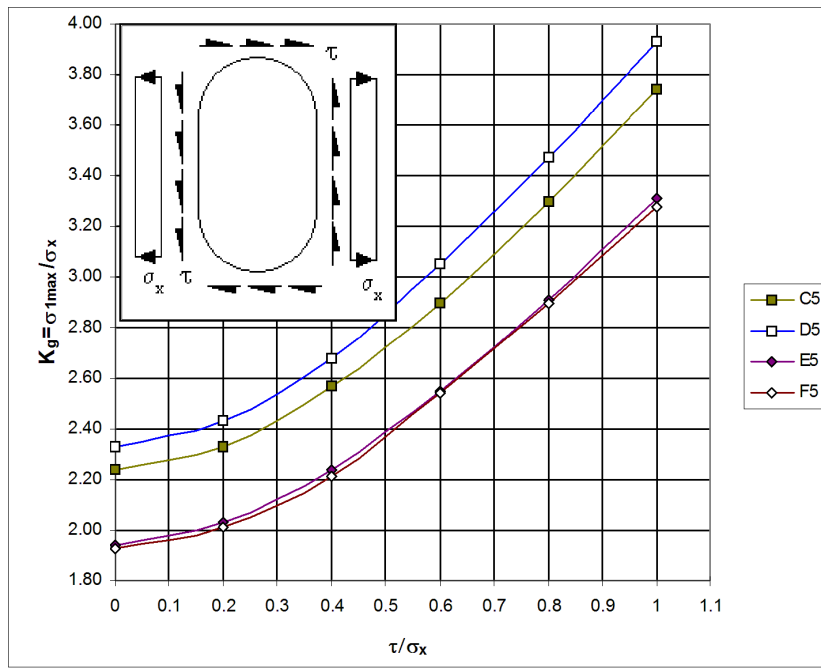


Figure C-49 Rectangular cut-out with rounded corners: 600 x 1200 mm, σ_x and τ

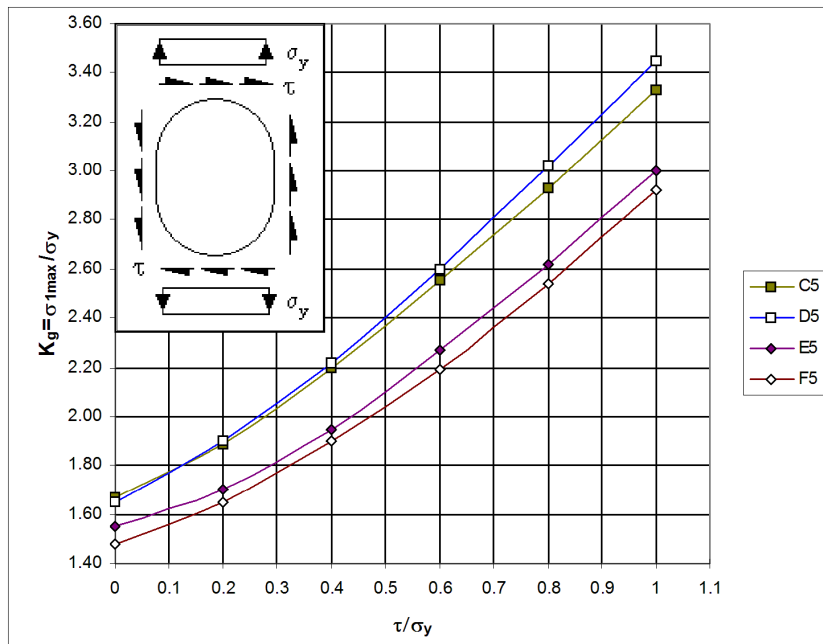


Figure C-50 Rectangular cut-out with rounded corners: 600 × 800 mm, σ_y and τ

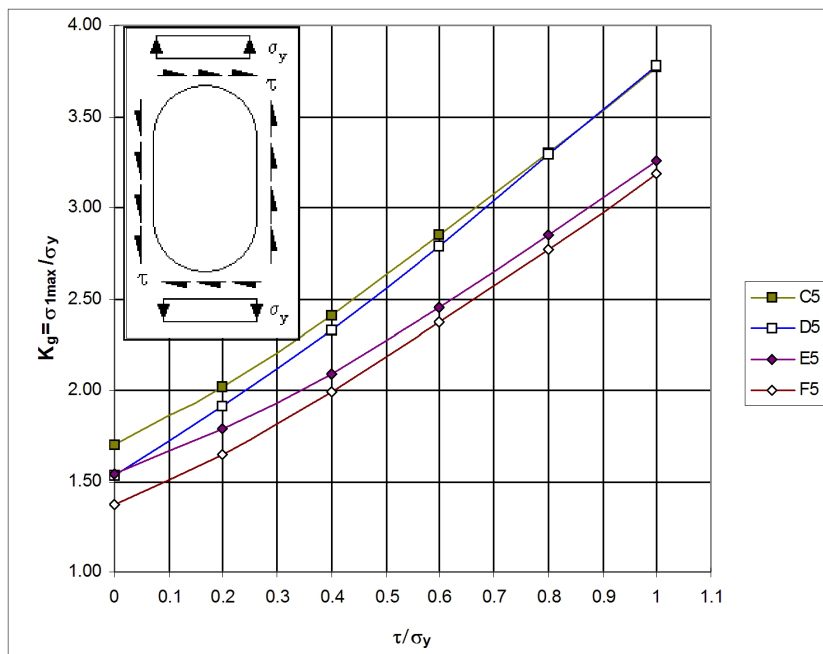


Figure C-51 Rectangular cut-out with rounded corners: 600 × 1200 mm, σ_y and τ

APPENDIX D S-N CURVES FOR BASE MATERIAL OF HIGH STRENGTH STEEL

D.1 S-N curves for components of high strength steel subjected to high mean tensile stress

For high strength steel other than cast steel with yield strength above 500 MPa and a surface roughness equal $R_a = 3.2\mu\text{m}$ or better the following design S-N curve can be used for fatigue assessment of the base material /58/. It should be noted that for instance grit blasting after final machining will increase the surface roughness compared to the surface roughness after final machining.

$$\log N = 17.446 - 4.70 \log \Delta\sigma \quad (\text{D.1.1})$$

In air a fatigue limit at $2 \cdot 10^6$ cycles at a stress range equal 235 MPa can be used. For variable amplitude loading with one stress range larger than this fatigue limit a constant slope S-N curve should be used. See also [2.12]. This S-N curve is developed for tether connections subjected to a high mean stress such that the stress range is fully tensile during all load cycles.

(The mean S-N curve is given by $\log N = 17.770 - 4.70 \log \Delta\sigma$.)

For seawater with cathodic protection a constant slope S-N curve should be used. (The same as for air to the left of $2 \cdot 10^6$ cycles, see Figure D-1.) If requirements to yield strength, surface finish and corrosion protection are not met, the S-N curves presented in [2.4.4], [2.4.5] and [2.4.9] should be used. For subsea application the S-N curves in [D.2] can be used. The thickness exponent $k = 0$ for this S-N curve.

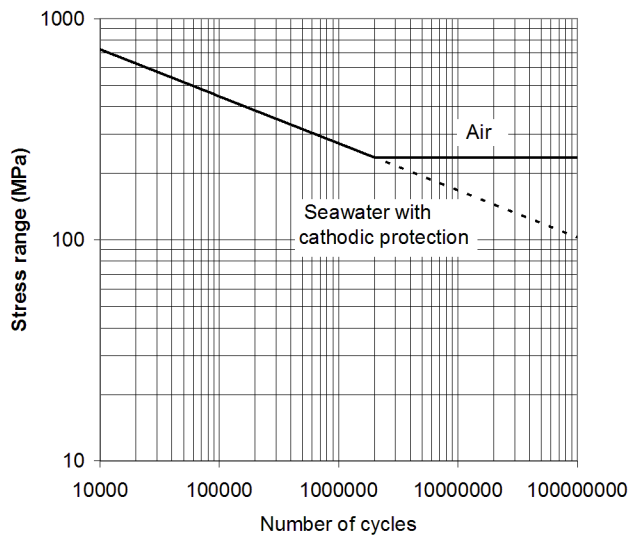


Figure D-1 S-N curve for high strength steel (HS-curve)

D.2 S-N curves for high strength steel for subsea applications

S-N curves for carbon and low alloy machined steel forgings in compliance with DNVGL-RP-0034 steel forging class 2, 3 or equivalent are provided in Table D-1 and Table D-3 for air environment and Table D-2 and Table D-4 for seawater with cathodic protection. The design S-N curves are valid for carbon and low alloy steels

with tensile strength up to 897 MPa (130 ksi). It is further required that the yield to tensile strength ratio is no higher than 0.90.

The standard deviation of $\log N$ is 0.2 and the thickness exponent $k = 0$ for all S-N curves in [D.2]. The S-N curve to be used for design should be selected based on final surface roughness and the minimum specified tensile strength (information on yield strength is included for information). The recommended S-N curves are intended for variable amplitude loading only. The use of the S-N curves with constant amplitude loading, especially at high stress levels, may provide non-conservative results.

The material non-linearity may be represented by an isotropic hardening rule to allow for local yielding during make-up, pressure testing and for simulating the first load cycle. The use of the presented S-N curves in this appendix requires that the local stress range at the considered hot spot is less than two times the yield strength.

D.2.1 Fatigue stress

The stress range $\Delta\bar{\sigma}$ be entered the S-N curve may be derived as:

$$\Delta\bar{\sigma} = \Delta\sigma \frac{f_m}{f_x} \quad (\text{D.2.1})$$

where $\Delta\sigma$ is the local stress range at the considered hot spot, f_m is a factor taking into account the mean stress influence and f_x is the notch support factor from equation (D.2.3).

The mean stress factor, f_m , is for the S-N curves in [D.2.2] equal to 1 ($f_m=1$). The mean stress factor, f_m , is derived from the following equation for the S-N curves in [D.2.3]:

$$f_m = \frac{1 + 0.5 \frac{\sigma_m}{\Delta\sigma}}{1.25} \quad (\text{D.2.2})$$

This mean stress factor is limited to $0.6 \leq f_m \leq 1.4$. The stress range $\Delta\sigma$ and mean stress σ_m calculated from equation (D.2.4) and equation (D.2.5), respectively.

The notch support factor may for all S-N curves in [D.2] be estimated from the notch radius r as:

$$f_x = \begin{cases} 1.37 & \text{if } r \leq 1 \text{ mm} \\ 10^{0.136[1 - \log r]} & \text{if } 1 \text{ mm} < r < 10 \text{ mm} \\ 1.0 & \text{if } r \geq 10 \text{ mm} \end{cases} \quad (\text{D.2.3})$$

The stress range may for fatigue analysis of notches in base material where initiation of a fatigue crack is a significant part of the fatigue life, be calculated based on von Mises form of component stress ranges as

$$\Delta\sigma = \sqrt{\Delta\sigma_x^2 + \Delta\sigma_y^2 + \Delta\sigma_z^2 - \Delta\sigma_x\Delta\sigma_y - \Delta\sigma_y\Delta\sigma_z - \Delta\sigma_x\Delta\sigma_z + 3(\Delta\tau_{xy}^2 + \Delta\tau_{yz}^2 + \Delta\tau_{zx}^2)} \quad (\text{D.2.4})$$

where:

$$\begin{aligned} \Delta\sigma_x &= \sigma_{x,\max} - \sigma_{x,\min}, \quad \Delta\sigma_y = \sigma_{y,\max} - \sigma_{y,\min}, \quad \Delta\sigma_z = \sigma_{z,\max} - \sigma_{z,\min}, \quad \Delta\tau_{xy} = \tau_{xy,\max} - \tau_{xy,\min}, \\ \Delta\tau_{yz} &= \tau_{yz,\max} - \tau_{yz,\min}, \quad \Delta\tau_{zx} = \tau_{zx,\max} - \tau_{zx,\min} \end{aligned}$$

Load condition max and min are at the same time instances for all stress components. The component stress ranges may be both negative and positive.

The following mean stress may be used in fatigue analysis of hot spots in base material:

$$\sigma_m = \sigma_{x,mean} + \sigma_{y,mean} + \sigma_{z,mean} = \frac{1}{2}(\sigma_{x,max} + \sigma_{x,min} + \sigma_{y,max} + \sigma_{y,min} + \sigma_{z,max} + \sigma_{z,min}) \quad (\text{D.2.5})$$

D.2.2 S-N curves for a high mean tensile stress

The design S-N curves in [Table D-1](#) and [Table D-2](#) are developed for subsea steel forgings subjected to a high mean tensile stress.

Table D-1 Design S-N curves for steel forgings in air and subjected to a high mean tensile stress

S-N curve	Tensile strength in [MPa] (ksi)	Typical yield strength for the given tensile strength in [MPa] (ksi)	$\log \bar{\alpha}$	
			$m = 5.0$	
			$Ra \leq 3.2 \mu\text{m}$	$Ra \leq 6.4 \mu\text{m}$
BM1	Including and above 517 (75) Up to 586 (85)	448 (65) and below	17.898	17.730
BM2	Including and above 586 (85) Up to 655 (95)	448 (65) - 586 (85)	18.098	17.910
BM3	Including and above 655 (95) Up to 897(130)	552 (80) - 759 (110)	18.275	18.069

Table D-2 Design S-N curves for steel forgings in seawater with cathodic protection and subjected to a high mean tensile stress

S-N curve	Tensile strength in [MPa] (ksi)	Typical yield strength for the given tensile strength in [MPa] (ksi)	$\log \bar{\alpha}$	
			$m = 5.0$	
			$Ra \leq 3.2 \mu\text{m}$	$Ra \leq 6.4 \mu\text{m}$
BM1	Including and above 517 (75) Up to 586 (85)	448 (65) and below	17.500	17.332
BM2	Including and above 586 (85) Up to 655 (95)	448 (65) - 586 (85)	17.700	17.512
BM3	Including and above 655 (95) Up to 897(130)	552 (80) - 759 (110)	17.877	17.671

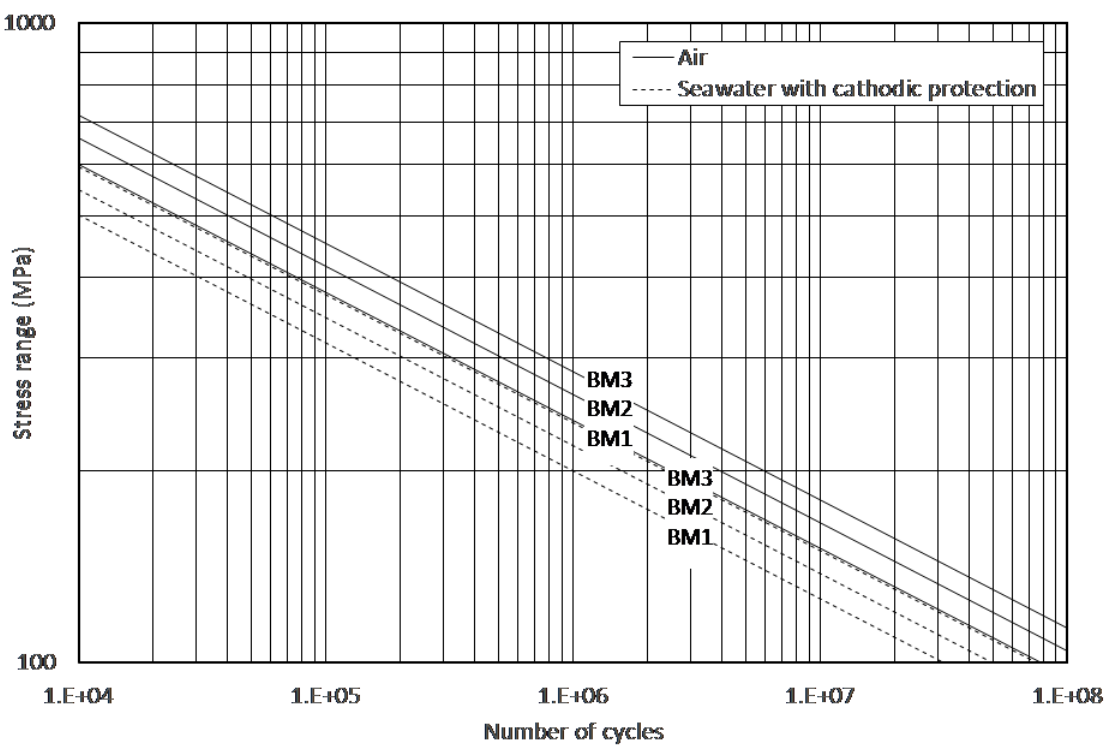


Figure D-2 Design S-N curves for steel forgings subjected to a high mean tensile stress and surface roughness $R_a \leq 3.2 \mu\text{m}$

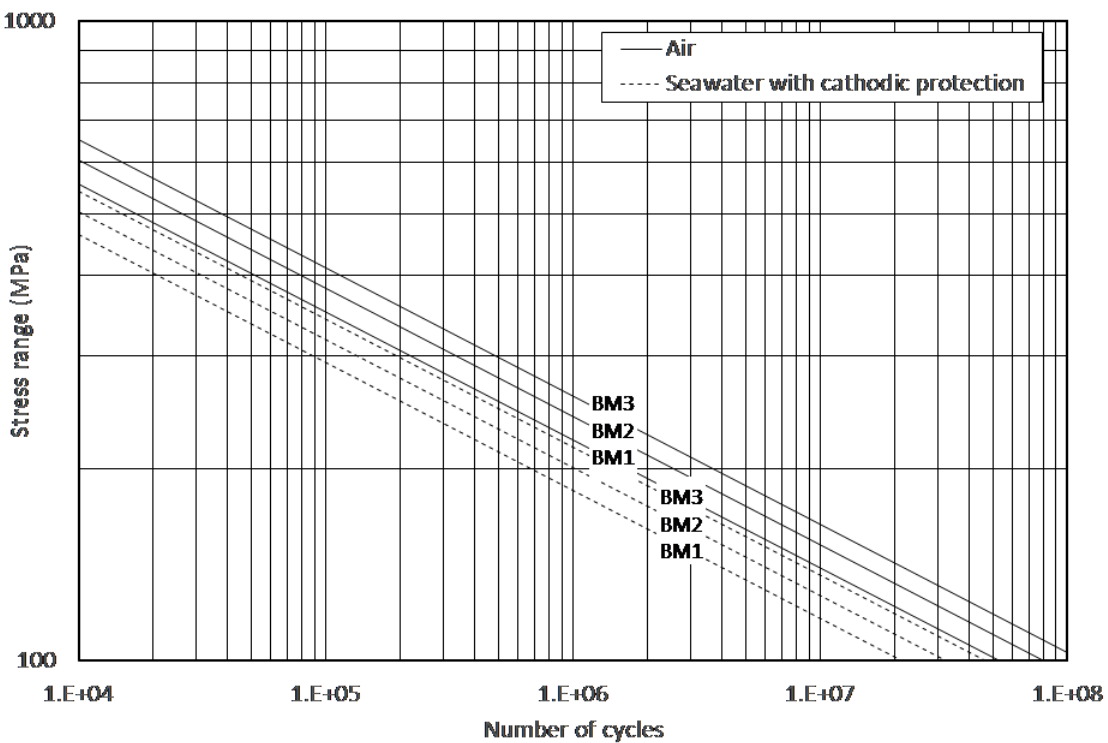


Figure D-3 Design S-N curves for steel forgings subjected to a high mean tensile stress and surface roughness $R_a \leq 6.4 \mu\text{m}$

D.2.3 S-N curves for a constant stress ratio

The design S-N curves in [Table D-3](#) and [Table D-4](#) are developed for a constant stress ratio of $R = \sigma_{min}/\sigma_{max} = 0$ ($\sigma_m/\Delta\sigma = 0.5$ or $\sigma_{min} = 0$ and $\sigma_{max} = \Delta\sigma$).

Table D-3 Design S-N curves for steel forgings in air

S-N curve	Tensile strength in [MPa] (ksi)	Typical yield strength for the given tensile strength in [MPa] (ksi)	$\log \bar{\alpha}$	
			$R_a \leq 3.2 \mu\text{m}$	$R_a \leq 6.4 \mu\text{m}$
BM1	Including and above 517 (75) Up to 586 (85)	448 (65) and below	20.402	20.275
BM2	Including and above 586 (85) Up to 655 (95)	448 (65) - 586 (85)	20.728	20.576
BM3	Including and above 655 (95) Up to 897(130)	552 (80) - 759 (110)	21.018	20.842

Table D-4 Design S-N curves for steel forgings in seawater with cathodic protection

S-N curve	Tensile strength in [MPa] (ksi)	Typical yield strength for the given tensile strength in [MPa] (ksi)	$\log \bar{a}$	
			$m = 6.0$	$R_a \leq 3.2 \mu\text{m}$
BM1	Including and above 517 (75) Up to 586 (85)	448 (65) and below	20.002	19.875
BM2	Including and above 586 (85) Up to 655 (95)	448 (65) - 586 (85)	20.328	20.176
BM3	Including and above 655 (95) Up to 897(130)	552 (80) - 759 (110)	20.618	20.442

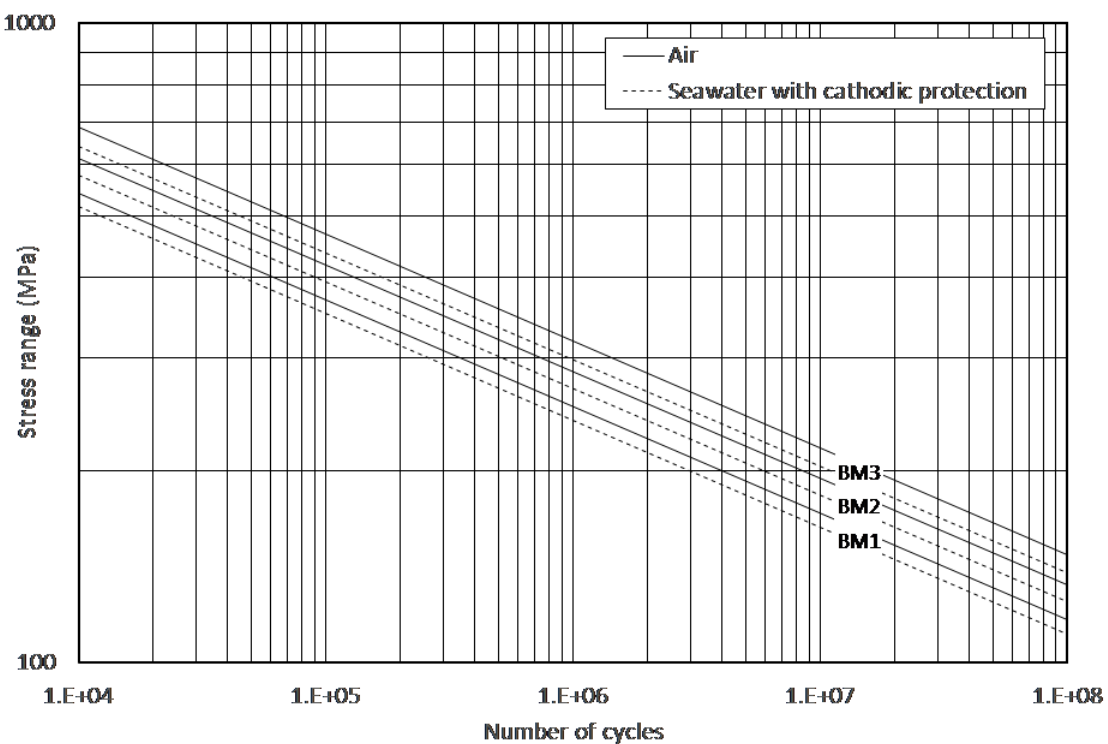


Figure D-4 Design S-N curves for steel forgings for $R = 0$ and surface roughness $R_a \leq 3.2 \mu\text{m}$

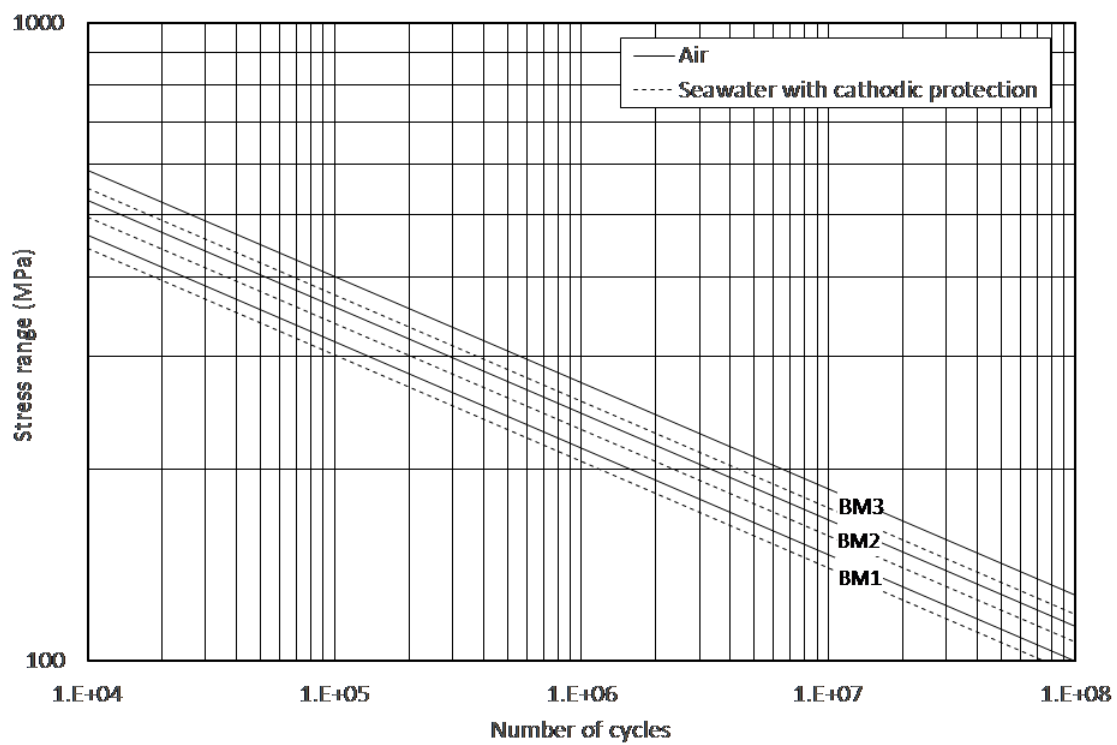


Figure D-5 Design S-N curves for steel forgings for $R = 0$ and surface roughness $R_a \leq 6.4 \mu\text{m}$.

APPENDIX E APPLICATION OF THE EFFECTIVE NOTCH STRESS METHOD FOR FATIGUE ASSESSMENT OF STRUCTURAL DETAILS

E.1 General

Effective notch stress is the total stress at the root of a notch, obtained assuming linear-elastic material behaviour. To take account of statistical nature and scatter of weld shape parameters, as well as of non-linear material behaviour at the notch root, the real weld is replaced by an effective one, see [Figure E-1](#). For structural steels an effective notch root radius of $r = 1.0$ mm has been verified to give consistent results. For fatigue assessment, the effective notch stress is compared with a common fatigue resistance curve.

The method is restricted to welded joints which are expected to fail from the weld toe or weld root. Other causes of fatigue failure, e.g. from surface roughness or embedded defects, are not covered. Also it is not applicable where considerable stress components parallel to the weld or parallel to the root gap exist.

The method is well suited for S-N classification of alternative geometries. Unless otherwise specified, flank angles of 30° for butt welds and 45° for fillet welds are suggested.

The method is limited to thicknesses $t \geq 5$ mm. For smaller wall thicknesses, the method has not been verified (or a smaller radius and another S-N curve is recommended used, see literature).

In cases where a mean geometrical notch root radius can be defined, e.g. after certain post weld improvement procedures such as grinding, the actual geometrical radius may be used in the effective notch stress analysis. Then the calculated notch stress should be entered into a relevant S-N curve. See [Table A-5](#) in [App.A](#) for potential fatigue crack growth from ground areas at welded regions.

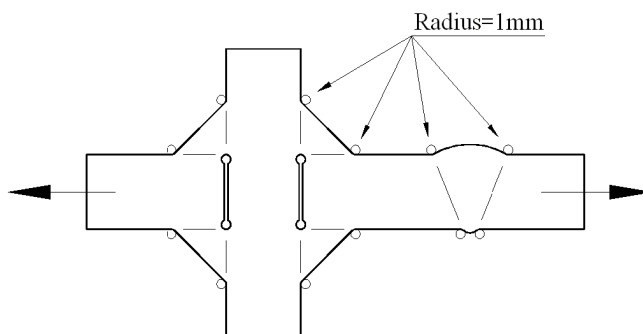


Figure E-1 Analysis of effective notch stress

E.2 Calculation of effective notch stress

Effective notch stresses or notch stress concentration factors can be calculated by parametric formulae, taken from diagrams or calculated from finite element analysis. The effective notch radius is introduced such that the tip of the radius touches the root of the real notch, e.g. the end of an un-welded root gap.

Calculation of effective notch stress by the finite element method requires that a fine element mesh is used around the notch region. The effective notch stress to be used together with the recommended S-N curve is the maximum calculated surface stress in the notch. This maximum surface stress may be obtained directly from the nodal stress calculated at the surface or from extrapolation of element stresses to the surface. In some finite element programs it may also be efficient to add bar elements with a small area (negligible area) along the notch surface. Then the surface stress is finally derived as force in the bar divided by area.

The requirement to mesh size is depending on elements used. If elements with quadratic displacement functions are used, a minimum of 4 elements should be used along a quarter of the circle circumference. If simpler elements are used, the mesh refinement should be improved correspondingly. The mesh should be

made with regular elements without transition to reduced refinement within the first three element layers from the notch surface. An element shape that is close to quadratic is preferred.

In case of uncertainty about elements ability to provide reliable surface stress it is recommended to perform a validation of the methodology against a well known case.

Notch Stress S-N Curves

The calculated notch stress should be linked to a notch stress S-N curve for fatigue design as described in [Table E-1](#). The S-N curves are presented as mean minus two standard deviations in logarithmic S-N format.

The thickness effect is assumed accounted for in the calculated notch stress. Thus a further reduction of fatigue capacity for larger thicknesses is not required.

The S-N curve is presented on the standard form:

$$\log N = \log \bar{a} - m \log \Delta\sigma \quad (\text{E.2.1})$$

where:

\bar{a} = intercept of the design S-N curve with the log N axis

m = negative inverse slope of the S-N curve.

Table E-1 Notch stress S-N curves

Environment	Log \bar{a}	
Air	$N \leq 10^7$ cycles $m_1 = 3.0$	$N > 10^7$ cycles $m_2 = 5.0$
	13.358	17.596
Seawater with cathodic protection	$N \leq 10^6$ cycles $m_1 = 3.0$	$N > 10^6$ cycles $m_2 = 5.0$
	12.958	17.596
Seawater with free corrosion	For all $N \log \bar{a} = 12.880$ and $m_1 = 3.0$	

E.3 Validation of analysis methodology

The notch stress concept using finite element analysis can be validated against a well tested detail that also can be assessed based on nominal stress approach.

A cruciform joint may be selected for analysis as shown in [Figure E-2](#) and this subsection.

The F curve may be used for fatigue assessment of the weld toe using the nominal stress approach.

Then target notch stress at the weld toe is obtained as 3.17 times the nominal stress in the plate for plate thickness equal 25 mm.

A fillet welded cruciform joint may be selected for analysis as shown in [Figure E-4](#) and [Figure E-5](#). Then the W3 curve may be used for fatigue assessment of the weld root using the nominal stress approach. The nominal stress in the weld is derived as:

$$\sigma_w = \sigma_{\text{Nominal}} t / 2a \quad (\text{E.3.1})$$

where:

t = thickness of member

a = throat thickness.

Then a target notch stress in the weld root is obtained as 6.25 times the nominal stress in the fillet weld.

If the calculated stress from validation analyses is far from the target values, it is recommended to consider the accuracy of the methodology used such as type of element in relation to mesh refinement and read out of notch surface stress.

The toe of the same detail would be classified as F3. This result in a target notch stresses 4.02 times the nominal stress.

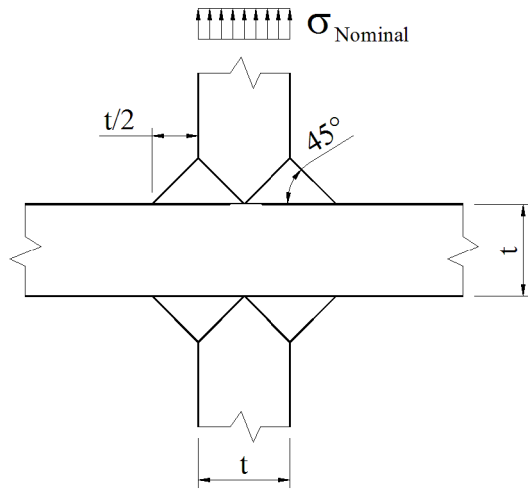


Figure E-2 Geometry for validation of analysis procedure for the weld toe

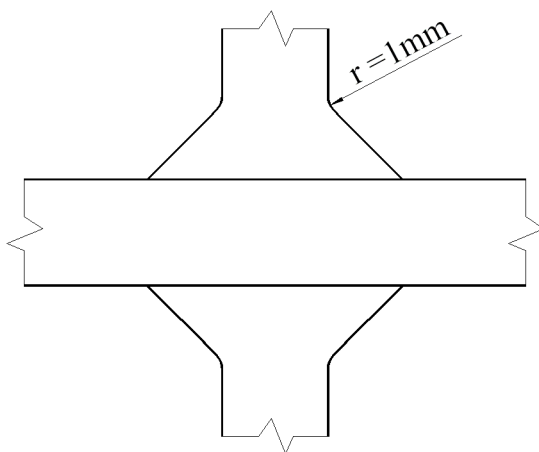


Figure E-3 Geometry of the transition from weld to base material to be used in the analysis

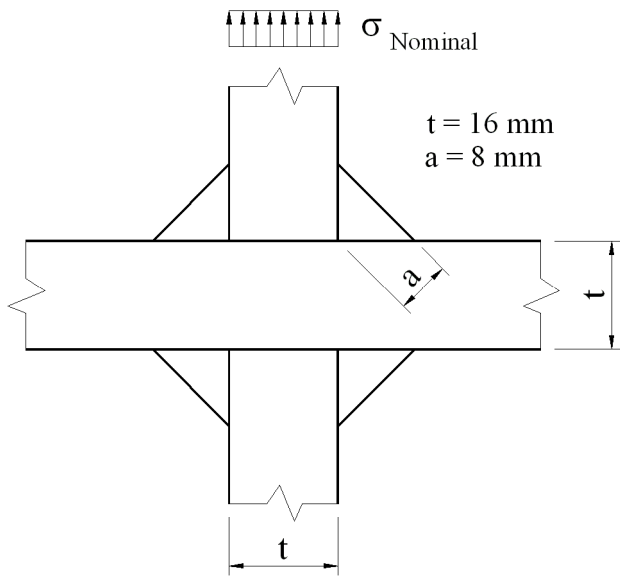


Figure E-4 Detail selected for validation of procedure for root of fillet welds

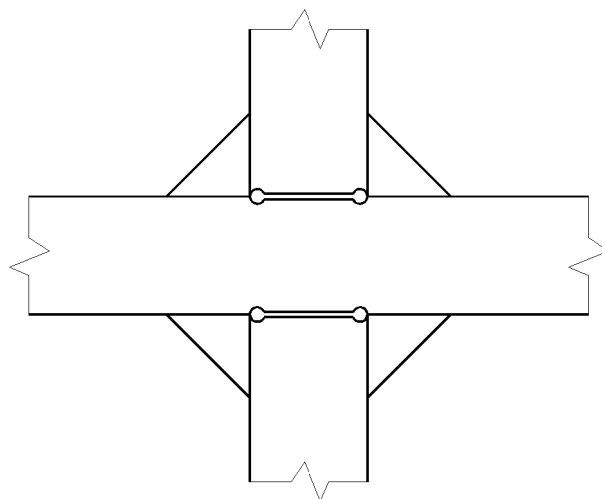


Figure E-5 Notch to be included in FE model for the weld root

APPENDIX F COMMENTARY

The purpose of this commentary section is to add background information, additional explanations and examples which may be useful for understanding the content of this recommended practice. Short explanations of the content of the different sections are given in the following:

[F.1]: This section shows how fatigue damage from low cycle fatigue can be combined with fatigue damage from high cycle fatigue.

[F.2]: This section shows the most significant part of the S-N curve when stress ranges are derived from typical environmental load responses such as wave loads. This is also considered relevant for wind loads.

[F.3]: This section shows a simplified way to combine fatigue damages from different dynamic processes.

[F.4]: This section explains that different S-N curves can be used depending on the main stress direction relative to the weld toe.

[F.5]: This section gives some background for how the S-N curves are derived and the scatter in the fatigue test data associated with the different S-N curves.

This section gives also some background for the thickness effect used in this RP and also an equation for the length effect is included. This may be useful for design of long pipes with weld seams for gas storage and girth welds subjected to a rather uniform stress range along the welds.

The relationship between the S-N curves in this RP and the S-N curves in IIW and Eurocode 3 is provided.

A section on size of defects inherent in the S-N data and requirements to non-destructive examination is included.

[F.6]: This section gives some background for corrosion protection of jacket structures in the splash zone area and for details in tanks in FPSOs.

[F.7]: This section gives some background on effect of residual stresses for derivation of fatigue test data and S-N curves for design. It gives also some considerations on how to assess few fatigue tests for purpose of deriving a reliable fatigue design procedure.

[F.8]: This section gives information on stress calculation in pipes and cylindrical tanks subjected to internal pressure variations.

[F.9]: This section gives some references to literature on stress concentration factors.

[F.10]: This section gives some information that can be used for fatigue assessment of tubular joints welded from the outside only.

[F.11]: This section is included as information about stress concentration factors for some defined geometries and load cases that can be used for calibration of analysis methodology. This section gives also some background for the methodology used for fatigue analysis of web stiffened cruciform joints in [4.3.8].

[F.12]: This section provides guidance on fatigue analysis where the principal stress direction changes significantly during a load cycle.

[F.13]: This section gives background for closed form equations that are frequently used for calculation of fatigue damage based on short term and long term stress responses.

A fatigue analysis of a drum is included to illustrate the use of the fatigue limit in design and for selection of nominal stress S-N curve at a ring stiffener together with calculation of the stress concentration factor at this ring stiffener.

[F.14]: This section is included to explain the stress condition at a girth weld in a pipe due to a fabrication tolerance.

[F.15]: This section is included as an alternative method for calculation of fatigue damage at improved details using S-N curves (as an alternative to the factors on fatigue life improvement in Table 7-1).

[F.16]: This example is included to show the complexity of fatigue analysis of different hot spots at a gusset plate connection. This example illustrates use of different hot spot S-N curves as described in [4.3.5].

[F.17]: Stress concentration factors for conical transitions.

F.1 Comm. 1.2.3 low cycle and high cycle fatigue

By fatigue strength assessment of offshore structures is normally understood capacity due to high cycle fatigue loading.

By high cycle loading is normally understood cycles more than 10 000. For example stress response from wave action shows typically 5 mill cycles a year. A fatigue assessment of response that is associated with number of cycles less than 10 000 is denoted low cycle fatigue.

This recommended practice is mainly made with the purpose of assessing fatigue damage in the high cycle region. The specified S-N curves are shown in the graphs above 10^4 cycles. Typical S-N test data are derived for number of cycles between 10^4 and $5 \cdot 10^6$ cycles. However, the S-N curves may be linearly extrapolated to fewer cycles for practical use in a fatigue assessment. This is not necessarily conservative and in case of a high utilisation, the approach described in NORSO N-006 may be used.

High cycle fatigue analysis is based on calculation of elastic stresses that are used in the assessment.

Low cycle fatigue is associated with load reversals that imply significant yielding at the hot spot also during the load reversal. Therefore calculated strain is often used as a parameter to account for non-linear material behaviour when low cycle fatigue is considered.

Offshore structures are normally designed for other limit states such as the ultimate limit state (ULS). Then a load and material coefficient is used in design to achieve sufficient safety. Even if stresses due to local notches are not accounted for in an ULS design the assessment of ULS implies that the actual strain ranges during an ULS loading is limited and that a further assessment of low cycle fatigue is normally not required. Thus for design of offshore structures in the North Sea it has in general not been practice to analyse the structures specifically for low cycle fatigue.

When non-linear methods are used for documentation of ULS e.g. for a storm loading on a platform, it is recommended to assess low cycle fatigue during that considered storm. See NORSO N-006 for further guidance.

Low cycle fatigue is also found to be of concern in some local areas in ship structures due to loading and unloading. The reason for this is that ship structures in general show a much higher utilisation in ULS than offshore structures.

FPSOs are rather similar structures with similar loading and unloading as tankers, therefore low cycle fatigue may be an issue to consider for these structures depending on procedure used for loading and unloading.

For calculation of fatigue damage at highly loaded details it is recommended to calculate a stress range from the wave action corresponding to the largest expected stress range during the time interval of a loading/unloading cycle. This stress range should be added to the low cycle stress range before the fatigue damage from the low cycle fatigue is calculated. This stress range from the wave action can be calculated as:

$$\Delta\sigma_w = \Delta\sigma_0 \left(1 - \frac{\log n_{LCF}}{\log n_0} \right)^{1/h} \quad (\text{F.1.1})$$

where:

$\Delta\sigma_0$ = largest stress range during n_0 cycles from wave action

n_{LCF} = number of loading/unloading cycles during the lifetime

h = Weibul shape parameter from the wave action.

Then an effective stress range to be used for calculation of low cycle fatigue can be obtained as:

$$\Delta\sigma_e = \Delta\sigma_{LCF} + \Delta\sigma_w \quad (\text{F.1.2})$$

This effective stress range is used for calculation of fatigue damage from low cycle fatigue: D_{LCF} . Then the resulting fatigue damage can be calculated as the sum:

$$D = D_{LCF} + D_{HCF} \quad (\text{F.1.3})$$

where D_{HCF} is fatigue damage from the wave action alone.

Due to large stress cycles implying local yielding at the hot spot the calculated stress range from a linear elastic analysis should be modified by a plasticity correction factor before the S-N curve is entered for calculation of fatigue damage, see e.g NORSO N-006.

F.2 Comm. 1.3 methods for fatigue analysis

Important part of action history

The contribution to fatigue damage for different regions of a Weibull distribution is shown in [Figure F-1](#) for fatigue damage equal 1.0 (and 0.5) for a 20-year period. The calculation is based on a Weibull long term stress range distribution with shape parameter $h = 1.0$ (in the range that is typical for a semi-submersible and an S-N curve with slope $m = 3.0$ for $N < 10^7$ and $m = 5.0$ for $N > 10^7$ cycles (typical S-N curve for a welded connection in air condition)).

It is noted that the most important part of the long-term stress range is for actions having a probability of exceedance in the range 10^{-3} to 10^{-1} during the lifetime. This corresponds to $\log n = 5-7$ in [Figure F-1](#).

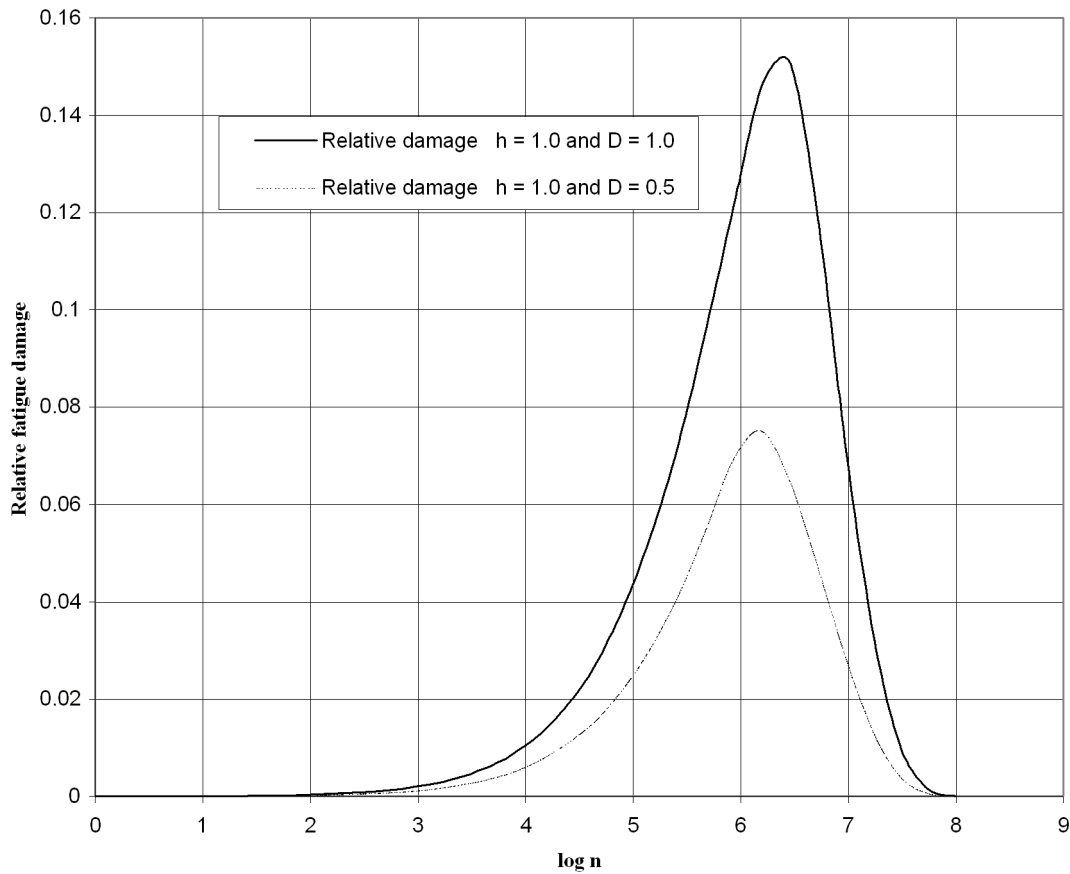


Figure F-1 Relative fatigue damage in Weibull distribution of stress ranges

F.3 Comm. 2.2 combination of fatigue damages from two dynamic processes

Background

In some design cases one fatigue damage is calculated for one dynamic process. Then another fatigue damage for the same hot spot is calculated for another dynamic process. Then the question arises on how to calculate the resulting fatigue damage for the considered hot spot. It is non-conservative to simply add the two fatigue damages together.

An example of such a design situation is swell response of an FPSO that also is subjected to wave response. Another example may be wave response of a floating platform that also may be subjected to wind response on a flare tower that are giving stress cycling at the same hot spot in the structure. In many cases it is practical to calculate the fatigue damage for each of these processes separately as the design may belong to different engineering contracts.

When a detailed stochastic analysis of the complete structural system is performed for each of the dynamic processes, a more accurate combined stress response can be calculated before the S-N curve is entered and the fatigue damage is calculated. See for example [DNVGL-OS-E301 Position mooring](#).

In the following a simple method for derivation of resulting fatigue damage from two processes is presented. This methodology is based on information of mean zero up-crossing frequency in addition to the calculated fatigue damages for each of the processes.

Combined fatigue damage for one slope S-N curve

Combined fatigue damage for the responses shown in [Figure F-2](#) can be obtained as:

$$D = D_1 \left(1 - \frac{v_2}{v_1}\right) + v_2 \left\{ \left(\frac{D_1}{v_1}\right)^{1/m} + \left(\frac{D_2}{v_2}\right)^{1/m} \right\}^m \quad (\text{F.3.1})$$

where:

D_1 = calculated fatigue damage for the high frequency response

D_2 = calculated fatigue damage for the low frequency response

v_1 = mean zero up-crossing frequency for the high frequency response

v_2 = mean zero up-crossing frequency for the low frequency response

m = inverse slope of the S-N curve = 3.0.

The combined fatigue damage is based on the assumption that each of the fatigue damages D_1 and D_2 are derived based on a one slope S-N curve. The equation is derived based on analogy with Rainflow stress range counting.

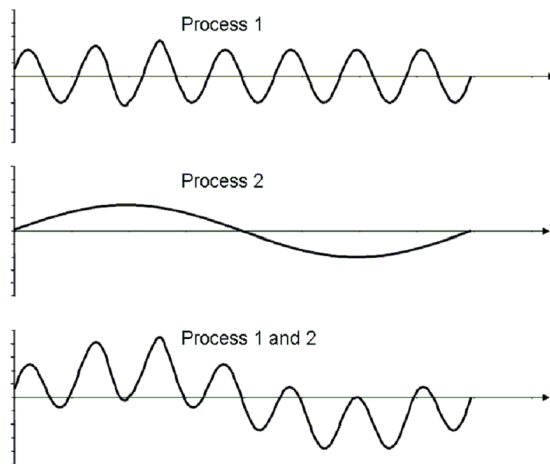


Figure F-2 Sketch showing high and low frequency response and combined response

Combined fatigue damage for two-slope S-N curves

For two-sloped S-N curves it is questioned if equation (F.3.1) can be used for calculation of resulting fatigue damage.

The S-N curves in air have a transition in slope from $m = 3.0$ to $m = 5.0$ at 10^7 cycles.

For a long term stress range distribution with Weibull shape parameter $h = 1.0$, 20 years service life, and a fatigue damage equal 1.0 the major contribution to fatigue damage occurs around 10^7 cycles. Approximately half the damage occurs at number of cycles below 10^7 cycles and the other half above 10^7 cycles. For lower fatigue damage than 1.0, which is the case in order to have acceptable resulting fatigue damage when considering two processes, the main contribution to fatigue damage will be at the S-N line with slope $m = 5.0$.

Thus, in order to have a methodology that is safe one should use a slope $m = 5.0$ in equation (F.3.1) if the fatigue damages for the two processes have been calculated based on this two-slope S-N curve.

An alternative to this is to calculate the fatigue damage for process no 2 with a straight S-N curve with slope $m = 3.0$. Then equation (F.3.1) can be used with D_1 calculated from a two-slope S-N curve and with $m = 3.0$.

F.4 Comm. 2.3.2 plated structures using nominal stress S-N curves

The fatigue capacities of welded connections are dependent on the principal stress range direction relative to the weld toe. See also [4.3.4]. The following guidance is based on assessment of fatigue test data.

Figure F-3 a) and b) are intended used for nominal stress analyses.

The selection of E or F curve for $\varphi = 0^\circ$ depends on thickness of attachment as presented in Table A-7 in App.A. For other φ values see Table F-1.

Figure F-3 c) can be used together with the hot spot stress methodology in general.

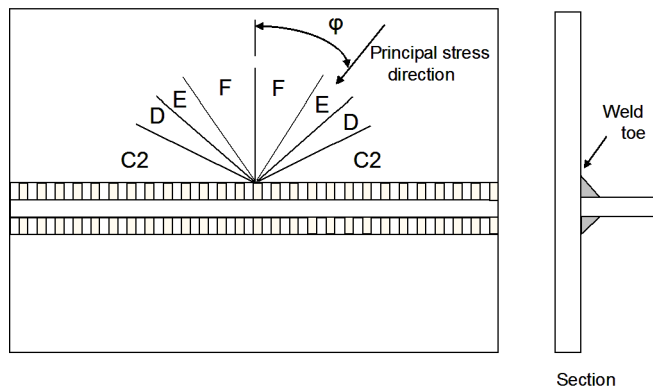
In general the stress range in both the two principal directions shall be assessed with respect to fatigue.

Table F-1 Classification of details and selection of S-N curve

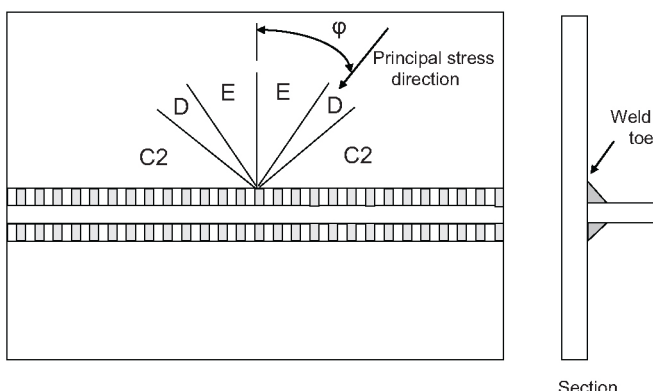
Angle φ in Figure F-3	Detail classified as F for stress direction normal to the weld	Detail classified as E for stress direction normal to the weld	S-N curve when using the hot spot stress methodology
0 - 30	F	E	D
30 - 45	E	D	C2
45 - 60	D	C2	C2
60 - 75	C2	C2	C2*)
75 - 90	C2*)	C2*)	C2*)

*) A higher S-N curve may be used in special cases. See Table A-3 for further information.

- a) Detail classified as F (plate thickness of attachment $t > 25$ mm) for stress direction normal to the weld, see [Table F-1](#) for φ .



- b) Detail classified as E (plate thickness of attachment $t \leq 25$ mm) for stress direction normal to the weld, see [Table F-1](#) for φ .



- c) S-N curve when using the hot spot stress methodology, see [Table F-1](#) for φ .

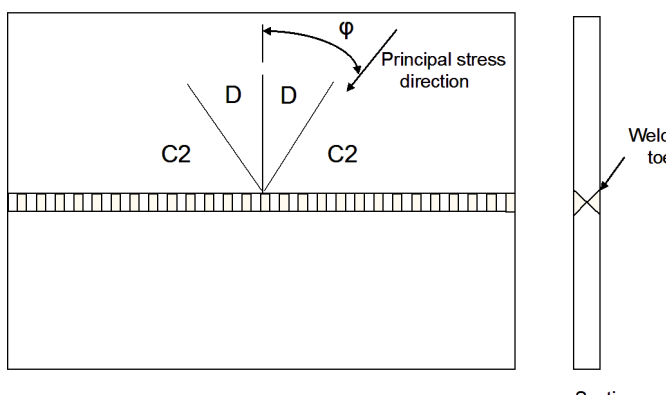


Figure F-3 Classification of details and selection of S-N curve

F.5 Comm. 2.4.3 S-N curves and joint classification

Normally the standard deviation of the log N is not required for design purpose as the design S-N curves are presented as mean-minus-two-standard-deviations as described in [2.4.1]. However, information about the standard deviation in the S-N curve is required for purpose of probabilistic analysis.

It is more complex to derive design S-N curves for real structures than that expressed by simple mathematical regression of test data for derivation of S-N curves as expressed in some literature. A main reason for this is lack of relevant fatigue test data for structures. Most of the fatigue test data are derived from testing of small scale test specimens. These specimens do not include the same amount of residual stresses as a full scale structure. The test data may also belong to different R-ratios. Further, the small scale test specimens are most often more perfect considering tolerances and defects than that of real structures. Thus, also engineering assessment is required for derivation of recommended design S-N curves in a design standard that can be used to achieve sound structures with respect to fatigue capacity.

One specific S-N curve may be used for different details. In principle different details can show different scatter when they are tested. The simple details show less scatter in test data than the more complex details.

Fatigue testing is normally performed under constant amplitude loading while actual structures are likely subjected to variable amplitude loading. This introduces additional uncertainty as explained in [2.4.14].

All this makes it difficult to present standard deviations that are representative for each specific S-N curve. However, without having test data made for a specific design and fabrication a typical standard deviation $s_{logN} = 0.200$ can be used for all the S-N curves in [2.4.4] to [2.4.9] and [2.4.11] and [D.2]. $s_{logN} = 0.162$ can be used for the high strength S-N curves in [D.1]. $s_{logN} = 0.225$ can be used for the S-N curve for umbilical pipes in [2.4.12].

Size effect

The size effect may be explained by a number of different parameters:

- thickness of plate – which is explained by a more severe notch with increasing plate thickness at the region where the fatigue cracks are normally initiated
- attachment length – which is explained by a more severe notch stress due to more flow of stress into a long attachment than a short
- volume effect – which for surface defects can be explained by increased weld length and therefore increased possibility for imperfections that can be initiated into fatigue cracks.

It might be added that some authors group all these 3 effects into one group of 'thickness effect' or size effect. In this recommended practice, the thickness exponent is assumed to cover the first item in the list above. This is accounted for by making the size effect depending on the attachment length in [2.4.3]. An increased attachment length reduces the S-N class as shown in App.A of this recommended practice. Examples of the third effect and how it can be accounted for in an actual design is explained in more detail in the following. See also /12/, /18/ and /19/ for more background and explanation of the thickness effect.

Test specimens used for fatigue testing are normally smaller than actual structural components used in structures. The correspondence in S-N data depends on the stress distribution at the hot spot region. For traditional tubular joints there is one local hot spot region, while at e.g. circumferential welds of TLP tethers there is a length significantly longer than in the test specimens having the similar order of stress range. Crack growth is normally initiated from small defects at the transition zone from weld to base material. The longer the weld, the larger is the probability of a larger defect. Thus, a specimen having a long weld region is expected to have a shorter fatigue life than a short weld. This can be accounted for in an actual design by probabilistic analysis of a series system, see e.g. *Methods of Structural Safety* /21/. See also /79/. Weld length in a tether system is one example where such analysis should be considered to achieve a reliable fatigue design. A mooring line consisting of chains is another example where reliability methods may be used to properly account for the size effect or system effect.

The system effect for the S-N curves in this RP has been investigated using reliability methods. The results are expressed analytically below.

The length of weld and number of similar connections subjected to the same stress range should be assessed based on engineering judgement. If a tether system is subjected to a dynamic axial force without significant bending the assessment becomes simple as all welds will be subjected to the same stress range. As soon as there is some bending over the diameter of the tether there will likely be some hot spots at some connections that are subjected to a larger stress range than the other connections. Then only the regions with the most severe stress ranges shall be included for weld length and number of connections.

For threaded bolts, the stress concentration at the root of the threads increases with increasing diameter. Based on fatigue tests, it is recommended to use $k = 0.25$ which can be assumed to include size effects both due to the notch itself, and due to increased length of notch around circumference with increased diameter. The thickness exponent may be less for rolled threads. Thus for purpose made bolts with large diameters, it may be recommendable to perform testing of some bolts to verify the fatigue capacity to be used for design. It should be remembered that the design S-N data is obtained as mean minus 2 standard deviation in a log S-log N diagram.

S-N curve with thickness effect

The design S-N curve with thickness effect included is given by:

Curve part (1), see [Figure F-4](#).

$$\log N = \log \bar{a}_1 - m_1 k \log \left(\frac{t}{t_{ref}} \right) - m_1 \log \Delta \sigma \quad (F.5.1)$$

Part (2) of the curve is established assuming continuity at $N_1=10^6$ or 10^7 cycles depending on the S-N curve is given for seawater with cathodic protection or in air is given by:

$$\log N = \frac{m_2}{m_1} \log \bar{a}_1 + \left(1 - \frac{m_2}{m_1} \right) \log N_1 - m_2 k \log \left(\frac{t}{t_{ref}} \right) - m_2 \log \Delta \sigma \quad (F.5.2)$$

where \bar{a}_1 is for S-N curve without thickness effect included. $\log \bar{a}_1$ is given in [Table 2-1](#), [Table 2-2](#) and [Table 2-3](#).

Part (2) of the S-N curve can also be written on a standard form:

$$\log N = \log \bar{a}_2 - m_2 k \log \left(\frac{t}{t_{ref}} \right) - m_2 \log \Delta \sigma \quad (F.5.3)$$

where:

$$\log \bar{a}_2 = \frac{m_2}{m_1} \log \bar{a}_1 + \left(1 - \frac{m_2}{m_1} \right) \log N_1 \quad (F.5.4)$$

See also [\[2.4.3\]](#).

S-N curve with system effect and thickness effect

The design S-N curve with system effect and thickness effect included is given by:
Curve part (1), see [Figure F-4](#).

$$\log N = \log \bar{a}_1 - \frac{s_{\log N}}{2} \log \left(\frac{l_{weld}}{l_{ref}} n_s \right) - m_1 k \log \left(\frac{t}{t_{ref}} \right) - m_1 \log \Delta\sigma \quad (\text{F.5.5})$$

where:

l_{weld} = length of weld subjected to the same stress range

l_{ref} = reference length corresponding to typical length of weld in tested specimen used for derivation of S-N curve. $l_{ref} = 100$ mm may be used.

n_s = number of similar connections subjected to the same stress range

$s_{\log N}$ = standard deviation in $\log N$.

Part (2) of the curve is established assuming continuity at $N_1=10^6$ or 10^7 cycles depending on whether the S-N curve is given for seawater with cathodic protection or in air:

$$\log N = \log \bar{a}_2 - m_2 k \log \left(\frac{t}{t_{ref}} \right) - m_2 \log \Delta\sigma \quad (\text{F.5.6})$$

with:

$$\log \bar{a}_2 = \frac{m_2}{m_1} \left(\log \bar{a}_1 - \frac{s_{\log N}}{2} \log \left(\frac{l_{weld}}{l_{ref}} n_s \right) \right) + \left(1 - \frac{m_2}{m_1} \right) \log N_1 \quad (\text{F.5.7})$$

where \bar{a}_1 is for S-N curve without thickness effect included. $\log \bar{a}_1$ is given in [Table 2-1](#), [Table 2-2](#) and [Table 2-3](#).

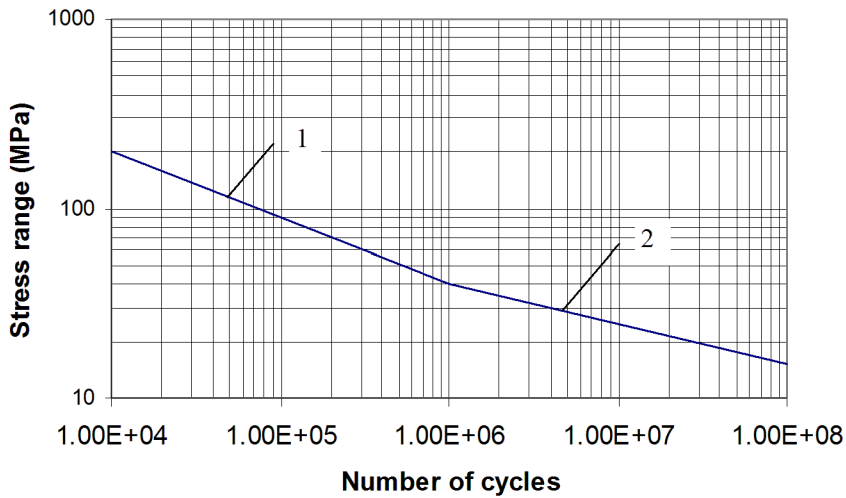


Figure F-4 Typical S-N curve with thickness effect included

Link to S-N curves in other design codes

The relationship between S-N curves in this document and those given by IIW /30/, Eurocode 3 /3/, for air environment is given in [Table F-2](#). It should be noted that the correspondence between S-N curves in this document and IIW relates only to number of cycles less than $5 \cdot 10^6$ in Eurocode 3. (The relationship is only approximate for the B1 and B2 curves.)

Table F-2 DNV GL notation in relation to Eurocode 3

DNV GL notation	IIW and Eurocode 3 notation
B1*)	160
B2*)	140
C	125
C1	112
C2	100
D	90
E	80
F	71
F1	63
F3	56
G	50
W1	45
W2	40

<i>DNV GL notation</i>	<i>IIW and Eurocode 3 notation</i>
W3	36
T	

- These curves are slightly different from IIW and Eurocode 3.
- Eurocode has transition in slope at $5 \cdot 10^6$ cycles and cut off at 10^8 cycles which is different from IIW.

Size of defects inherent in S-N data and requirements to non-destructive examination

This recommended practise is being used in classification by DNV GL and as a reference document in NORSO. This means that this RP is related to two different reference documents with respect to extent of NDT and acceptance criteria:

- [DNVGL-OS-C102 Design of offshore steel structures, general - LRFD method](#), [DNVGL-OS-C401 Fabrication and testing of offshore structures](#) and [ISO 5817 Welding - Fusion-welded joints in steel, nickel, titanium and their alloys \(beam welding excluded\) Quality levels for imperfections](#).
- NORSO N-004 *Design of steel structures* and M-101 *Structural steel fabrication*.

Most fatigue cracks are initiated from undercuts at weld toes. There can be different reasons for undercuts. It is recommended to prepare a good welding procedure to avoid large undercuts during production welding. No undercut is included in S-N classes better than the D-curve. Maximum allowable size of undercuts equal to 0.5 mm in depth may be considered inherent in the different design S-N classes D, E and F. For the S-N class F1 and lower an undercut equal to 1.0 mm may be accepted.

The weld details are being subjected to larger stress ranges as one goes to the higher S-N classes. A double sided butt weld belongs to D or E depending on fabrication. Butt welds are more critical with respect to internal defects than many other details. Planar defects like cracks and lack of fusion are not allowed. It should be noted that use of S-N classes above that of D imply special consideration with respect to requirements to NDT and acceptance criteria. Thus, reference for these S-N classes is made to Annex C of ISO 5817:2014 and to quality level ISO 5817 – B125. Radiographic testing is not suitable for detection of planar imperfections, hence ultrasonic testing should be used for detection of planar defects. See NORSO M-101 and ISO 5817 regarding requirements to volumetric defects like porosity and slag inclusions.

An example of crack growth through a plate thickness equal 25 mm from maximum surface defects that fulfil some different S-N curves is shown in [Figure F-5](#). A semi-elliptic surface defect is assumed with half axes $a/c = 0.2$. This calculation is based on a Weibull long term stress range distribution with 10^8 cycles during life time of 20 years. The shape parameter is $h = 1.0$ and the scale parameter is determined such that the accumulated Miner damage is equal 1.0 during the life time of the structure based on design S-N curves. It is observed that larger surface defects can be accepted for an F detail as compared with that of D and C. In [Figure F-5](#) $a_{initial} = 1.28$ mm for F class, 0.23 mm for D and 0.37 mm for C. The reason for the low value for the D class as compared with C is the notch effect at the weld toe which is not present for a machined surface (C class). The situation becomes different for internal defects where very small defects are acceptable for a C class due to high stresses inside the weld.

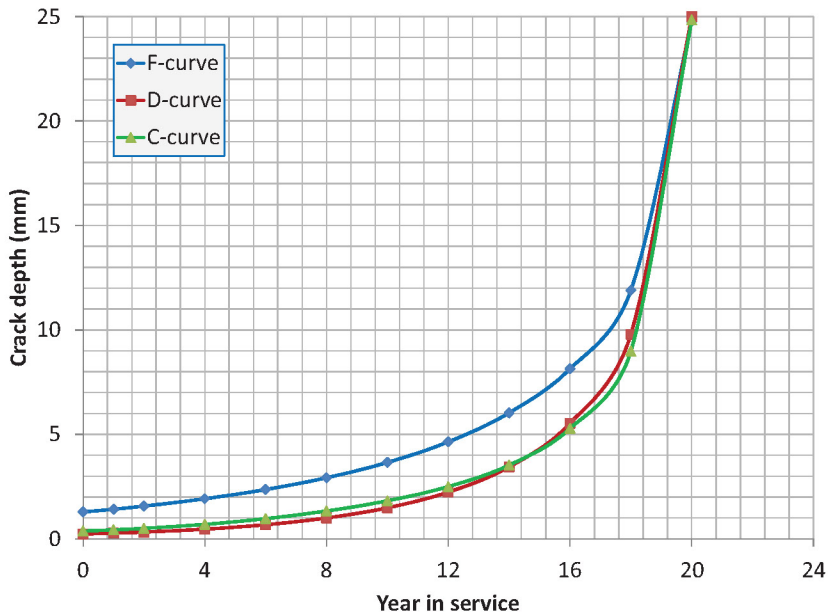


Figure F-5 Crack growth development from maximum surface defects in some different S-N classes

F.6 Comm. 2.4.9 S-N curves and efficiency of corrosion protection

S-N curve for joints in the splash zone

In Norway it has been the practice to use seawater S-N curve with cathodic protection for joints in the splash zone and a larger design fatigue factor (DFF) in the splash zone than in other areas in jacket structures. It is assumed that the joints also have a good coating in this area.

A high DFF is used because it is considered to be difficult to perform inspection and repair in this area. Increasing the DFF implies that the probability of a fatigue cracking becomes reduced. For example a DFF = 10 implies that the probability of a fatigue crack during the lifetime becomes very small (accumulated probability less than 10^{-4} and annual less than 10^{-5} the last year in service).

Quite a lot of the fatigue life is associated with initiation of a fatigue crack and growth of small cracks. The cracks have to grow to some size before the coating is broken. As long as the coating is not broken the condition corresponds to that of air.

The probability of having a fatigue crack that is so large that the coating is broken is considered to be low within the major part of the design life using a DFF = 10.

Based on this it is considered acceptable to calculate fatigue damage with an S-N curve that is somewhat reduced compared with that of air. Then the seawater curve with cathodic protection can be used in lack of documented S-N curves in seawater in free corrosion for coated joints (in the high cycle region above 10^6 cycles).

This recommendation is linked to use of a high DFF and a good coating. Then the probability of presence of an open fatigue crack subjected to free corrosion becomes small in the major part of the service life of the platform life as explained above.

S-N curve for details in tanks in FPSOs

Tanks in FPSOs are not designed with the same high DFF as used for splash zone joints in jackets. Also the coating is not so durable. The coating becomes more brittle with time and it is most likely to crack at hot spot regions with large strain cycles. In tanks without anodes the efficiency of the coating should be specially considered.

In [DNVGL-CG-0129](#) it is assumed that the coating is efficient for some years and then the condition is that of free corrosion. A similar procedure may be used for design of tanks in FPSOs. The time with efficient coating depends on type and quality of the coating used. See [DNVGL-CG-0129](#) for more details.

F.7 Comm. 2.4.14 qualification of new S-N curves based on fatigue test data

Effect of residual stresses

The residual stresses at weld toes of small scale test specimens are normally small as compared with that in actual full size structures due to different restraints during fabrication. Also if small scale test specimens are produced from cutting from larger structures a significant part of the residual stresses will likely be lost. This should be kept in mind when planning the testing and when assessing the test results in terms of an S-N curve.

A reduced residual stress in the test specimens may be compensated for by performing the testing at a high R-ratio. (By a high R-ratio is understood $R = \sigma_{\min}/\sigma_{\max}$ around 0.5 and low R –ratio in region 0 to 0.1.) As the maximum nominal stress is limited by the yield of the material it is easier to achieve a high R-ratio for the longer fatigue lives where a low stress range is expected than for the short fatigue lives. This may lead to testing at R-ratios that are not constant within one test series. This may be different from earlier practice, however, this is considered to be fully acceptable. Another approach that has been followed to derive design S-N curves for welded structures based on fatigue test data from small scale test specimens has been to force the curves through the centre of gravity of the test data with a predefined slope that is representative for crack growth in large scale structures with large residual stresses from fabrication. If testing is performed at a low R-ratio, IIW (/30/) recommend reducing the fatigue strength at 2 mill cycles by 20%.

Statistical assessment of fatigue test data

To plan fatigue testing that will provide a reliable basis for derivation of design S-N curves requires experience from fatigue assessment of structures and knowledge about statistics. Some guidance can be found in literature such as in /76/. However, engineering judgement is required in each case to specify type of test specimen, number of tests and loading to be used in the tests. Engineering judgement is also required for assessment of recommended slope in S-N curve to be used for fatigue assessment of real structures as compared with that derived from small scale test specimens due to difference in residual stresses at the hot spots. See also /86/ and /89/.

A design S-N curve should provide a 97.7% probability of survival where the mean curve is determined with 75% confidence. The design curve can be derived as the mean minus two standard deviations as obtained from a plot of experimental data assuming the data to follow a Gaussian distribution on a logarithmic scale for the number of cycles to failure (for a large number of test data). This will give an unbiased estimate of the design S-N curve, but this estimate will be uncertain when it is based on limited test data.

The statistical uncertainty in fatigue test data shall be accounted for when a limited number of tests is performed to establish design S-N curves. It is required that the design curve is estimated with at least 75% confidence. When a total of n observations of the number of cycles to failure N are available from n fatigue tests carried out at a number of representative stress ranges S, then the design S-N curve estimated with confidence can be expressed as:

$$\log \bar{a} = \log a - cs_{\log N} \quad (\text{F.7.1})$$

where:

$\log a$ = intercept of the mean value of the n test data with the log N axis

$S_{\log N}$ = the standard deviation of the n test data of $\log N$, and c is a factor whose value depends on number of fatigue test data and is shown in [Table F-3](#) and [Figure F-6](#) for the case where the standard deviation is known and also when it is unknown.

The values for the factor c given in [Table F-3](#) and [Figure F-6](#) are derived for independent variables. For an example of independent variables, consider the case that the slope of the S-N curve is kept constant when the regression analysis is performed, such that the regression is reduced to estimation of one parameter only, i.e. the cut-off with the $\log N$ axis, and $\log N$ can be considered independent. This is often the assumption for assessment of S-N curves for welded structures, such as assessments performed by IIW. For an example of dependent variables, consider the case that the regression is performed with estimation of two parameters, i.e. the slope of the S-N curve and the cut off with the $\log N$ axis, and $\log N$ is dependent on $\log S$.

When $\log N$ is considered a dependent variable, the values for the factor c given in [Table F-3](#) and [Figure F-6](#) are approximate only and should not be used for extrapolation outside of the interval for $\log S$ covered by the test data. For accurate values for the factor c for this case, both within the interval for $\log S$ covered by the test data and for extrapolation outside of this interval, the methodology described in /76/ for dependent variables may be used.

A derivation of a design S-N curve may follow different approaches. It may be useful to understand the difference between the following two approaches:

- pure statistical approach
- engineering approach.

By following a pure statistical approach a mean S-N curve and a standard deviation of test data can be derived. This corresponds to standard deviation being unknown when determining c values in [Table F-3](#) and [Figure F-6](#) to be used in equation (F.7.1). This requires a significant number of test specimens (as seen from the figure). This recommendation is sometimes used in small scale testing but can hardly be afforded when performing full scale type testing.

When doing a lot of testing that results in much the same values of standard deviations, one can assume the standard deviation as known. Thus the main challenge is to derive mean values. This gives reduced requirements for c values to be used in equation (F.7.1). This may also be seen as an engineering approach that one may consider to use in well-defined tests (instrumented full scale test specimens with strain gauges). For standard deviation from fatigue test data see [\[F.5\] Commentary](#). For complex connections a larger standard deviation can be expected. It should be checked that the fatigue test data look homogeneous and that the scatter is not larger than that normally observed in fatigue testing.

It should be added that a few large scale tests can add significant confidence to a design S-N curve dependent on type of structural detail to be designed. A prototype test specimen that is fabricated in a similar way as the actual connection is considered to represent a physical behaviour in a representative manner as it is similar in geometry, material characteristics, residual stress, and fabrication tolerances. In addition it can likely be subjected to a more relevant loading as compared with that of small scale test specimens. Thus, even if only one large scale test is performed, it is reasonable to put as much significance into that test result as can be substantiated by a total engineering judgement rather than a statistical assessment.

An engineering assessment may also take knowledge from performed analysis into account. This assessment may depend on how the analysis has been performed and on the safety inherent in the procedure that is used, see [\[5.4\]](#).

Table F-3 Number of standard deviations to be subtracted from the mean to derive a design S-N curve with 97.7% probability of survival

Number of tests	Standard deviation known		Standard deviation unknown	
	75% confidence	95% confidence	75% confidence	95% confidence
	2.39	2.95	3.78	9.24
3	2.30	2.74	2.95	5.01
10	2.21	2.52	2.53	3.45
15	2.17	2.42	2.40	3.07
20	2.15	2.37	2.33	2.88
30	2.12	2.30	2.25	2.65
50	2.10	2.23	2.19	2.48
100	2.07	2.16	2.12	2.32
∞	2.00	2.00	2.00	2.00

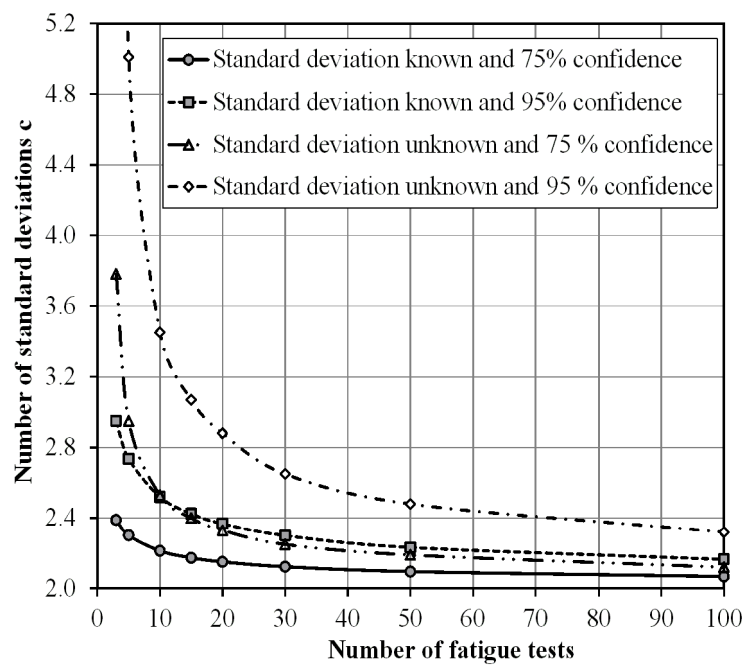


Figure F-6 Number of standard deviations to be subtracted from the mean to derive a design S-N curve with 97.7% probability of survival

Justifying the use of a given design curve from a new data set

This section presents a methodology to validate the use of a particular design S-N class on the basis of a limited number n of new fatigue tests. It is assumed that the design S-N curve is described on a form as presented in [2.4] and that the standard deviation in the S-N curve is known.

It is assumed that the fatigue testing is performed until a well-defined failure is achieved such as a fatigue crack through the connection (and not a run-out due to other failures such as leakage or loss of pretension in connectors).

Due to a limited number of new test data it is assumed that the slope of a mean S-N curve for the new data is the same as for the considered design S-N curve. Based on this assumption of a fixed m - value for the test data a mean value of $\log N$ and $\Delta\sigma$ can be established. A mean S-N curve based on the new test data can be established as:

$$\log N = \log a - m \log(\Delta\sigma SMF) + \frac{x_c}{\sqrt{n}} s_{\log N} \quad (\text{F.7.2})$$

where:

N = number of cycles (mean value of new test data at stress range $\Delta\sigma$)

$\log a$ = Intercept of considered mean standard S-N curve in this RP with the $\log N$ axis

m = slope of standard S-N curve

$\Delta\sigma$ = stress range

SMF = stress modification factor

n = number of test samples

x_c = confidence with respect to mean S-N data as derived from a normal distribution

xc = 0.674 for 75% confidence level and 1.645 for 95% confidence level.
A 75% confidence level is used in the following equations.

$s_{\log N}$ = standard deviation in the standard S-N curve.

From the equation above the SMF can be derived as:

$$SMF = 10^{(\log a - \log N - m \log \Delta\sigma + \frac{0.674}{\sqrt{n}} s_{\log N}) / m} \quad (\text{F.7.3})$$

and with n fatigue test data to derive mean S-N curve from these data:

$$SMF = 10^{(\log a - \frac{1}{n} \sum_{i=1}^n \log N_i - \frac{m}{n} \sum_{i=1}^n \log \Delta\sigma_i + \frac{0.674}{\sqrt{n}} s_{\log N}) / m} \quad (\text{F.7.4})$$

Then a revised design S-N curve can be derived as:

$$\log N = \log a - 2s_{\log N} - m \log(\Delta\sigma SMF) \quad (\text{F.7.5})$$

or

$$\log N = \log a - 2s_{\log N} - m \log SMF - m \log(\Delta\sigma)$$

Example of analysis case A:

Assume testing of connectors with test data as shown in [Table F-4](#). It is assumed that the test data follow a shape of the S-N curve similar to the high strength curve in [\[D.1\]](#) with $m = 4.7$. The test data are presented in [Figure F-7](#) together with the mean curve derived from the 6 test results and design S-N curve derived from the same test data. It is assumed that the testing is performed in the order as listed in [Table F-4](#) from S1 to S6. In principle one may assume the testing to be stopped after any number of the tests and perform an assessment of resulting SMF. This is done in this example in the following.

Stress modification factors (SMFs) derived from statistics using a student t distribution and considering standard deviation as unknown is shown in [Table F-4](#) and [Figure F-8](#). SMFs derived from equation (F.7.4) by considering the standard deviation as known is also shown in [Table F-4](#) and [Figure F-8](#). The present data set (from all 6 tests) shows a resulting standard deviation equal 0.160 in $\log N$. The standard deviation in the high strength S-N curve as presented in [\[D.1\]](#) is 0.162. This standard deviation is derived from testing of the base material only. Thus, if one considers uncertainty in actual fabrication, fabrication tolerances and make-up torque, it is likely that a larger standard deviation should be used. This may be assessed based on general fatigue test data of such connections, if available. (See also example case B below.)

Based on this example it is seen that a few tests may provide very useful information about the fatigue design procedure. Even only one test may give very useful information and estimate of SMF to be used for design. The recommended number of tests will in principle be somewhat dependent on the test results from the first tests that are performed. If one plot the test results in a graph like that shown in [Figure F-8](#) one can judge the convergence in derived SMF factor before one decide on further testing. In this example it is seen that a significant confidence in the estimated SMF is achieved after the first 3 tests.

It is observed from [Table F-4](#) that if the testing is stopped after the two first tests (S1+S2), a SMF equal 5.22 is derived. After three tests (S1+S2+S3) the SMF is changed to 5.10, which is not very far from the SMF derived after 6 tests in this example.

If one plan to perform only 2 tests it is recommended to select stress ranges such that failure of the first specimen is aimed at 100 000-500 000 cycles and the second at 1-10 mill cycles.

Tables for student t distributions can be found in statistical handbooks, Ang and Tang, [DNVGL-RP-C207](#) and also from spread sheets.

Table F-4 Example of test data and derivation of stress modification factor (St. dev 6 test data = 0.160)

	Stress Range [MPa]	Number of test cycles	SMF derived from student t distribution	SMF derived from assumed known and constant standard deviation (75% confidence)
S1	80	490 000		4.90
S2	36	8 900 000	22.20	5.28
S3	54	2 700 000	6.55	5.14
S4	47	3 100 000	5.70	5.21
S5	60	900 000	5.52	5.27
S6	40	11 000 000	5.31	5.20

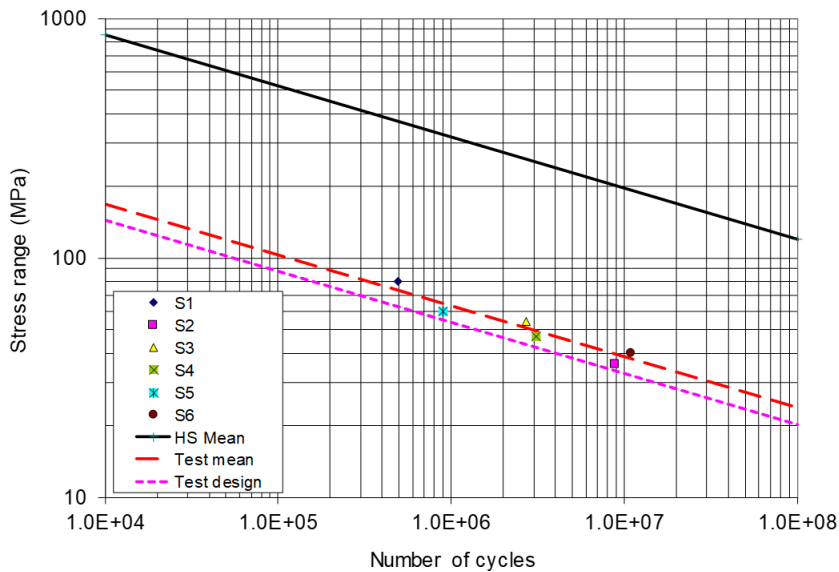


Figure F-7 Test data used for derivation of SMF in example (St. dev 6 test data = 0.160)

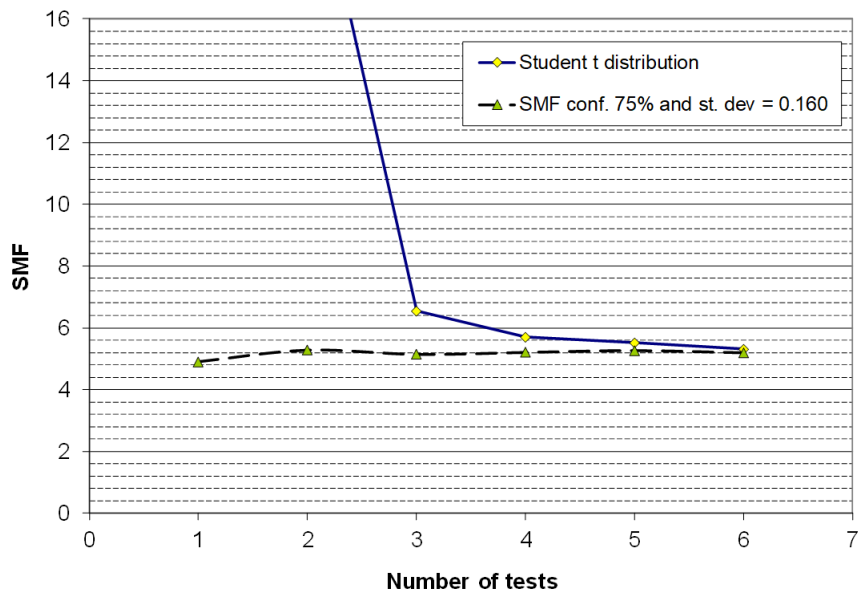


Figure F-8 SMF factor as function of number of test specimens (St. dev 6 test data = 0.160) (By one test is understood test S1 in Table F-4, by 2 tests is understood S1 and S2, etc.)

Example of analysis case B:

This example is made to check the robustness of the proposed analysis procedure. The test data from Table F-4 is modified in a fictitious manner such that the scatter is significantly increased by approximately doubling the standard deviation to 0.318 for the 6 test data. The mean S-N curve from the test data is kept

the same as in example case A. In addition the ordering of the test data is changed into a worst situation with the first tests furthest away from the basis high strength S-N curve, see also [Figure F-9](#) and [Figure F-7](#).

The SMF from the student t distribution includes the actual calculated standard deviation after 2, 3 tests etc. Test number 6 falls significantly outside the mean S-N curve which increases the standard deviation significantly. This explains the SMF based on student t after 6 tests as compared with 5 tests ([Figure F-5](#) and [Figure F-10](#)).

First it is assumed that the standard deviation in the new test data follow that of the high strength steel curve (with standard deviation equal 0.162 while the calculated standard deviation for the 6 test data is 0.318). The effect of assuming different confidence levels for this assumption is illustrated in [Figure F-10](#). The difference in calculated SMF is not that large for different confidence levels.

The resulting SMFs are also shown in [Figure F-5](#) and [Figure F-10](#) when the standard deviation in equation (F.7.4) is increased to 0.318 (for 75% confidence level). It is observed that this results in a higher SMF. This illustrates that one should try to use a relevant value of an expected (or conservative) standard deviation into equation (F.7.4).

From [Figure F-10](#) it is seen that the calculated SMF reduces with number of test data. This effect is likely augmented due to the sequence of the test data used in this fictitious example which is less likely to be similar to this example at least for more test data than 3 to 4.

From the example in [Figure F-10](#) one might get the impression that it is conservative with one test. However, the resulting decrease of SMF with number of tests is a result of sequence of the test data used. Another case could be to present the test data in a reversed order. This would result in the lowest calculated SMF for one test and a slightly increasing SMF with including additional number of tests as is shown in [Figure F-11](#).

Table F-5 Example of test data and derivation of stress modification factor (St. dev 6 test data = 0.318)

	Stress range [MPa]	Number of test cycles	SMF			
			Student t distribution	75% conf. and $s_{log N} = 0.162$	95% conf. and $s_{log N} = 0.162$	75% conf. and $s_{log N} = 0.318$
S1	35	9 000 000		6.03	6.51	7.39
S2	48	2 800 000	40.66	5.74	6.06	6.63
S3	48	3 200 000	7.93	5.58	5.84	6.28
S4	35	13 000 000	6.52	5.53	5.74	6.12
S5	63	1 600 000	5.90	5.34	5.53	5.85
S6	80	1 400 000	6.27	5.04	5.20	5.47

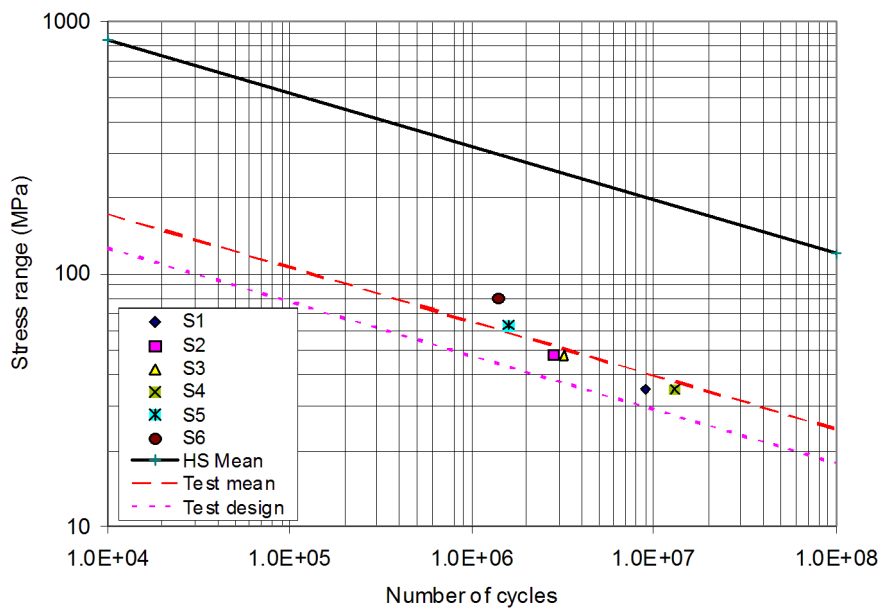


Figure F-9 Test data used for derivation of SMF in example (St. dev 6 test data = 0.318)

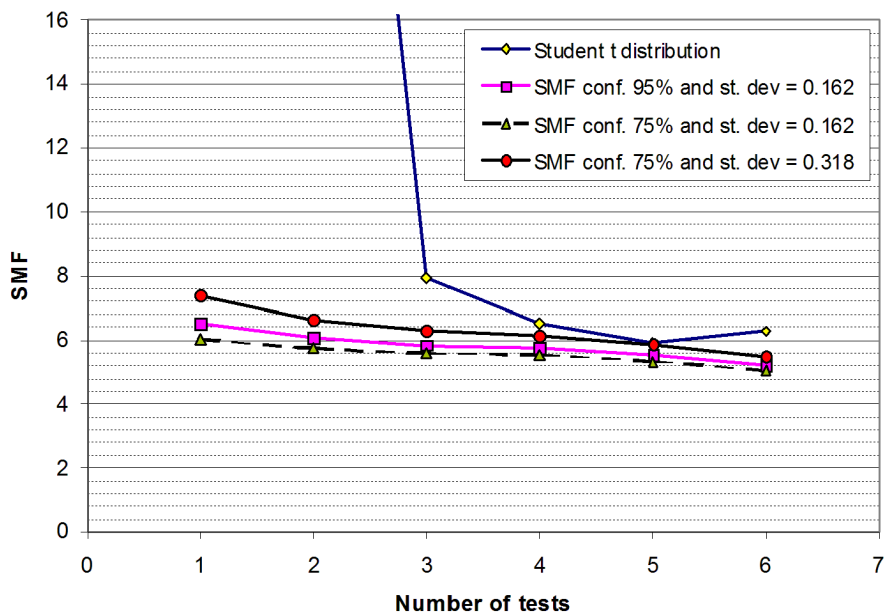


Figure F-10 SMF factor as function of confidence, standard deviation and number of test specimens for test data shown in Figure F-9

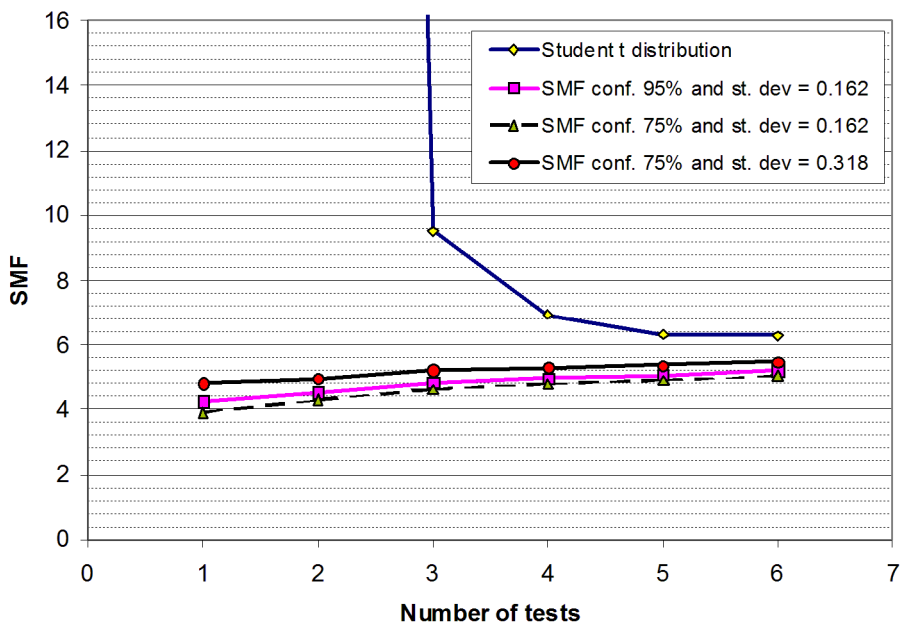


Figure F-11 SMF factor as function of confidence, standard deviation and number of test specimens with test data in reversed order as compared with Figure F-10

F.8 Comm. 2.10.3 fatigue analysis of pipes and cylindrical tanks subjected to cyclic internal pressure

The following sections can be used for fatigue assessment of pipes or cylindrical tanks used for transportation of gas subjected to low cycle fatigue from loading and unloading of content. The following sections give stress concentration factors for thickness transitions at girth welds and at ring stiffeners/supports. It also gives stress concentration factors for the longitudinal welds (or seam weld) due to out-of-roundness of pipes and cylindrical tanks. For very long welds the fatigue capacity is considered to be reduced due to a system effect. (The longer the weld is, the larger is the probability that there is a significant defect that can initiate a fatigue crack.) The fatigue capacity for long welds can be accounted for as described under System effects in [F.5].

Tapered thickness transitions

For tapered thickness transitions in pipes and cylinders as shown in Figure F-12 the bending stress over the wall thickness at the weld is mainly due to the axial stress in the pipe wall. This means that at thickness transitions the stress concentration factors presented in [3.3.7] can be used directly together with the nominal stress in the pipe wall for calculation of hot spot stress at the weld. Nominal stress in the pipe wall due to global bending moment can be calculated based on section modulus of the mid wall pipe section.

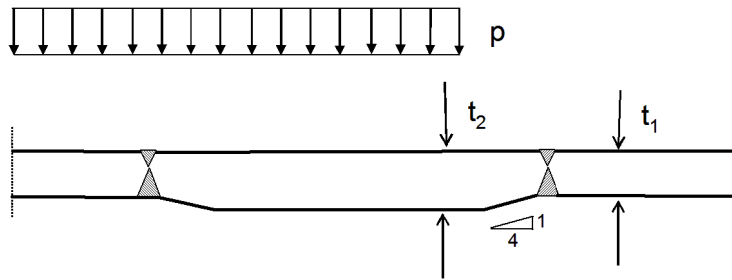


Figure F-12 Tapered thickness transition in pipe or cylinder

Thickness transitions with step in thickness

A transition with a step in thickness from t_1 to t_2 in a pipe or cylinder as shown in Figure F-13 is considered. It is assumed that the radius of the pipe or cylinder $r \gg t_1$. The stress due to the end cap pressure is calculated as:

$$\sigma_a = \frac{pr}{2t_1} \quad (\text{F.8.1})$$

The total stress at the inner side and the outer side is calculated as:

$$\sigma_t = \sigma_a \pm \sigma_b \quad (\text{F.8.2})$$

This equation can also be written as:

$$\sigma_t = \sigma_a \left(1 \pm \frac{\sigma_b}{\sigma_a} \right) = \sigma_a SCF \quad (\text{F.8.3})$$

where the stress concentration factor for the inner side is:

$$SCF = 1 + \frac{2-\nu}{\gamma} \sqrt{\frac{3}{1-\nu^2}} \left(1 - \frac{t_1}{t_2} \right) \quad (\text{F.8.4})$$

and the stress concentration factor for the outer side of the pipe is:

$$SCF = 1 - \frac{2-\nu}{\gamma} \sqrt{\frac{3}{1-\nu^2}} \left(1 - \frac{t_1}{t_2} \right) \quad (\text{F.8.5})$$

The γ is defined as:

$$\gamma = \frac{2(t_1^{2.5} + t_2^{2.5})}{t_2^{2.5} - t_2^{0.5} t_1^2} \left(1 + \left(\frac{t_1}{t_2} \right)^{1.5} \right) + \left(\frac{t_1}{t_2} \right)^2 - 1 \quad (\text{F.8.6})$$

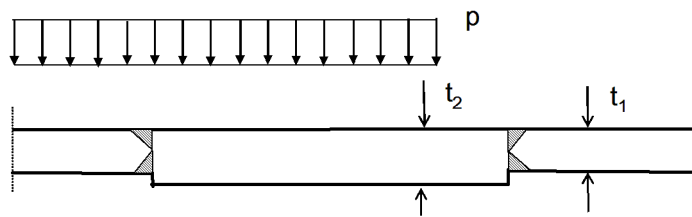


Figure F-13 Thickness transition in pipe or cylinder

Ring stiffeners at supports in storage tanks and at flange connections in risers

A ring stiffener in a cylinder as shown in [Figure F-14](#) is considered. This applies also to a bolted flange connection that is frequently used in risers for oil and gas production, see [Figure F-15](#) where the most critical hot spot is found at point B.

The stress concentration at a ring stiffener is obtained as:

$$SCF = 1 \pm \frac{\sqrt{3}(2-\nu)}{\sqrt{1-\nu^2}} \frac{1}{\beta} \quad (\text{F.8.7})$$

where the plus sign applies to the inner side and minus to the outer side. This stress concentration includes effect from internal pressure and end cap pressure. It shall be used together with the nominal stress acting in the axial direction of the pipe wall due to end cap pressure.

β is defined as:

$$\beta = 1 + \frac{2t\sqrt{rt}}{A_r \sqrt[4]{3(1-\nu^2)}} \quad (\text{F.8.8})$$

With $\nu = 0.3$ for steel the expression for β becomes:

$$\beta = 1 + \frac{1.56t\sqrt{rt}}{A_r} \quad (\text{F.8.9})$$

and the stress concentration factor for the inner side becomes:

$$SCF = 1 + \frac{3.087}{\beta} \quad (\text{F.8.10})$$

and the stress concentration factor for the outer side becomes:

$$SCF = 1 - \frac{3.087}{\beta} \quad (\text{F.8.11})$$

Due to the notch of the weld itself the fatigue strength of the weld at the ring stiffener itself becomes less than for the other shell side. As the stress is lesser on the outside than at the inside it is thus recommended to place ring stiffeners on the outside of a shell structure subjected to internal pressure. This is a different conclusion from that of ring stiffeners in tubular members subjected to pure external axial force, see /25/.

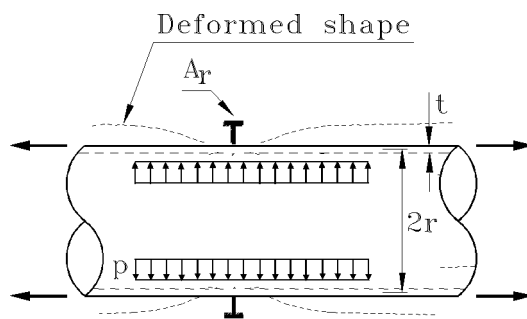


Figure F-14 Ring stiffener on cylinder with internal pressure

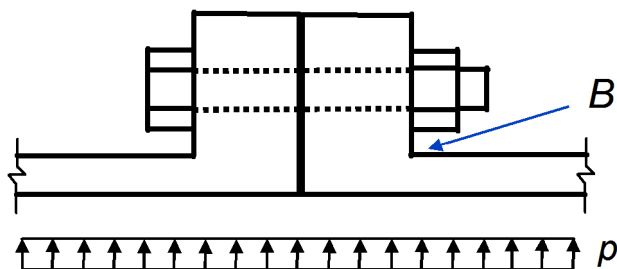


Figure F-15 Section through bolted flange connection

Longitudinal welds with bending stress over the pipe wall resulting from out-of-roundness of fabricated pipes
The out-of-roundness of fabricated pipe elements results in increased stress due to a bending moment over the wall thickness, see [Figure F-17](#). The eccentricity due to out-of-roundness is a function of tension in the hoop direction of the pipe. This eccentricity is reduced as the internal pressure is increased and the hoop tension is increased. Thus the bending stress over the wall thickness is a non-linear function of the internal pressure.

It is assumed that the out-of-roundness results in an eccentricity δ_0 without any hoop tension force from internal pressure.

In terms of out of roundness the equation for stress concentration factor can be derived as:

$$SCF = 1 + \frac{1.5\delta_{OOR}}{t\lambda l} \tanh(\lambda l) \quad (F.8.12)$$

where the out of roundness is defined as $\delta_{OOR} = d_{max} - d_{min}$, $l = \pi d/8$ and l which is a function of the membrane hoop stress σ_m is defined as follows:

$$\lambda = \sqrt{\frac{12\sigma_m}{Et^2}} \quad (F.8.13)$$

Tolerance requirements for pipelines are given in [DNVGL-ST-F101](#).

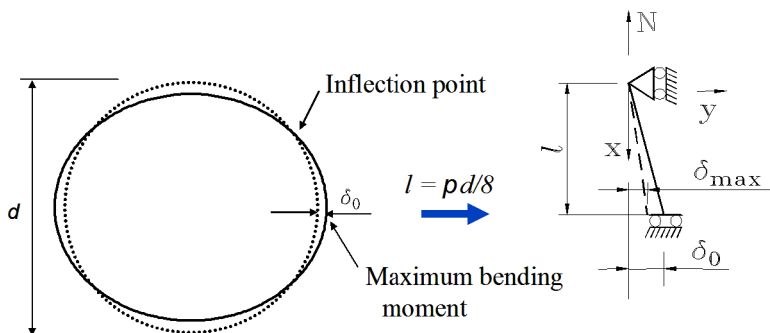


Figure F-16 Section through pipe showing out-of-roundness and analysis model

F.9 Comm. 3.3 stress concentration factors

See *An Analytical study of Stress Concentration Effects in Multibrace Joints under Combined Loading* /9/, for further background on this procedure of calculating a resulting hot spot stress from superposition of stress components. /2/ is the main reference for stress concentration factors for simple tubular joints. See also /85/ for analysis of T-joints.

The formula for SCF at a tubular butt weld can be outlined based on theory for thin walled structures, see /25/ and /85/.

F.10 Comm. 3.3.3 tubular joints welded from one side

F.10.1 General

The fatigue design of the root area of tubular joints welded from one side may be considered based on [3.3.3] as follows. Guidance on selection of S-N curve is provided in [\[F.10.2\]](#). The use of the F3 curve

requires a reliable non-destructive examination of the weld root. If this requirement is not met or larger defects than the basis for the S-N curve are detected during fabrication, it is recommended to use a reduced S-N curve that may be derived by fracture mechanics as shown in [F.10.5].

If a detailed finite element analysis of the actual tubular joint is made, [F.10.3] may be followed for fatigue life calculation of the weld root. Otherwise [F.10.4] may be used for fatigue life calculations of the weld root based on parametric equations for simple tubular joints from App.B.

F.10.2 Selection of S-N curve

Lack of penetration is hard to control by non-destructive examination and it is considered more difficult to detect possible defects at a root area of a tubular joint welded from one side than for a butt weld welded from one side. Lack of penetration in combination with other defects like lack of fusion may result in fatigue crack into the weld. This crack growth may occur in a direction normal to the main fluctuating stress in the brace as indicated on the inside weld root in Figure F-17.

The fatigue design of the root area of tubular joints welded from one side may be considered as follows:

Brace side:

- Girth welds welded from one side may be classified as F3 on the brace side. The defect size inherent in this curve is less than 1-2 mm. The F3 curve may also be considered the highest S-N curve to be used for potential defects in the weld root growing into the weld due to stress fluctuations in the brace if a reliable non-destructive examination of this region is performed.

Chord side:

- The size of potential defects that might grow into the chord on the weld root side is likely small and the weld to the brace may be considered like an attachment on a plate for the fluctuating stresses in the chord, i.e. that stress caused by chord action can be used. This means that the E-curve can be used for brace thickness less or equal 25 mm and the F-curve for brace thickness larger than 25 mm when the stress range in the chord root is used for fatigue analysis. If the methodology from [4.3.4] is used for hot spot stress calculation on the chord side, the E or F curve depending on the brace thickness can be used as hot spot S-N curve as explained in [4.3.5].
- The reference thickness associated with the listed S-N curves (E, F and F3) is $t_{ref} = 25$ mm.
- S-N curves in air may be used for the inside weld root where the braces are filled with air.

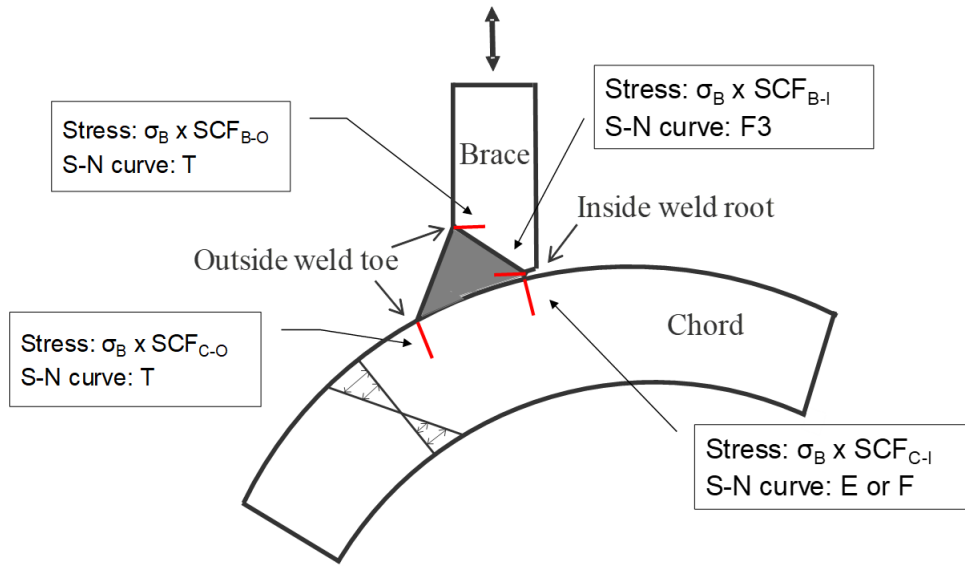


Figure F-17 Potential fatigue cracks, nominal stress and SCF in simple tubular joints

Potential fatigue cracks together with the proposed procedure for analysis of stresses and S-N curves to be used for fatigue assessment of the saddle at a tubular joint is shown in [Figure F-17](#). The same principle for fatigue assessment can also be used for the crown position with respect to action effect from the brace and by use of R for the weld root from [Table F-6](#) if parametric equations are used for the analysis. At the crown position there may also be stress due to chord action. If this stress contributes significantly to the total stress range, the nominal stress, σ_c , should be added to the resulting stress due to the brace action.

σ_B = nominal stress caused by brace action (resulting in stress in both chord and brace side of weld)

σ_C = nominal stress caused by chord action (resulting in stress in chord side of weld only)

SCF_{B-O} = stress concentration factor - brace side - outside (weld toe)

SCF_{C-O} = stress concentration factor - chord side - outside (weld toe)

SCF_{B-I} = stress concentration factor - brace side - inside (weld root)

$$SCF_{B-I} = SCF_{B-O} \cdot R \text{ (if parametric equations in [F.10.4] are used)}$$

SCF_{C-I} = stress concentration factor - chord side - inside (weld root)

$$SCF_{C-I} = SCF_{C-O} \cdot R \text{ (if parametric equations in [F.10.4] are used)}$$

$$SCF_{C-I} = 1.0 \text{ when hot spot analysis is used}$$

R = reduction factor from [Table F-6](#).

F.10.3 Fatigue assessment of the weld root based on detailed finite element analysis of simple tubular joints

If a detailed finite element analysis of a simple tubular joint is performed, the hot spot stresses representative for the brace side weld root and the chord side weld root may be based on extrapolation of stresses to the weld root as described in [4.3.4]. See [F.10.2] for selection of S-N curve.

F.10.4 Fatigue assessment of the weld root based on parametric equations for simple tubular joints

The following approach for fatigue life assessment of the weld root based on parametric equations may be performed.

- Normally the stress on the outside of the brace at the hot spot is larger than at the root area. Hence the stress on the inside of the brace or chord at the root may be used for fatigue assessment of the weld root. The methodology presented by Lee (1999) may be used if not documented otherwise by for example a detailed finite element analysis, see /99/.
- The stress at the root to be combined with an S-N curve from [F.10.2] may be determined based on the calculated stress concentration factors derived for the outside brace and chord side multiplied by a reduction factor R that is derived from Table F-6. Different stress concentration factors apply to the outside brace side and the outside chord side. Different S-N curves apply for crack growth into the weld using stresses in the brace and for crack growth into the chord as explained in [F.10.2]. Therefore, this procedure would be easier understandable if separate R values for the brace side and the chord side were developed and presented in the literature. However, only one set of R-factors is available for calculation of stress in the weld root relative to that of the outside weld toe. Due to different SCFs and different S-N curves one should still calculate fatigue lives both from the weld root into the weld on the brace side and into the chord separately even if the same R factor is used in both cases as assumed here.
- If the stresses on the outside hot spots are so large that weld improvement on the outside is needed, it is also necessary to check the inside weld root for the actual stress at the weld root. If the stress on the outside is a factor X larger than that can be accepted without weld improvement, it should be noted that the stress on the inside of the tubular joints is also larger by the same factor. Thus, another assessment of the weld root is required where the stress at the root is increased by the factor X for this new fatigue analysis. This shall be assessed before weld improvement of the outside can be recommended. If the stresses in the weld root is derived from a detailed finite element analysis, these stresses can be used directly for fatigue assessment (without any stress increase factor).

This procedure is applicable for simple tubular joints only.

F.10.5 Assessment of defects in the weld root larger than 1-2 mm

- Defect larger than that accounted for in the F3 curve may be evaluated by fracture mechanics calculations and the calculated value will depend on plate thickness. A long defect should be considered here with the defect size measured in the thickness direction of the tubular. A factor for reduction of fatigue life due to a possible large root defect in a tubular joint compared to a butt weld may be evaluated based on fracture mechanics analysis.
- The stress field at the root may be derived from a finite element analysis. The crack growth may be assumed to be normal to the direction of the maximum principal stress. The fatigue life is first calculated for an initial defect size corresponding to that of the F3 curve: $F(\text{Life } a_i = 1 \text{ mm})$. Then the fatigue life is calculated for an initial defect size corresponding to that of a tubular joint welded from one side: $F(\text{Life } a_i = \text{larger root defect})$. The fatigue life reduction factor, FR , is obtained from equation (F.10-1).
- A modified S-N curve below F3 is calculated from equation (F.10-2). An S-N curve corresponding to this log a value (or below) may now be used for fatigue life analysis based on nominal stress at the root as calculated by a detailed finite element analysis.

$$FR = \frac{F(Life \quad a_i = larger \ root \ defect)}{F(Life \quad a_i = 1 \ mm)} \quad (F.10.1)$$

$$\log a = 11.546 + \log(FR) \quad (F.10.2)$$

If other information about the reliability of the non-destructive testing is not available, a defect size into the weld root of magnitude 5 mm may be assumed. This corresponds approximately to a defect size inherent the W3 curve that might be used in such a situation.

Table F-6 Reduction factors for calculation of stress at root area of single sided welds in tubular joints

Type of joint	Load	Reduction factor	Validity range
K-joint	Axial	$R = 2.60 (0.203 + 1.66 \beta - 1.30 \beta^2)$ $(0.47 + 0.024 \gamma - 0.00054 \gamma^2)$ $\left(\frac{0.187 \tau}{(\tau^2 + 0.52^2)^2} + 0.39 \right) \left(1.64 - 0.005 \frac{0.0012}{\zeta} \right) \quad (F.10.3)$ $(0.808 + 1.053 \theta - 1.029 \theta^2)$	$0.2 \leq \beta \leq 0.9$ $10 \leq \gamma \leq 30$ $0.2 \leq \tau \leq 1.0$ $0.042 \leq \zeta \leq 0.175$ $30^\circ \leq \theta \leq 60^\circ$
	Balanced in-plane bending	$R = 3.04 \left(\frac{0.31 \beta}{(\beta^2 + 0.77^2)^2} + 0.37 \right)$ $\left(\frac{0.44 \tau}{(\tau^2 + 0.67^2)^2} + 0.13 \right) (1.97 - \zeta^{-0.13}) \quad (F.10.4)$ $(6.22 - 10.60 \theta + 5.034 \theta^2)$	
	Balanced out-of-plane bending	$R = 4.82 (1.04 - 1.17 \beta + 0.70 \beta^2) \gamma^{-0.175}$ $\left(\frac{0.28 \tau}{(\tau^2 + 0.57^2)^2} + 0.17 \right) (\zeta^{-0.017} - 0.45) (1.56 - 0.663 \theta) \quad (F.10.5)$	
T- and Y-joint	Axial	$R = 2.35 (-1.802 \beta^2 + 1.557 \beta + 0.318) (-0.556 \tau + 0.850) \quad (F.10.6)$ $(0.007 \gamma + 0.50) (-0.246 \theta^2 + 0.679 \theta + 0.540)$	$0.40 \leq \beta \leq 0.85$ $10 \leq \gamma \leq 30$ $0.35 \leq \tau \leq 0.85$ $30^\circ \leq \theta \leq 90^\circ$
	Balanced in-plane bending	$R = 2.55 (0.334 \beta + 0.419) (-0.648 \tau^2 + 0.252 \tau + 0.611) \quad (F.10.7)$ $(0.0002 \gamma^2 - 0.002 \gamma + 0.578) (2.314 \theta^2 - 5.536 \theta + 3.985)$	
	Balanced out-of-plane bending	$R = 2.4 (-1.051 \beta^2 + 0.856 \beta + 0.469) (-0.6 \tau + 0.856) \quad (F.10.8)$ $(-0.0002 \gamma^2 + 0.014 \gamma + 0.456) (0.117 \theta^2 - 0.454 \theta + 1.426)$	
X-joint	Axial	$R = 2.25 (-1.734 \beta^2 + 1.565 \beta + 0.326) \quad (F.10.9)$ $(2.687 \tau^3 - 5.117 \tau^2 + 2.496 \tau + 0.297)$ $(0.0065 \gamma + 0.53)$	$0.40 \leq \beta \leq 0.85$ $10 \leq \gamma \leq 30$ $0.35 \leq \tau \leq 0.85$

Type of joint	Load	Reduction factor	Validity range
	Balanced in-plane bending	$R = 2.5(0.25\beta + 0.548)(3.772\tau^3 - 7.478\tau^2 + 4.136\tau - 0.0730)$ (F.10.10) $(0.008\gamma + 0.472)$	
	Balanced out-of-plane bending	$R = 2.4(-1.188\beta^2 + 0.981\beta + 0.453)(3.414\tau^3 - 6.330\tau^2 + 3.101\tau + 0.194)$ (F.10.11) $(-0.0002\gamma^2 + 0.014\gamma + 0.460)$	

θ shall be given in radians. See also definition of notations in [App.B](#).

For joints with $\beta > 0.85$ the stress on the inside may be interpolated between the value for $\beta = 0.85$ and $\beta = 1.0$ where $R = 0.85$ may be assumed for $\beta = 1.0$.

The same R-factor may be used for unbalanced loading as for balanced loading.

F.11 Comm. 4.3.7 verification of analysis methodology for finite element hot spot stress analysis

Specimens for verification of analysis methodology are shown in [Figure F-18](#) to [Figure F-23](#). The leg lengths for fillet welds in [Figure F-18](#) to [Figure F-22](#) are 5 mm.

The hot spot stress analysis methodology may be verified based on analysis of these details with derived target hot spot stress.

Loading on the specimens for calculation of hot spot stress is shown in [Table F-7](#).

The target hot spot stresses for the specified load cases are listed in [Table F-8](#).

A correction factor to be applied to the analyses may be established if the calculated hot spot stress in general is different from the target hot spot stress. This correction factor is obtained as:

$$f = \frac{\sigma_{\text{Hot spot Target}}}{\sigma_{\text{Hot spot Calculated}}} \quad (\text{F.11.1})$$

Table F-7 Loading on the specimens

Specimen	Position of loading	Nominal stress
1	Stress in the axial direction over end area equal 0.667 MPa (= 900 mm ²)	1.00 MPa
2	Stress in the axial direction over end area equal 0.667 MPa (= 900 mm ²)	1.00 MPa
3	Stress in the axial direction over end area equal 0.700 MPa (= 1000 mm ²)	1.00 MPa

<i>Specimen</i>	<i>Position of loading</i>	<i>Nominal stress</i>
4	Point load 219 N above bracket in cantilever at a distance 625 mm from the support plate in test rig	Nominal stress at weld toe to be calculated as bending moment calculated in this section divided by the elastic section modulus in this section. The specified point load is made to provide a nominal stress at this position equal 1.00 MPa.
5	Point load 123 N above bracket in cantilever at a distance 435 mm from the support plate in test rig	
6	Stress in the axial direction of plate equal 1.00 MPa	1.00 MPa

Table F-8 Target hot spot stress values/stress concentrations linked to the D curve

<i>Specimen</i>	<i>Hot spot target values</i>
1	1.32
2	1.86 - 1.96
3	1.33
4	1.64 - 1.84
5	1.69
6	3.13

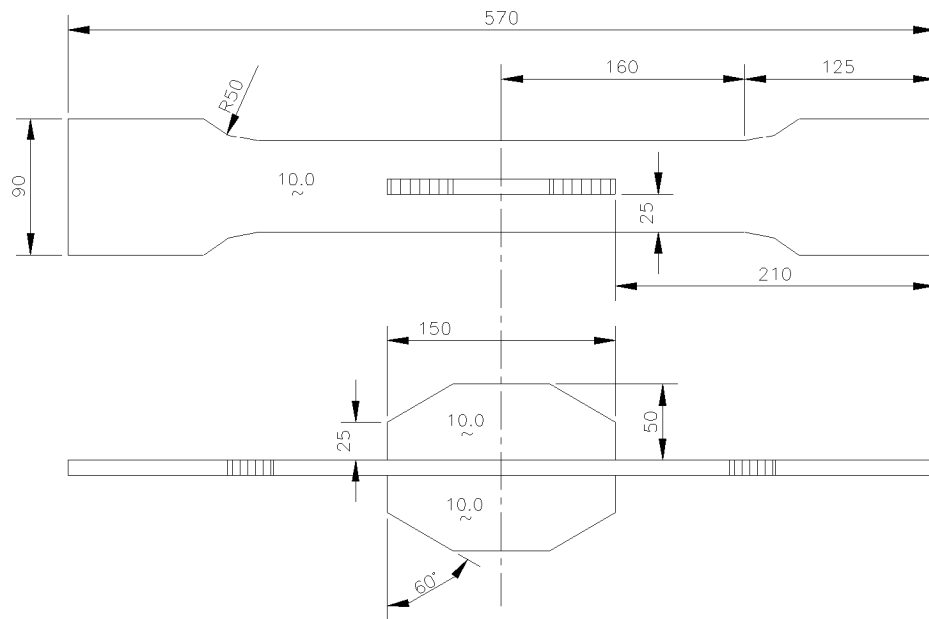


Figure F-18 Specimen 1

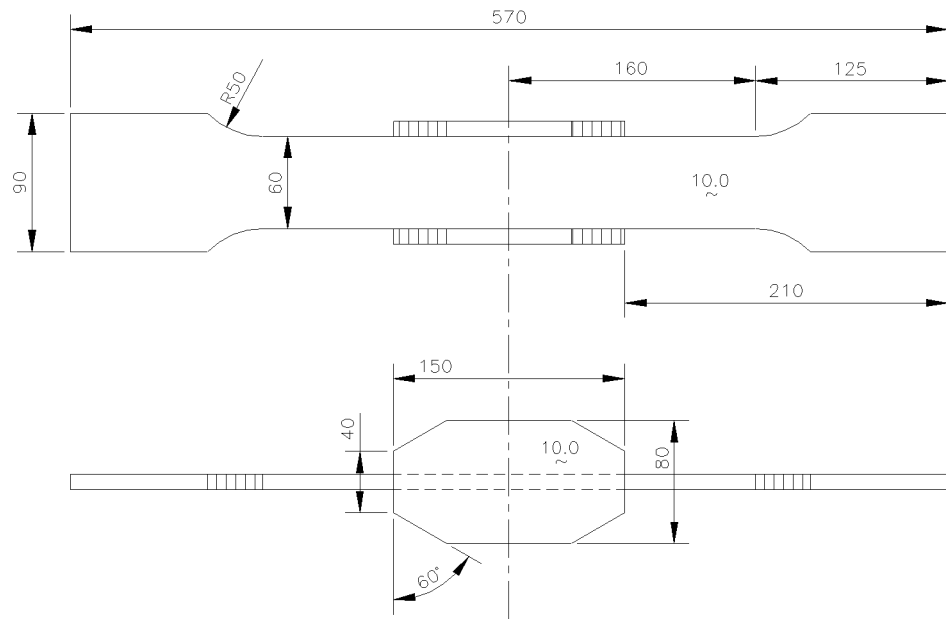


Figure F-19 Specimen 2

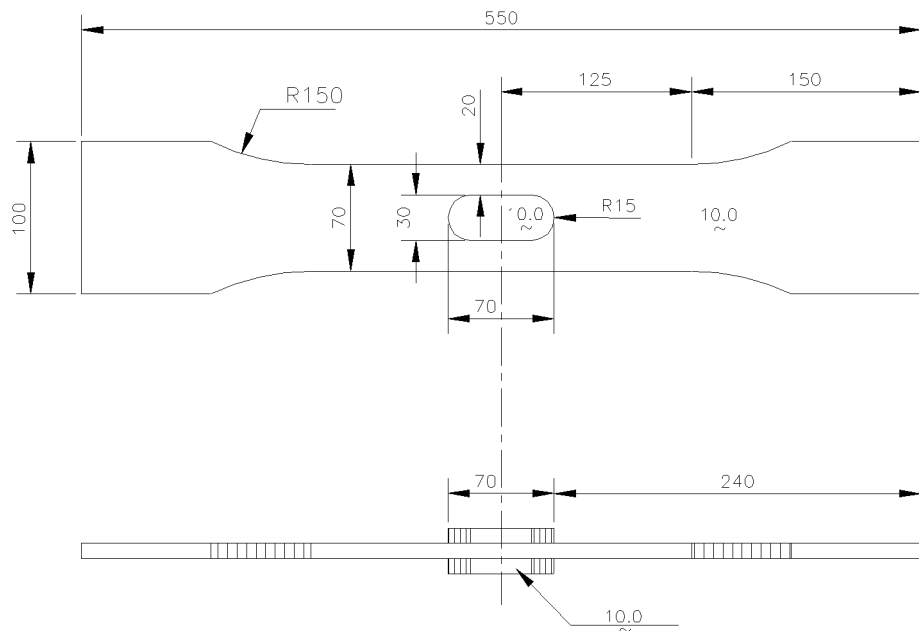
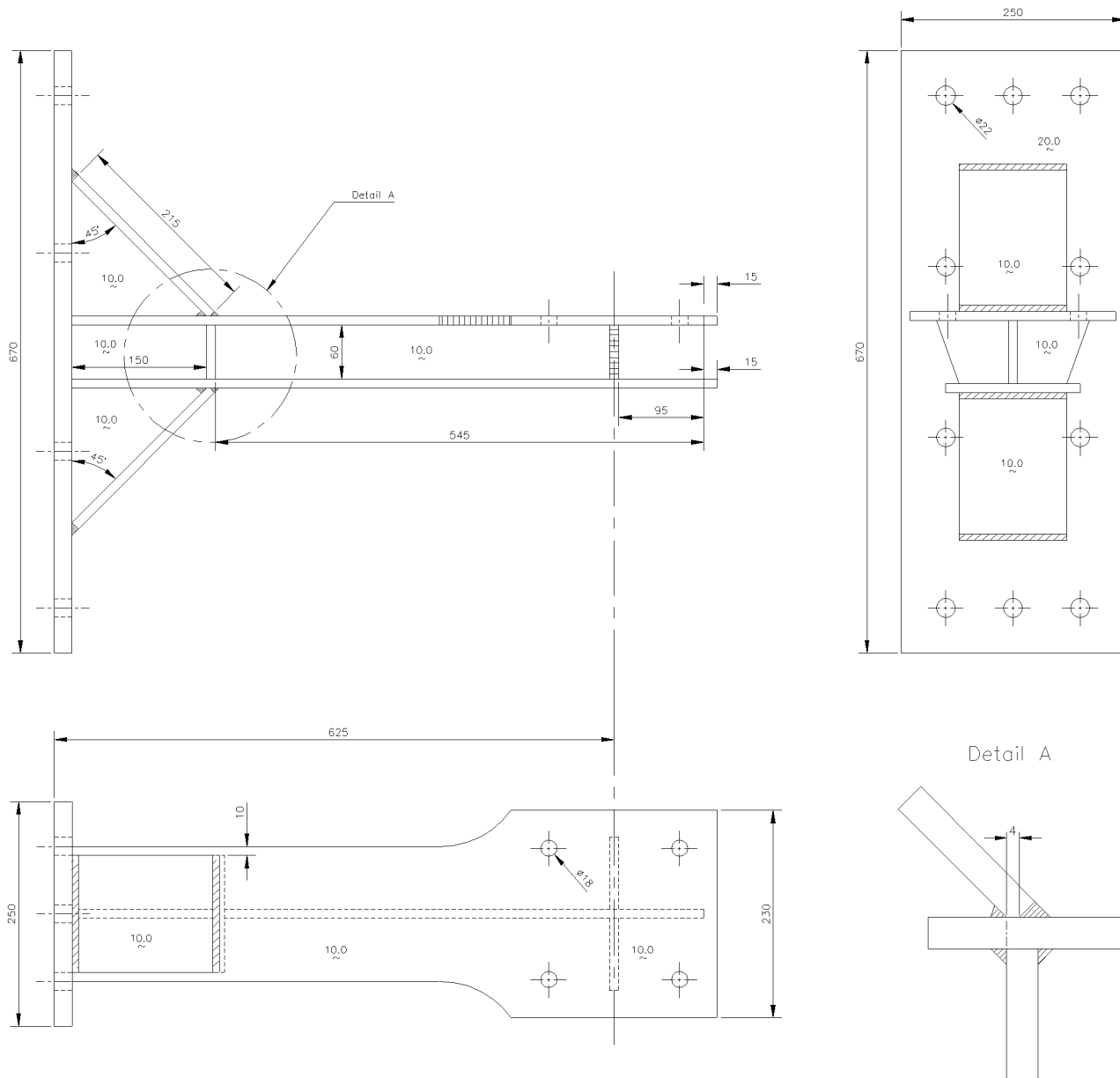


Figure F-20 Specimen 3

a)



b)

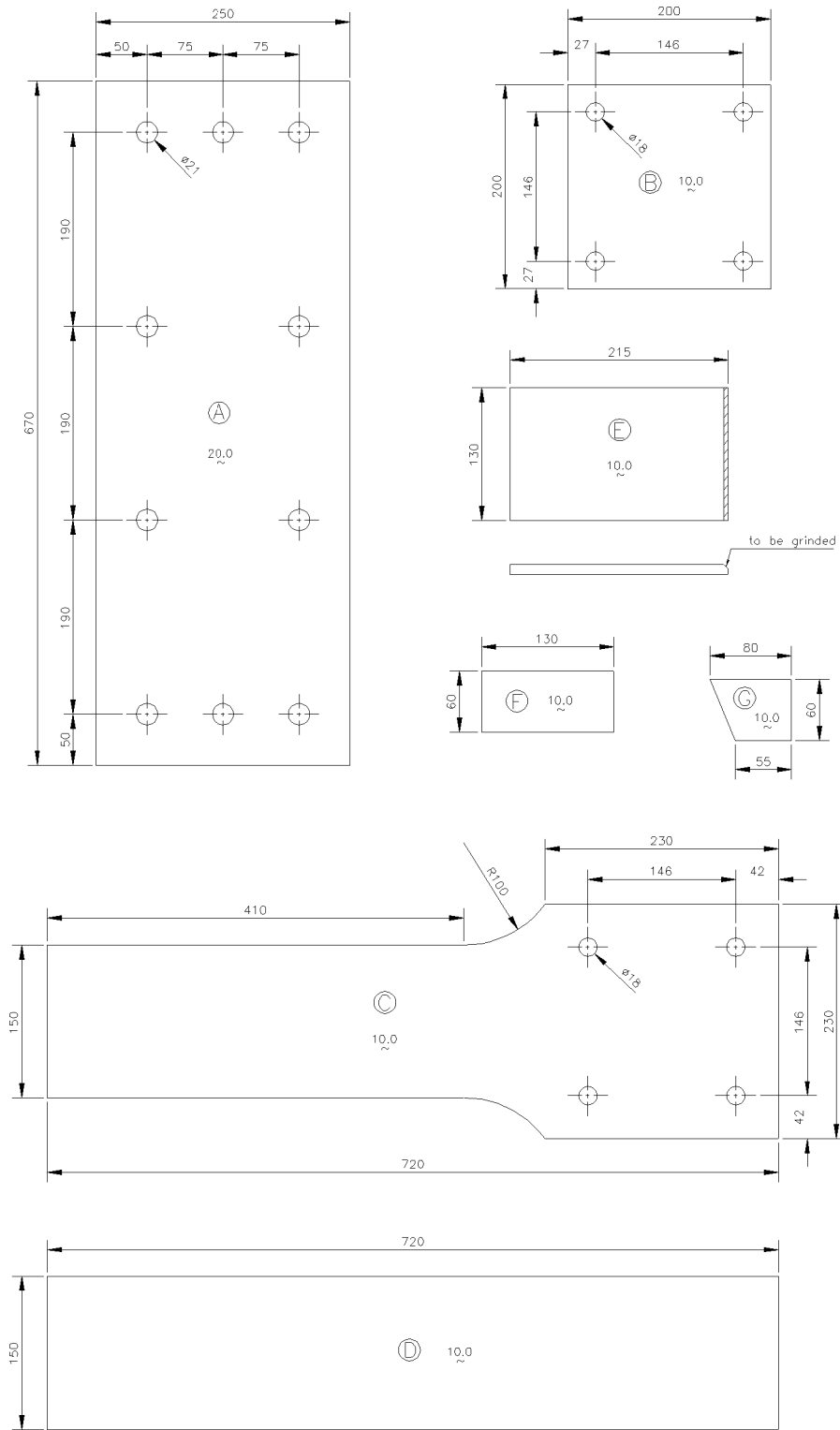


Figure F-21 Specimen 4

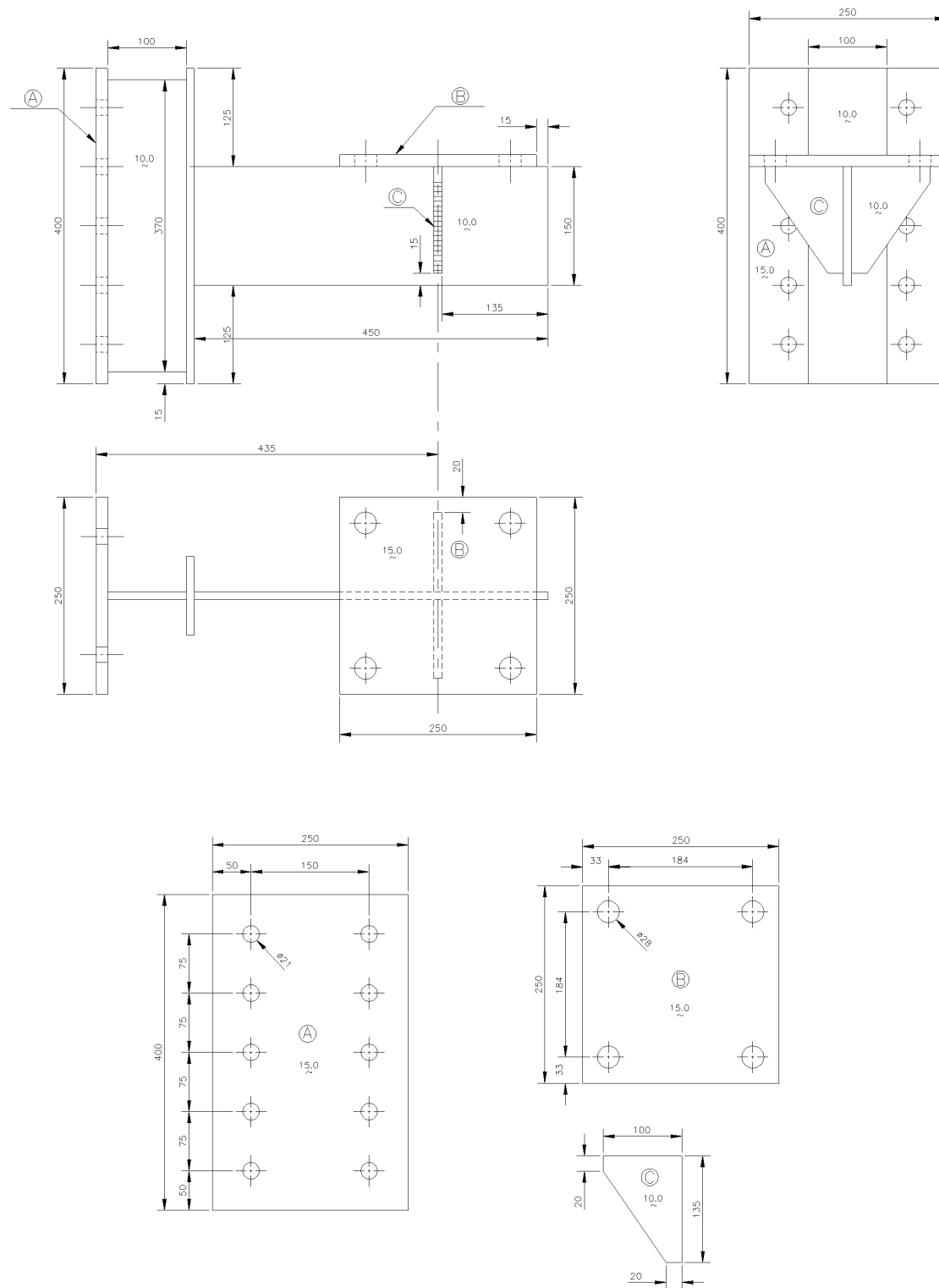


Figure F-22 Specimen 5

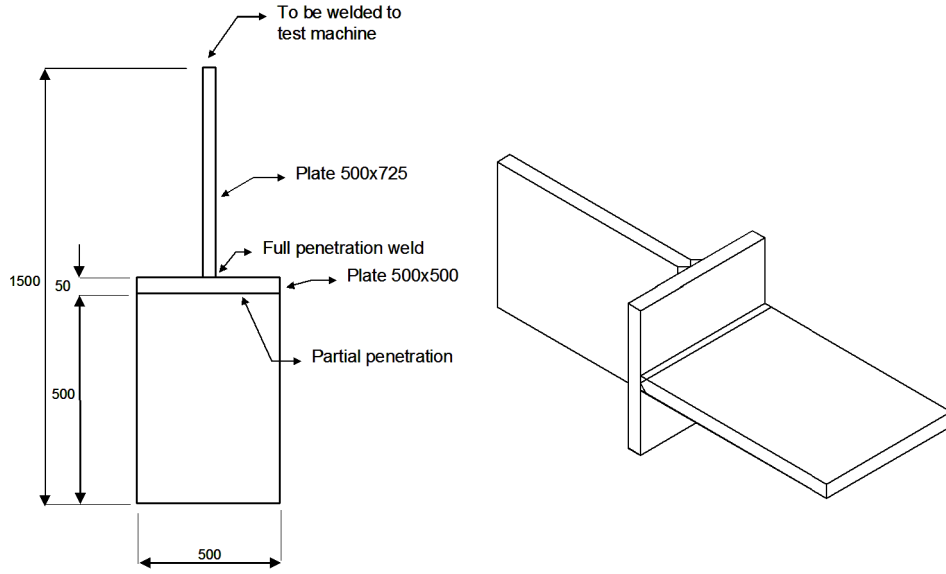


Figure F-23 Specimen 6 thickness all plates $t = 50$ mm.

Plate thickness to be used in analysis procedure

The main calibration of the procedure in [4.3.8] was performed on fatigue tested specimens with $t_1 = t_2 = 10$ mm. The readout position is made dependent on the plate thickness t_1 .

$$x_{shift} = \frac{t_1}{2} + x_{wt}$$

It may be questioned if the read out point should rather be made as a function of plate thickness t_2 .

The following considerations are made with respect to this question:

- It is assessed that it is the stress in plate 1 that is governing for the fatigue capacity at the weld toe on plate 1 side of Figure 4-10 at hot spot 1, and it is the stress in the vertical plate 2 that is governing for the fatigue capacity of the weld toe on the transition from the weld to the plate 2 at hot spot 2. Thus for finite element modeling of the hot spot regions and read out of hot spot stress it is the thickness t_1 that is governing for the stress at weld toe to plate 1 and it is the thickness t_2 that is governing for the stress at weld toe to plate 2.
- The stress distribution at a 45° hopper connection in Figure F-24 is shown in Figure F-25 without additional weld and in Figure F-26 with additional weld. The local bending stress in the plate 1 is the major contribution to increase in hot spot stress as compared with nominal membrane stress. The membrane stresses and the bending stresses are extrapolated back to the weld toe for illustration (extrapolation from stresses at $t_1/2$ and $3t_1/2$ to the weld toe is shown).
- The stress distribution at the hot spot 1 is not expected to change significantly even if the thickness t_2 is increased to a large value. However, one would shift the read out point to the right in the sketch of Figure 4-11 resulting in a corresponding reduced read out stress from the shell analysis model. Thus, this would provide a non-conservative hot spot stress. Based on this the thickness t_2 is not considered to be a relevant parameter governing the distance from the intersection line to the read out point of stress in the shell element analysis.

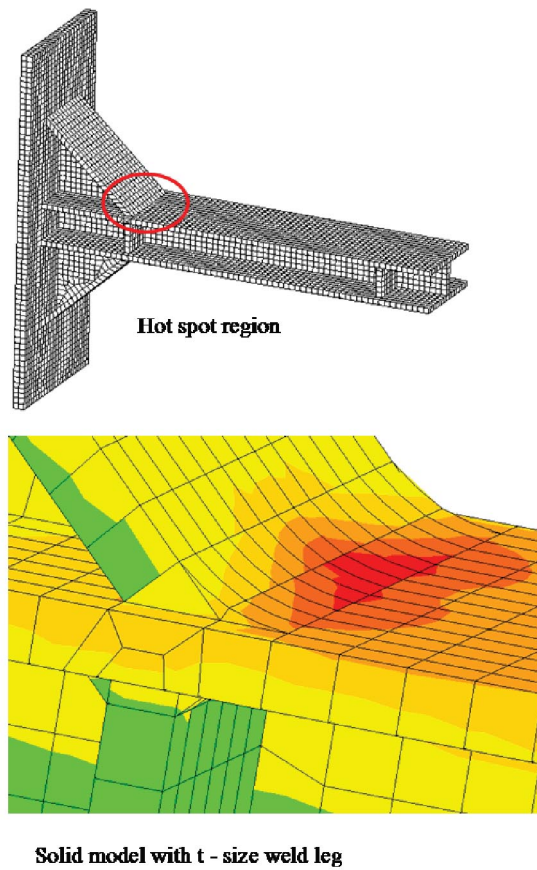


Figure F-24 Solid element model of tested specimen

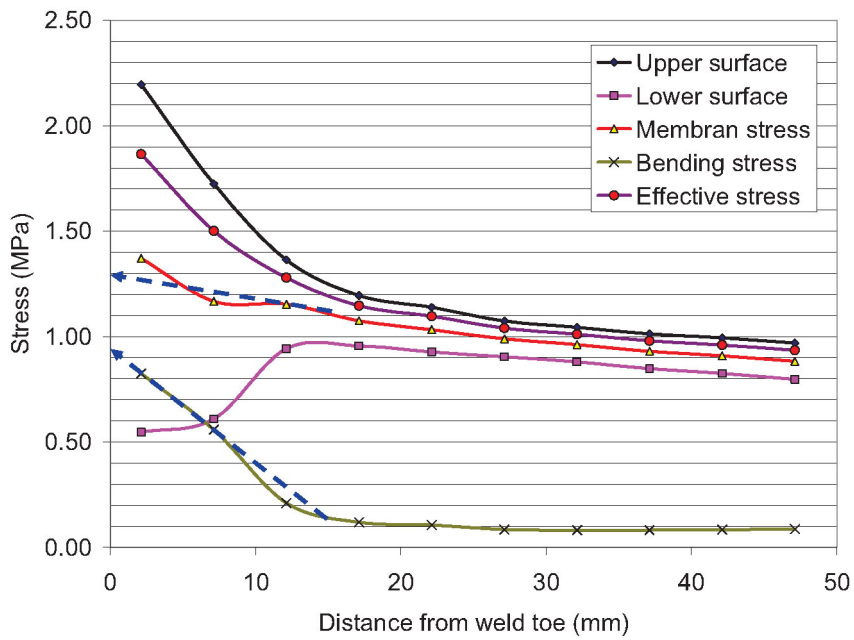


Figure F-25 Stress distribution in plate 1 without additional weld

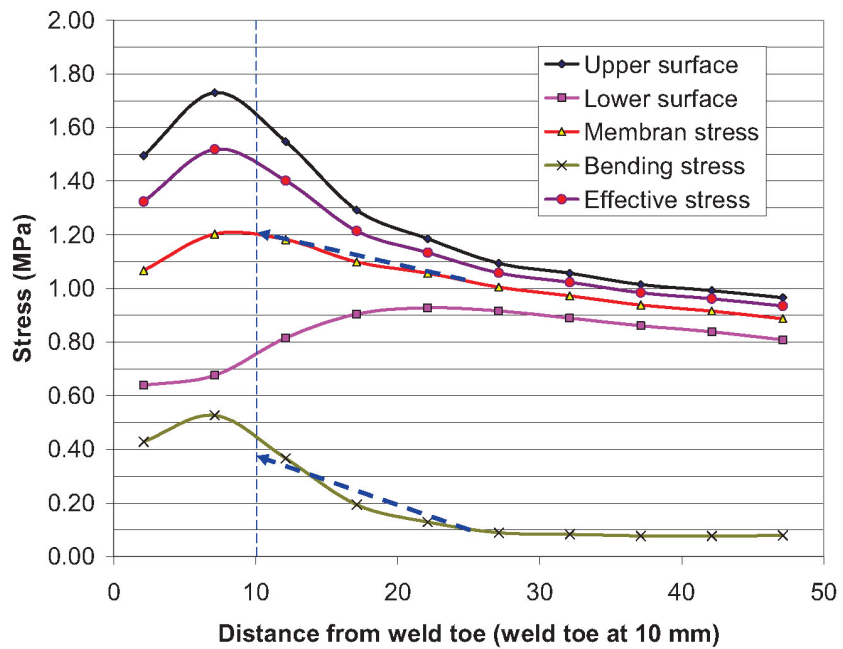


Figure F-26 Stress distribution in plate 1 with additional weld leg 10 mm

F.12 Comm. 4.3.4 Multidirectional fatigue analysis

The following example of a multidirectional fatigue analysis methodology is related to tubular joints, however, the same methodology may also be used for multidirectional fatigue analysis of details in plated structures. For plated structures both the method A and the method B in [4.3.4] may be used for read out of hot spot stresses. For tubular joints, [4.2] defines the read out of hot spot stresses.

For tubular joints, it is recommended in [2.3.4] that the range of the hot spot stress is defined by the extrapolated maximum principal stress in combination with the T-curve. As explained in [4.3] the principal stress need not always be perpendicular to the weld toe in tubular joints in all types of structures. Nor is this necessarily the case for plated structures in general.

As a further complication, the principal stress direction at a specific hot spot may vary with loading conditions. Here, assessing fatigue damage accumulation in only one specified stress direction would underestimate the total damage. On the other hand, combining the damage from multiple directions may prove excessive and overestimate the total damage. The latter as principal stress ranges having directions closer to perpendicular to the weld toe will give rise to a crack parallel with the weld toe, i.e. along the weld (see [Figure 2-3](#)) whereas principal stress ranges having directions closer to parallel with the weld toe will give rise to a crack that will be transverse to the weld toe, i.e. across the weld (see [Figure 2-4](#)). For these principal stress ranges more parallel with the weld toe a higher S-N curve may be assumed as explained in [F.4].

In these cases, with varying principal stress direction, fatigue is typically assessed based on several time simulations of the structural response to various loading conditions from which time series of stress are established and rainflow counted for stress ranges. Indeed, in the following it is implicitly assumed that all stresses vary with time, hence may exhibit a varying principal stress direction not only between time series but also within each individual time series. Further, it is assumed that all variations in loading, be it assumed direction, magnitude, stochastic seed, etc., are explicitly accounted for through an adequate number of simulations each resulting in a time series of the stress at the hot spot.

The proposed analysis methodology addresses the challenges of multidirectional fatigue presented above by evaluating two damages for each hot spot: one representing the damage due to stresses normal to the weld toe, D_{\perp} , and one due to the damage accumulation from stress ranges more parallel with the weld toe, D_{\parallel} .

For any given principal stress direction defined by the angle θ from the perpendicular to weld direction at any given hot spot, [Figure F-28](#), the stress in said direction $\sigma(\theta)$ may be analysed - one time series at a time - by rainflow counting of the directional stresses $\sigma(\theta)$ and using corresponding S-N curves to evaluate the unidirectional damage $D(\theta)$ where for $\theta \leq 30^\circ$ the T-curve can be assumed and the C2-curve can be assumed for $\theta > 30^\circ$. This is based on the guidance in [F.4]. For plated structures the D-curve can be assumed for $\theta \leq 30^\circ$.

The accumulated multidirectional damage may then be derived as the largest of the two calculated fatigue damages where all unidirectional damages $D(\theta)$ counted in the angle range $\pm 60^\circ$ relative to perpendicular to the weld direction is summed into the damage D_{\perp} and all unidirectional damages $D(\theta)$ counted outside the angle range $\pm 45^\circ$ is summed into the damage D_{\parallel} , i.e. as:

$$D = \max \begin{cases} D_{\perp} = \sum_{\text{timeseries}} D(\theta) \text{ for } -60^\circ \leq \theta \leq 60^\circ \\ D_{\parallel} = \sum_{\text{timeseries}} D(\theta) \text{ for } -45^\circ \leq \theta \leq 45^\circ \end{cases} \quad (\text{F.12.1})$$

It should be noted that there is an overlap zone between $\pm 45^\circ$ and $\pm 60^\circ$ in which the damage $D(\theta)$ is considered to contribute to both the damage D_{\perp} and the damage D_{\parallel} , see [Figure F-29](#).

The methodology assumes that the full stress tensor at the hot spot is adequately described by the relevant extrapolation method along the direction perpendicular to the weld, i.e. governed by the stress gradient in

said direction. Hence, the method may be used with any relevant hot spot extrapolation method or indeed directly on the notch stress, see [App.E](#).

Following the notation of [Figure F-28](#), this means that the three stress components σ_x , σ_y , and τ_{xy} of the plane stress tensor at the hot spot each are assumed described by the same extrapolation.

From the plane stress tensor at the hot spot, the direct stress in any direction defined by the angle θ relative to the x -direction (i.e. perpendicular to the weld) by transformation becomes:

$$\sigma(\theta) = \sigma_x \cos^2 \theta + \sigma_y \sin^2 \theta + 2\tau_{xy} \cos \theta \sin \theta \quad (\text{F.12.2})$$

Moreover, the first principal direction will be at an angle φ relative to the x -direction given by:

$$\tan 2\varphi = \frac{2\tau_{xy}}{\sigma_x - \sigma_y} \quad (\text{F.12.3})$$

with the other principal direction being perpendicular to this, i.e. at $\sigma(\varphi) + 90^\circ$.

Assuming then that the principal direction φ is constant for the entire duration of the time series assessed, the stress in the two possible principal directions can be calculated as $\sigma(\varphi)$ and $\sigma(\varphi + 90^\circ)$. Each of which can be counted using rainflow counting and combined with the relevant S-N curve for its direction, φ or $\varphi + 90^\circ$ respectively, and the cumulative fatigue damage $D(\sigma(\varphi))$ and $D(\sigma(\varphi + 90^\circ))$ for each principal stress direction can be calculated.

Analysing all the time series one by one this way, the total damage can be established for each time series and ultimately summed together using equation (F.12.1) to give the overall total damage. Notably addressing the multidirectional fatigue accumulation by summing damage for potentially different principal directions for two different crack possibilities.

As mentioned initially, the principal stress direction may vary not only between time series but also within each time series. Therefore, as the validity of the procedure necessitates that the principal stress direction is rather constant for each time series, it will in cases where a time series exhibits a significant variation in the principal stress direction be necessary to split such a series into sub-series such that each have a rather constant principal stress direction.

In practice, any time series of hot spot stress derived from dynamic response simulations will likely exhibit some small variation of the principal stress direction implying a likely need for subdivisions to formally comply with the above stated requirements. Recognizing that this, apart from being impractical, potentially will compromise the rainflow counting methodology, it is recommended that an allowable tolerance on the principal stress direction φ of, say $\pm 5^\circ$ is adopted and that only time series exhibiting variations greater than this, i.e. larger than 10° are split before being analysed individually. With this tolerance requirement assessed in a pre-processing of each time series, once sub-divided as needed, the per series average principal stress direction may be used in the assessment of the fatigue damage.

If the time series of hot spot stress exhibits a significant variation of the principal stress direction, the above described methodology is compromised and cannot be used to assess the damage from a non-proportional response. This because it can then no longer be assumed that the fatigue damage will be governed by the principal stress direction, why it is necessary to include the shear stress contribution to the damage accumulation. A sub-division of the time series into what then essentially is a series of proportional cases each at a unique average principal stress direction as described above is therefore not a viable methodology.

In these cases, a modified effective hot spot stress measure:

$$\Delta\sigma_{eff} = \gamma \sqrt{\Delta\sigma_\perp^2 + 0.81\Delta\tau_{||}^2} \quad (\text{F.12.4})$$

may be adapted in a critical plane approach to address the non-proportional response by taking the critical plane to be defined by an angle θ defined in [Figure F-28](#) and then substituting the normal to weld stress

range $\Delta\sigma_{\perp}$ with the direct stress range in the critical plane $\Delta\sigma_{\theta}$ and correspondingly the parallel shear stress range $\Delta\tau_{\parallel}$ by the shear stress range perpendicular to the critical plane $\Delta\tau_{\theta+90^\circ}$.

The factor γ may be taken equal to 1.0 for proportional loading. It is observed that shorter fatigue endurance is derived in fatigue testing under non-proportional loading than under proportional loading. This experience is also reflected in some fatigue design standards where stricter acceptance criteria are provided for non-proportional loading as compared to proportional loading, /30/ and /118/. The reduced endurance for non-proportional loading is considered to depend on type of material, the phase angle between the normal stress and the shear stress, and the relation between the shear stress and the normal stress. The reduced endurance under non-proportional loading is negligible if the principle stress direction is within $\pm 10^\circ$, or if the shear stress is less than 15% of the normal stress. Testing is proposed to derive more reliable data to provide an improved design guidance for relevant load conditions for these structures. At present it is recommended that the value of the γ factor to be used in design for non-proportional loading is assessed for the actual case based on the governing parameters listed above and available literature.

For any given time series of hot spot stress, assuming the variation in direct stress σ_{θ} to be the master and the perpendicular shear stress $\tau_{\theta+90^\circ}$ to be slave hereof, once a half cycle direct stress range $\Delta\sigma_{\theta}$ is identified in the master time series, a corresponding shear stress range $\Delta\tau_{\theta+90^\circ}$ can be identified in the slave series as illustrated in [Figure F-27](#).

Alternative to identifying the slave shear stress range $\Delta\tau_{\theta+90^\circ}$ corresponding to each master direct stress range $\Delta\sigma_{\theta}$ the overall maximum shear range $\Delta\tau_{\theta+90^\circ} = \max(\Delta\tau_{\theta+90^\circ}) - \min(\Delta\tau_{\theta+90^\circ})$ may be used as a constant shear stress range to be added to each counted direct stress range.

The critical plane direction is then obtained by conducting the above for all possible directions θ which the direction yielding the largest damage $D_{\sigma\varphi}$ is then derived as the critical plane direction φ .

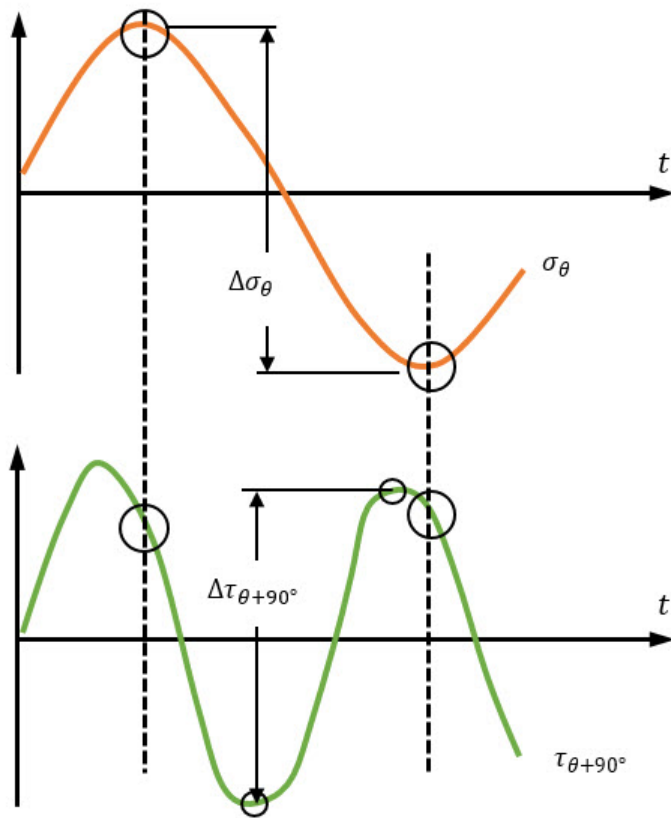


Figure F-27 Illustration of master direct stress range and slave shear stress range

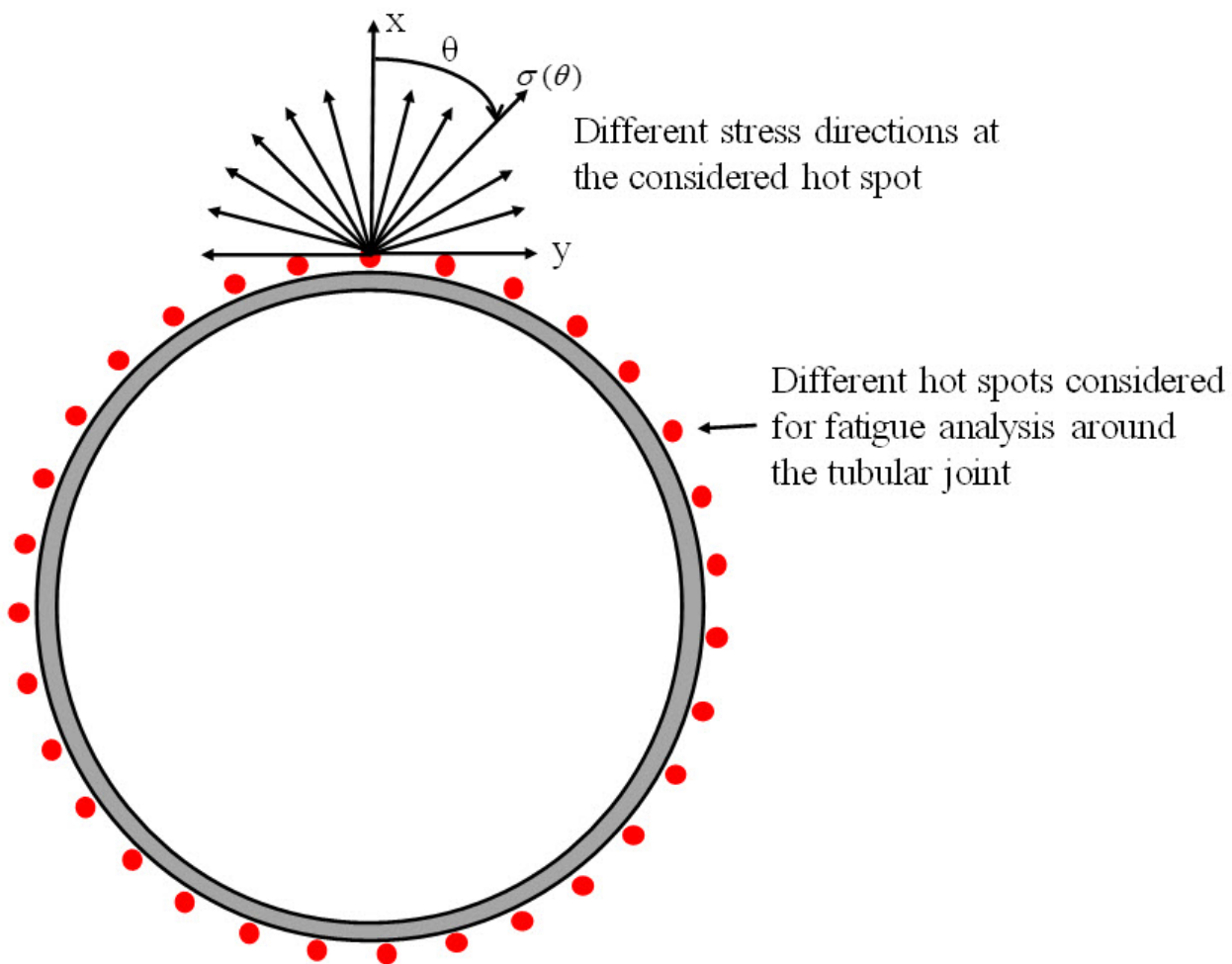


Figure F-28 Stress direction and different hot spots at tubular joints

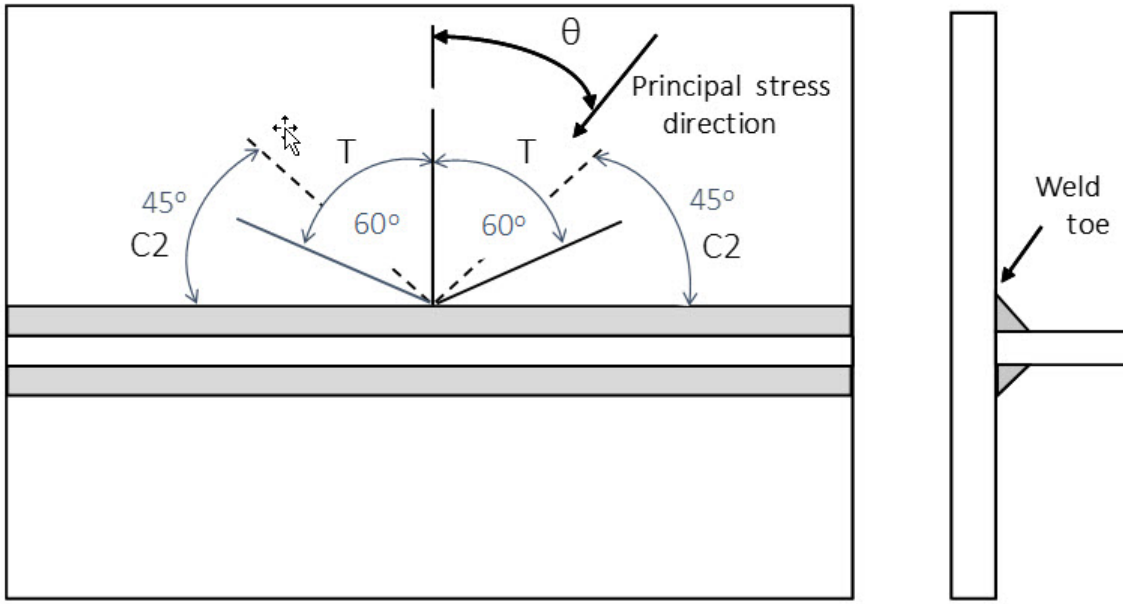


Figure F-29 Illustration of sectors to be analysed for crack along the weld toe and transverse to the weld

F.13 Comm. 5 simplified fatigue analysis

Weibull distributed stress range and bi-linear S-N curves

When a bi-linear or two-slope S-N curve is used, the fatigue damage expression is given by:

$$D = v_0 T_d \left[\frac{q^{m_1}}{\bar{a}_1} \Gamma \left(1 + \frac{m_1}{h}; \left(\frac{S_1}{q} \right)^h \right) + \frac{q^{m_2}}{\bar{a}_2} \gamma \left(1 + \frac{m_2}{h}; \left(\frac{S_1}{q} \right)^h \right) \right] \leq \eta \quad (\text{F.13.1})$$

where:

S_1 = stress range for which change of slope of S-N curve occur

\bar{a}_1, m_1 = S-N fatigue parameters for $N < 10^7$ cycles (air condition)

\bar{a}_2, m_2 = S-N fatigue parameters for $N > 10^7$ cycles (air condition)

$\gamma(\)$ = incomplete gamma function, to be found in standard tables

$\Gamma(\)$ = complementary incomplete gamma function, to be found in standard tables.

For definitions and symbols see also [1.5], [1.6] and [5.1].

Alternatively the damage may be calculated by a direct integration of damage below each part of the bilinear S-N curves:

$$D = \int_0^{S_1} \frac{v_0 T_d f(S, \Delta\sigma_0, h)}{N_2(S)} dS + \int_{S_1}^{\Delta\sigma_0} \frac{v_0 T_d f(S, \Delta\sigma_0, h)}{N_1(S)} dS \quad (F.13.2)$$

where the density Weibull function is given by:

$$f(S, \Delta\sigma_0, h) = h \frac{S^{h-1}}{q(\Delta\sigma_0, h)^h} \exp\left(-\left(\frac{S}{q(\Delta\sigma_0, h)}\right)^h\right) \quad (F.13.3)$$

$$q(\Delta\sigma_0, h) = \frac{\Delta\sigma_0}{(\ln(n_0))^{1/h}} \quad (F.13.4)$$

S-N curves for air condition are assumed here such that the crossing point of S-N curves is here at 10^7 cycles. However, this can easily be changed to that of seawater with cathodic protection where the crossing point is at 10^6 cycles, see [2.4.5]. The stress range corresponding to this number of cycles in air is:

$$S_1 = \left(\frac{\bar{a}_1}{10^7}\right)^{\frac{1}{m_1}} \quad (F.13.5)$$

The left part of S-N curve is described by notation 1, while the right part is described by notation 2.

Short term Rayleigh distribution and linear S-N curve

When the long term stress range distribution is defined through a Rayleigh distribution within each short term period for the different loading conditions, and a one-slope S-N curve is used, the fatigue criterion reads:

$$D = \frac{v_0 T_d}{\bar{a}} \Gamma\left(1 + \frac{m}{2}\right) \cdot \sum_{i=1, j=1}^{\text{all seastates all headings}} r_{ij} (2\sqrt{2m_{0ij}})^m \leq \eta \quad (F.13.6)$$

where:

- r_{ij} = the relative number of stress cycles in short-term condition i, j
- v_0 = long-term average zero-up-crossing-frequency (Hz)
- m_{0ij} = zero spectral moment of stress response process.

The gamma function, $\Gamma(1+\frac{m}{2})$ is equal to 1.33 for $m = 3.0$.

Short term Rayleigh distribution and bi linear S-N curve

When a bi-linear or two-slope S-N curve is applied, the fatigue damage expression is given as,

$$D = v_0 T_d \sum_{i=1, j=1}^{\text{all seastates}} r_{ij} \left[\frac{(2\sqrt{2m_{0ij}})^{m_1}}{\bar{a}_1} \Gamma\left(1 + \frac{m_1}{2}; \left(\frac{S_1}{2\sqrt{2m_{0ij}}}\right)^2\right) + \frac{(2\sqrt{2m_{0ij}})^{m_2}}{\bar{a}_2} \gamma\left(1 + \frac{m_2}{2}; \left(\frac{S_1}{2\sqrt{2m_{0ij}}}\right)^2\right) \right] \quad (\text{F.13.7})$$

Example fatigue analysis of a drum

A drum used for transportation of equipment is assessed with respect to fatigue. See [Figure F-30](#). The maximum allowable tension force in the wire on the drum shall be determined. There are three different spaces for wire on the drum, separated by external ring stiffeners 200 · 20 mm. The ring stiffeners are welded to the drum by double sided fillet welds. A high bending stress in the drum occurs when the wire is at the centre of the drum. Then the reaction force at each support becomes equal $P/2$ and the maximum bending moment at the highest stressed ring stiffener is $Pa/2$. When the drum is rotated 180 degrees the bending moment at the same position is reversed and the range in bending moment is derived as:

$$\Delta M = Pa \quad (\text{F.13.8})$$

The section modulus for the drum is calculated as:

$$W = \frac{\pi}{32} (D^4 - (D - 2t)^4) \frac{1}{D} \quad (\text{F.13.9})$$

where D = diameter = 600 mm and t = thickness = 20 mm. Then $W = 5114 \cdot 10^3 \text{ mm}^3$.

For the outside of the drum a stress concentration factor is calculated from [\[3.3.8\]](#):

$$\alpha = 1 + \frac{1.56t\sqrt{rt}}{A_r} = 1 + \frac{1.56 \cdot 20\sqrt{300 \cdot 20}}{200 \cdot 20} = 1.60 \quad (\text{F.13.10})$$

$$SCF = 1 + \frac{0.54}{\alpha} = 1 + \frac{0.54}{1.60} = 1.34 \quad (\text{F.13.11})$$

The nominal stress at the outside of the drum at the considered ring stiffener is obtained as:

$$\Delta\sigma = \frac{\Delta M}{W} SCF \cong \frac{Pa}{W} SCF \quad (\text{F.13.12})$$

The distance from the drum support to the considered ring stiffener $a = 1200$ mm.

A design fatigue factor of 2 is specified: DFF = 2.

The number of rotations of the drum is not specified and is considered to be uncertain. Therefore a stress range below the constant amplitude fatigue limit is aimed for. The detail classification is found from Table A-7 detail 8: the classification is E.

Then the allowable stress range is obtained from Table 2-1 for an E -detail and from [2.12] as:

$$\Delta\sigma_{allowable t=25mm} = \frac{\Delta\sigma \text{ at } 10^7 \text{ cycles}}{DFF^{1/3.0}} = \frac{46.78}{2^{1/3.0}} = 37.13 \text{ MPa} \quad (\text{F.13.13})$$

Then the maximum tension force is derived as:

$$P = \frac{\Delta\sigma_{allowable} W}{a SCF} = \frac{37.13 \cdot 5114 \cdot 10^3}{1200 \cdot 1.34} = 118.1 \text{ kN} \quad (\text{F.13.14})$$

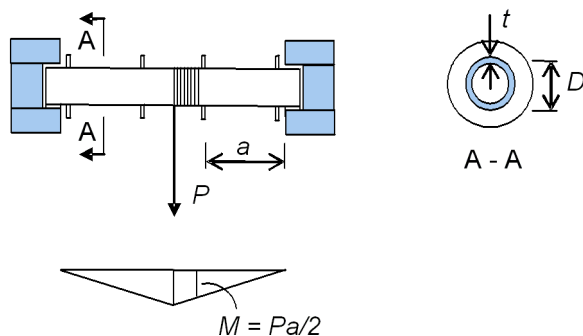


Figure F-30 Drum for transportation

F.14 Comm. 2.10.1 stresses at girth welds in pipes and S-N data

When pipes are subjected to a global bending moment only, the stress on the inside is lower than that of the stress on the outside as shown in Figure F-31. For a pipe with diameter 772 mm and thickness 36 mm the ratio between the stress on the inside and the outside is 0.91.

It should be noted that the local bending stress due to thickness transition and fabrication tolerances is due to the membrane stress over the thickness. This stress is denoted σ_{gm} in Figure F-31 and this stress shall be used together with equation (2.10.6) for derivation of local bending stress.

The resulting stress at welded connections may be calculated as a sum of the stress from global bending and that from local bending on inside and outside as relevant.

The local bending moment at a distance x from a weld with an eccentricity may be calculated based on shell theory as:

$$M(x) = M_0 e^{-\xi} \cos \xi \quad F.14.1$$

where the eccentricity moment M_0 is derived from as:

$$M_0 = \frac{\delta_m}{2} \sigma_a t \quad F.14.2$$

where:

δ_m = shift in neutral axis due to change in thickness and fabrication tolerance

σ_a = membrane axial stress in the tubular

t = thickness of pipe.

A reduced co-ordinate is defined as:

$$\xi = \frac{x}{l_e} \quad F.14.3$$

where the elastic length is calculated as:

$$l_e = \frac{\sqrt{r t}}{\sqrt[4]{3(1-\nu^2)}} \quad F.14.4$$

where:

r = radius to mid surface of the pipe

t = thickness of the pipe

ν = Poisson's ratio.

The results from this analytical approach are compared with results from axisymmetric finite element analysis in [Figure F-32](#).

The presented equations may be used to design connections with built in eccentricity to decrease the stress at the root that has a lower S-N curve than at the weld cap (toe). This will, however, increases the stress at the weld toe and may require weld improvement at the weld toe. The principal of purpose made eccentricity can be used in special situations where a long fatigue life is required, see /80/.

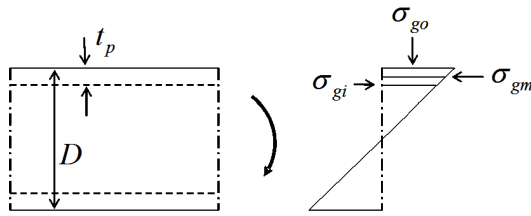


Figure F-31 Stress in pipe due to global bending moment

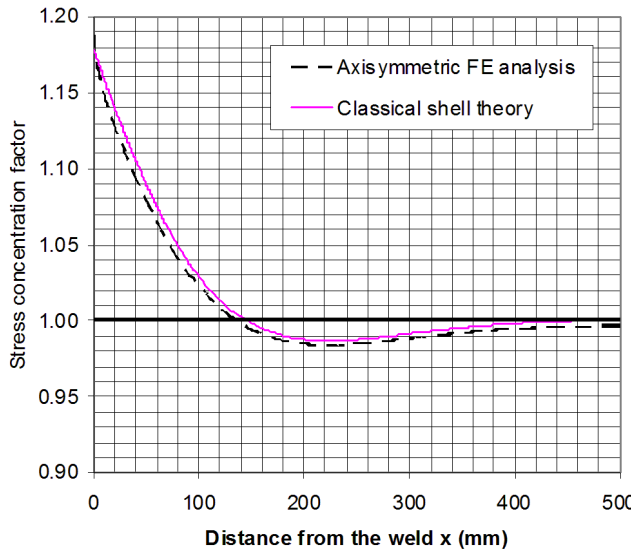


Figure F-32 Stress concentration as function of distance from weld

With reference to [Figure F-31](#) the stress on the outside is calculated as:

$$\sigma_{\text{outside}} = (\text{SCF}_{\text{outside}} - 1)\sigma_{\text{gm}} + \sigma_{\text{go}} \quad (\text{F14.5})$$

where $\text{SCF}_{\text{outside}}$ is stress concentration factor for calculation of stress for the outside and the other parameters are defined in [Figure F-31](#).

The stress on the inside is calculated as:

$$\sigma_{\text{inside}} = (\text{SCF}_{\text{inside}} - 1)\sigma_{\text{gm}} + \sigma_{\text{gi}} \quad (\text{F14.6})$$

where $\text{SCF}_{\text{inside}}$ is stress concentration factor for the inside and the other parameters are defined in [Figure F-31](#). $\text{SCF}_{\text{inside}}$ for pipelines is presented in [\[2.10.1\]](#) and for tubulars in [\[3.3.7\]](#).

F.15 Comm. 7. improvement of fatigue life by fabrication

See *Recommendations on Post weld Improvement of Steel And Aluminium Structures*, /16/, for effect of weld improvements on fatigue life. See also *API Provisions for SCF, S-N, and Size-Profile Effects*, /22/, for effect of weld profiling on thickness effect. See *Fatigue of Welded Joints Peened Underwater*, /13/, for fatigue of welded joints peened underwater.

An alternative to the improvement factors in [Table 7-1](#) is to use S-N curves with a more correct slope that represents the improved details. An example of such S-N curves is shown in [Figure F-33](#).

Characteristic S-N curves for improved details can be found in [Table F-9](#) for air environment and [Table F-10](#) for seawater with cathodic protection. S-N curve to be selected is linked to the S-N classification of details shown in [App.A](#).

The S-N curves for improvement are in line with the recommendations from IIW for increased stress ranges at $2 \cdot 10^6$ cycles (increase in stress range by a factor 1.3 for grinding and a factor 1.5 for hammer peening). The resulting improvement may likely be found to be larger when using these S-N curves than using factors from [Table 7-1](#) as the main contribution to fatigue damage is accumulated to the right of $2 \cdot 10^6$ cycles in the high cycle range of the S-N curve.

It should be noted that S-N curves above that of D should be used with caution for welded connections where fatigue cracks can initiate from internal defects. In general the selection of appropriate S-N curve depends on NDE method used and acceptance criteria. This needs to be assessed when improvement methods are used and corresponding S-N curves are selected.

Where grit blasting of the surfaces is performed after improvement, it is recommended to increase the stress range by factor ψ as explained in [\[7.3\]](#) before the S-N curve is entered for calculation of number of cycles to failure.

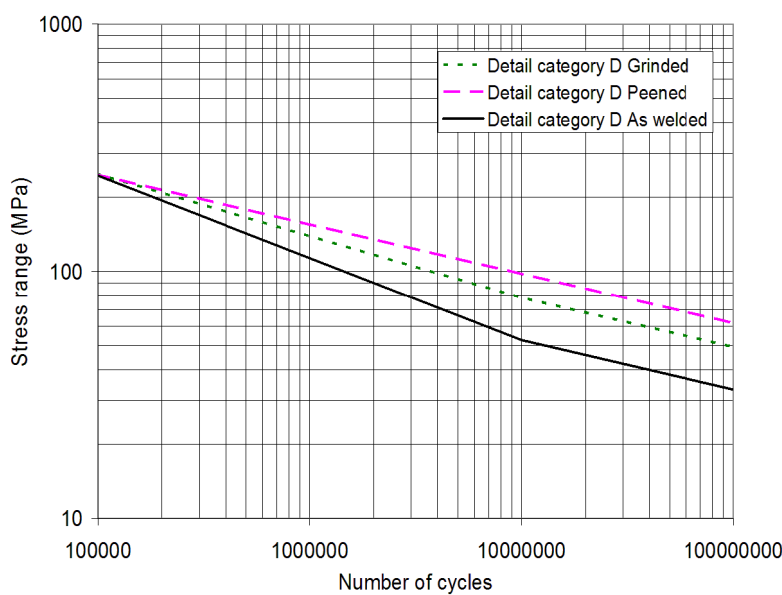


Figure F-33 Example of S-N curves (D-curve) for a butt weld in as welded condition and improved by grinding or hammer peening

Table F-9 S-N curves for improved details by grinding or hammer peening in air environment

S-N curve	Improvement by grinding			Improvement by hammer peening
	$N \leq 10^7$ cycles $m_1 = 3.5$	$N > 10^7$ cycles $m_2 = 5.0$	Thickness exponent	For all N $m = 5.0$
	$\log \bar{a}_1$	$\log \bar{a}_2$	k	$\log \bar{a}$
D	13.540	16.343	0.15	16.953
E	13.360	16.086	0.15	16.696
F	13.179	15.828	0.20	16.438
F1	12.997	15.568	0.20	16.178
F3	12.819	15.313	0.20	15.923
G	12.646	15.066	0.20	15.676
W1	12.486	14.838	0.20	15.448
W2	12.307	14.581	0.20	15.191
W3	12.147	14.353	0.20	14.963
T	13.909	16.869	0.20	17.480

Table F-10 S-N curves for improved details by grinding or hammer peening in seawater with cathodic protection

S-N curve	Improvement by grinding		Improvement by hammer peening
	$N \leq 10^6$ cycles $m_1 = 3.5$	$N > 10^6$ cycles $m_2 = 5.0$	For all N $m = 5.0$
	$\log \bar{a}_1$	$\log \bar{a}_2$	$\log \bar{a}$
D	13.142	16.203	16.555
E	12.962	15.946	16.298
F	12.781	15.687	16.040
F1	12.599	15.427	15.780
F3	12.421	15.173	15.525
G	12.248	14.926	15.278
W1	12.088	14.697	15.050
W2	11.909	14.442	14.793
W3	11.749	14.213	14.565

F.16 Comm. 3.3.12 joints with gusset plates

An example related to gusset joints and cruciform joints is considered in Figure F-34. This example is included in order to illustrate the complexity of fatigue design at such connections.

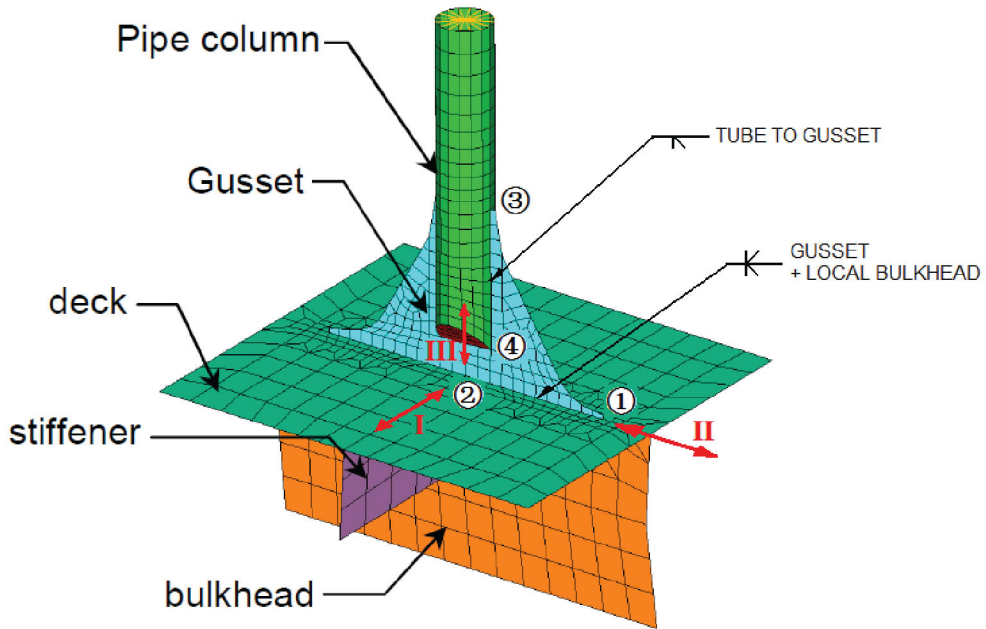


Figure F-34 Gusset and cruciform joint

A gusset connection to a structural deck in which one may have cyclic varying stresses in the 3 directions (I, II, III) as shown in Figure F-34 is considered. Full penetration welds between the gusset and the deck are assumed, in the local region under the deck, and in the tube which is slotted over the gusset which has been profiled for 'favourable' geometry. One may expect to find stress peaks at the points indicated as ①, ②, ③ and ④. Now it is assumed in this example that fabrication misalignments between the gusset and the underlying bulkhead have not been modelled, but have been defined by way of a tolerance, say 15% of the gusset plate thickness. Furthermore it is assumed that stresses are extracted from plate/shell elements by method B in [4.3.4].

Considering stresses in the deck plate for direction I, [4.3.5] with Table A-7 (8) leads to the use of the E-curve or the F-curve depending on the thickness of the gusset plate (even if a fillet weld for the gusset is used). This would apply all along the gusset and applies to stresses at the top and bottom surface of the elements in the deck plate adjacent to the weld. Stresses are not factored by 1.12.

Considering stresses in the deck plate for direction II, [4.3.5] leads to the use of the D-curve when extrapolation of stresses to the plane of the gusset plate is performed and further extrapolation of stresses to the hot spot are made as shown in [4.3]. This principally applies at point ①. However, typically with method B one will extract stresses at the centre of the elements located on either side of the axis of the gusset toe. Then extrapolation of stresses to the gusset plane should be performed at 0.5t before this stress is multiplied by 1.12 for calculation of hot spot stress.

Considering stresses in the gusset (and in the bulkhead below), a peak stress may be found at point 2 because of the presence of the stiffener for stress direction III. Here, the hot spot stress method can be used together with S-N curve D (due to the presence of the stiffener below the deck plate). For a region some distance away from the stiffener and stress direction III, [4.3.5] with Table A-8 (1) leads to the use of the F-curve (without the 1.12 factor) if it is assumed that the deck plate is thicker than 25 mm. This approach should be used for all gusset surface stresses extracted from the bottom row of gusset plate elements. In order to have a better understanding of this, a simple shell element model could be visualized in which the

transverse deck plating does not attract additional stress, due to the lack of transverse stiffness, as explained in [4.3.5].

If the fabrication eccentricity has not been modelled, it is not necessary to apply an additional correction factor to either the deck or the gusset/bulkhead stresses provided the defined tolerance is less than δ_0 , 0.15 t_i from [3.1.3].

Considering stresses extracted from the tubular column one may expect a concentration at point ③. From the root of the single-sided weld one can use the stresses extracted from the inner surface of tube elements adjacent to the gusset and one should use the F3 curve (without the 1.12 factor) (due to the weld root). For stresses extracted from the external surface of the tube elements one should use the D-curve (as hot spot stress S-N curve).

One may also find a concentration of stress in the gusset at point ④, where the welding is usually quite complex due to the presence of a cover plate. Interpreting [3.3.12], one should also use the F3 curve applied to the gusset plate surface stresses in this area (without the 1.12 factor), and one should use W3 to assess cracks through the weld from the root (based on stresses calculated in the weld).

An example of stress concentration factors for gusset plate joints analysed in a project is shown in Table F-11.

Table F-11 Stress concentration factors for joints with gusset plate

Geometry	SCF
RHS 250 x16 with favourable geometry of gusset plate	2.9
RHS 250 x16 with simple shape of gusset plate	3.8
Ø250 x16 with favourable geometry of gusset plate	2.3
Ø250 x16 with simple shape of gusset plate	3.0

F.17 Comm. 3.3.9 stress concentration factors for conical transitions

The following analysis procedure for calculation of stress concentration factor for conical connections are slightly more accurate than that presented in [3.3.9] especially for a cone thickness different from that of the tubular.

The stress concentration factor for nominal stress in the tubular is derived as:

$$SCF_t = 1 + \frac{6\zeta l_{et}}{t_t} \quad (\text{F.17.1})$$

where:

$$\zeta = \frac{\psi\lambda(2\kappa + 2) - \kappa\epsilon\operatorname{tg}\alpha}{(2\kappa + 2)(\eta\psi - \epsilon)} \quad (\text{F.17.2})$$

and:

$$\begin{aligned}
 \eta &= \frac{1}{2} - \frac{l_{ec}\cos(\alpha)}{2\kappa l_{et}} \\
 \epsilon &= \frac{l_{ec}\cos(\alpha)}{2\kappa l_{et}} + \frac{l_{et}(\sin(\alpha)\tan(\alpha) + \cos(\alpha))}{\square} - \frac{\nu r k_{st}}{E t_c l^2 e t l_{ec}} \sin(\alpha) \\
 \lambda &= \frac{\tan(\alpha)}{2} + \frac{\nu r k_{st}}{E l_{et}^3} \left(\frac{1}{t_t} - \frac{1}{t_c} \right) \\
 \psi &= \frac{(\sin(\alpha)\tan(\alpha) + \cos(\alpha))\kappa l_{et} - l_{ec}}{(2\kappa + 2)l_{ec}} \\
 \kappa &= \frac{l_{et} k_{sc}}{l_{ec} k_{st}} \\
 k_{st} &= \frac{E t_t^3}{12(1 - \nu^2)} \\
 k_{sc} &= \frac{E t_c^3}{12(1 - \nu^2)} \\
 l_{et} &= \frac{\sqrt{r t_t}}{\sqrt[4]{3(1 - \nu^2)}} \\
 l_{ec} &= \frac{\sqrt{r t_c}}{\sqrt[4]{3(1 - \nu^2)}}
 \end{aligned} \tag{F.17.3}$$

where:

- k_{st} = shell stiffness of tubular
- k_{sc} = shell stiffness cone
- E = Young's modulus
- ν = Poisson's ratio
- t_t = thickness of the tubular
- t_c = thickness of the cone
- r = radius of the tubular or cone at the junction measured from the axis of the tubular to the middle of the shell surface (tubular or cone at junction)
- k_{st} = shell stiffness of tubular
- k_{sc} = shell stiffness of cone
- l_{et} = elastic length for tubular
- l_{ec} = elastic length for cone.

The stress concentration factor on the cone side is derived with respect to the nominal stress in the tubular as reference:

$$SCF_c = \left(\frac{\eta\zeta - \lambda}{\epsilon} \frac{l_{et}}{l_{ec}} \tan(\alpha) + \frac{1}{\cos(\alpha)} + \frac{6\zeta l_{et}}{t_c} \right) \frac{t_t}{t_c} \tag{F.17.4}$$

Example calculation:

$$\begin{aligned} E &= 2.1 \cdot 10^{11} \text{ N/m}^2 \\ v &= 0.3 \\ \alpha &= 8^\circ \\ t_t &= 0.030 \text{ m} \\ t_c &= 0.040 \text{ m} \\ l_{et} &= 0.113 \text{ m} \\ l_{ec} &= 0.130 \text{ m} \\ k_{st} &= 5.192 \cdot 10^5 \text{ Nm} \\ k_{sc} &= 12.31 \cdot 10^5 \text{ Nm} \\ \kappa &= 2.053 \\ \eta &= 0.221 \\ \varepsilon &= 0.715 \\ \psi &= 0.130 \\ \lambda &= 0.073 \\ \zeta &= 0.035 \\ SCF_t &= 1.796 \\ SCF_c &= 1.197 \end{aligned}$$

CHANGES – HISTORIC

April 2016 edition

Main changes April 2016

• Sec.1 Introduction

- [1.2.1] The validity of the recommended practice for use in seawater with and without cathodic protection is increased from 550 MPa to 690 MPa.

• Sec.2 Fatigue analysis based on S-N data

- [2.4.6] New S-N curve for simple tubular joint for harmonisation with ISO 19902.
- [2.4.10] The HS curve for high strength steel is moved to [D.1] to be in the same appendix as the S-N curves for subsea application in [D.2].
- [2.5.1] New information on residual stresses after cold forming is inserted. This may for example be important for design of penetrations in monopiles for J-tube transfer.
- [2.5.2] Text is added for additional explanation of content.
- [2.10.1] Text is revised to align with DNV-OS-F101 and to include improved S-N data derived in a joint industry project.
- [2.10.2] The content is revised to be aligned with DNV-OS-F101.

• Sec.3 Stress concentration factors

- [3.1.1] More background information on δ_0 is included.
- [3.1.2] Added SCF equation for the back side of thickness transition as asked for by the industry.
- [3.1.5] This section is revised with improved figures. It is noted that also a compressive force range in the axial direction can give tensile stress normal to the main stress direction and lead to fatigue of fillet weld.
- [3.3.4] The change to a higher S-N curve for simple tubular joints implies that some more information is needed also on stiffened tubular joints, and some more information is added.
- [3.3.7.2] The value of δ_0 is reduced to make this safer based on new information about actual fabricated tolerances.
- [3.3.7.3] Limit on thickness ratio for use of Equation (3.3.5) is deleted.
- [3.3.9] Information is added on effect of placement of thickness transition.

• Sec.4 Calculation of hot spot stress by finite element analysis

- [4.3.4] Section added for purpose of fatigue life calculation using time domain and Rainflow analysis.
- [4.3.6] More explanation is included as the use of this section is considered difficult to document in projects.
- [4.3.9] Factor in Equation (4.3.15) is increased due to possible start and stop positions around circumference when welding.

• Sec.7 Improvement of fatigue life by fabrication

- [7.3] Section added because a different requirement to roughness is made regarding coating than for fatigue strength in standards.

The reference list has been updated.

- App.D S-N curves for base material of high strength steel
 - [D.2] A new section with S-N curves for high strength carbon and low alloy machined forgings for subsea applications is included.
- App.E Application of the effective notch stress method for fatigue assessment of structural details
 - App.E The content on notch stress analysis is moved from the commentary section and is included as a new appendix to get it in more line with accepted procedures when using finite element analysis.
- App.F Commentary
 - [F.5] ISO 5817 revised in 2014 and existing text had to be updated.
 - [F.7] Table F-3 and Figure F-6 are corrected. The former was not precise with respect to confidence level.

April 2014 edition

Main changes

- General
 - A number of minor editorial changes have been made such as to correct equation numbering.
- Sec.2 Fatigue Analysis Based on S-N Data
 - [2.4.3]: A section on thickness effect for butt welds and cruciform joints has been added. The thickness exponent for S-N class C and C1 has been modified in Table 2-1 and Table 2-2.
 - [2.4.13]: “S-N curves for piles” has been added. The consecutive text has been renumbered accordingly.
 - [2.5]: Absolute signs have been included in Equation (2.5.1).
- Sec.3 Stress Concentration Factors
 - [3.3.3]: “Tubular joints welded from one side” has been revised. Also the commentary section on this part has been changed and text with design equations is added.
 - [3.3.7]: Additional Figure 3-11 b has been included to demonstrate that the methodology can also be used for double sided joints. Some improvement of text.
 - [3.3.12]: This section has been revised and a commentary section to this part, [D.16] has been added.
- Sec.4 Calculation of hot spot stress by finite element analysis
 - [4.2]: This section has been amended.
 - [4.3.5] has been restructured to include previous 4.3.7.
 - Previous 4.3.8 has been renumbered to [4.3.7].
 - [4.3.8]: A new section on web stiffened cruciform joints is added in the main section and in the commentary, [D.16].
- App.A Classification of Structural Details

Changes - historic

- Change in S-N classification made on longitudinal welds in Table A-9 detail category 2. Also information on requirements to NDT and acceptance criteria is given together with a new section on this for information in the commentary section.
- App.D Commentary
 - Section Commentary [D.15]. The slope of the S-N curve for ground welds has been changed from $m = 4.0$ to $m = 3.5$.

About DNV GL

DNV GL is a global quality assurance and risk management company. Driven by our purpose of safeguarding life, property and the environment, we enable our customers to advance the safety and sustainability of their business. We provide classification, technical assurance, software and independent expert advisory services to the maritime, oil & gas, power and renewables industries. We also provide certification, supply chain and data management services to customers across a wide range of industries. Operating in more than 100 countries, our experts are dedicated to helping customers make the world safer, smarter and greener.